Linking structural traits, non-structural carbohydrates and tree ecological strategies in different climates

Guangqi Zhang

THÈSE POUR OBTENIR LE GRADE DE DOCTEUR DE L'UNIVERSITÉ DE MONTPELLIER

En Écologie Fonctionnelle et Sciences Agronomiques

École doctorale GAIA

Unité de recherche UMR AMAP

Linking structural traits, non-structural carbohydrates and tree ecological strategies in different climates

Présentée par Guangqi ZHANG

Le 24 Juin 2022

Sous la direction de Alexia STOKES et Pascale MAILLARD

Devant le jury composé de

[Dr Alexia STOKES, DR1-HDR, INRAE Montpellier, France]	[Directrice de thèse]
[Dr Pascale MAILLARD, CR-HDR, INRAE Nancy, France]	[Co-Directrice de thèse]
[Dr Bruno CLAIR, DR2-HDR, CNRS Montpellier, France]	[Président du jury]
[Dr Stéphane BAZOT, Professor, Université Paris-Saclay, France]	[Rapporteur]
[Dr Lourens POORTER, Professor, Wageningen University, Netherlands]	[Rapporteur]
[Dr Anaïs BOURA, Professor, CNRS-MNHN-Sorbonne Université, France]	[Examinateur]
[Dr Zexin FAN, Professor, XTBG CAS, China]	[Examinateur]
[Dr Zhun MAO, CR, INRAE Montpellier, France]	[Invité, co-encadrant]

UNIVERSITÉ DE MONTPELLIER

Acknowledgements

Firstly, a heartfelt thanks to my supervisor, Alexia Stokes, for her conscientious and kind mentorship during my PhD. It was always a pleasure to work with her and I have learned a lot from her, including her rigorous work attitude, optimistic and cheerful personality, witty and humorous conversation and keen scientific insight. I appreciated a lot for her contributions not only to my manuscripts and thesis writings, but also to my understandings of research.

Secondly, I would like to thank my co-supervisor, Zhun Mao, who was always passionate about research and inspired me when I got negative mood about my work. I am deeply grateful for his help with statistics learning, constructive and supportive comments to my work. During my PhD journey, especially during the Chinese traditional festivals, he always made me feel at home every time. I would also like to thank another co-supervisor, Pascale Maillard, who variously helped with study design, field work, lab methods, and reviewing manuscript drafts. Her friendliness and kindness have always been an example for me to follow and inspire me.

Many thanks to the members of my PhD committee: Isabelle Chuine, Brigitte Meyer-Berthaud, Patrick Heuret, Claire Fortunel, Jordi Martinez-Vilalta for their effort and constructive comments to improve my PhD work. Thanks to the reviewers and members of my PhD jury for taking time to evaluate this thesis work.

A special thanks to the head of the AMAP institute, Thierry Fourcaud, for making me feel welcome at the lab. Thanks to Nathalie Hodebert and Miléna Dordevic-Giroud for their administrative help, and without their enthusiasm, maybe I would not be able to eat with my colleagues in the canteen. I would also like to thank Merlin Ramel, Sophie Nourissier-Mountou, Stéphane Fourtier, Jean-Luc Maeght, Julien Engel, for their help in the fieldwork. My PhD work cannot be finished without their support.

A special thanks to China Scholarship Council (CSC) for providing me with a four-year PhD bursary. Thanks to Bastien Gerard and the SILVATECH facility for their help on measurement of non-structural carbohydrate. Thanks to Loic Brancheriau and Nabila Boutahae for their help on near infra-red spectroscopy analysis. Thanks to Brice Dupin for permission to sample trees on private property at Luz-Saint-Sauveur, France. Thanks to the colleagues of UMR EcoFog lab and the staff of Paracou research station for their hep on the fieldwork in French Guiana.

I would like to thank all my friends and colleagues in the lab, for sharing their experience. It was enjoyable to get along with them, especially during the coffee time and lunch time, which relieves the pressure of academics. I would also like to thank my Chinese friends in Montpellier, because I had a very pleasant life other than scientific research. All of them make my spare time more colourful.

Finally, I want to thank my family, especially my mother and sister. They are my strong backing. Their selfless dedication and silent support are the motivation for me to persist in a foreign country until now. A special mention goes to my girlfriend, Yanan Li. Very lucky to meet her as partner in my life. Without her encouragement, support and companionship, I could not finish my PhD.

Table of Content

Abstract

Functional traits which impact plant fitness indirectly via their effects on growth, reproduction and survival are considered the widely accepted tool for studying the plant strategies. As an important functional trait, non-structural carbohydrates (NSC) are considered as indicator of balance between carbon sources and sinks in plants and reflect the adaptive strategies of plants. In xylem, NSC are mostly stored as soluble sugars and starch in radial and axial parenchyma (RAP). The design of the xylem space of woody plant species also plays important roles in tree growth and multiple functions including water transport, mechanical integrity and carbohydrate storage. However, little is known about how NSC impacts xylem multi-functionality, nor how the relationship between NSC and parenchyma fractions vary among species and climates. Whether NSC content in different organs coordinates with traits linked to the economic spectrum, that design plant ecological strategies, is still less known. In this thesis, we firstly carried out a systematic review by compiling a database of NSC, RAP, wood density and maximum tree height data for 68 tree species to explore the relationships among these traits, especially the relationship between NSC and parenchyma fraction. Then, we collected leaves, stems and roots from 90 tree species in temperate, Mediterranean and tropical climates and measured functional traits including NSC, carbon, nitrogen, leaf mass per area, stem and root wood density and xylem anatomical traits to disentangle how NSC and xylem traits are linked to tree physiological processes and ecological strategies and explore the trade-off of xylem structure and function. We found NSC content was positively correlated with RAP fractions confirming the important role of stem parenchyma cells in NSC storage. The analysis of evolutionary relationships demonstrated that RAP fractions and NSC content were always closely related, suggesting that RAP can act as a reliable proxy for potential NSC storage capacity in tree stems. We also found that all xylem traits showed marked interspecific variation and varied significantly across climates and xylem arrangement

types. Wood density was positively correlated with total parenchyma fractions in both stems and roots, while it was negatively correlated with vessel fraction, vessel mean diameter and specific xylem hydraulic conductivity (SXHC), which revealed a trade-off between xylem mechanical support and hydraulic conductivity. Moreover, there were positive correlation patterns between NSC and SXHC in stems, but negative correlation in roots, suggesting hydraulic-storage strategies differed between these organs, with more closer ties existing in the stem than in root. In addition, our results revealed there was a covariation between leaf NSC content and leaf economics traits, whereas the variations between woody organs, especially stem NSC content and economics traits were largely decoupled. Tree ecological strategies were influenced by climate and species with different leaf habit exhibit different resource strategies: deciduous species tended to gather on acquisitive side, whereas evergreen species gathered more on conservative side. The results presented in the thesis have not only broadened the scope of our knowledge about the storage and physiology of NSC in trees, but also provided insight on functional strategies related design of xylem space in angiosperms, especially across a broad range of species and climates.

Key words: climate, economics spectrum, functional trait, non-structural carbohydrate, radial and axial parenchyma, storage, wood density, structure-function, trade-offs, xylem anatomy

Résumé

Les traits fonctionnels qui ont un impact indirect sur l'aptitude des plantes par le biais de leurs effets sur la croissance, la reproduction et la survie sont considérés comme un outil largement accepté pour étudier les stratégies des plantes. En tant que trait fonctionnel important, les glucides non structurels (NSC) sont considérés comme des indicateurs de l'équilibre entre les sources. Dans le xylème, les NSC sont principalement stockés sous forme de sucres solubles et d'amidon dans le parenchyme radial et axial (RAP). La construction du xylème des espèces végétales ligneuses joue également des rôles importants dans la croissance des arbres et de multiples fonctions, notamment le transport de l'eau, l'intégrité mécanique et le stockage des glucides. Cependant, on sait peu de choses sur l'impact de NSC sur la multifonctionnalité du xylème, ni sur la manière dont la relation entre les NSC et les fractions du parenchyme varie selon les espèces et les climats. On sait encore moins si la teneur en NSC dans les différents organes est coordonnée avec les traits liés au spectre économique, qui conçoivent les stratégies écologiques des plantes. Dans cette thèse, nous avons d'abord effectué une revue systématique de la littérature internationale sur le sujet et compilé une base de données de NSC, RAP, densité du bois et hauteur maximale de l'arbre pour 68 espèces d'arbres afin d'explorer les relations entre ces traits, en particulier la relation entre NSC et fraction parenchyme. Nous avons ensuite prélevé des feuilles, des tiges et des racines de 90 espèces d’arbres dans des climats tempérés, méditerranéens et tropicaux et mesuré les caractéristiques fonctionnelles, afin de démêler la façon dont les caractéristiques des NSC et du xylème sont liées aux processus physiologiques et aux stratégies écologiques des arbres et d'explorer le compromis entre la structure et la fonction du xylème. Nous avons constaté que la teneur en NSC était positivement corrélée aux fractions RAP, ce qui confirme le rôle important des cellules du parenchyme du tronc dans le stockage des NSC. Nous avons également constaté que tous les traits du xylème présentaient une variation interspécifique marquée et variaient de

manière significative entre les climats et les types d'agencement du xylème. La densité du bois était positivement corrélée avec les fractions totales du parenchyme dans le tronc et la racine, tandis qu'elle était négativement corrélée avec la fraction des vaisseaux, le diamètre moyen des vaisseaux et la conductivité hydraulique spécifique du xylème (SXHC), ce qui a révélé un compromis entre le support mécanique du xylème et la conductivité hydraulique. De plus, il y avait des corrélation positive entre NSC et SXHC dans les troncs, mais une corrélation négative dans les racines, suggérant que les stratégies de stockage hydraulique différaient entre ces deux organes, avec des liens plus étroits existant dans le tronc que la recine. En outre, nos résultats ont révélé une covariation entre la teneur en NSC des feuilles et les caractéristiques économiques des feuilles, tandis que la variation entre les organes ligneux, en particulier la teneur en NSC des tiges et les caractéristiques économiques, était largement découplée. Les stratégies écologiques des arbres ont été influencées par les climats et les espèces ayant des caractéristiques foliaires différentes présentent des stratégies de ressources différentes: les espèces à feuilles caduques ont tendance à se rassembler du côté de l'acquisition, tandis que les espèces à feuilles persistantes ont tendance à se rassembler du côté de la conservation. Les résultats présentés dans la thèse ont non seulement élargi le champ de nos connaissances sur le stockage et la physiologie des NSC chez les arbres, mais ont également fourni un aperçu des stratégies fonctionnelles liées à la conception de l'espace du xylème chez les angiospermes, en particulier à travers une large gamme d'espèces et de climats.

Mots clés: climat, spectre économique, traits fonctionnel, glucides non structuraux, parenchyme radial et axial, stockage, densité du bois, structure-fonction, compromis, anatomie du xylème

List of Abbreviations

AP: axial parenchyma

APG: angiosperm phylogeny group

C: carbon

CFI: comparative fit index

CV: coefficient of variation

D: diameter

DBH: diameter at breast height

FFT: fibers, fiber-tracheids and tracheids

H_{max}: maximum tree height

LC: leaf carbon content

LESPC: leaf economics spectrum principal component axis

LMA: leaf mass per area

LN: leaf nitrogen content

LNSC: leaf non-structural carbohydrates

LPC: leaf principal component

LSS: leaf soluble sugars

LST: leaf starch

MAP: mean annual precipitation

MAT: mean annual temperature

MHD: vessel mean hydraulic diameter

N: nitrogen

NIRS: near infra-red spectroscopy

NSC: non-structural carbohydrates

NSC_{mean}: mean value of non-structural carbohydrates over 1 year

NSC_{max}: maximum value of non-structural carbohydrates in 1 year

PC: principal component axis

PCA: principal component analysis

PGLS: phylogenetic generalized least squares

PICs: phylogenetically independent contrasts

PLSR: partial least squares regression

RAP: radial and axial parenchyma

RC: root carbon content

RFFT: fiber (including tracheid) fractions

RMSECV: root mean square error of cross validation

RMSEP: root mean square error of prediction

RN: root nitrogen content

RNSC: root non-structural carbohydrates

RP: radial parenchyma

RPC: root principal component axis

RRAP: root total parenchyma fractions

RSS: root soluble sugars

RST: root starch

RVF: root vessel fractions

RWD: root wood density

S: vessel composition index

SC: stem carbon content

SEC: standard error of calibration

SEM: structural equation model

SFFT: stem fiber (including tracheid) fractions

SMA: standardized major axis

SN: stem nitrogen content

SNSC: stem non-structural carbohydrates

SPC: stem principal component axis

SRAP: stem total parenchyma fractions

SRMR: standardized root mean square residual

SS: soluble sugars

SSS: stem soluble sugars

SST: stem starch

ST: starch

SVF: stem vessel fraction

SWD: stem wood density

SXHC: specific xylem hydraulic conductivity

VD: vessel density

VF: vessel fraction

VMD: vessel mean diameter

WD: wood density

WPC: whole-plant principal component axis

CHAPTER 1: General introduction

In the process of growth, plants would perform a series of physiological activities and ecological functions, such as photosynthesis, respiration, water transport, defense, etc. Different plants would show different ways, that is to say, plants have different ecological strategies. In other words, plant ecological strategies refer to how a species sustains a population by perform its functions, and as operating in the presence of competing species, in varied landscapes, and under regimes of disturbance (Westoby, 1998). Functional traits which impact plant fitness indirectly via their effects on growth, reproduction and survival are considered the widely accepted tool for studying the plant strategies (Westoby *et al.*, 2002; Violle *et al.*, 2007). The patterns in traits have been described using various concepts, with the "economics spectrum" currently being one of the best models to describe the relationships among functional traits. For example, the leaf economics spectrum, for the first time at global scale, summarized the variation and interrelationships among leaf economics traits, reflecting a gradient of fast (acquisitive) to slow (conservative) strategies in terms of investment and use of nutrients and other resources (Wright *et al.*, 2004; Donovan *et al.*, 2011; Osnas *et al.*, 2013; Pan *et al.*, 2020). Along the leaf economics specturm, species with higher specific leaf area tend to have higher leaf nitrogen content and lower leaf life span, allowing a better acquisition of resources to adapt to harsh environments, while the opposite is that species with lower specific leaf area generally have a longer leaf life span but lower leaf nitrogen content and lower photosynthetic rates as species' strategies tend towards the conservation of resources. In analogy with the leaf economic spectrum, a "wood economics spectrum (Chave *et al.*, 2009) and a "root economic spectrum" (Kramer-Walter *et al.*, 2016; Roumet *et al.*, 2016) have been hypothesized to represent trait covariation, from fast-growing species with acquisitive traits (organs that are cheap to construct, with high uptake capacity, respiration, high surface area and nitrogen content), to slow-growing species with conservative traits (long-lived organs

with a high-carbon cost). However, the link between the different organs in terms of ecological strategies is still poorly understood, particularly with regard to stem and root organs.

1.1 ANATOMICAL TRAITS IN SECONDARY XYLEM

Woody organs play great role in tree survival and functional performance. Woody xylem traits are increasingly recognized as core functional traits in plants, and increasing understanding of xylem functions is also increasingly important. To thrive in a forest environment, and withstand both biotic and abiotic constraints, tree xylem is multifunctional, simultaneously providing hydraulic functioning, mechanical support, storage and defense against insect/pathogen attack. Because wood performs more than one task, the requirements for wood structure are conflicting, and understanding the interconnectedness of xylem structure and function is critical to understanding the diversity of physiology, structure, and life-history types found in woody plant species (Pratt and Jacobsen, 2017). The secondary xylem of angiosperms is generally composed of three specialized cell types including parenchyma, vessels and fibers (tracheids and fiber-tracheids may also be present) (Fig. 1.1), that contribute to these distinct functions. Variations in the size, form, arrangement, and frequency of these cell types lead to the diversity of woods that perform these functions in a range of ecological contexts (Chave *et al*., 2009).

1.1.1 Parenchyma cells in xylem

Xylem parenchyma cells are produced by ray and fusiform initials of the cambium and are living tissues with variation in size, orientation, form and wall pitting (Fig. 1.2). The parenchyma cells of secondary xylem can be divided into radial parenchyma (RP) and axial parenchyma (AP), with the former stretching radially, perpendicular to the long axis of a stem and latter generally elongated parallel to the long axis of a stem (Ziemińska, 2014; Morris,

2016). The living parenchyma cells can represent a large component of the tissue volume and the proportion of those varies across plant organs, species and environment (Spicer, 2014; Ziemińska, 2014). The high variability in parenchyma cells and tissues suggests similar variation in functions (Beeckman, 2016). These function range from defense/wound repair (Morris *et al.*, 2020), to respiration (Rodríguez-Calcerrada *et al.*, 2015), nutrient and water storage (Plavcová *et al.*, 2016; Secchi *et al.*, 2017), and mechanical contribution, particularly by RP (Burgert and Eckstein, 2001; Rana *et al.*, 2009). Wood rays usually have large amounts of lignin packed among parenchyma cells and fibers, that will also increase overall wood density and mechanical strength (Burgert and Eckstein, 2001; Rana *et al.*, 2009). In addition, xylem parenchyma cells in contact with xylem conduits are assumed to perform embolism repair function, which allow water to flow into empty conduits and supply water for refilling (Zwieniecki and Holbrook, 2009; Brodersen *et al.*, 2010). However, there is no consensus on the exact repair mechanism of the hydraulic system, including vessel refilling (Beeckman, 2016). Moreover, AP normally is associated with the maintenance of hydraulic conductivity, as tree species with higher fractions of AP tend to have larger vessels (Morris *et al.*, 2018a). Axial parenchyma can be divided into two major types (paratracheal axial parenchyma and apotracheal axial parenchyma, Fig. 1.3) according to their arrangement. Paratracheal AP cells are highly grouped around the vessels, but scanty paratracheal arrangement is very frequent, occuring in up to 28% of all hardwoods (Wheeler *et al.*, 2007). Apotracheal AP cells are not associated or contiguous with vessels in transverse section and some random contacts may exist, although they are infrequent (Morris and Jansen, 2016). The two types of axial parenchyma, especially the paratracheal AP, have distinct distribution patterns and are frequently used for their taxonomic and identifying values, but are rarely directly related to function. More attention should be paid to the structure and arrangement of parenchyma cells

and it might indeed be more important to distinguish between contact cells and isolation cells from a functional point of view.

1.1.2 Vessel cells in xylem

Xylem is the tissue in vascular plants which conducts water upwards in a plant. The xylem vessel is one of the two cell types of tracheary elements which are the water conducting elements in vascular plants, the other is the tracheid. Most angiosperms have both xylem vessels and tracheids but the xylem vessels serve as the major conductive element. (Tyree and Ewers, 1991; Sperry *et al.*, 2006). A vessel consists of a vertical series of vessel members that vary from elongated to squat, drum-shaped cells the walls of which are secondarily thickened with rings, spirals, or networks of cellulose, that later become lignified (Fig. 1.4). Vessel anatomical characteristics have been also associated with many xylem functions, especially for hydraulic function. Xylem vessels are main channels for axial water transport in plants and their traits greatly affect the flow rate of water, maintenance of water potential gradient and vulnerability to xylem cavitation (Wheeler *et al.*, 2005). Vessel fraction, defended as the portion of sapwood occupied by vessel lumens, is found be closely related to wood mechanical robustness and hydraulic conductivity (Scholz *et al.*, 2013). Vessel sizes (e.g., diameter) are directly used to calculate both mean hydraulic diameter (i.e., the actual conductance of conduits) and specific xylem hydraulic conductivity (i.e., conductance per unit root surface area), two fundamental hydraulic variables widely used in literature (Tyree and Ewers, 1991; Poorter *et al.*, 2010a; Fortunel *et al.*, 2014). According to the Hagen-Poiseuille equation, the lumen conductivity increases with the fourth power of the lumen diameter (Tyree and Ewers, 1991). A higher mean vessel diameter favors conducting efficiency, but may decrease conducting safety due to the increasing risk of vessel implosion and cavitation (Loepfe *et al.*, 2007). Additionally, the vessel size to vessel number per area ratio is also the

main driver of hydraulic conductivity, with high the ratio associated with high hydraulic conductivity, although the risk of freeze-induced embolisms also increased (Zanne *et al.*, 2010). Therefore, for a given total vessel fraction, mean vessel size shall be closely related to vessel density, thereby affecting the plant's hydraulic strategy in water use (Hacke *et al.*, 2006). Furthermore, when viewed from the cross-section, the species, especially for the temperate species, can be divided in three main categories according to the distribution of vessels: diffuse-porous, ring-porous and semi-ring-porous (Fig. 1.5). Diffuse-porous species usually have similar vessel size, with no clear earlywood-latewood vessel arrangement. Ring-porous species have vessels with two essentially distinct diameters, with relatively large vessels concentrated in the earlywood and considerably smaller vessels in the latewood. Semi-ring-porous species are not strictly either ring porous or diffuse porous in structure and exhibit vessel distributions somewhere in between these two categories. Diffuse-porous species are usually found in tropical regions, whereas ring-porous species are always deciduous and are therefore more abundant in cooler regions, or regions with a marked dry season (Boura and De Franceschi, 2007). Large earlywood vessels in ring-porous species are important for rapid water transport after leaf abscission and dormancy, whereas in diffuse porous species, root pressure drives vessel refilling at the end of the winter/dry season. However, it remains uncertain if and how other anatomical characters differ between the porosity types and the associated functions among species.

1.1.3 Fiber cells in xylem

The xylem fibers are usually non-living sclerenchyma cells as they lose their protoplasts at maturity and can be found in between the tracheids and xylem vessels of the xylem tissue. Fiber cells are much-elongated cells with many times longer than the breadth, tapering to a wedge-shape at both ends and usually have very thick secondary walls made up of lignin or

cellulose (Fig. 1.6). It is well known that the main function of fibers is mechanical support and mechanical properties of wood are mainly determined by cell wall tissues. It was reported that fiber wall proportion was positively correlated with modulus of rupture (an indicator of mechanical strength) in 17 evergreen shrub species of South Africa (Jacobsen *et al.*, 2007). Ziemińska *et al*. (2013) showed similar results across 24 Australian angiosperms which found wood density was not related to total fiber fraction, but positively correlated with fiber wall fraction and negatively with fiber lumen fraction, as well as shown in Janssen *et al.* (2020) for large number of neotropical trees. Hence, it is clear to say that strongly related to fiber properties is wood density. For example, a study exploring the relationships between wood specific gravity (Wood specific gravity and wood density are often viewed as interchangeable, despite the fact that they are slightly different. Specifically, wood specific gravity used water density as a baseline normally expressed as 1, to express the ratio of a wood density as compared to water.) and anatomical traits in branches and roots of 113 rainforest tree species also confirmed that fiber traits are major contributors to wood specific gravity (Fortunel *et al.*, 2014). And the wood specific gravity was independent of vessel traits in branches. Although vessels were demonstrated to have some effect on density at roots, the positive correlation between fiber wall fraction and wood specific gravity was particularly high. In addition to mechanical support, studies have also reported that fibers can be alive and thus store starch (Yamada *et al.*, 2011; Plavcová *et al.*, 2016), although fiber cells are generally considered dead cells. For example, Yamada *et al*. (2011) found that more than 70% of the starch grains in the outermost ring were stored in living wood fibers during winter for the species *Robinia pseudoacacia*. Plavcová *et al*. (2016) also found the living fibers are strongly related to the starch storage capacity in sapwood of temperate deciduous trees, with living fibers being densely packed with starch grains. Furthermore, there is no definite conclusion on whether fibers are involved in hydraulic function, although studies have reported that fiber traits had

no relationships with hydraulic conductivity or minimum water potential (Jacobsen *et al.*, 2007; Pratt *et al.*, 2007). However, Jacobsen *et al.*, (2005) for the first time reported that at the cellular level, increased cavitation resistance was correlated with increased fiber wall area and decreased fiber lumen area, which suggested a mechanical role for fibers in cavitation resistance. Therefore, we still need to further study the function of the fiber and the connection with other anatomical traits.

1.1.4 Trade-offs among anatomical traits with xylem functions

Although the three cell types in the xylem perform their main functions, it is not difficult to see that their functions are nonetheless entwined and connected in complex ways. Trees have evolved in response to a multitude of diverse environmental signals, that have led to trade-offs in structure and function within the xylem space. As the largest metabolically active fraction in the xylem space, parenchyma cells, and the NSC stored within them, are fundamental to driving survival processes, such as resprouting after a disturbance like a wildfire (Smith *et al.*, 2018a). In particular, AP is associated with the maintenance of hydraulic conductivity, as tree species with higher fractions of AP tend to have larger vessels (Morris *et al.*, 2018a) and greater hydraulic capacitance (Aritsara *et al.*, 2021; Ziemińska *et al.*, 2020). Paratracheal AP is an accessible source of NSC for embolism refilling in vessels (Tomasella *et al.*, 2020). However, a large AP fraction decreases wood density and results in high stem respiration, reducing tree growth rate (Jacobsen *et al.*, 2007; Fortunel *et al.*, 2014; Rodríguez-Calcerrada *et al.*, 2015). The RP are also major sinks of NSC, but can contain a large amount of lignin between individual parenchyma cells and surrounding fibers, thus increasing overall wood density and improving radial strength (Burgert and Eckstein, 2001), but decreasing the available xylem space for other cell types. Vessels, however, decrease wood density, but a large lumen fraction is vital for increased hydraulic conductivity (Zanne *et al.*, 2010),

potentially creating a trade-off between hydraulics and xylem mechanical integrity (Christensen-Dalsgaard *et al.*, 2007a, b; Chen *et al.*, 2020), although studies provide conflicting results (Woodrum *et al.*, 2003). In addition, the covariation between hydraulic safety and efficiency is one of the most frequently studied relationships. The evidence for this trade-off between safety and efficiency is supported by a study across the world's woody plant species, showing that no species had high efficiency and high safety, although correlations between them were weak (Gleason *et al.*, 2016). Moreover, studies have also shown there is a strong negative relationship between vessel size and vessel density (Sperry *et al.*, 2008; Poorter *et al.*, 2010a; Zanne *et al.*, 2010; Fortunel *et al.*, 2014). Big vessels are important for achieving the highest levels of efficiency, while high vessel density is important for safety as it reduces the overall impact of cavitation in a single vessel (Ewers *et al.*, 2007; Gleason *et al.*, 2016). Although there have been some studies on the trade-offs of xylem structural functions, these studies focused on limited functions and number of species, or on shrubs. Better understanding of connection between the multiple structure and function of the xylem across a broad of species and climate is still needed.

When analyzing relationships among xylem structure and function, most studies are often restricted to main stems and branches (Gleason *et al.*, 2016; Barotto *et al.*, 2018; Chen *et al.*, 2020; Aritsara *et al.*, 2021; Pratt *et al.*, 2021a), mainly because of their importance in water transport and mechanical support and also their accessibility. However, the growth of trees depends not only on the synergy of aboveground structure and function, but also on the condition of transportation and storage in the underground xylem. Normally, the distribution of anatomical traits is different between stem and root, as parenchyma content is higher and fiber content is lower in root than in the stem (Stokes and Guitard, 1997). Additionally, root's mechanical environment is a soil matrix and roots typically experience less negative hydrostatic pressure than stems and thus resulting in the root having different mechanical and

transport constraints compared to the stem (Pratt *et al*., 2007). The stem and root also tend to focus on different functions. Stems have to hold the crown up and suck the water up to the leaves, while roots uniquely function in underground anchoring and storage. Therefore, the combined study of xylem structure in both aboveground and underground woody organs may explain the structure and function relationships better than the study of an individual organ.

1.1.5 Effect of climates on xylem traits

Species from different climatic backgrounds with divergence of wood structure patterns can have specific functional strategies that reflect differences in plant resource allocation and use (Wright *et al.*, 2005; Violle *et al.*, 2007; Yu *et al.*, 2020). Temperature and precipitation are the two most commonly considered variables in studying how climate affects plant traits on a global scale (Clarke and Gaston, 2006; Moles *et al.*, 2014). Studies showed that climatic factors have some impact on anatomical traits. For example, Morris *et al*. (2016) found there was a strong and positive correlation between RAP and mean annual temperature (MAT), albeit non-linear, whereas the relationship between RAP and mean annual precipitation (MAP) was weakly negative. Ziemińska (2014) also found total parenchyma fractions tended to be higher in warmer and wetter locations in twigs of 69 Australia species. Additionally, tropical species have higher level of RAP fractions than that of temperate and subtropical species (Morris *et al*., 2016). When studying the relationship between climate and vessel, however, studies showed that vessel fraction was not related to temperature and precipitation in both stem and twigs (Martínez-Cabrera *et al.*, 2009; Gleason *et al.*, 2012). The relationship between vessel size and temperature was positive (Morris *et al.*, 2018a) across a large of woody angiosperms, and tropical species do have larger vessel diameter than temperate species (McCulloh *et al.*, 2010; Morris *et al.*, 2018a), although some studies suggested vessel size was mainly driven by the size of a plant rather than by a climate (Olson and Rosell, 2013).

Little study has been done on the relationship between fiber and climate, but see Martínez-Cabrera *et al.* (2009) which found fiber traits showed stronger correlations with precipitation than with temperature, with fiber wall areas increasing with decreasing MAP. Wood density which emerges from the interaction of different xylem properties would also vary across environmental gradients. For example, in North and South America, mean wood density increased with increasing MAT, but increased with decreasing annual precipitation sum (Šímová *et al.*, 2018). Clough *et al.* (2017) also found a positive relationship between wood density and MAT in tree species of eastern United States, which suggested that climate influences investment in stem wood within tree species and contributes to biogeographical patterns in wood density. Additionally, wood density has also been shown to vary with latitude: although the wood density of tropical and temperate tree species is not significantly different, more variability is found in tropical species compared to temperate species (Wiemann and Williamson, 2002). Despite there are many studies focusing on variation and functional significance of xylem properties, it remains unclear how wood xylem traits and functions are internally connected across different climates and whether the functional trade-off varies due to climate differences.

1.2 NON-STRUCTURAL CARBOHYDRATES

As an important functional trait, non-structural carbohydrates (NSC) are the primary substrates and the key energy source for plant metabolic processes (Fig. 1.7), which play a vital role in plant multiple functions including respiration, osmoregulation, reproduction, defence and survival (Kozlowski, 1992; Morin *et al*., 2007; Sala *et al.*, 2012; Dietze *et al.*, 2014; Hartmann and Trumbore, 2016), as well as having major consequences for downstream processes such as microbial activity in the rhizosphere (Schiestl-Aalto *et al.*, 2019). Non-structural carbohydrates are a product of photosynthesis and comprise mainly soluble sugars

which are involved in transport or immediate functions, and starch that is stored for future use, when carbon demand is higher than supply (e.g., under severe drought stress; Anderegg and Anderegg, 2013; Wiley *et al.*, 2013; Klein and Hoch, 2015; Furze *et al.*, 2019), which represent a major carbon storage pool in woody plants.

1.2.1 Relationships between NSC and parenchyma

Carbon storage in sapwood buffers the imbalance between carbon supply and demand, helping trees to survive changing environments, especially in drought conditions (Hartmann and Trumbore, 2016 ; Kawai *et al.*, 2021). An understanding of potential factors that can affect NSC storage pool size is essential for better evaluating the role of NSC in tree physiological processes, especially across a broad range of species and climates. Non-structural carbohydrates are generally found in the live tissues within a tree and fluctuate between organs throughout the year. The role of wood parenchyma in storage is often highlighted and the quantity of NSC in sapwood xylem should depend largely on the volume of parenchyma cells present. Supporting this point, studies in temperate regions have revealed significant positive correlations between parenchyma fractions and NSC contents across species (Plavcová *et al.*, 2016; Godfrey *et al.*, 2020; Chen *et al*., 2020; Kawai *et al.*, 2021), providing insights into the size and dynamics of wood parenchyma carbohydrate pool. For example, Chen *et al*. (2020) found that the xylem NSC content was positively related to RAP and axial parenchyma (AP), but not related to radial parenchyma (RP) in 19 temperate broadleaf tree species, suggesting that the roles of RP and AP are distinct among species, while Kawai *et al*. (2021) showed both AP and RP were associated to NSC content in the branches of 15 subtropical woody species, emphasizing the importance of anatomical constraints for sapwood carbon stores. In addition, Plavcová *et al*. (2016) found significantly lower NSC content but higher RAP volume in stems of four tropical species compared to 12

temperate species. Nevertheless, these studies focused on a limited number of species and climates, and it remains unclear to what extent relationships would hold for a broad diversity of tree species and across biomes.

1.2.2 Seasonal variation of NSC

Most studies monitor the NSC levels in more than one organ, as a single organ is not a good indicator of NSC storage at the whole-tree level (Richardson *et al.*, 2013a; Furze *et al.*, 2019). Taking into account the expected positived correlations between NSC and parenchyma fractions mentioned above, it seems easy to think of the high variability in NSC content across species and woody organs as there exist large differences in wood parenchyma fractions across species and woody organs. As expected, it is well established that NSC contents can vary among organs, and woody roots are particularly important storage pool which accumulate large amounts of NSC (Würth *et al.*, 2005). NSC reserves in roots are functionally important in trees, irrespective of their capacity to resprout. High NSC contents in roots allow for fast root growth in the spring and hence uptake of water and nutrients for budburst. A previous study indicated that the carbon demands of metabolism and routine functions in roots are greater than in stems across temperate eucalypt species, which suggests higher NSC contents in roots are needed (Smith *et al.*, 2018b). However, accurate measurements of whole-tree NSC storage and allocation among organs are logistically difficult, although some studies present NSC storage at a whole-tree level (Mei *et al.*, 2015; Smith *et al.*, 2018a; Furze *et al.*, 2019). In addition, the NSC content is also known for its seasonal variability, which is supported by a seminal review (Kozlowski, 1992). The total NSC contents typically peaked at the end of growing season and declined throughout the winter, reaching a minimum during or shortly after bud break. Similar seasonal trends were also observed in deciduous trees in tropical climates, where stemwood NSC content decreased

during leaf expansion and reproduction, and were higher in the dry season than in the rainy season (Newell *et al.*, 2002). Martínez-Vilalta *et al.* (2016) examined broad patterns of seasonal NSC variation across organs (i.e., leaf, stem, belowground organs), plant functional types (deciduous, evergreen, etc.) and biomes (boreal, temperate, Mediterranean, tropical) by assembling global database, which confirmed the seasonal NSC fluctuations, with a strong depletion of starch during the growing season and a general increase during winter months, particularly in boreal and temperate biomes. Therefore, understanding how patterns of NSC vary in trees and across climates will enable us to better evaluate the role of NSC in tree physiological processes and ecological strategies, especially across a broad range of species and climates.

1.2.3 The roles of NSC

Non-structural carbohydrate storage is particularly important for trees to improve tolerance to disturbance and unfavorable environmental conditions. During periods of environmental stress, trees can actively mobilize high NSC contents from various sources to maintain basic metabolic functions (Sala *et al.*, 2012; Dietze *et al.*, 2014). As mentioned above, NSC mainly comprise soluble sugars and starch. Soluble sugars are mainly synthesized from newly assimilated carbon by daytime photosynthesis and transferred to different organs by mass flow, which are used for short-term metabolism or stored (Kozlowski, 1992). Starch may serve as long-term storage pool which contribute to regrowth after disturbance and provide carbohydrates to new organs (Wiley *et al.*, 2013; Klein and Hoch, 2015). When carbon assimilation is insufficient to support metabolic activity, starch can be converted back to soluble sugars (Chapin *et al.*, 1990; Gibon *et al.*, 2009) and starch reserves are also fundamental for providing sugars to rebuild the foliage of deciduous tree species, after leaf fall (trees lose autotrophy ability and function using their C reserves) (EI Zein *et al.*, 2011;

Gilson *et al*., 2014). It is also known that NSC may be involved in reversal of embolism (Bucci *et al.*, 2003; Nardini *et al.*, 2011; Sala *et al.*, 2012). For example, Bucci *et al*. (2003) found that xylem hydraulic conductivity caused by embolism was lost in the morning and then recovered in the afternoon and this diurnal variation was related to a starch and sugar interconversion with disappearance of starch and increase of sugars in petioles from morning to afternoon. Sugars may also be involved in phloem transport which is thought to be driven by a pressure build-up in source tissues. The sugars accumulated in the phloem create osmotically driven pressure gradient to drive long-distance phloem transport (Ryan and Asao, 2014). In addition, the importance of NSC in repair of drought-induced embolism and maintenance of xylem transport has been highlighted. Previous study suggested that embolism can be repaired by water influx from surrounding non embolized vessels, driven by an osmotic gradient established by importing sugars into embolized vessels (Brodersen *et al*., 2010). Additionally, the NSC could also have critical osmotic functions (via continuous exchange of the soluble, osmotically active fraction) to avoid tissue water deficit and to maintain turgor and vascular transport (Hartmann and Trumbore, 2016).

In addition to being used for growth and respiration, NSC accumulation could passively occur when carbon supply exceeds demand (Chapin *et al.*, 1990), which reflects the translation of growth and photosynthesis regulation strategies. However, there has been a vigorous debate which focuses on if storage is an passive or active process (Sala *et al*., 2012; Wiley and Helliker, 2012). "Active" means that storage is increased at the expense of growth, even when the conditions for growth are favorable (Dietze *et al*., 2014). Regardless, both active and passive storage involve a trade-off between storage and growth. The allocation-based trade-off between carbon demand and supply depends largely on tree ecological strategies, which has been linked to plant resource acquisitive and conservative strategies. Furthermore, the content of NSC and allocation patterns in leaves, stems and roots are considered as indicators

of balance between carbon sources and sinks in plants (Chapin *et al.*, 1990; Hoch *et al.*, 2003; Körner, 2003; Würth *et al.*, 2005; Martínez-Vilalta *et al*., 2016). For example, fast-growing tree species with a high specific leaf area or low leaf mass per area tend to have high light capture potential and high net photosynthetic rate, which may result in an increase of photosynthates available for rapid growth of plant (Wright *et al.*, 2002; Li *et al.*, 2016). Additionally, slow-growing tree species with tough leaves, high leaf mass per area (LMA) and dense wood usually invest more carbon in reserve and defence than fast-growing species allowing them to persist longer when carbon demand is higher than supply (e.g., under severe drought stress) (Poorter and Kitajima, 2007; Poorter *et al.*, 2010b; Anderegg and Anderegg, 2013). Our current understanding of how NSCs interact with the fast-slow tree species continuum is fragmented, mostly derived from studies on seedlings (Signori-Müller *et al.*, 2021). For example, Poorter and Kitajima (2007) found that stem sugar concentrations were positively correlated with sapling survival rate, but negatively correlated with sapling growth rate in the moist forest in Bolivia. However, patterns observed in seedlings may not be easily extrapolated to mature trees (Signori-Müller *et al.*, 2021). To elucidate the functional role of storage in the fast-slow continuum, NSC dynamics across multiple plant organs in adult tree species with contrasting life-history strategies need to be assessed. Until now, it is still less known whether NSC content in different organs coordinate with tree functional economic traits which design plant ecological strategies.

1.3 RESEARCH GAPS, OBJECTIVES AND OUTLINE OF THE THESIS

Parenchyma fractions might act as a proxy for NSC storage capacity and recent studies found positive correlations between RAP and NSC content in woody stems and branches (Plavcová *et al*., 2016; Godfrey *et al*., 2020; Chen *et al*., 2020; Kawai *et al*., 2021; Pratt *et al*., 2021a). However, these studies focused on a limited number of species or on single biomes. Moreover,

these field measurements provide useful data, but large-scale studies are difficult to conduct due to the variation of NSC, especially the seasonality of NSC fluxes, as repeated sampling must be performed throughout the year (Martínez-Vilalta *et al*., 2016). The difficulties reside also in the trees and their size at adult stage, their location in forests, biomes etc. A systematic review of available data with multiple seasonal sampling points would be necessary to provide an alternative perspective and complementary evidence to validate the relationship between NSC and RAP in tree stems across species and climates.

Functions linked different xylem cell types are interdependent, and because wood xylem performs more than one task, there are conflicting demands leading to structure and function trade-offs (Grubb, 2016; Pratt and Jacobsen, 2017; Pratt *et al*., 2021a). Additionally, differences in function among species may be due to the spatial arrangement of cells, such as porosity, within the xylem space, but the link between cell function and their spatial arrangement is poorly understood. The resulting design of the xylem space actively influences physiological processes occurring within trees, potentially driving survival or failure when local environmental conditions change (Lachenbruch and McCulloh, 2014). Understanding design of the xylem space therefore, will allow us to identify strategies that contribute to tree survival in different climates.

NSC produced by photosynthesis can be quickly used for immediate functions or stored for reserves and defence (Wiley *et al.*, 2013; Klein and Hoch, 2015; Weber *et al.*, 2019), which suggest an allocation-based trade-off between carbon demand and supply. Several studies have reported the resource economics trade-off at different tissues, i.e., at leaf (Wright *et al*., 2004; Osnas *et al*., 2013), wood (Chave *et al.*, 2009), and root tissues (Prieto *et al.*, 2015; Roumet *et al.*, 2016), as well as at whole-plant level (Freschet *et al.*, 2010; de la Riva *et al.*, 2016; Zhao *et al.*, 2017; Li *et al.*, 2022). These studies demonstrated the traits of leaves, stems

and roots are coordinated and thus provide a useful framework for exploring the trade-off between acquisition and conservation of resources at entire plant level (Reich, 2014). Yet, although there are many studies on plant economic strategy, little research has been conducted to explore the direct coordination between NSC in different organs and functional economic traits which design plant ecological strategies.

Following above research gaps, the specific objectives of the thesis were to answer the overarching scientific question about how functional traits are interconnected and reflect tree resource allocation and ecological strategies, and test the following main hypotheses:

1) There should be a direct positive relationship between NSC contents and parenchyma fractions in a wide array of tree species, providing a new outlook and further insight on their relationships across climates and tree evolutionary subdivision based on a systematic review.

2) The design of the xylem space coordinates trade-offs between the xylem multiple structures and functions related to anatomical, hydraulic, mechanical and storage traits across a broad range of species and climates.

3) NSC contents coordinate with tree functional traits linked to the economics spectrum from a whole-tree level, revealing the role of NSC in tree physiological processes and ecological strategies across a broad range of species and climates.

The outline of main three chapters in this thesis is shown in Figure 1.8. The Chapter 2 describes the direct links between parenchyma fractions and NSC contents which mainly involved the function of nutrient storage in stem organs. In Chapter 3, we further expanded our research to include mechanical, hydraulic and storage functions and also extended to two woody organs (stem and coarse root). The Chapter 3 not only verified the content of Chapter 2, but also further revealed the complicated structure-function trade-offs at the xylem scale,

while also comparing the differences between different woody organs. In Chapter 4, we expand the organ scope to explore the role of NSC storage in ecological strategies at the whole tree level including leaf, stem and root. The Chapter 4 broadened the horizons of trade-offs in resource allocation by investigating the links between NSC and plant economic spectrum. More specifically:

In **Chapter 2**, we carried out a systematic review by compiling a database of NSC contents, RAP fractions, wood density and maximum tree height data for 68 tree species that span a wide spectrum of characteristics, to provide a new outlook and further insight on their relationships across climates and evolutionary subdivisions. In line with previous findings, we hypothesize that tree stems with large RAP fractions also have high NSC content and that RP fractions play a greater role in NSC storage than AP fractions; RAP fractions and NSC content increase with increasing wood density but are smaller in taller trees; RAP fractions, NSC content and wood density all increase with mean annual temperature, but decrease with mean annual precipitation.

In **Chapter 3**, we investigated the design of the xylem space in stems and coarse roots of 60 tree species from temperate, Mediterranean and tropical climates, and examined how RAP patterns affected NSC content of these organs. We asked if the design of the xylem space coordinates the trade-offs between structure and function in stems and roots, and if this coordination is linked to climate, and expect that any variance in xylem patterns is affected by evolutionary history, but that evolutionary history itself would not change the fundamental trade-off between xylem structure and function. If the design of the xylem space depends on climate and organ function, are patterns of apotracheal and paratracheal AP linked to porosity that change between the stem and the root? As the hydraulic function is largely assured by the new vessels formed in the earlywood of temperate/Mediterranean ring-porous species, we

hypothesize that apotracheal AP exists in greater quantities in the stems of ring-porous species in temperate climates, and paratracheal AP is more abundant in diffuse porous xylem, including in roots that are usually diffuse porous with large vessels. We also expect that xylem with large vessels and increased hydraulic conductivity has reduced density and increased NSC content that maintains osmoregulation and assists the filling of embolized vessels, especially in Mediterranean regions that undergo long dry periods.

In **Chapter 4**, we explored the coordination of functional traits along with plant economics spectrum linking leaf habit by measuring suites of similar traits representing leaf, stem and root across 90 angiosperm species from temperate, Mediterranean and tropical forests. We sought to answer the following questions: Whether NSC content in leaf, stem and root coordinated with functional traits associated with acquisitive and conservative resource strategies? We hypothesized that leaf NSC content would coordinate with functional economics traits, while stem and root NSC content would be independent of acquisitive and conservative resource strategy spectrum. Whether leaf, stem and root traits covaried and integrated along with plant economics spectrum? We hypothesized that leaf, stem and root traits would be correlated towards a whole plant economic spectrum. Whether the plant economics spectrum is structured by climate zones and leaf habits? We hypothesized that plant economics spectrum is influenced by climate zones and deciduous species would perform acquisitive resource strategy, whereas evergreen species would exhibit conservative resource strategy in large-scale and cross-regional tree species.

In **Chapter 5**, we summarize key findings in the thesis and discuss the consistence and differentiation with other studies. We also provided some study perspectives for the future.

FIGURES

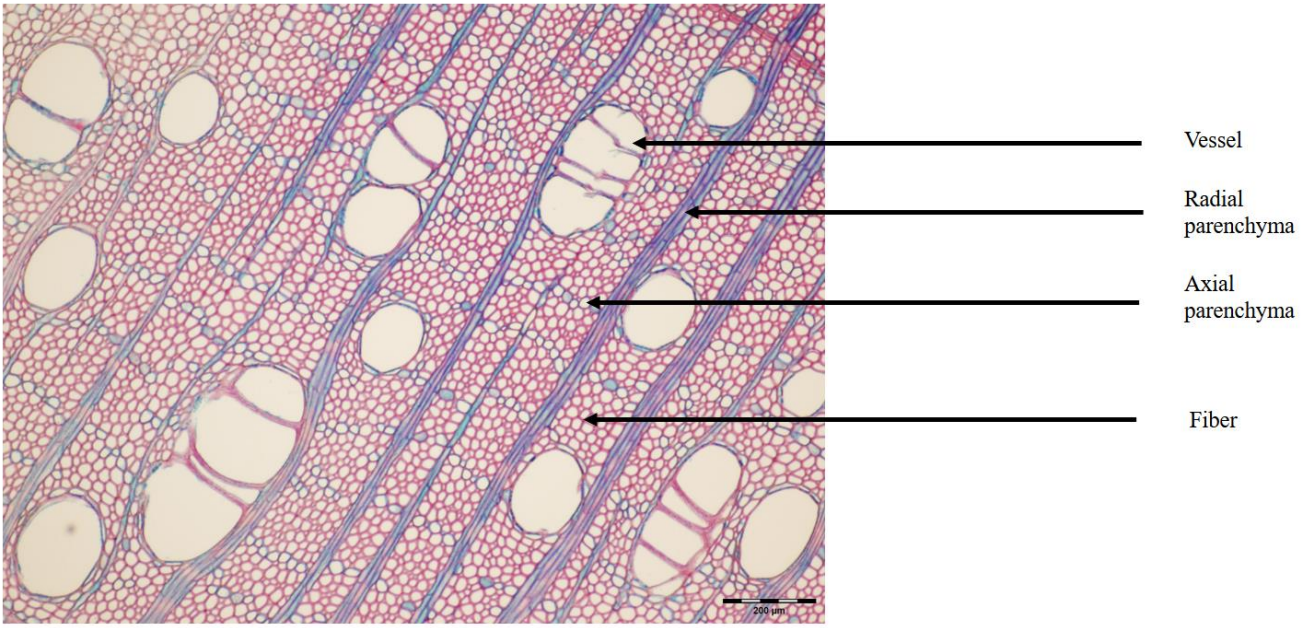

Fig. 1.1 Light micrographs of transverse sections of *Juglans nigra* with illustration of wood tissues.

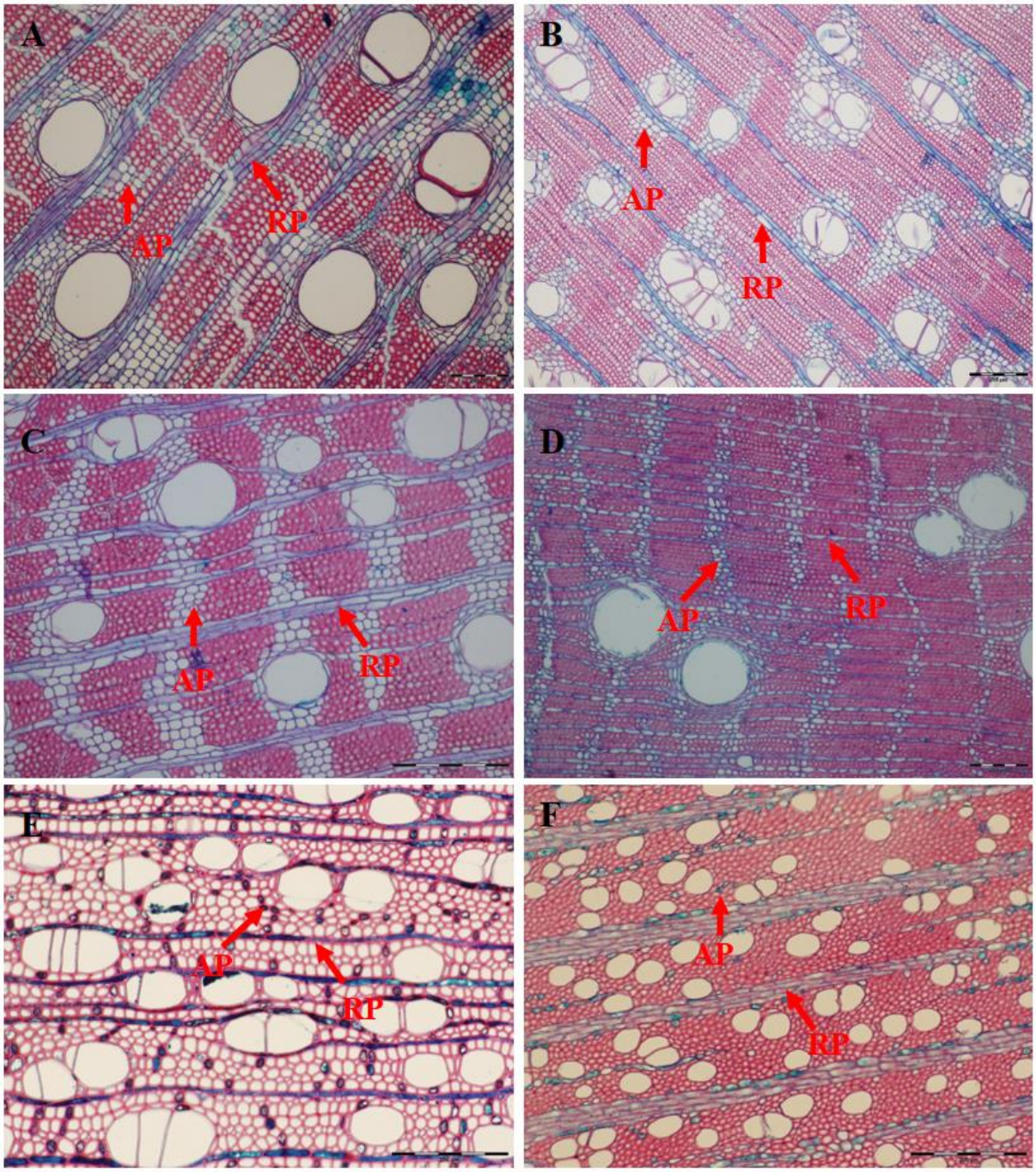

Fig. 1.2 Light micrographs of transverse sections of stem wood with different parenchyma distribution, showing a gradient from high to low fraction. (A) *Cecropia obtusa*, (B) *Qualea rosea*, (C) *Symphonia globulifera*, (D) *Parinari campestris*, (E) *Alnus glutinosa*, and (F) *Prunus spinosa*. AP is axial parenchyma; RP is radial parenchyma.

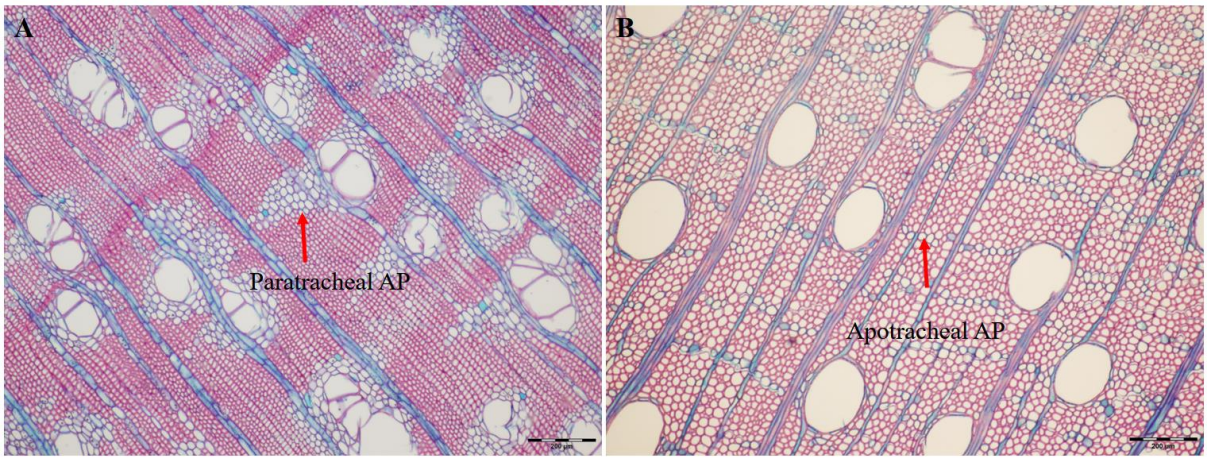

Fig. 1.3 Light micrographs of transverse sections of two species with different axial parenchyma (AP) arrangements: (A) *Qualea rosea* with paratracheal AP and (B) *Juglans nigra* with apotracheal AP.

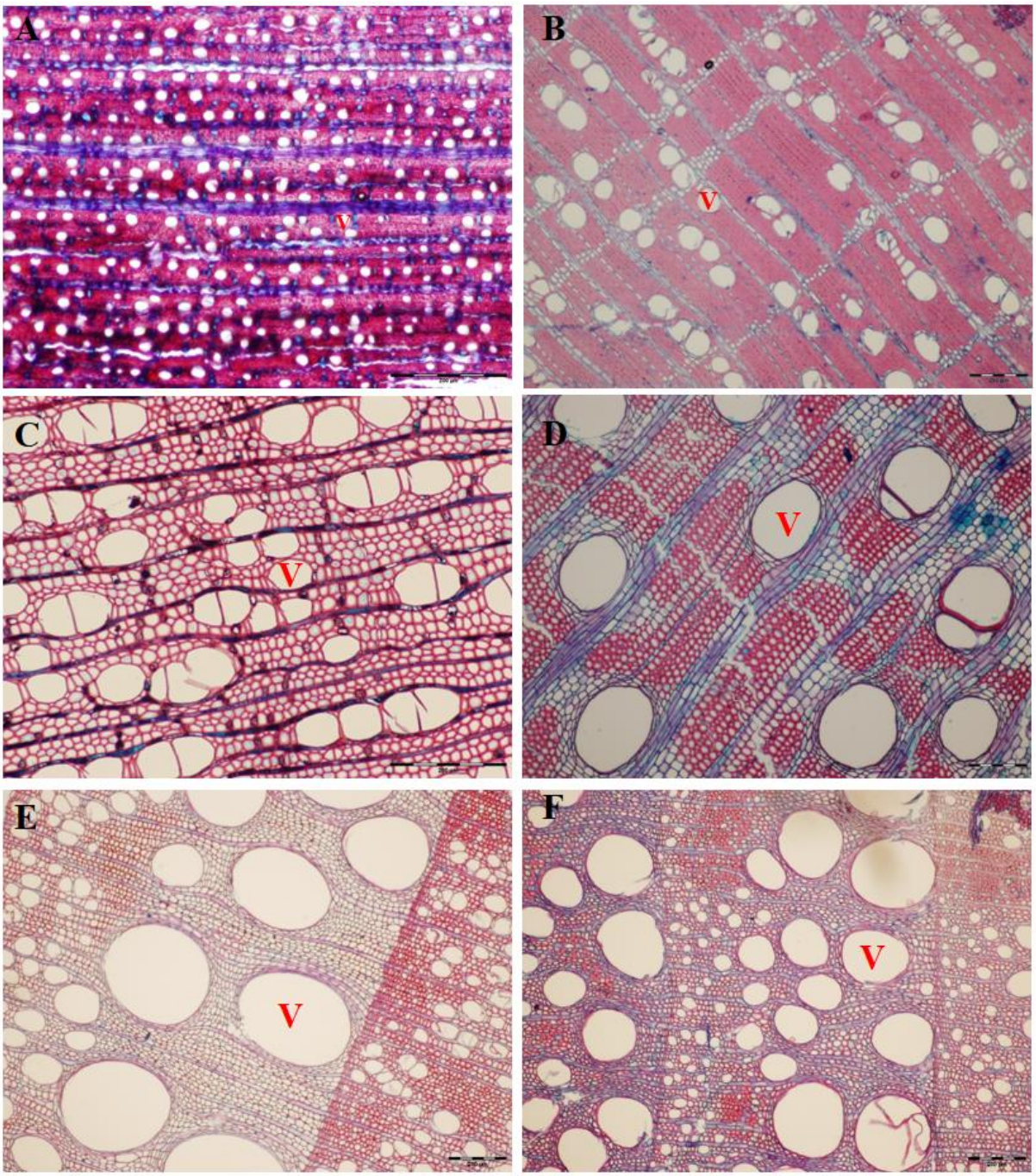

Fig. 1.4 Light micrographs of transverse sections of stem wood with different vessel distribution, showing a gradient from small to big size. (A) *Buxus sempervirens*, (B) *Pogonophora schomburgkiana*, (C) *Alnus glutinosa*, (D) *Cecropia obtusa*, (E) *Castanea sativa*, and (F) *Quercus petraea*. V is vessel.

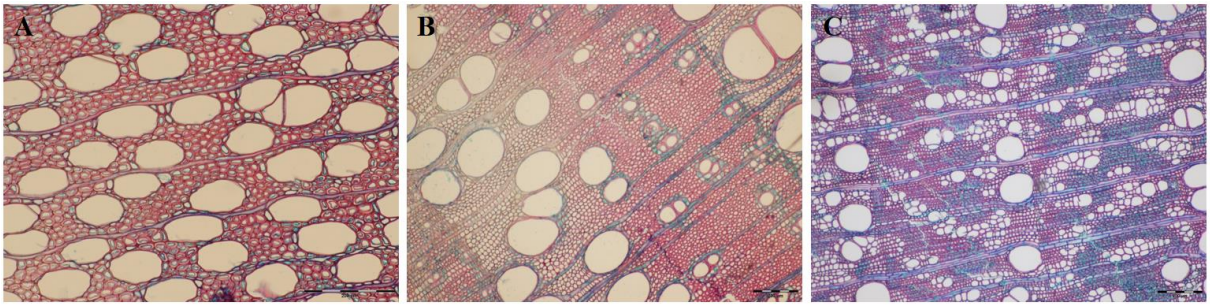

Fig. 1.5 Light micrographs of transverse sections of three species with different vessel distributions: (A) *Salix alba* with diffuse-porous vessel distribution, (B) *Fraxinus excelsior* with ring-porous vessel distribution and (C) *Pistacia terebinthus* with semi-ring-porous vessel distribution.

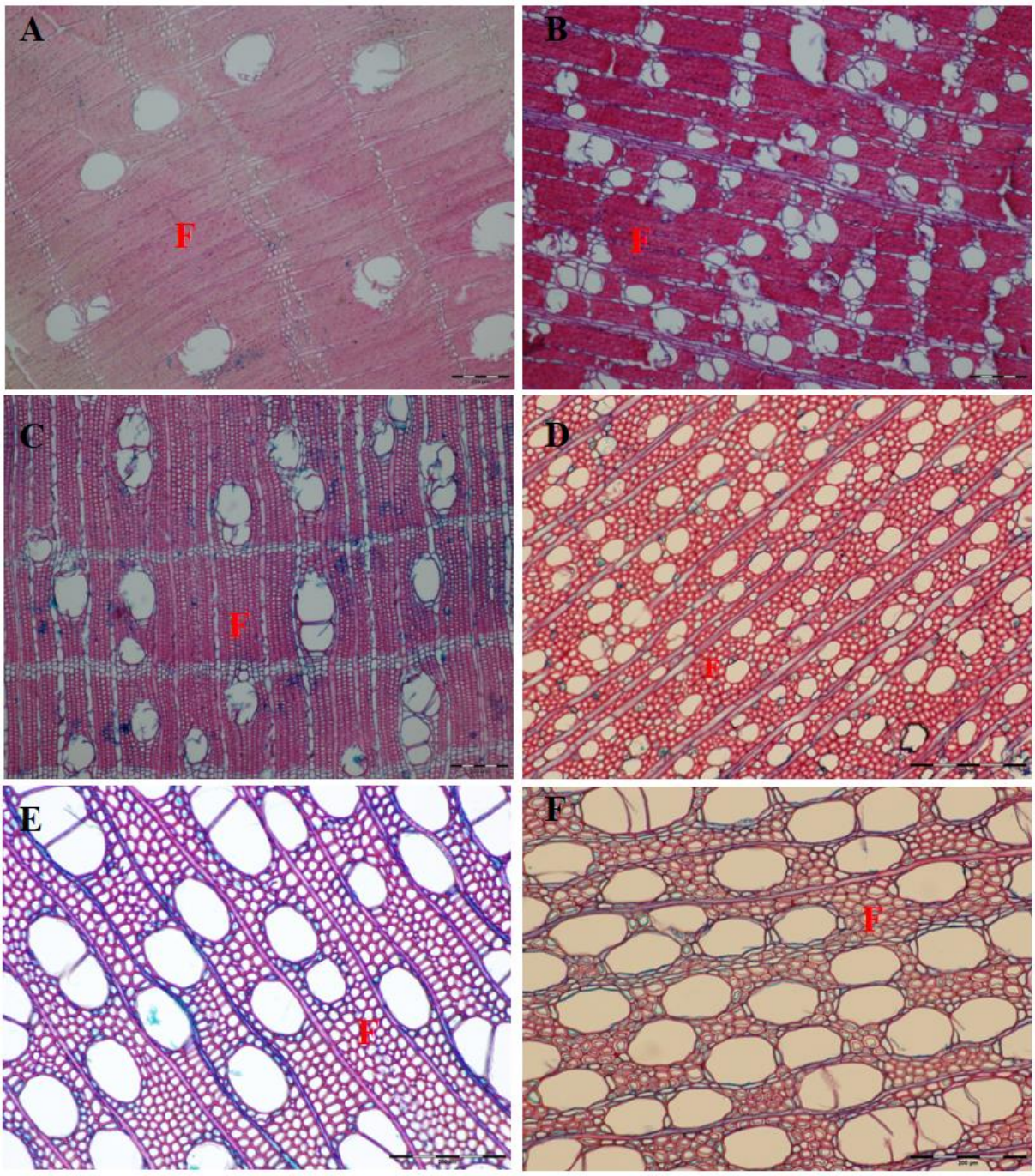

Fig. 1.6 Light micrographs of transverse sections of stem wood with different fiber distribution, showing a gradient from high to low density. (A) *Bocoa prouacensis*, (B) *Tapura capitulifera*, (C) *Iryanthera hostmannii*, (D) *Pyrus communis*, (E) *Populus alba*, and (F) *Salix alba*. F is fiber.

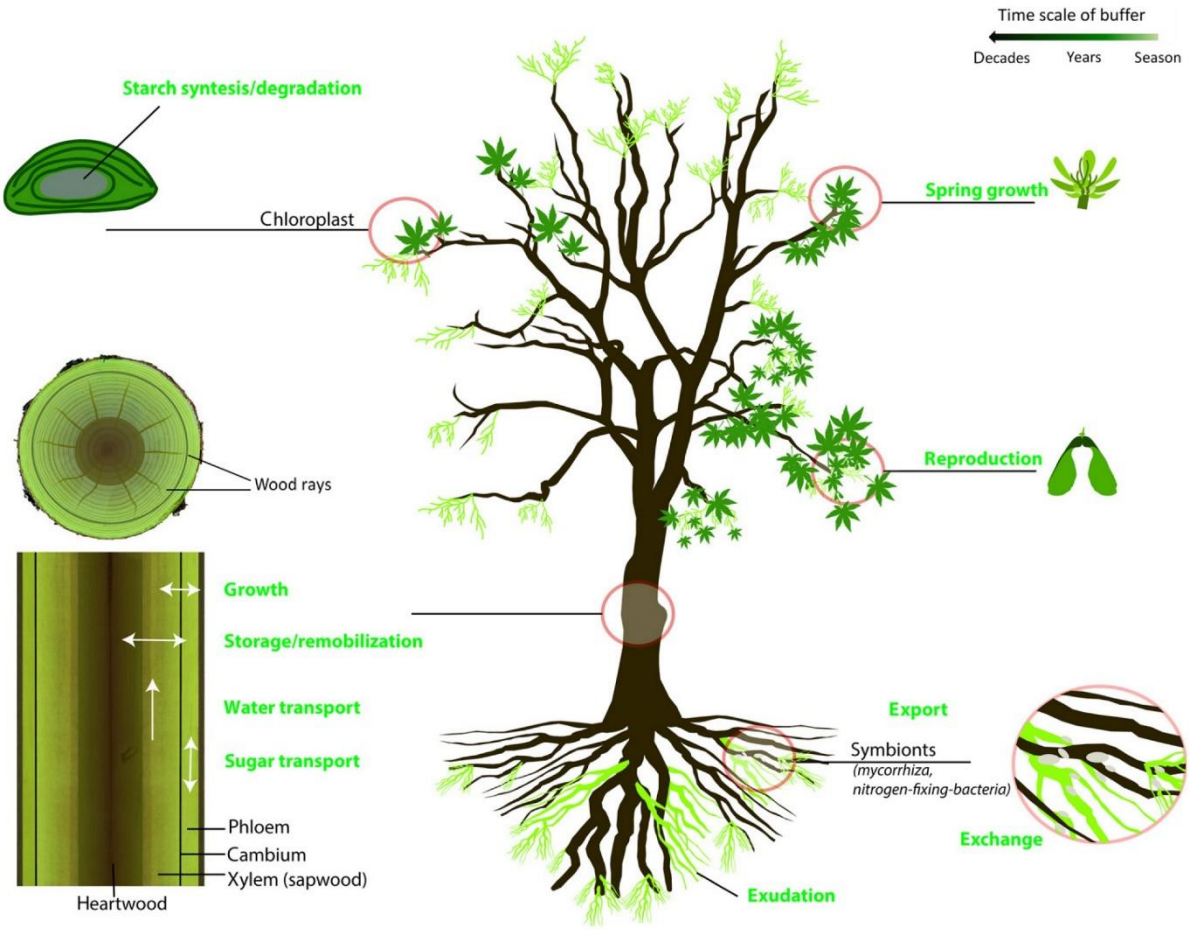

Fig. 1.7 Non-structural carbohydrates storage sites within the tree body with temporal scales and its functional roles. This figure was extracted from Hartmann and Trumbore (2016).

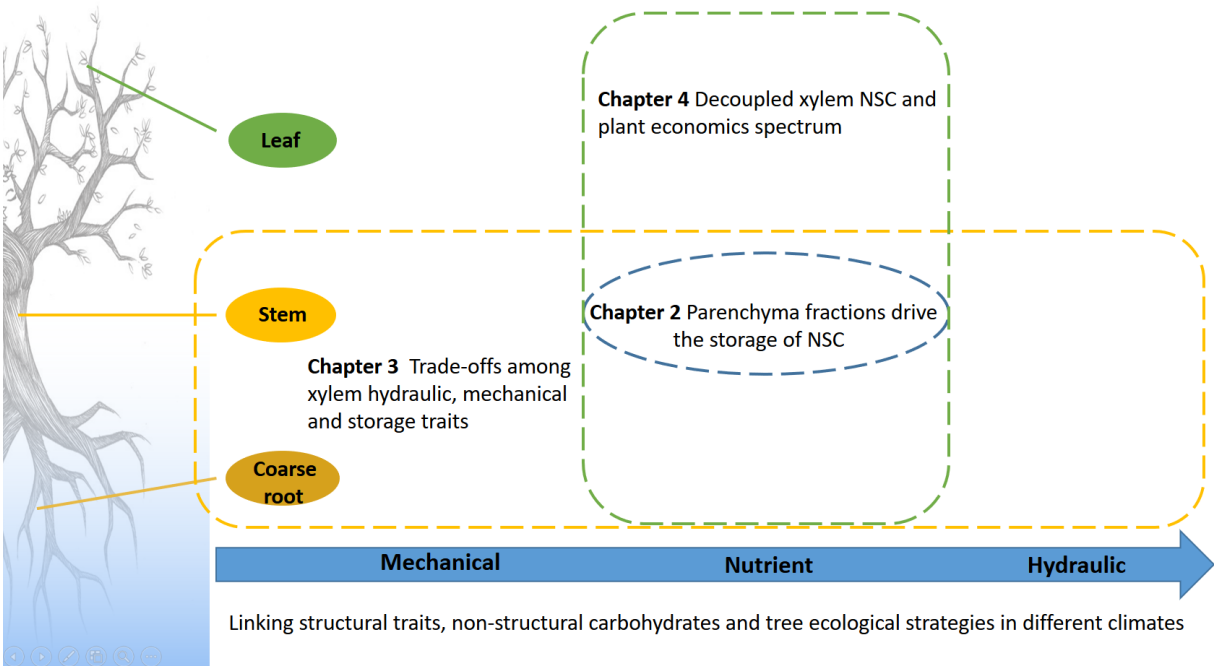

Fig. 1.8 Conceptual scheme of the thesis with three chapters.

CHAPTER 2: Parenchyma fractions drive the storage capacity of non-structural carbohydrates across a broad range of tree species

Guangqi Zhang[1*], Zhun Mao[1], Claire Fortunel[1], Jordi Martínez-Vilalta[2,3], Gaëlle Viennois[1], Pascale Maillard[4], Alexia Stokes[1]

1 AMAP, Univ Montpellier, CIRAD, CNRS, INRAE, IRD, 34000 Montpellier, France
2 CREAF, E08193 Bellaterra (Cerdanyola del Vallès), Catalonia, Spain
3 Universitat Autònoma Barcelona, E08193 Bellaterra (Cerdanyola del Vallès), Catalonia, Spain
4 SILVA, INRAE, Université de Lorraine, Agroparistech, Centre de Recherche Grand-Est Nancy, 54280 Champenoux, France
*Corresponding author: zh.guangqi@gmail.com

Published in *American Journal of Botany*, https://doi.org/10.1002/ajb2.1838

ABSTRACT

Premise: Nonstructural carbohydrates (NSCs) play a key role in tree performance and functioning and are stored in radial and axial parenchyma (RAP) cells. Whether this relationship is altered among species and climates or is linked to functional traits describing xylem structure (wood density) and tree stature is not known.

Methods: In a systematic review, we collated data for NSC content and the proportion of RAP in stems for 68 tree species. To examine the relationships of NSCs and RAP with climatic factors and other functional traits, we also collected climatic data at each tree's location, as well as wood density and maximum height. A phylogenetic tree was constructed to examine the influence of species' evolutionary relationships on the associations among NSCs, RAP, and functional traits.

Results: Across all 68 tree species, NSCs were positively correlated with RAP and mean annual temperature, but relationships were only weakly significant in temperate species and angiosperms. When separating RAP into radial parenchyma (RP) and axial parenchyma (AP),

both NSCs and wood density were positively correlated with RP but not with AP. Wood in taller trees was less dense and had lower RAP than in shorter trees, but height was not related to NSCs.

Conclusions: In trees, NSCs are stored mostly in the RP fraction, which has a larger surface area in warmer climates. Additionally, NSCs were only weakly linked to wood density and tree height. Our analysis of evolutionary relationships demonstrated that RAP fractions and NSC content were always closely related across all 68 tree species, suggesting that RAP can act as a reliable proxy for potential NSC storage capacity in tree stems.

Key words: climates, non-structural carbohydrates, radial and axial parenchyma, storage, wood density

2.1 INTRODUCTION

Nonstructural carbohydrates (NSCs) are essential substrates for metabolic processes such as maintenance respiration, osmoregulation, growth, and defense (Kozlowski, 1992; Morin *et al*., 2007; Sala *et al*., 2012). The dynamics of NSCs are considered as indicators of carbon source–sink balance in trees (Körner, 2003; Mei *et al*., 2015) and have major consequences for downstream processes such as mycorrhizal activity (Schiestl-Aalto *et al*., 2019). Generally, carbon fixed during photosynthesis is transported as NSCs, which mainly comprise soluble sugars and starch (Hoch *et al*., 2003). Soluble sugars are mostly involved in transport and various immediate functions, while starch is stored in different plant organs for future remobilization, allowing trees to maintain functionality when carbon demand is higher than supply (e.g., under severe drought stress) (Anderegg and Anderegg, 2013; Wiley *et al*., 2013; Klein and Hoch, 2015; Furze *et al*., 2019). Drought-related tree mortality has been linked to NSC starvation (McDowell *et al*., 2008; Galiano *et al*., 2011; Chuste *et al*., 2020), although evidence points to hydraulic failure as the main trigger of mortality (Rowland *et al*., 2015;

Adams *et al*., 2017). Nonstructural carbohydrates also play an important role in drought resistance as sources of solutes for osmoregulation and turgor maintenance (O'Brien *et al*., 2014; Sapes *et al*., 2019, 2021). Therefore, an understanding of potential factors that can affect the size of the NSC storage pool is essential for better evaluating the role of NSC in tree physiological processes, especially across a broad range of species and climates.

Nonstructural carbohydrates are stored in vegetative tissues in the form of soluble sugars and starch and, besides in storage organs such as rhizomes and stolons, are usually most abundant in actively growing tissues such as leaves, fine roots, and sapwood (Hartmann and Trumbore, 2016; Ramírez *et al*., 2018; Wang *et al*., 2018a). Within the sapwood, NSCs are mostly stored in radial and axial parenchyma (RAP) cells (Spicer, 2014; Plavcová and Jansen, 2016). Stem parenchyma cells are produced by ray and fusiform initials of the vascular cambium, which develop into radial parenchyma (RP) and axial parenchyma (AP) strands, respectively (Carlquist, 2001; Morris *et al*., 2016). The RAP fractions play a key role in defense against pathogenic fungi, as both RP and AP can accumulate antimicrobial compounds such as suberin (Biggs, 1987; Morris *et al*., 2016). The RP and AP can also have different functions. For example, the tensile strength of individual xylem rays was found to be three times higher than the radial strength of all xylem cells in *Fagus sylvatica* (Burgert and Eckstein, 2001), suggesting the importance of RP for tree mechanical integrity (Zheng and Martinez-Cabrera, 2013). Although total RAP proportion was not correlated with hydraulic properties (Jacobsen *et al*., 2007; Pratt *et al*., 2007; Poorter *et al*., 2010a; Fortunel *et al*., 2014), the amount of AP was positively correlated with hydraulic capacitance in tropical species that had higher AP fractions around wide vessels (Morris *et al*., 2018a; Aritsara *et al*., 2021).

Parenchyma fractions might act as a proxy for NSC storage capacity, and recent studies showed positive correlations between RAP and NSC content in woody stems and branches

(Plavcová *et al*., 2016; Godfrey *et al*., 2020; Chen *et al*., 2020; Kawai *et al*., 2021; Pratt *et al*., 2021b). Although, these studies focused on a limited number of species, data suggest that the roles of RP and AP are distinct among species and climates. For example, Chen *et al*. (2020) found that NSC content was related to RAP and AP, but not RP in 19 temperate broadleaf tree species, while Kawai *et al*. (2021) showed both AP and RP were associated with NSC content in the branches of 15 subtropical woody species. In addition, Plavcová *et al*. (2016) found significantly lower NSC content but higher RAP volume in juvenile stems of four tropical species compared to 12 temperate species. Nevertheless, it remains unclear to what extent relationships would hold for a broad diversity of tree species and across biomes. Field measurements provide useful data, but due to the seasonality in NSC fluxes, large-scale studies are difficult to perform because repeated sampling must be performed throughout the year (Martínez-Vilalta *et al*., 2016). A systematic review of available data with multiple seasonal sampling points can therefore provide an alternative perspective and complementary evidence to validate the relationship between NSCs and RAP in tree stems across species and climates.

Along with vessels and fibers, RAP is a key component of wood structure and partially determines wood density (Ziemińska *et al*., 2013; Fortunel *et al*., 2014; Osazuwa-Peters *et al*., 2017). Martínez-Cabrera *et al*. (2009) showed that RP surface area decreased with increasing wood density in shrubs. Conversely, other studies on trees have shown that there is a positive correlation between wood density and xylem ray volume (Taylor, 1969; Rahman *et al*., 2005), although this result may be biased by the proportion of lignified cell wall present. In addition, the distribution patterns of RAP cells within xylem and the variation in ray geometry can also play an important role in wood mechanical properties (Fujiwara, 1992; Ziemińska *et al*., 2015). Wood density can be linked to different ecological functions (Chave *et al*., 2009; Fortunel *et al*., 2014), including growth, life span, stem respiration, and successional status

(Enquist *et al*., 1999; Roderick, 2000; Muller-Landau, 2004; Larjavaara and Muller-Landau, 2010; Martínez-Vilalta *et al*., 2010), that may also be affected by NSC availability (Körner, 2003; Hartmann and Trumbore, 2016). In particular, wood density tends to be inversely related to growth rate as a greater investment in mass per unit of wood volume slows down volumetric growth (Enquist *et al*., 1999; Poorter *et al*., 2008; Martínez-Vilalta *et al*., 2010; Fortunel *et al*., 2016; Rüger *et al*., 2018). Additionally, the relationships among wood density, RAP, and NSCs are regulated by trade-offs that affect growth rate and ultimately tree height. Taller trees tend to have stiffer stems (Jagels *et al*., 2018), less-dense wood (Díaz *et al*., 2016), and wider vessels (Morris *et al*., 2018a). However, we are still lacking a general consensus on the link between NSCs, RAP, wood density, and maximum tree size across a broad diversity of species.

Species from different climatic backgrounds can have specific functional strategies that reflect differences in resource allocation and use (Wright *et al*., 2005; Violle *et al*., 2007; Yu *et al*., 2020). For example, in North and South America, both mean wood density and tree height increased with increasing mean annual temperature (MAT), but wood density increased as the sum of annual precipitation decreased (Šímová *et al*., 2018). Morris *et al*. (2016) also found there was a strong and positive correlation between RAP and MAT, albeit nonlinear, whereas the relationship between RAP and mean annual precipitation (MAP) was weakly negative.

Evolutionary subdivisions such as angiosperms and gymnosperms may drive functional strategies (Carnicer *et al*., 2013; Piper *et al*., 2019). Herrera-Ramírez *et al*. (2020), who studied one angiosperm and two gymnosperm species, found that NSC age and transit time differed between groups, with older NSCs occurring in stems of angiosperm species. Generally, deciduous species have higher levels of NSCs than in evergreen species because deciduous species have greater asynchrony between supply and demand (Chapin *et al*., 1990;

He *et al*., 2020; Jiang *et al*., 2021), so seasonal fluctuations of NSCs are assumed to be greater in deciduous than in evergreen species because of leaf-fall (Piispanen and Saranpää, 2001; Schädel et al., 2009; Martínez-Vilalta *et al*., 2016).

Phylogenetic relationships between species can also be leveraged to evaluate the evolutionary drivers of functional strategies (Cadotte *et al*., 2008; Gravel *et al*., 2012; Schweiger *et al*., 2018). Previous studies found a strong signal of evolutionary history in the relationships between wood density and anatomical traits (Chave *et al*., 2006; Swenson and Enquist, 2007; Zanne *et al*., 2010; Baraloto *et al*., 2012; Gleason *et al*., 2012; Poorter *et al*., 2012; Fortunel *et al*., 2014). However, empirical evidence is not always consistent (Hoch *et al*., 2003; Richardson *et al*., 2013a), suggesting that we need more data to understand the contrast between angiosperms and gymnosperms as well as between deciduous and evergreen species. By analyzing NSCs, RAP, and wood density across species and climates, we can further clarify the contribution of climate and evolutionary factors.

Here we compiled a database of NSC content, RAP fractions, wood density, and maximum tree height for 68 tree species that span a wide spectrum of characteristics, to provide a new outlook and further insight on their relationships across climates and evolutionary subdivisions. In line with previous findings, we hypothesized that (1) tree stems with large RAP fractions also have high NSC content and that RP fractions play a greater role in NSC storage than AP fractions; (2) RAP fractions and NSC content increase with increasing wood density but are smaller in taller trees; (3) RAP fractions, NSC content, and wood density all increase with warmer MAT, but decrease with increasing MAP.

2.2 MATERIALS AND METHODS

2.2.1 Description of the data set

We combined available NSC and RAP data from specialized databases and a literature survey. We focused on data from tree stems only. Firstly, data on radial parenchyma (RP), axial parenchyma (AP) and RAP for a total of 1439 tree species were taken from the global wood parenchyma database (Morris *et al*., 2016) and Zheng and Martinez-Cabrera (2013) via the TRY Plant Trait Database (https://www.try-db.org/TryWeb/Home.php; Kattge *et al*., 2011). Data on NSCs for 177 tree species were taken from a global NSC database (https://doi.org/10.5061/dryad.j6r5k; Martínez-Vilalta *et al*., 2016). When a tree species in the original database had multiple values, we calculated the mean. A comparison of the global wood parenchyma and NSC databases showed that 39 tree species had both NSC and RAP data. Secondly, according to the selection criteria of Martínez-Vilalta *et al*. (2016), we used the terms "NSC" or "nonstructural carbohydrates" in Google Scholar to search for peer-reviewed scientific papers that were published after the year 2015 (i.e., were not included in the database developed by Martínez-Vilalta *et al*., 2016), and that reported NSC content (Appendix S2.1). We found NSC data for another 18 tree species that were also included in the global wood parenchyma database. NSC data were obtained from tables or extracted from figures using Engauge Digitizer 4.1 (Mitchell *et al*., 2022). In addition, we also searched the xylem collection at CIRAD (Montpellier, France) that comprises microscope slides (tangential, transversal and radial sections of stem wood). In the CIRAD xylem collection, we found 11 tree species for which NSC data also existed in the global NSC database. Three microphotographs of transversal sections for each species were taken with an APO x5 lens using a digital camera (EOS 500D; Canon, Tokyo, Japan) mounted on a light microscope (BX 60F; Olympus, Tokyo, Japan). Parenchyma areas were manually colored in Photoshop

(Adobe, San Jose, CA, USA) and the proportions of RAP (the total surface area of parenchyma divided by xylem surface area, %) for each species were quantified using ImageJ 1.52 software (National Institutes of Health, Bethesda, MD, USA). An example of an image is shown in Appendix S2.2.

In most studies, NSC content was expressed as milligrams per gram dry mass; any NSC values in other units were converted to milligrams per gram for comparison. All RAP units were expressed as percentages. The database of NSC and RAP contained data for 68 tree species (Appendix S2.3), and only species' averages were used. Because NSC data were collected in different months, we collated the mean and maximum of NSC values and recorded them as NSC_{mean} and NSC_{max}, respectively. NSC_{mean} represents the average state of the NSC during the year and thus balances the influence of seasonal variation. NSC_{max} is the maximum content of NSC throughout the year. In addition to NSC (n = 65) and RAP (n = 60) values, data for mean values of soluble sugars (n = 58), mean values of starch (n = 62), AP (n = 39), and RP (n = 64) were also included in this database. All species' names were checked against standard taxonomic nomenclature. Based on tree evolutionary subdivision, tree species were divided into angiosperms (n = 49) and gymnosperms (n = 19). We also divided tree species into deciduous species (n = 27) and evergreen species (n = 41) according to leaf habit.

We recovered wood density data (n = 65) for the above tree species from the global wood density database (Chave *et al*., 2009; https://doi.org/10.5061/dryad.234, Zanne *et al*., 2009) and additional literature sources (Appendix S2.1), where wood density is defined as the oven-dry mass divided by green volume. We also obtained maximum tree height (H_{max}) data (n = 63) via the TRY Plant Trait Database (https://www.try-db.org/TryWeb/Home.php; Kattge et al., 2011) and additional literature sources (Appendix S2.1).

We identified the locations (latitude and longitude) from the original publications that contained the NSC data for the 68 tree species. When mean annual temperature (MAT) and mean annual precipitation (MAP) were not presented in the original articles, we used their locations to extract them from Bioclim layers based on the WorldClim Global Climate Database (Fick and Hijmans, 2017) for the period 1970–2000 using ArcMap software (version 10.5, ESRI, San Jose, California, USA). According to this geographical information, the climates where species were growing were divided into temperate (n = 41), subtropical (n = 6), and tropical (n = 21) climate.

As in any systematic review of data, there are several caveats. First, studies may differ in trait measuring protocols. Second, some species are widespread and, accordingly, NSC, RAP, and wood density data from independent studies may be sampled in different countries, continents or climates, reducing the quality of the data matching (due to intraspecific variability in traits). To limit these effects, the following criteria for data selection were applied. First, for a given trait, we considered that species included in the same published database followed the same or similar protocols, and thus are comparable by default. For data from supplementary individual papers, we checked the measuring protocol and assessed whether it was compatible with those described in the global wood parenchyma database and global NSC database cited above. Finally, for each species, we checked the sampling location and year for each of the traits. Eighteen species were found to have trait values from different continents or climates. We conducted the main statistical analyses with and without those species, and the results were not significantly different. Therefore, we present the results for all 68 species. We also analyzed the variability of RAP, NSCs, and wood density within a single species across the different locations. We calculated the coefficient of variation for %RAP, NSC_{mean}, NSC_{max}, and wood density of the same tree species from different locations (when more than three values were available). The maximum coefficient of variation for %RAP was 0.41 (for

Swietenia macrophylla King) and the minimum was 0.06 (for *Pterocarpus angolensis* DC.). Most of the coefficients of variation were less than 0.2. The maximum coefficient of variation for NSC_{mean} was 0.58 (for *Pinus sylvestris* L.) and the minimum was 0.08 [for *Picea abies* (L.) H. Karst]. The maximum coefficient of variation for NSC_{max} was 0.58 (for *Fagus sylvatica* L.), and the minimum was 0.02 (for *Carpinus betulus* L.). The maximum coefficient of variation for wood density was 0.30 [for *Leucaena leucocephala* (Lam.) de Wit], and the minimum was 0.01 (for *Baikiaea plurijuga* Harms).

2.2.2 Statistical analysis

We used one-way analysis of variance (ANOVA) followed by Tukey's honestly significant difference (HSD) post hoc test to test for differences in NSC_{mean} and NSC_{max} and a Kruskal–Wallis test to investigate differences in %RAP (1) between gymnosperms and angiosperms and (2) between climates. We ran linear regressions to examine the effects of MAT and MAP on NSC_{mean}, NSC_{max}, %RAP, wood density, and maximum tree height. To check whether the strength of relationships among NSC_{mean}, NSC_{max}, %RAP, wood density, and maximum tree height held in all species pooled and in each evolutionary subdivision and climate, we used linear models (1) with all species pooled, (2) separately for angiosperms and gymnosperms, and (3) by climatic region. We also investigated the relationships between NSC_{mean}, NSC_{max}, wood density, and %RAP using linear models for deciduous and evergreen species, respectively.

To test for multivariate correlations and bivariate relationships between NSC_{mean}, NSC_{max}, %RAP, wood density, and H_{max}, we performed (1) a principal component analysis (PCA) between wood traits (including climate as supplementary variables) and (2) Pearson correlation tests across wood traits and climate variables (MAT, MAP, and latitude). The PCA and correlation analyses were repeated using phylogenetically independent contrasts

(PICs; Felsenstein, 1985). In addition, phylogenetic generalized least squares (PGLS; Freckleton et al., 2002) were used to examine the role of species' evolutionary relationships on the associations between NSC_{mean}, NSC_{max}, %RAP, wood density, and H_{max}. To this aim, we generated a phylogenetic tree for our 68 species with Phylomatic version 3 (Webb and Donoghue, 2005) using Phylomatic tree version R20120829 as the backbone, based on the Slik *et al*. (2018) phylogenetic hypothesis. We also performed a Mantel test between correlation matrices with and without PICs to determine whether correlation patterns differ when including PICs. As correlation tests are sensitive to missing data, we removed the species for which wood trait data were missing (n = 15) when running the PCA. Some tree species were located in the southern hemisphere, therefore latitude values were negative, so we took the absolute value of the latitude value when performing PCA and Pearson analyses.

Data in text are means ± SE. All analyses were performed in R software (R Core Team, 2019) using packages APE (Paradis *et al*., 2004), caper (Orme *et al*., 2018), lmerTest (Kuznetsova *et al*., 2017), multcomp (Hothorn *et al*., 2008), and VEGAN (Dixon, 2003).

2.3 RESULTS

2.3.1 Variation in mean and maximum NSC content and parenchyma fractions across evolutionary subdivisions and climates

NSC_{mean} and NSC_{max} of tree stems for all species were 64.4 ± 5.1 mg g^{-1} and 87.9 ± 7.2 mg g^{-1}, respectively, and varied between evolutionary subdivisions and climates (Table 2.1). NSC_{mean}, NSC_{max}, soluble sugar, and starch content were greater in angiosperms than gymnosperms. NSC_{mean}, NSC_{max}, soluble sugar, and starch content were also greater in subtropical and tropical species, compared to temperate species (Table 2.1).

Mean stem %RAP for all species was 22.0 ± 1.8%, with differences in %RAP between evolutionary subdivisions and climates (Table 2.1). Stem %RAP and %RP were greater in angiosperms compared to gymnosperms. However, %AP was not significantly different between evolutionary subdivisions. In addition, stem %RAP and %AP were also greater in subtropical and tropical species compared to temperate species, respectively (Table 2.1).

NSC_{mean}, NSC_{max}, and %RAP were positively correlated with MAT (Figure 2.1A, C, E). MAP was weakly and positively correlated with NSC_{mean} and NSC_{max} but not with %RAP (Figure 2.1B, D, F). Neither wood density or maximum tree height were correlated with either MAT or MAP (Appendix S2.4).

2.3.2 Correlations between mean and maximum NSC content, parenchyma fractions, wood density and maximum tree height across evolutionary subdivisions and climates

As expected, NSC_{mean} was positively correlated with %RAP (Figure 2.2A). However, this correlation was found in angiosperms but not gymnosperms (Figure 2.2B) and only in temperate species when focusing on climatic regions (Figure 2.2C). In both deciduous and evergreen species, NSC_{mean} was positively correlated with %RAP (Appendix S5). Across all species, NSC_{mean} was positively correlated with %RP but not with %AP (Figure 2.2D, G). When analyzing separately angiosperms and gymnosperms, no relationships were found between %AP or %RP and NSC_{mean} (Figure 2.2E, H). When dividing by climate zones, NSC_{mean} was positively correlated with RP in temperate species (Figure 2.2F, I). Similar patterns were found between NSC_{max} and %RAP, %RP and %AP (Appendices S2.5, S2.6).

We found no relationship between NSC_{mean}, NSC_{max}, and wood density (Appendix S2.7), but we found a positive correlation between %RAP and wood density (Figure 2.3A). However, when evolutionary subdivisions and climates were taken into account, significant correlations between %RAP and wood density occurred in gymnosperm species (Figure 2.3B) and

temperate species (Figure 2.3C) only. Wood density was positively correlated with %RAP in both deciduous and evergreen species (Appendix S2.5). Across all species, wood density was positively correlated with %RP, but not with %AP (Figure 2.3D, G). We found the same pattern when separately analyzing angiosperm and gymnosperm species (Figure 2.3E, H). Within climate zones, %AP and %RP were correlated with wood density only in temperate species (Figure 2.3F, I).

We found that H_{max} was strongly and negatively correlated with wood density and %RAP, but not with NSC_{mean} and NSC_{max} when all species were pooled together (Appendix S2.8). When analyzing separately angiosperms and gymnosperms, only wood density was significantly correlated with H_{max} (Appendix S2.8). When data were divided by climate zones, NSC_{mean} was weakly and negatively correlated with H_{max} in temperate species (Appendix S2.8), and this relationship was largely driven by the presence of tall, coniferous and temperate species in the data set. Both NSC_{mean} and NSC_{max} were positively correlated with H_{max} in tropical species (Appendix S2.8). Wood density and %RAP were negatively correlated with H_{max} in temperate species only (Appendix S2.8). Similar patterns were found between %RP and H_{max}, while no significant correlations were found between %AP and H_{max} (Appendix S2.9).

Among the 68 species, only 53 species had complete data for NSC_{mean}, NSC_{max}, %RAP, wood density, H_{max}, MAT, MAP, and latitude. The first two PCA axes for the five plant traits explained 56.9% and 24.0% of overall trait variation, respectively (Figure 2.4A). NSC_{mean}, NSC_{max}, and %RAP loaded strongly on the first PCA axis, while wood density and H_{max} mainly contributed to the second PCA axis (with opposite signs). Pearson correlation showed that %RAP was significantly and positively correlated with NSC_{mean}, NSC_{max}, and wood density, while H_{max} was significantly and negatively correlated with %RAP and wood density (Table 2.2).

When PICs were used in trait PCA analyses, we found that there were no changes in the patterns of correlations among wood traits. The first PCA axis explained 40.6% of overall variation, mainly loading with NSC_{mean}, NSC_{max}, and %RAP and the second PCA axis explained 27.9%, through coordinated tree traits such as H_{max} and wood density (Figure 2.4B). In a Pearson correlation, when PICs were included, NSC_{max} and %RAP, wood density and H_{max} were significantly correlated, but there were no significant correlations among other traits (Table 2.2). The matrices of pairwise correlations among wood traits were similar between Pearson correlation matrices with and without PICs ($R_{Mantel} = 0.58$, $P < 0.01$). The PGLS models showed that both NSC_{mean} and NSC_{max} content and wood density were significantly correlated with %RAP, while NSC_{mean} and NSC_{max} content were not correlated with wood density (Appendix S2.10).

2.4 DISCUSSION

We found that trees with large RAP fractions also had more NSCs but only in angiosperms. In addition, we did not find more NSCs in denser wood, although the radial parenchyma (but not axial parenchyma) fraction was positively related to wood density. Taller trees had less dense wood and less RAP, but we found no significant relationships between NSCs and tree height. NSCs and RAP were more abundant in tropical species, as a result of strong positive relationships with MAT. Our analysis of evolutionary relationships demonstrated that RAP fractions and NSCs were always closely related, suggesting that RAP can act as a reliable proxy for maximum NSC storage capacity. Unless specified otherwise, as patterns for NSC_{mean} and NSC_{max} were similar, we use the generic term NSCs from here onward.

2.4.1 Relationships between NSC content and RAP fractions

In agreement with our first hypothesis, that tree stems with large RAP fractions have more NSCs, we found a positive relationship between NSCs and %RAP across 68 species and three

climate regions (Figure 2.2A). Nevertheless, variability in data was high, partially due to the combination of data originating from diverse sources and seasons (Martínez-Vilalta *et al*., 2016; Furze *et al*., 2019). Also, we found a positive relationship between NSCs and %RAP in both deciduous and evergreen species, which emphasized our first hypothesis and highlighted the storage role of parenchyma. However, we found no significant relationships between NSCs and %RAP in gymnosperms, but %RAP did diverge between angiosperms and gymnosperms, as also found by Morris *et al*. (2016). Angiosperms have a wide range of ray types and dimensions, whereas gymnosperms usually only have uni-/biseriate rays. The amount of NSCs was also greater in angiosperms than in gymnosperms, which translated into different associations between NSCs and RAP. In conifers, the proportion of axial parenchyma that constitutes secondary xylem is usually much lower than that of angiosperms (Spicer, 2014; Aritsara *et al*., 2021), although we found no significant differences. This configuration may emphasize the role of axial parenchyma in maintaining water transport in the angiosperm vessels (Spicer, 2014). Also, distinct differences in wood structure and function between angiosperms and gymnosperms could mask effects, e.g., live wood fibers in angiosperms can accumulate starch and further contribute to NSC storage (Yamada *et al*., 2011; Carlquist, 2014; Plavcová *et al*., 2016). Additionally, von Arx *et al*. (2017) explained the lack of relationships between NSCs and RAP in *Pinus sylvestris* by suggesting that radial parenchyma fractions usually indicate the maximum potential NSC storage capacity in tree stems, and not the actual NSC content at any one time.

When we examined the relationships between NSCs and radial and axial parenchyma separately, we found a positive relationship between NSCs and radial parenchyma across all species, but no relationships with axial parenchyma (Figure 2.2D, G). These results indicate that radial parenchyma plays a greater role in NSC storage than axial parenchyma. It has been suggested that axial parenchyma can influence hydraulic capacitance in angiosperms by

releasing water into vessels in periods of drought (Morris *et al*., 2018a). Additionally, vessel to axial parenchyma connectivity would facilitate xylem hydraulic optimization, suggesting that plants may need axial parenchyma to surround and service vessels (Aritsara *et al*., 2021; Ziemińska *et al*., 2020). Therefore, the physiological function of both types of parenchyma could be very different, calling for a careful consideration of xylem structure for a better understanding of tree ecological strategies.

We did not find significant relationships between NSCs and %RAP in subtropical and tropical tree species, therefore partially refuting our first hypothesis. Because our results are contradictory to the results of Kawai *et al*. (2021), who found that RAP fractions were significantly associated with NSC content in the branches of 15 subtropical woody species, our low sample size (21 species) might not fully represent the variability in NSCs and RAP encountered in these climates. Additionally, RAP performs several major functions in tropical species, such as water storage and defense against pathogens, that may be less important in temperate species (Plavcová *et al*., 2016). Also, photosynthesis and growth can continue throughout the year in the tropics (in the absence of marked dry seasons), minimizing seasonal mismatches between carbon source and sinks. Future studies adding more data from tropical and subtropical species are needed to further clarify the relationship between parenchyma fractions and NSC content.

2.4.2 Relationships among NSC, RAP, wood density and maximum height

We did not find any relationships between NSC content and wood density across species (Appendix S2.7), but we found that %RAP increased in more dense wood, partially corroborating our second hypothesis. Although wood density was positively correlated with %RAP and radial parenchyma across all species, it was not related to axial parenchyma. Because parenchyma cells are relatively thin-walled, parenchyma-rich wood may need

relatively more tracheids or fibers to contribute to mechanical strength (Martínez-Cabrera *et al*., 2009). Wood rays usually have large amounts of lignin packed among parenchyma cells, that will also increase overall wood density and stem bending strength (Burgert and Eckstein, 2001; Rana *et al*., 2009). However, in 61 shrubs from North and South America, Martínez-Cabrera *et al*. (2009) reported that radial parenchyma was negatively correlated with wood density, while axial parenchyma showed the opposite trend, suggesting that radial parenchyma may possess different roles in shrubs and trees, that have different needs in terms of mechanical strength. In addition, fibers and fiber tracheids contribute to mechanical strength in angiosperms (Ziemińska *et al*., 2013; Fortunel *et al*., 2014), while the mechanical strength in gymnosperm xylem is largely provided by tracheid cells (Patten *et al*., 2010). Apart from providing a storage function, axial parenchyma also has a role related to hydraulics. For example, Zheng and Martínez-Cabrera (2013) found axial parenchyma was directly related to conducting efficiency, and could provide extra water storage and embolism repair capacity in low density wood. Additionally, Janssen *et al*. (2020) found that axial parenchyma was not related to wood density but increased with sapwood specific hydraulic conductivity in neotropical tree species, which may be due to the role of parenchyma cells in the refilling of embolized vessels (Secchi *et al*., 2017). When dividing species by climatic zones, we found significant correlations between wood density and parenchyma fractions in temperate species only, potentially because of lower variation in wood density in temperate than tropical tree species (Swenson and Enquist, 2007).

In our study, wood density was negatively correlated with potential maximum tree height, as also found by Thomas (1996). Taller trees have wider conduits in their trunks because they have longer path lengths and therefore need wider vessels (thus reducing wood density) to maintain hydraulic conductivity and minimize the increase in hydraulic resistance (Coomes *et al*., 2008; Olson *et al*., 2021). In tropical species, NSCs were more abundant in taller trees,

although this pattern was not explained by increases in axial or ray parenchyma. Taller angiosperms usually have more axial parenchyma cells packed around vessels, reducing overall wood density, and protecting against xylem embolism through the controlled water release into vessels (Preston *et al*., 2006; Morris *et al*., 2018a). However, our angiosperm data set was limited to trees with a maximum potential height of 10–60 m, compared to 20–110 m for temperate conifers. Therefore, the smaller height range, combined with the increased diversity of cell types in angiosperms, may mask patterns of xylem variability linked to tree height.

Recent studies have emphasized the importance of including information on phylogenetic relationships between species to better understand the role of evolutionary history on trait variation (Chave *et al*., 2006; Cadotte *et al*., 2012; Fortunel *et al*., 2014; Schweiger *et al*., 2018). In our study, the only significant relationships found after accounting for species phylogenetic relationships were %RAP with NSC_{max}, and wood density with maximum potential tree height (Table 2.2). The underlying cause for these patterns may be that traits are labile, for instance, when distant relatives show convergent evolution or when close relatives show trait differentiation (Cavender-Bares *et al*., 2004; Gravel *et al*., 2012). The relationship between %RAP and NSC_{max} indicates that RAP is a reliable proxy for maximum potential NSC storage capacity, supported by phylogenetically corrected regression analyses (PGLS), showing that NSCs and wood density were always related with %RAP. Also, the matrices of pairwise correlations with and without PICs among wood traits were similar, indicating that phylogenetic relatedness did not affect the relationships among wood traits. Therefore, our results show for the first time, the close evolutionary relationship between stem parenchyma cells and NSC storage.

2.4.3 Effect of climatic factors on wood traits

In agreement with our third hypothesis, we found that NSCs and %RAP increased with warmer temperatures. The strong, positive relationships we found among latitude, NSC content, and RAP fractions reinforce the relationships that we found with MAT because there were more NSCs and RAP in tropical tree species. Our results suggest that as temperature increases, photosynthesis increases more rapidly than the combination of all carbon sinks (growth, respiration, defense), and thus, more photosynthates are stored in NSC pools, providing an important mechanism to offset rising metabolic costs (Hoch and Körner, 2009; Gough *et al*., 2010). We found that NSCs and %RAP were positively correlated with MAT, but only NSCs were positively correlated with MAP. This result is similar to that found by Moles *et al*. (2014), who demonstrated that most plant traits correlate more strongly with temperature than precipitation. Precipitation is usually interpreted as an indicator of water availability to plants, which could be affected by a suite of factors including hydrology, soil type, soil depth, and access to groundwater (Gardner, 1965). Global variation in any or all of these factors would weaken the relationship between MAP and plant traits (Moles *et al*., 2014). Although RAP and NSCs were influenced by climate, we found no significant relationships between MAT, MAP, and wood density, which is inconsistent with results from a study by Šímová *et al*. (2018). Our result indicates that other factors not considered here, such as soil fertility, stem diameter, tree age, and stand density, are more important determinants of wood density variation (Larjavaara and Muller-Landau, 2010; Nabais *et al*., 2018).

2.5 CONCLUSION

We investigated the relationships among NSCs, RAP, wood density, and potential maximum tree height, together with climatic factors, for 68 tree species. We found that NSC content was

strongly related to RAP when all species were pooled together, demonstrating that parenchyma cells are a major repository for NSCs. Wood density was positively correlated with the proportion of ray parenchyma in tree stems, but there were no significant relationships between wood density and NSCs. Tree height and wood density were negatively related overall, but NSCs were more abundant in taller, tropical species. Both NSCs and RAP increased in tropical species, reflecting the strong, positive relationship with mean annual temperature. Phylogenetic relatedness did not affect the correlation patterns among wood functional traits showing that RAP is a suitable proxy for potential NSC storage capacity in stems. Our study helps to better understand the trade-offs among xylem ecological strategies, but more data, especially from the tropics and subtropics, are required on a large scale to build a robust understanding of how different sapwood functions (including NSC storage, water transport, respiration, mechanical integrity, and resistance to pathogens) are related across species, growth forms, and climate.

Acknowledgements

This work was supported by China Scholarship Council (Ph.D. bursary for G.Z.). This work has benefited from support of a grant from Investissement d'Avenir grants of the Agence Nationale de la Recherche (CEBA: ANR-10-LABX-25-01). This study was co-financed by a French–Chinese program PHC XU GUANGQI 2019 (ref.: 43379XF). We thank Dr. P. Langbour (CIRAD, France) for access to the CIRAD Xylotech, Montpellier. We thank Prof. Y. Y. Zhang (Xiamen University, China.) for her valuable suggestions on data analysis. We are very thankful for the constructive comments by the Associated Editor and reviewers, which greatly improved this manuscript.

Author contributions

G.Z and A.S designed the study and collected data. G.Z and Z.M analyzed data. G.Z wrote the first draft of the manuscript that was further improved by inputs from all co-authors. All the authors contributed critically to the drafts and gave final approval for publication.

Data availability statement

Data used in the systematic review can be accessed at https://doi.org/10.15454/H5RLTP.

TABLES

Table 2.1 Mean values of soluble sugars, starch, NSCs, RP, AP, and RAP in tree stems in different climates and for angiosperms and gymnosperms (mean ± SE). Different lowercase letters indicate significant differences among climates; different uppercase letters indicate significant differences between evolutionary subdivisions ($P < 0.05$). NSC_{mean}, mean value of nonstructural carbohydrates over one year; NSC_{max}, maximum value of nonstructural carbohydrates in one year; AP, axial parenchyma; RP, radial parenchyma; RAP, radial and axial parenchyma; *n*, sample size. See Appendix S2.11 for statistical results of the difference analyses.

Group	**Soluble sugars**	**Starch**	**NSC_{mean}**	**NSC_{max}**	**%RP**	**%AP**	**%RAP**
Temperate	23.02±2.86 a *n* = 33	19.07±3.14 a *n* = 37	47.30±5.21 a *n* = 38	61.76±6.71 a *n* = 38	11.89±1.00 a *n* = 41	5.16±1.21 a *n* = 18	13.63±1.36 a *n* = 33
Subtropical	51.86±21.63 b *n* = 4	45.10±27.30 ab *n* = 4	85.09±20.23 b *n* = 6	104.87±18.17 ab *n* = 6	20.16±5.66 a *n* = 5	27.50±10.20 b *n* = 3	38.36±9.52 b *n* = 6
Tropical	36.25±3.77 b *n* = 21	53.66±7.80 b *n* = 21	89.37±8.42 b *n* = 21	130.34±13.52 b *n* = 21	13.48±0.94 a *n* = 18	15.47±2.10 b *n* = 18	30.57±1.92 b *n* = 21
Angiosperm	34.01±3.67 B *n* = 40	42.38±5.24 B *n* = 43	77.51±5.91 B *n* = 47	105.36±8.54 B *n* = 47	15.34±0.99 B *n* = 45	12.33±1.77 A *n* = 36	28.60±1.90 B *n* = 41
Gymnosperm	20.45±2.10 A *n* = 18	10.01±1.60 A *n* = 19	30.09±2.73 A *n* = 18	42.29±4.47 A *n* = 18	7.40±0.46 A *n* = 19	3.26±2.39 A *n* = 3	7.86±0.77 A *n* = 19
Total	29.80±2.73 *n* = 58	32.47±4.12 *n* = 62	64.38±5.07 *n* = 65	87.90±7.20 *n* = 65	12.99±0.84 *n* = 64	11.64±1.68 *n* = 39	22.04±1.82 *n* = 60

Table 2.2 Pearson correlations (ρ values) among NSC content, RAP fractions, wood density, and climatic factors in 68 species. Phylogenetic independent contrasts are not considered below the central diagonal line of the matrix, but are considered above the diagonal line. Significant effects are in bold ($P < 0.05$). Density, wood density; H_{max}, maximum tree potential height; MAP, mean annual precipitation; MAT, mean annual temperature; NSC_{mean}, mean value of nonstructural carbohydrates over 1 year; NSC_{max}, maximum value of nonstructural carbohydrates in 1 year; RAP, radial and axial parenchyma.

Component	Density	%RAP	NSC_{mean}	NSC_{max}	H_{max}	Latitude	MAT	MAP
Density	1	0.24	-0.01	0.09	**-0.33**	0.02	0.04	0.03
%RAP	**0.46**	1	0.16	**0.29**	-0.16	0.14	-0.12	0.10
NSC_{mean}	0.23	**0.63**	1	**0.90**	0.02	0.11	-0.20	0.11
NSC_{max}	0.20	**0.59**	**0.93**	1	0.04	0.16	-0.25	0.04
H_{max}	**-0.54**	**-0.47**	-0.23	-0.16	1	0.03	-0.07	-0.21
Latitude	-0.09	**-0.54**	**-0.45**	**-0.52**	0.22	1	**-0.85**	**-0.77**
MAT	0.14	**0.56**	**0.55**	**0.58**	-0.22	**-0.84**	1	**0.68**
MAP	-0.17	0.19	**0.24**	**0.37**	-0.10	**-0.56**	**0.44**	1

FIGURES

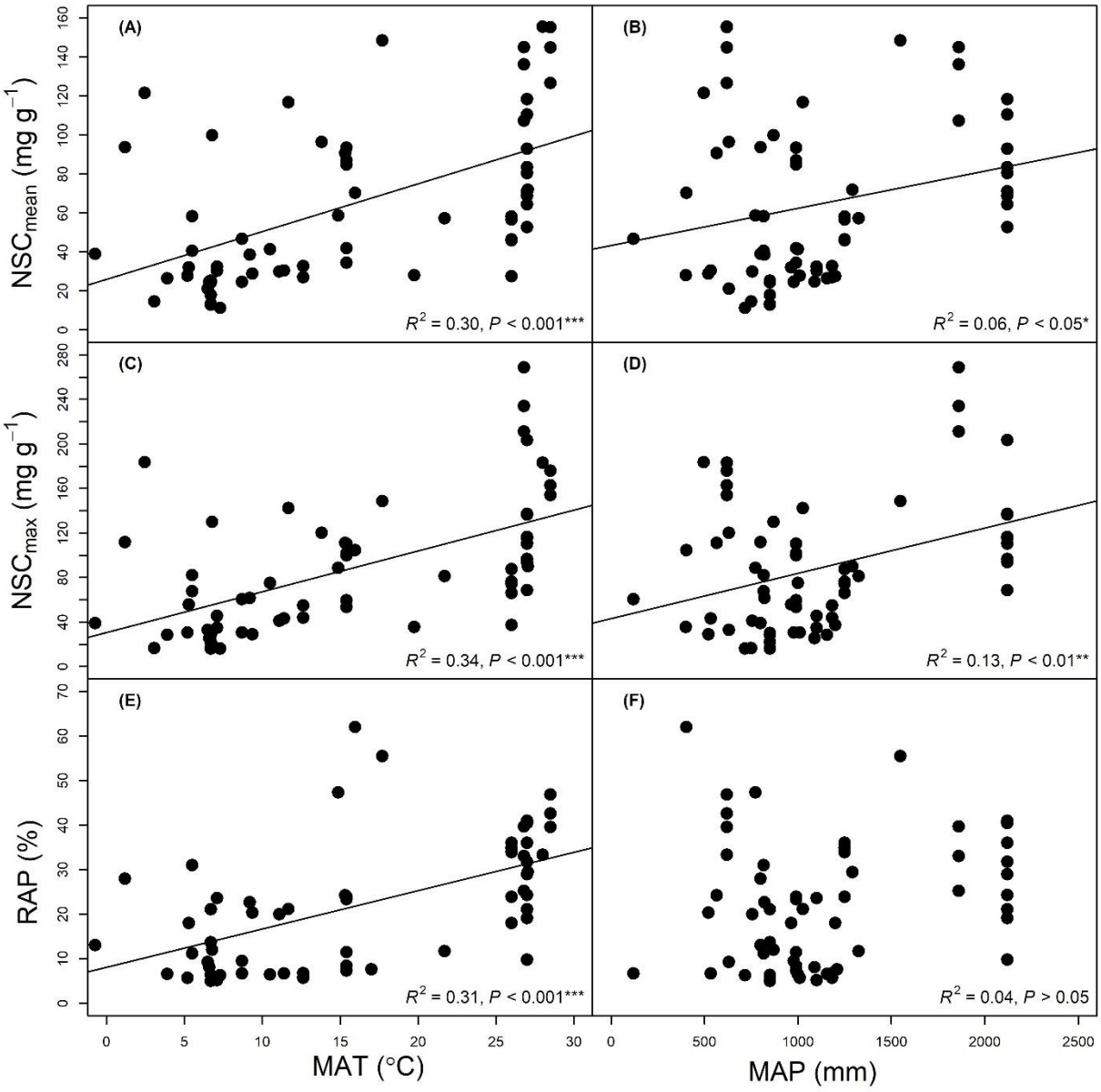

Fig. 2.1 Relationships between NSC_{mean} and (A) MAT and (B) MAP, between NSC_{max} and (C) MAT and (D) MAP, and between RAP and (E) MAT and (F) MAP. MAP, mean annual precipitation; MAT, mean annual temperature; NSC_{mean}, mean value of nonstructural carbohydrates over 1 year; NSC_{max}, maximum value of nonstructural carbohydrates in 1 year; RAP, radial and axial parenchyma.

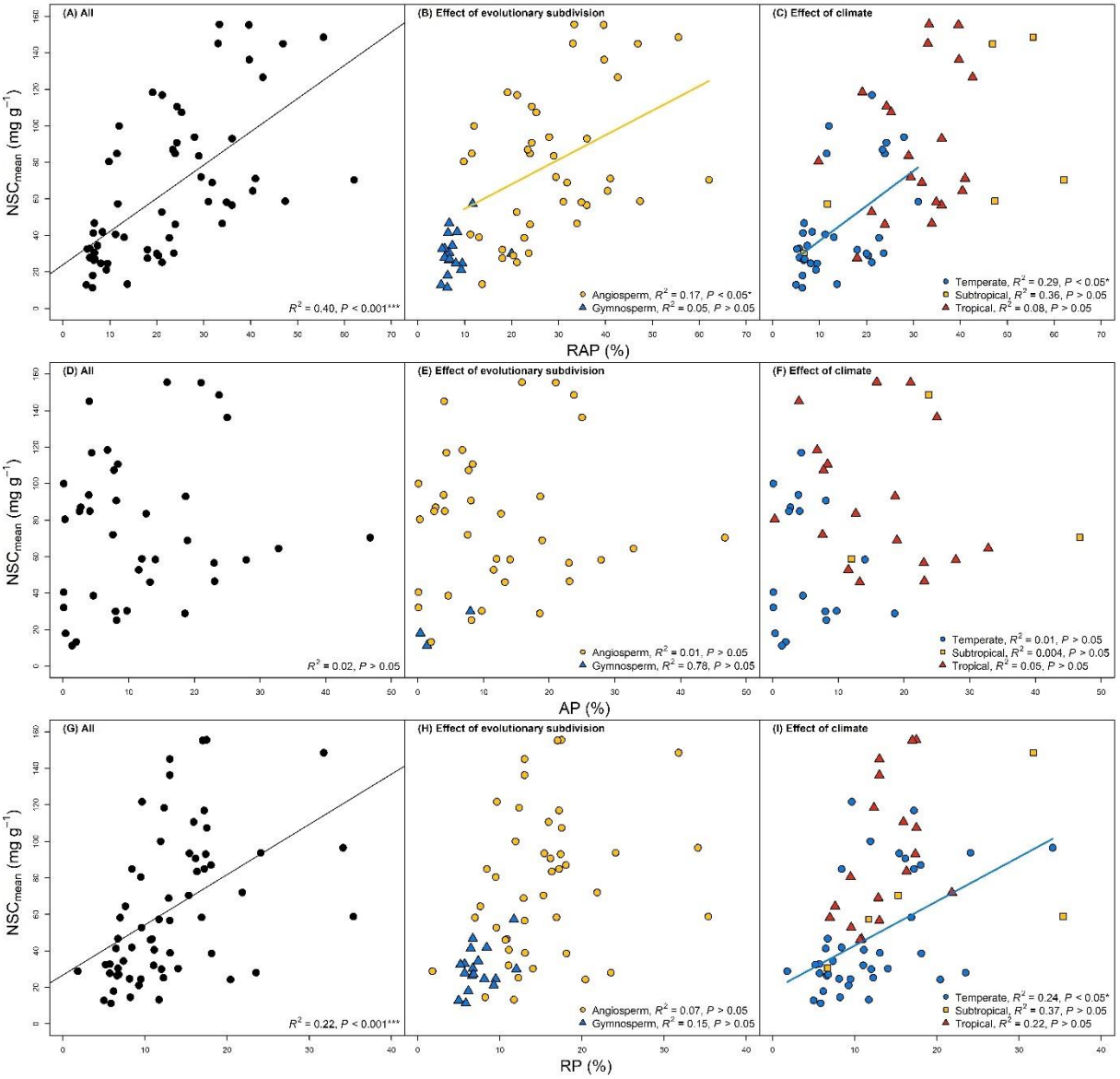

Fig. 2.2 Relationships between NSC_{mean} and (A–C) RAP, (D–F) AP, and (G–I) RP fractions with all species pooled across evolutionary subdivisions and climates. AP, axial parenchyma; NSC_{mean}, mean value of nonstructural carbohydrates over 1 year; RP, radial parenchyma; RAP, radial and axial parenchyma.

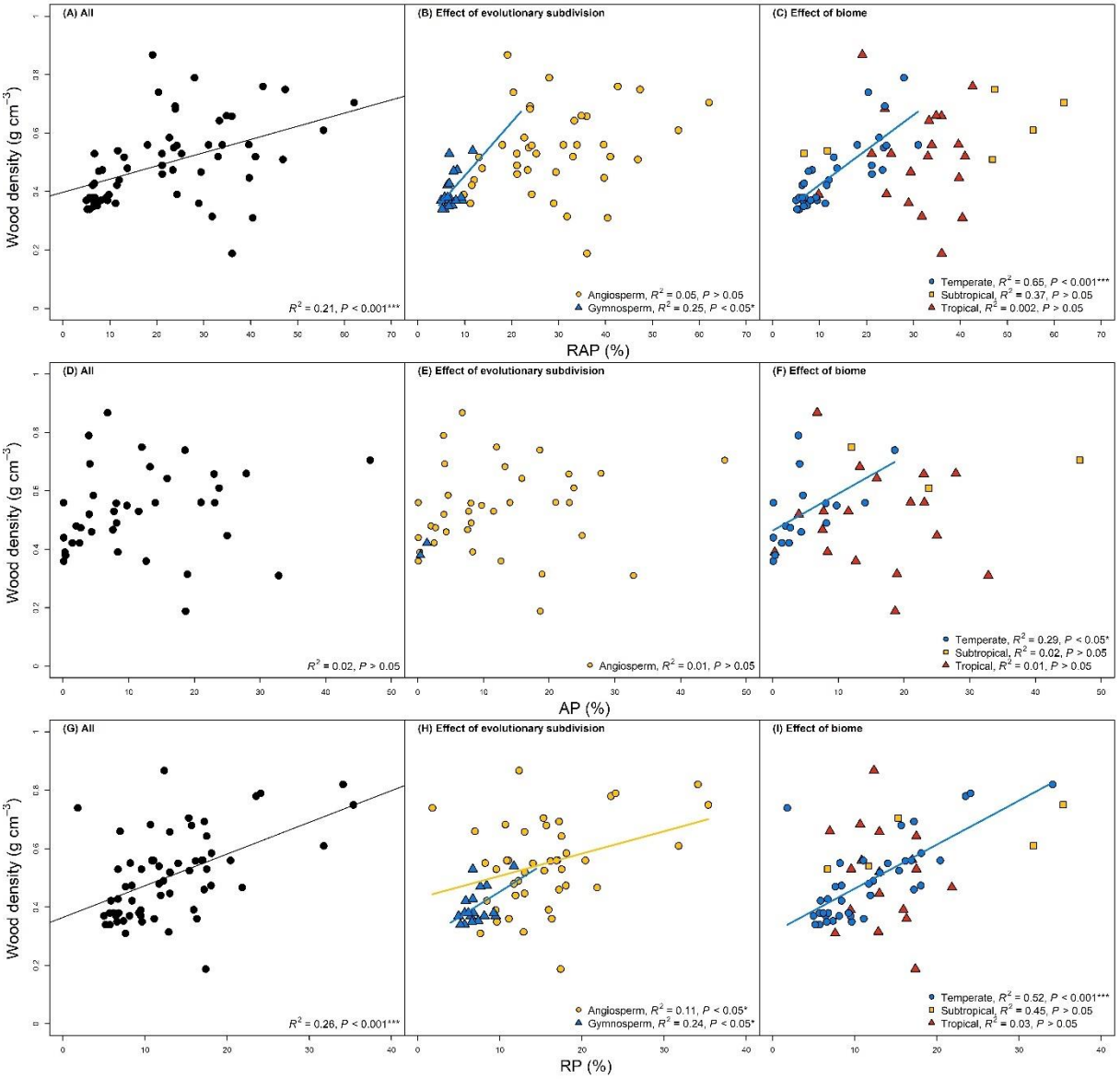

Fig. 2.3 Relationships between wood density and (A–C) RAP, (D–F) AP, and (G–I) RP fractions with all species pooled across evolutionary subdivisions and climates. AP, axial parenchyma; RP, radial parenchyma; RAP, radial and axial parenchyma.

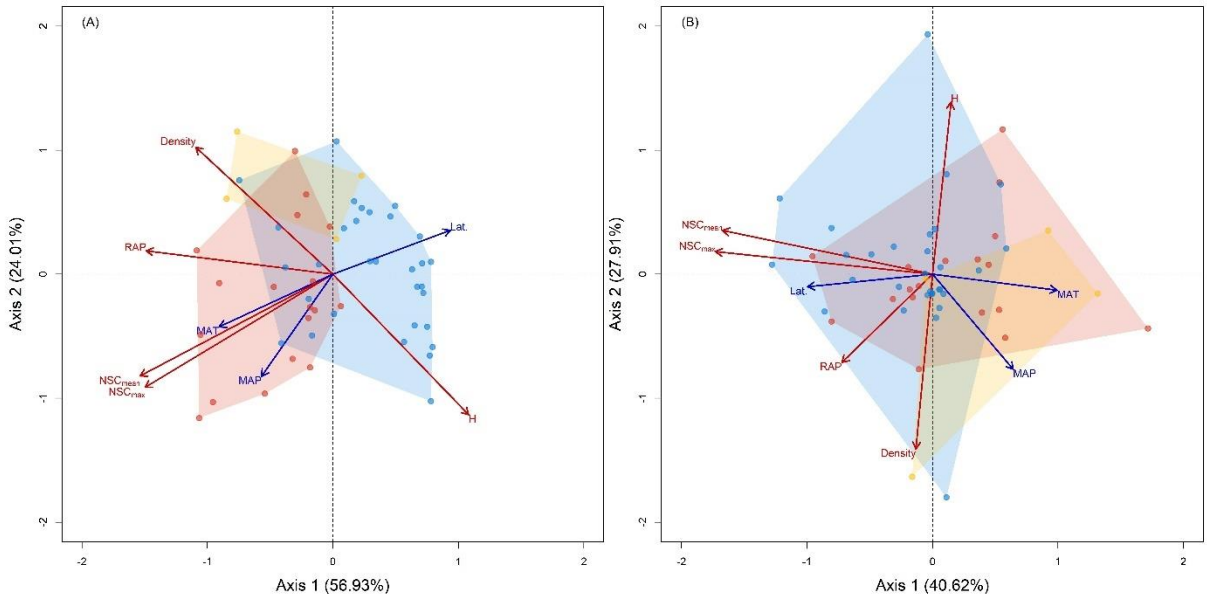

Fig. 2.4 Loadings plot of wood traits on the first two principal components axes (A) using raw data and (B) using phylogenetically independent contrasts (PICs). Mean annual temperature (MAT), mean annual precipitation (MAP), and latitude (Lat.) were added as supplementary variables without any effect on the analyses. Density, wood density; *H*, potential maximum tree height; NSC_{mean}, mean value of nonstructural carbohydrates over 1 year; NSC_{max}, maximum value of nonstructural carbohydrates in 1 year; RAP, radial and axial parenchyma. The light blue area represents temperate tree species; the yellow area represents subtropical tree species; the light red area represents tropical tree species. Blue and red arrows represent abiotic variables and wood traits, respectively.

SUPPLEMENTARY MATERIALS

Appendix S2.1 Supplementary references for extracting data which were not included in the databases.

Annighöfer P, Mölder I, Zerbe S, Kawaletz H, Terwei A, Ammer C. 2012. Biomass functions for the two alien tree species *Prunus serotina* Ehrh. and *Robinia pseudoacacia* L. in floodplain forests of Northern Italy. *European Journal of Forest Research* **131**: 1619–1635.

Bouffier LA, Gartner BL, Domec JC. 2003. Wood density and hydraulic properties of ponderosa pine from the Willamette Valley vs. the Cascade Mountains. *Wood and Fiber Science*, **35**

Cao Y, Li Y, Chen Y. 2018. Non-structural carbon, nitrogen, and phosphorus between black locust and chinese pine plantations along a precipitation gradient on the Loess Plateau, China. *Trees* **32**: 835–846.

DeSoto L, Olano JM, Rozas V. 2016. secondary growth and carbohydrate storage patterns differ between sexes in *Juniperus thurifera*. *Frontiers in Plant Science* **7**: 723.

Earles JM, Stevens JT, Sperling O, Orozco J, North MP, Zwieniecki MA. 2018. Extreme mid-winter drought weakens tree hydraulic-carbohydrate systems and slows growth. *New Phytologist* **219**: 89–97.

Eid T, Tuhus E. 2001. Models for individual tree mortality in Norway. *Forest Ecology and Management* **154**: 69–84.

Ezeibekwe IO, Okeke SE, Unamba CIN, Ohaeri JC. 2009. An investigation into the potentials of *Dactyladenia bacteri*; *Dialum guineense*; and *Anthonota macrophylia* for paper pulp production. *Report and Opinion* **1**: 18–25.

Fujii S, Kubota Y, Enoki T. 2009. Resilience of stand structure and tree species diversity in subtropical forest degraded by clear logging. *Journal of Forest Research* **14**: 373–387.

Furze ME, Huggett BA, Aubrecht DM, Stolz CD, Carbone MS, Richardson AD. 2019. Whole-tree nonstructural carbohydrate storage and seasonal dynamics in five temperate species. *New Phytologist* **221**: 1466–1477.

Godfrey JM, Riggio J, Orozco J, Guzmán-Delgado P, Chin ARO, Zwieniecki MA. 2020. Ray fractions and carbohydrate dynamics of tree species along a 2750 m elevation gradient indicate climate response, not spatial storage limitation. *New Phytologist* **225**: 2314–2330.

Hoch G, Popp M, Körner C. 2002. Altitudinal increase of mobile carbon pools in *Pinus cembra* suggests sink limitation of growth at the Swiss treeline. *Oikos* **98**: 361–374.

Liang E, Wang Y, Eckstein D, Luo T. 2011. Little change in the fir tree-line position on the southeastern Tibetan Plateau after 200 years of warming. *New Phytologist* **190**: 760–769.

Liu W, Su J, Li S, Lang X, Huang X. 2018. Non-structural carbohydrates regulated by season and species in the subtropical monsoon broad-leaved evergreen forest of Yunnan Province, China. *Scientific Reports* **8**: 1083.

Mei L, Xiong Y, Gu J, Wang Z, Guo D. 2015. Whole-tree dynamics of non-structural carbohydrate and nitrogen pools across different seasons and in response to girdling in two temperate trees. *Oecologia* **177**: 333–344.

Mirabel A, Ouédraogo DY, Beeckman H, Delvaux C, Doucet JL, Hérault B, Fayolle A. 2019. A whole-plant functional scheme predicting the early growth of tropical tree species: evidence from 15 tree species in Central Africa. *Trees* **33**: 491–505.

Nardini A, Casolo V, Borgo AD, Savi T, Stenni B, Bertoncin P, Zini L, McDowell NG. 2016. Rooting depth, water relations and non-structural carbohydrate dynamics in three woody angiosperms differentially affected by an extreme summer drought. *Plant, Cell & Environment* **39**: 618–627.

Palacio S, Camarero JJ, Maestro M, Alla AQ, Lahoz E, Montserrat-MartíG. 2018. Are storage and tree growth related? Seasonal nutrient and carbohydrate dynamics in evergreen and deciduous Mediterranean oaks. *Trees* **32**: 777–790.

Ramírez AJ. 2017. The functional role of carbohydrate reserves in the growth and survival of trees. Ph.D. dissertation, Université du Québec, Montréal Québec, Canada.

Shi P, Körner C, Hoch G. 2008. A test of the growth-limitation theory for alpine tree line formation in evergreen and deciduous taxa of the eastern Himalayas. *Functional Ecology* **22**: 213–220.

Tixier A, Guzmán-Delgado P, Sperling O, Amico Roxas A, Laca E, Zwieniecki MA. 2020. Comparison of phenological traits, growth patterns, and seasonal dynamics of non-structural carbohydrate in Mediterranean tree crop species. *Scientific Reports* **10**: 347.

Appendix S2.2 Light micrographs of transverse sections of *Gliricidia sepium* (Jacq.) Kunth ex Walp with clear axial parenchyma and radial parenchyma. (a) Original image stained with alcian blue, (b) image colored using Photoshop, the blue area is axial parenchyma, the red area is radial parenchyma. All bars, 200 μm.

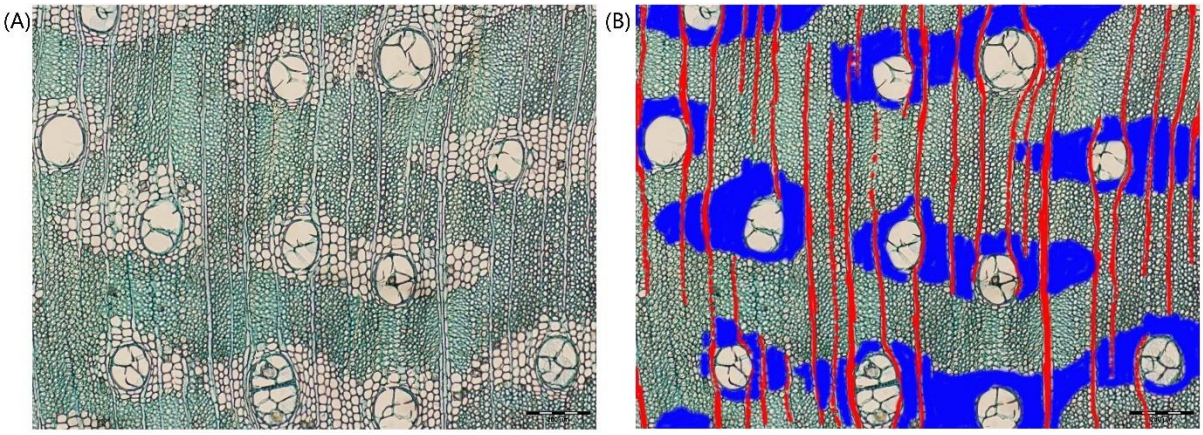

Appendix S2.3 Phylogenetic tree for the 68 focal species. The cladogram is based on the Angiosperm Phylogeny Group III (*Botanical Journal of the Linnean Society* 161: 105–121) classification.

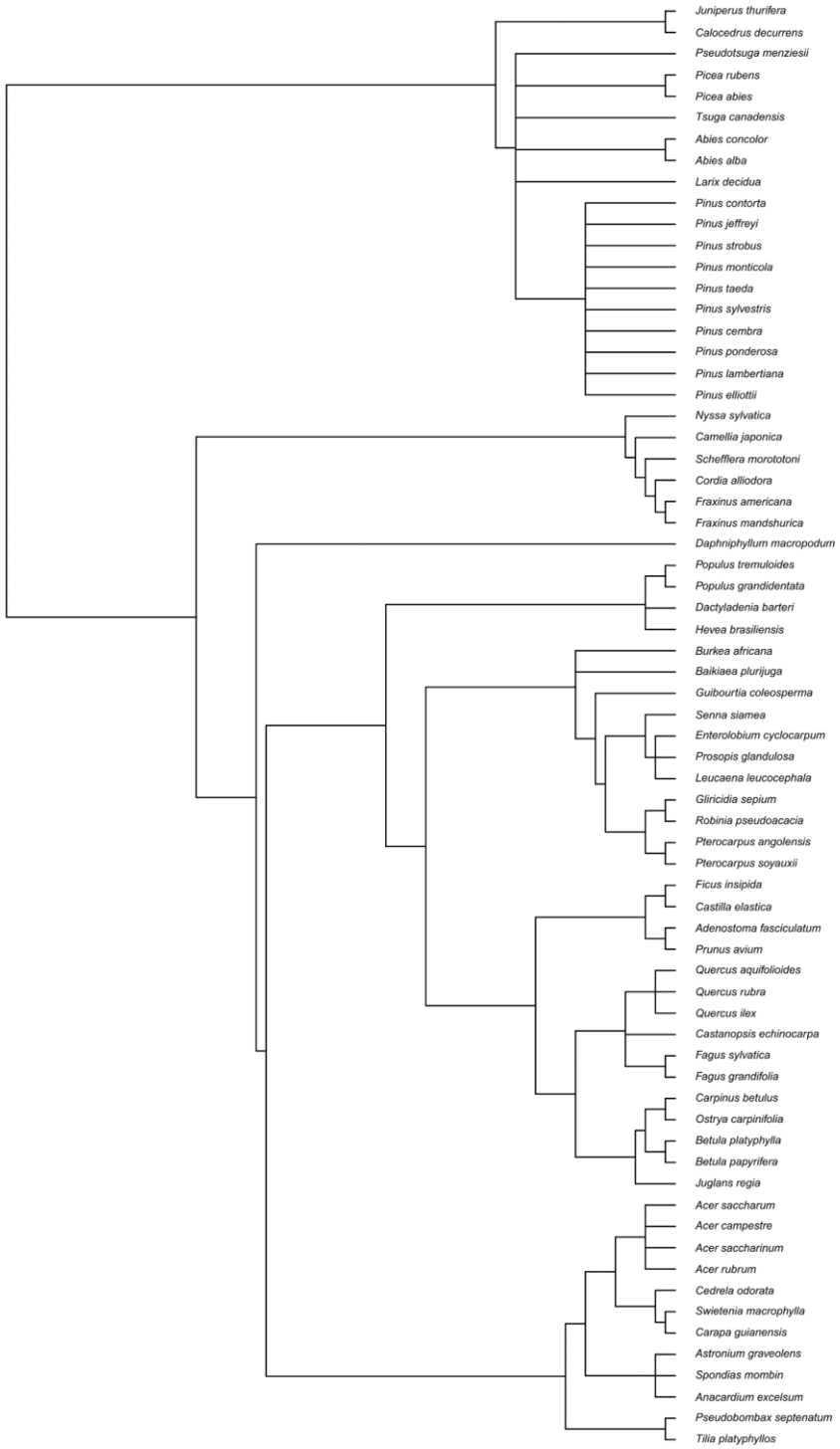

Appendix S2.4 Relationships between (A) wood density and MAT, (B) wood density and MAP, (B) maximum tree height and MAT, and (D) maximum tree height and MAP. MAP: mean annual precipitation. MAT: mean annual temperature.

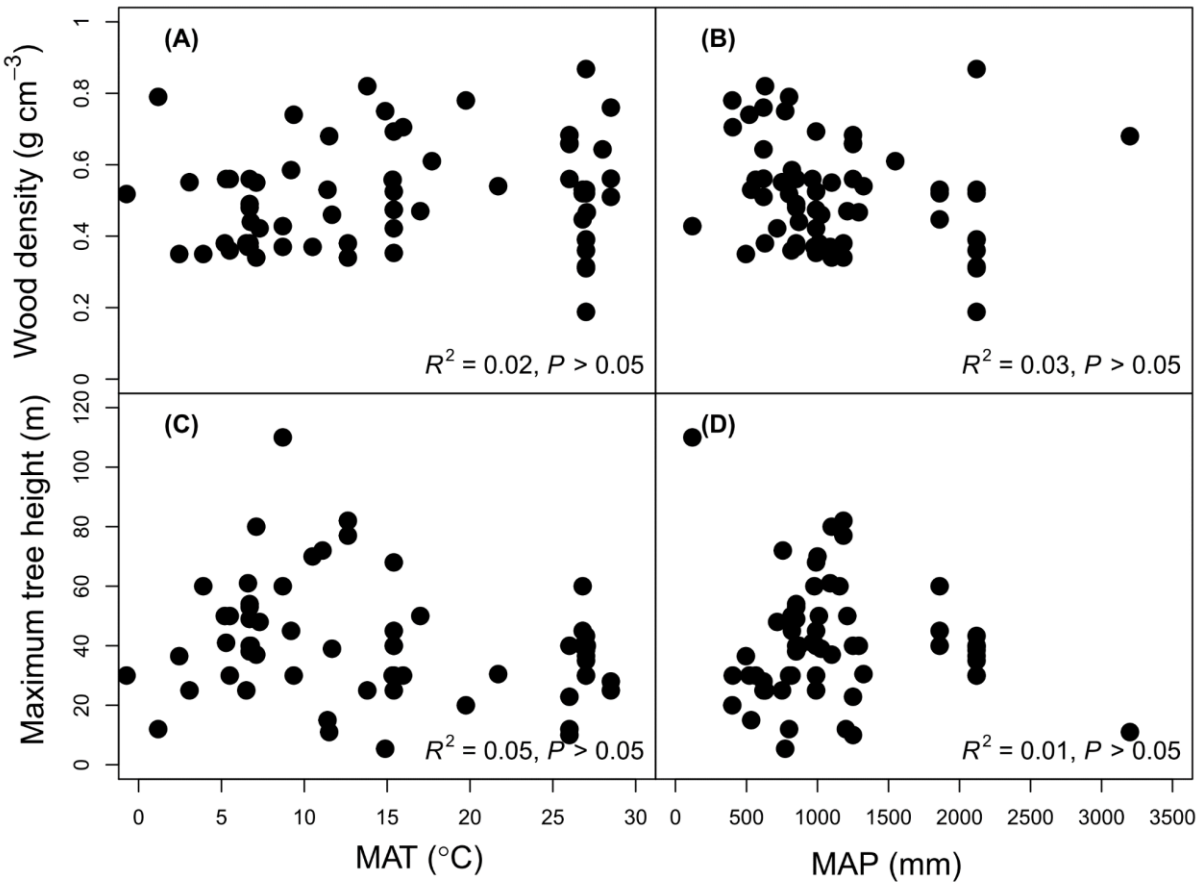

Appendix S2.5 Relationships between parenchyma fractions and NSC_{mean} (A, B, C), NSC_{max} (D, E, F), and wood density (G, H, I) across leaf habits. AP: axial parenchyma, NSC_{mean}: mean value of nonstructural carbohydrates. NSC_{max}: maximum value of nonstructural carbohydrates in 1 year; RP: radial parenchyma; RAP: radial and axial parenchyma.

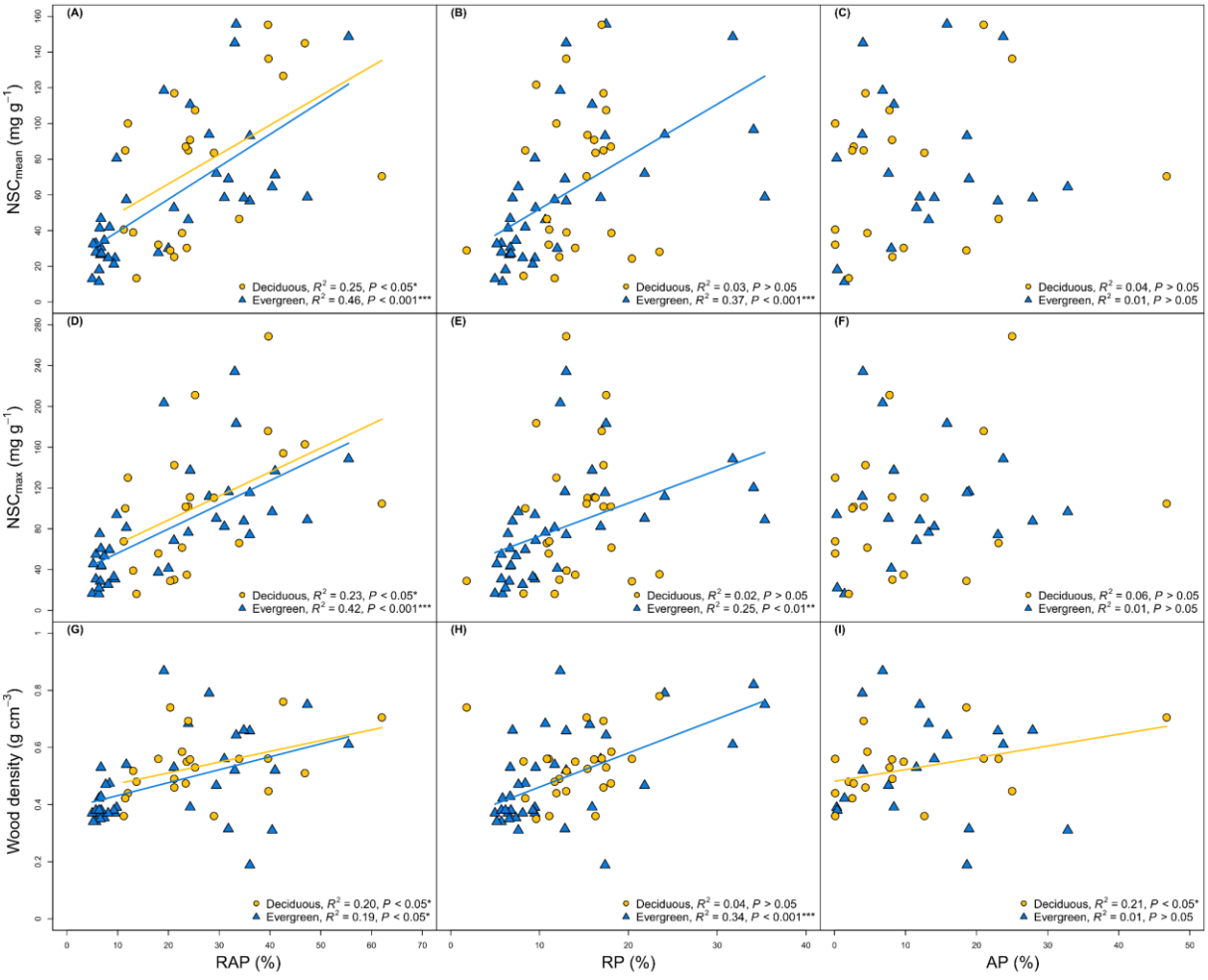

Appendix S2.6 Relationships between NSC_{max} and RAP (A, B, C), AP (D, E, F), and RP (G, H, I) fractions with all species pooled and across evolutionary subdivisions and climates. AP: axial parenchyma; NSC_{max}: maximum value of nonstructural carbohydrates in 1 year; RP: radial parenchyma; RAP: radial and axial parenchyma.

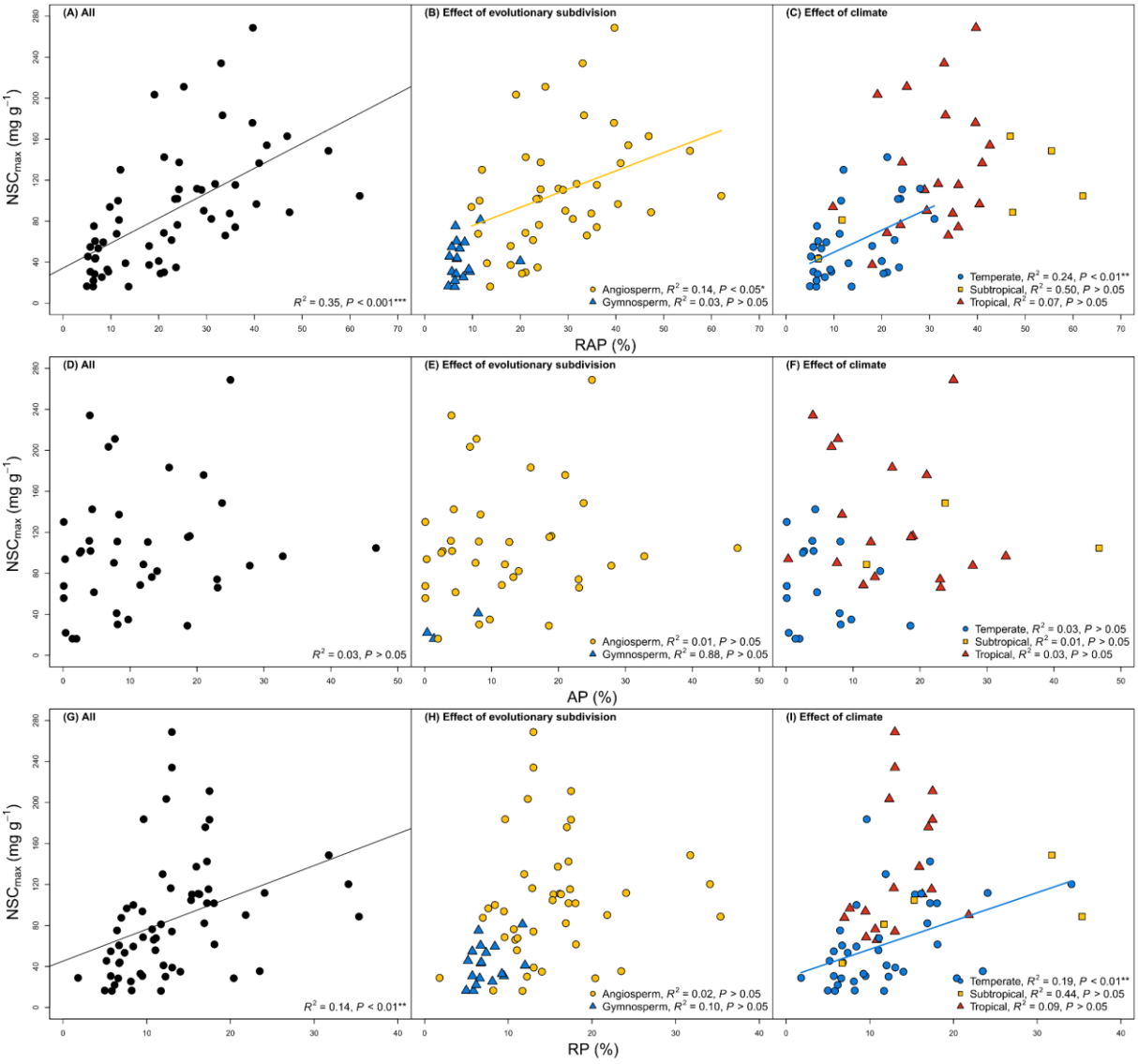

Appendix S2.7 Relationships between NSC_{mean} and wood density (A, B, C) or between NSC_{max} and wood density (D, E, F), with all species pooled, and across evolutionary subdivisions and climates. NSC_{mean}: mean value of nonstructural carbohydrates over 1 year; NSC_{max}: the max value of nonstructural carbohydrates in 1 year.

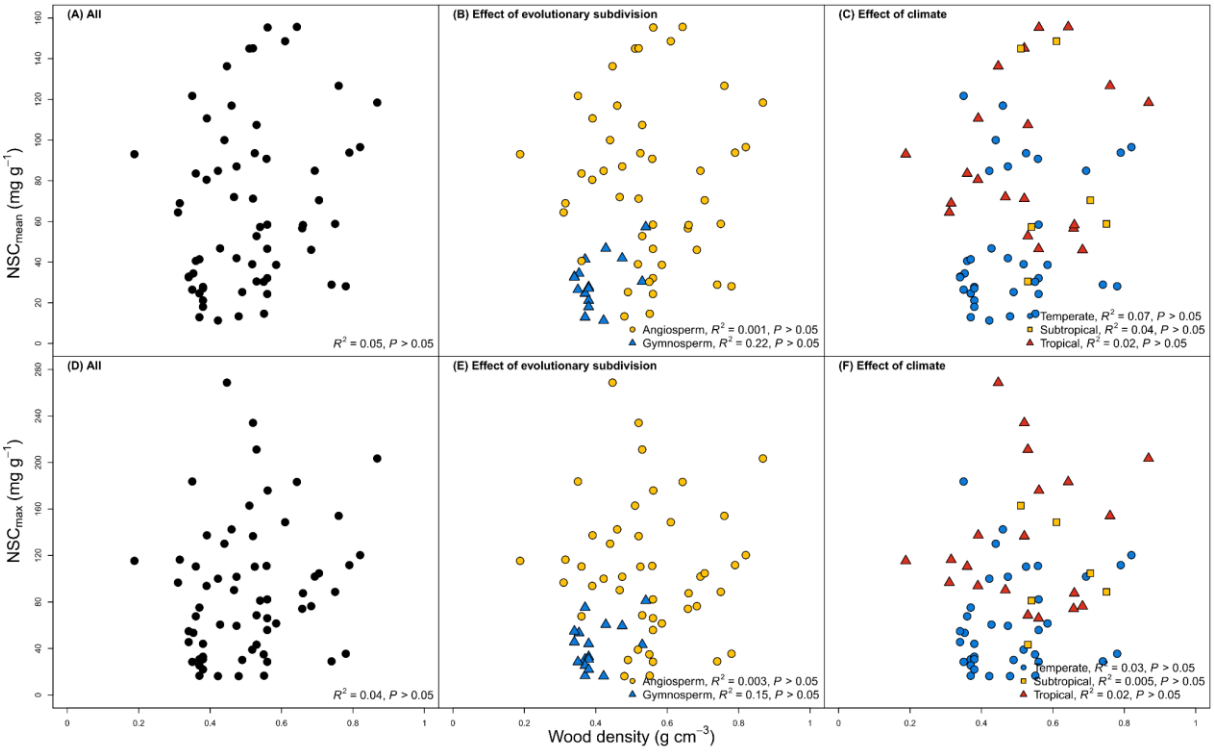

Appendix S2.8 Relationships between maximum tree height and NSC_{mean} (A, B, C), NSC_{max} (D, E, F), RAP (G, H, I) and wood density (J, K, L) with all species pooled and across evolutionary subdivisions and climates. NSC_{mean}: mean value of nonstructural carbohydrates over 1 year; NSC_{max}: maximum value of nonstructural carbohydrates in 1 year; RAP: radial and axial parenchyma.

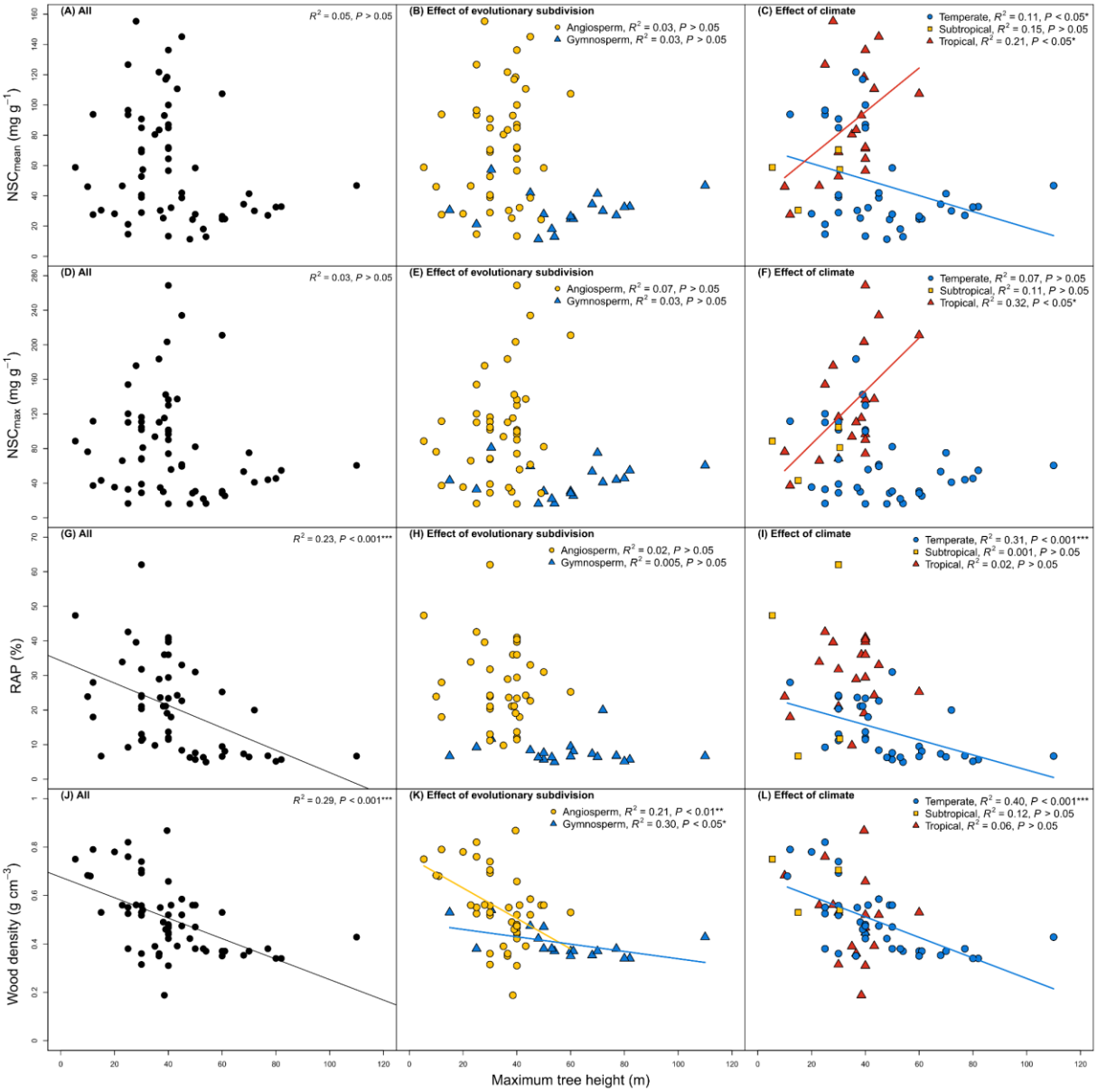

Appendix S2.9 Relationships between maximum tree height and RP (A, B, C) and AP (D, E, F) with all species pooled and across evolutionary subdivisions and climates. AP: axial parenchyma; RP: radial parenchyma.

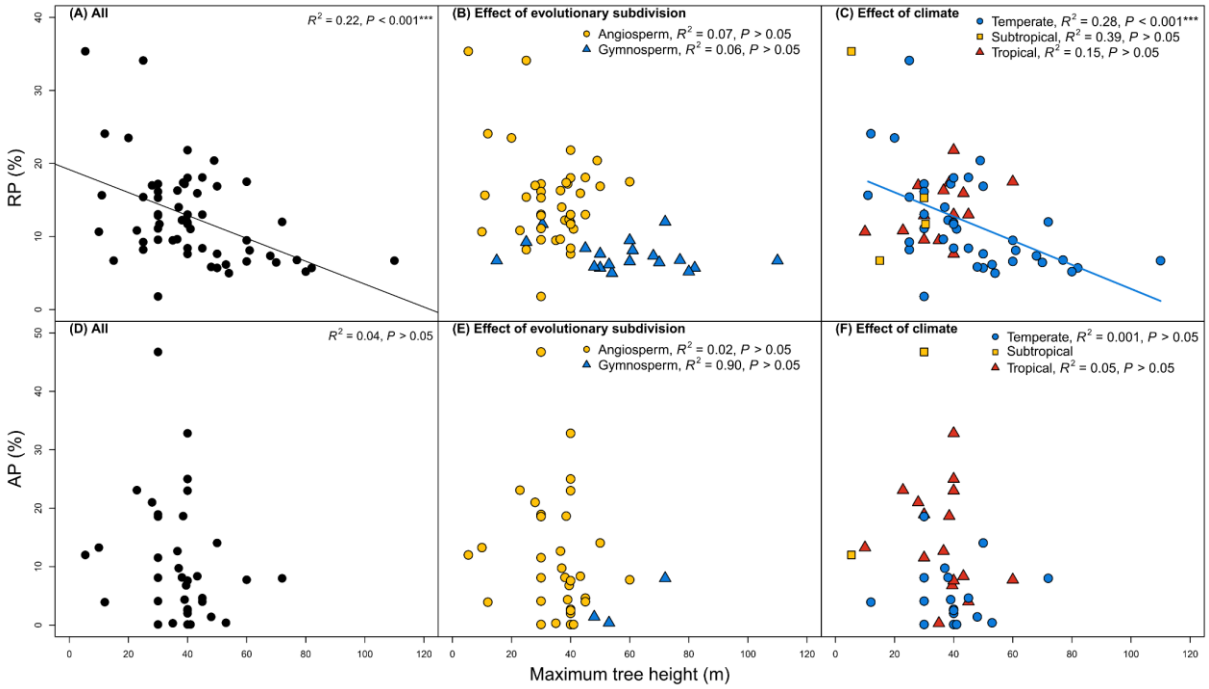

Appendix S2.10 Models of phylogenetic generalized least squares (PGLS) to explain the correlations among NSC_{mean}, NSC_{max}, wood density, RAP, and H_{max}. H_{max}: maximum tree height. NSC_{mean}: mean value of nonstructural carbohydrates over 1 year. NSC_{max}: maximum value of non-structural carbohydrates in 1 year. RAP: radial and axial parenchyma. WD: wood density.

Model	R^2	P
NSC_{mean} – RAP	0.17	**<0.01****
NSC_{max} – RAP	0.20	**<0.001*****
WD – RAP	0.20	**<0.001*****
NSC_{mean} – WD	0.01	>0.05
NSC_{max} – WD	0.02	>0.05
NSC_{mean} – H_{max}	0.00	>0.05
NSC_{max} – H_{max}	0.00	>0.05
RAP – H_{max}	0.03	>0.05
WD – H_{max}	0.26	**<0.001*****

Appendix S2.11 Statistics for one-way ANOVA analysis for soluble sugars, starch, NSC and Kruskal–Wallis test for RP, AP, and RAP across climates (temperate, subtropical and tropical) and evolutionary subdivisions (angiosperm and gymnosperm). NSC_{mean}: mean value of nonstructural carbohydrates over 1 year. NSC_{max}: maximum value of nonstructural carbohydrates in 1 year. RP: radial parenchyma. AP: axial parenchyma. RAP: radial and axial parenchyma.

Model	Statistic	Soluble sugars	Starch	NSC_{mean}	NSC_{max}	Statistic	%RP	%AP	%RAP
	F	5.89	10.36	10.35	13.55	χ^2	4.02	15.52	26.91
Climates	df	2, 55	2, 59	2, 62	2, 62	df	2	2	2
	P	0.005	<0.001	<0.001	<0.001	*P*	0.134	<0.001	<0.001
	F	5.73	16.42	23.73	19.92	χ^2	29.17	2.67	35.99
Evolutionary subdivisions	df	1, 56	1, 60	1, 63	1, 63	df	1	1	1
	P	0.020	<0.001	<0.001	<0.001	*P*	<0.001	0.102	<0.001

CHAPTER 3: The design of the xylem space coordinates trade-offs among hydraulic, mechanical and storage traits across tree species and climates

Guangqi Zhang[1], Zhun Mao[1], Pascale Maillard[2], Loic Brancheriau[3], Bastien Gérard[2], Julien Engel[1], Claire Fortunel[1], Jean-Luc Maeght[1], Jordi Martínez-Vilalta[4,5], Alexia Stokes[1]

1 AMAP, Université de Montpellier, CIRAD, CNRS, INRAE, IRD, 34000 Montpellier, France
2 SILVA, INRAE, Université de Lorraine, Agroparistech, Centre de Recherche Grand-Est Nancy, 54280 Champenoux, France
3 CIRAD, Université de Montpellier, UR BioWooEB, 34000 Montpellier, France
4 CREAF, E08193 Bellaterra (Cerdanyola del Vallès), Catalonia, Spain
5 Universitat Autònoma Barcelona, E08193 Bellaterra (Cerdanyola del Vallès), Catalonia, Spain

ABSTRACT

Premise: Xylem must perform several functions to ensure tree survival and the design of the xylem space leads to trade-offs among water transport, mechanical support and carbohydrate storage. However, it is not known how these trade-offs are affected by inherent xylem design (such as porosity and parenchyma arrangement) and whether the coordination among xylem traits is consistent across species and climates. Testing hypotheses about the design of the xylem space is facilitated by studying both stem and root xylem: regardless of porosity (ring, semi- and diffuse porous) in the stem, lateral roots are always diffuse porous. Therefore, cell arrangement should reflect trade-offs as xylem function changes throughout a tree.

Methods: We sampled 60 adult angiosperm tree species from temperate, Mediterranean and tropical climates. A total of 13 traits linked to multiple xylem functions were measured in stems and roots, including wood density and fiber fraction (mechanical traits), non-structural carbohydrates (NSC), ray (RP) and axial parenchyma (AP) arrangement (storage traits), vessel size and density (hydraulic traits). We also evaluated the strength of phylogenetic signals for each xylem trait calculated.

Results: We found NSC and specific xylem hydraulic conductivity (SXHC) were positively correlated in stems, but negatively in roots, highlighting trade-offs in the xylem space between shoots and roots, due to their different functions. Wood density was lowest in temperate species and across all species, it was positively correlated with total parenchyma fraction in both stems and roots, but was negatively correlated with vessel fraction and SXHC. Species with paratracheal AP and ring-porous xylem tended to have greater SXHC, and SXHC was positively related to AP but negatively to RP fraction in roots across all species. Mediterranean species had the lowest SXHC, while tropical species had the lowest vessel density but the largest vessels. Phylogenetic trends affected xylem traits, but was not the main factor impacting the coordination of trade-offs among traits.

Conclusions: The design of the xylem space is optimised for multifunctionality and that space is reorganised depending on the main functions that xylem must perform. Trade-offs occur among mechanical, storage and hydraulic traits in stems and roots, with roots possessing traits more linked to storage capacity and hydraulics. Climate is a major factor affecting both the design of the xylem space and the trade-offs that occur, with evolutionary history playing a minimal role in the coordination among traits.

Key words: climates, phylogenetic, trade-offs, structure-function, xylem anatomy

3.1 INTRODUCTION

To thrive in a forest environment and withstand both biotic and abiotic constraints, tree xylem is multifunctional, simultaneously providing hydraulic functioning, mechanical support and defense against insect/pathogen attack. The secondary xylem of angiosperms comprises three main cell types (parenchyma, vessels and fibers), that contribute to these distinct functions. The metabolically active axial and ray parenchyma cells play a fundamental role in defense and wound repair (Morris *et al.*, 2020), respiration (Rodríguez-Calcerrada *et al.*, 2015),

nutrient and water storage (Plavcová *et al.*, 2016; Secchi *et al.*, 2017); vessels mainly provide long-distance water and nutrient transport (Tyree and Ewers, 1991; Pratt and Jacobsen, 2017) and fibers, as well as ray parenchyma, provide mechanical strength (Burgert and Eckstein, 2001; Rana *et al*., 2009; Ziemińska *et al.*, 2013; Fortunel *et al.*, 2014). However, trees have evolved in response to a multitude of diverse environmental signals, that have led to trade-offs in structure and function within the xylem space (Grubb, 2016; Pratt and Jacobsen, 2017; Pratt *et al.*, 2021a). The resulting design of the xylem space actively influences physiological processes occurring within trees, potentially driving survival or failure when local environmental conditions change. Understanding design of the xylem space therefore, will allow us to identify strategies that contribute to tree survival in different climates.

Despite the apparently distinct roles of different xylem cells, their functions are nonetheless entwined and connected in complex ways, resulting in trade-offs that enhance survival strategies. As the largest metabolically active fraction in the xylem space, parenchyma cells, and the non-structural carbohydrates (NSC) stored within them, are fundamental to driving survival processes, such as resprouting after a disturbance like a wildfire (Smith *et al*., 2018a). In particular, axial parenchyma (AP) is associated with the maintenance of hydraulic conductivity, as tree species with higher fractions of AP tend to have larger vessels (Morris *et al.*, 2018a) and greater hydraulic capacitance (Aritsara *et al.*, 2021; Ziemińska *et al.*, 2020). Paratracheal AP (associated to vessels, Fig. S3.1A) can influence hydraulic capacitance in angiosperms by releasing water and NSC into vessels in periods of drought (Morris *et al*., 2018a), maintaining osmoregulation and assisting in the refilling of embolized vessels (Secchi *et al*., 2017; Tomasella *et al*., 2020). However, a large AP fraction decreases wood density and results in high stem respiration, reducing tree growth rate (Jacobsen *et al.*, 2007; Fortunel *et al.*, 2014; Rodríguez-Calcerrada *et al.*, 2015; Zhang *et al*., 2022a). Ray parenchyma (RP) are also major sinks of NSC, but can contain a large amount of lignin between individual

parenchyma cells and surrounding fibers, thus potentially increasing overall wood density and improving radial strength (Burgert and Eckstein, 2001; Zhang *et al*., 2022a), but decreasing the available xylem space for other cell types. The presence of large or abundant vessels, however, decreases wood density, but a large lumen fraction is vital for increased hydraulic conductivity (Zanne *et al.*, 2010), potentially creating a trade-off between hydraulics and xylem mechanical integrity (Christensen-Dalsgaard *et al.*, 2007a,b; Chen *et al*., 2020), although studies provide conflicting results. For example, Woodrum *et al.* (2003) found no relationship between hydraulic conductivity and xylem modulus of elasticity (i.e., resistance to being deformed elastically), in several diffuse porous *Acer* species. Differences in function among species may be due to the spatial arrangement of cells, such as porosity, within the xylem space, but the link between cell function and their spatial arrangement is poorly understood. Although there have been several studies on the trade-offs in functions performed by different cell types within the xylem space (Table 3.1), these studies have mostly focused on stem xylem in shrubs, or a limited number of tree species.

Diffuse-porous species are usually found in tropical regions, and tropical species generally have wider vessels and more abundant parenchyma than temperate tree species (McCulloh *et al.*, 2010; Morris *et al.*, 2016; 2018a). However, ring-porous species are always deciduous and are therefore more abundant in cooler regions, or regions with a marked dry season (Boura and De Franceschi, 2007). Large earlywood vessels in ring-porous species are important for rapid water transport after leaf abscission and dormancy, whereas in diffuse porous species, root pressure drives vessel refilling at the end of the winter/dry season (Hacke and Sauter, 1996; Utsumi *et al*., 1998). Therefore, although large vessels are usually found in the earlywood of ring-porous species, paratracheal AP does not contribute to restoring transport functions, that must be assured by the formation of new vessels in xylem produced simultaneously with budburst (Boura and De Franceschi, 2007). Paratracheal AP should

therefore be more abundant in diffuse porous xylem. As the role of apotracheal AP (isolated from vessels, Fig. S3.1B) is more likely to be linked to defense, water and NSC storage, it should therefore exist in greater quantities in ring-porous species, as well as in temperate climates (Morris *et al*., 2016). However, this hypothesis has not been tested across species and climates.

Testing hypotheses about the spatial arrangement of cells in the xylem space can be facilitated by studying both stem and root xylem. Regardless of the porosity type in angiosperm stems (ring or diffuse porous), xylem becomes more diffuse porous with distance from the stem in coarse roots. Roots usually have wider but less dense vessels, fibre content is lower than in the stem and RAP fraction is greater (Stokes and Guitard, 1997), thus increasing NSC storage capacity. This gradient in cell size is advantageous for an improved hydraulic efficiency, especially in horizontal lateral roots that take up water from the most superficial soil layers (Fahn, 1967; Pratt *et al*., 2007). Also, when responding to mechanical stress, such as wind loading, anchorage efficiency is better improved through morphological changes, rather than modifications in xylem anatomy (Stokes and Guitard, 1997). Therefore, a trade-off should exist in the xylem of coarse, lateral roots, that favours hydraulic functioning against mechanical functioning, and the quantity of paratracheal AP could increase as roots become more diffuse porous. However, it is not known if patterns of paratracheal and apotracheal AP are altered in roots, nor if there are subsequent changes to NSC content, that could in turn alter ecological strategies, such as resprouting. As vessels increase in size in roots, they will become more susceptible to drought-induced embolism, therefore any increases in NSC, especially in a drier climate, would help maintain hydraulic integrity.

The design of the xylem space is therefore determinant of several functional strategies in angiosperms. Whether these strategies are driven by coordinated evolutionary factors is not

yet fully clear. Exploring phylogenetically independent relationships among xylem functional traits should provide us with a more genuine insight for correlated evolutionary shifts and their impact on trait variation (Felsenstein, 1985). For example, phylogeny explained more than half of the variation in *individual* functional traits in the stem xylem of 700 angiosperm tree species in China (Zheng *et al.*, 2019). However, when examining the relationships *between* traits (e.g., wood density and fibre fraction, hydraulic conductivity and embolism resistance, or NSC content and parenchyma fractions), studies have shown that these relationships are not affected by evolutionary history (Fortunel *et al.*, 2014; Pratt *et al.*, 2021b; Zhang *et al*., 2022a). If this is indeed the case, phylogenetic relatedness will not affect relationships or trade-offs among functional traits, within either stem or root xylem, even though the design of the xylem space differs significantly between the two organs.

We investigated the design of the xylem space in stems and coarse roots of 60 tree species from temperate, Mediterranean and tropical climates, and examined how RAP patterns affected NSC content. We asked if the design of the xylem space coordinates the trade-offs between structure and function in stems and roots, and if this coordination is linked to climate, and (H1) expect that any variance in xylem patterns is affected by evolutionary history, but that evolutionary history itself would not change the fundamental trade-off between functional traits. If the design of the xylem space depends on climate and organ function, are patterns of apotracheal and paratracheal AP linked to porosity that changes between the stem and the root? As hydraulic function is largely assured by the formation of new vessels in the earlywood of temperate/Mediterranean ring-porous species, we (H2) hypothesize that apotracheal AP exists in greater quantities in the stems of ring-porous species in temperate and Mediterranean climates, and paratracheal AP is more abundant in diffuse porous xylem, including in roots that are usually diffuse porous with large vessels. We also expect (H3) that xylem with large vessels and increased hydraulic conductivity has reduced wood density and increased NSC

content, that maintains osmoregulation and assists the filling of embolized vessels, especially in Mediterranean regions that undergo long dry periods.

3.2 MATERIALS AND METHODS

3.2.1 Study sites and species

This study was conducted on trees from forests growing in three different climates: a temperate forest (Luz-Saint-Sauveur, France; 43°08'N, 0°03'E), a Mediterranean forest (Montpellier, France; 43°42'N, 4°00'E) and a tropical forest (Paracou, French Guiana; 5°15'N, 52°55'W). The site at Luz-Saint-Sauveur has a temperate mountain climate, with the heaviest rainfall in April and May. Mean annual precipitation is 1200 mm and mean annual temperature is 12.5 ℃ (mean summer temperature is 19.0 ℃ and mean winter temperature is 6.0 ℃, Rius *et al*., 2014). The site at Montpellier has a typical Mediterranean climate with hot dry summers and cool, wet winters. Mean annual precipitation is 907 mm with about 80% of the annual rainfall occurring between September and April. Mean annual temperature is 13.4 ℃ (July is the warmest month and January is the coldest, Allard *et al.*, 2008). The site at Paracou has a typical tropical rainforest climate with a distinct dry season from mid-August to mid-November and a long rainy season, often interrupted by a short drier period, between March and April. The mean annual precipitation is 3041 mm with a minimum in September and maximum in May. The mean annual temperature is 26 ℃ with an annual range of 1 - 1.5 ℃ (https://paracou.cirad.fr/website).

A total of 60 angiosperm species was selected, with 20 species in each climate, spanning 43 genera and 32 families (Table S3.1, Zhang *et al*., 2022b). For each species, three healthy, adult, single-stemmed trees were identified, with a distance of at least 20 m between them. Stems chosen were between 0.1 m and 0.5 m wide at a height of 1.3 m (however, in some adult, small-stature species, diameter was as low as 0.05 m, Table S3.1). For Mediterranean

and tropical trees, samples were collected at the end of August and September 2019, and for temperate trees, samples were collected in September 2020. We sampled all trees between 7am and midday, to reduce variability in NSC content linked to photosynthate production. At a height of 1.3 m, three 0.05 m long cores were extracted from tree stems with a 4.3 mm diameter increment borer (n = 540). To collect samples of roots, we excavated a single lateral root (0.02 - 0.05 m in diameter) and at a distance of 0.3 - 0.5 m from the base of the tree, we extracted three increment cores or removed three 0.02 m long segments of root, depending on accessibility (n = 540). All samples were immediately placed in moist paper, put in a cooler box and taken to the laboratory prior to midday, where they were kept in a fridge at 4°C.

3.2.2 Measurement of xylem anatomical traits

Within 24 h, one of the three replicate increment cores was trimmed and a 0.02 m long section was taken from the outer sapwood and placed in a 50% solution of alcohol and water. A 0.02 m long section of root was also placed in the solution of alcohol and water. These sections were kept for the analysis of xylem anatomical traits. Increment cores were embedded in paraffin individually after dehydration by immersing in a sequence of alcohol solution, whereas sections of root were just clamped in the microtome. We used a sliding microtome to cut 15 - 20 um thick cross-sections. Cross-sections were stained with a mixture of safranin and alcian blue (0.35 g safranin in 35ml 50% alcohol with 0.65 g alcian blue in 65 ml deionized water) and dehydrated using an ethanol series (50, 75, 95 and 100%). Finally, sections were mounted on glass slides and observed under a light microscope (Olympus BX 60F; Olympus Co. Ltd, Japan). Three microphotographs of transversal sections (one or two for very few sections) for each stem and root sample were taken with an APO x5 lens using a digital camera (Canon EOS 500D; Canon Inc., Tokyo, Japan). A total of 532 stem and 527 root microphotographs were taken (see an example in Fig. S3.1).

Radial parenchyma (RP) and axial parenchyma (AP) were manually colored using Photoshop (Adobe Systems Incorporated, USA) (Fig. S3.2). The proportions of RP (radial parenchyma area divided by xylem cross-section area, %) and AP (axial parenchyma area divided by xylem cross-section area, %) were estimated using ImageJ 1.52 software (https://imagej.nih.gov/ij/). The proportion of total radial and axial parenchyma (RAP, i.e., the sum of RP and AP, %), was then calculated. Using the same image, we also determined vessel fraction (VF, i.e., the total vessel area divided by xylem cross-section area, Fig. S3.2), vessel density (VD, vessel number per unit area), vessel mean diameter (VMD), vessel mean hydraulic diameter (MHD) and theoretical specific xylem hydraulic conductivity (SXHC). VMD, MHD and SXHC were calculated based on the diameter (D) of each vessel in the xylem cross-section.

D for a vessel *i* was calculated using Eqn 1 (Lewis, 1992):

$$D = \sqrt{\frac{2a^2b^2}{a^2+b^2}} \qquad \text{Eqn. 1}$$

where *a* is the maximum diameter of a vessel and *b* is the minimum diameter of a vessel. VMD was calculated as in Eqn 2:

$$VMD = \frac{\sum_{i=1}^{n} D_i}{n} \qquad \text{Eqn. 2}$$

where *n* is the number of vessels ($i \in [1, n]$). MHD was calculated (Scholz *et al.*, 2013) as in Eqn 3:

$$MHD = \sqrt[4]{\frac{\sum_{i=1}^{n} D_i^4}{n}} \qquad \text{Eqn. 3}$$

SXHC was calculated using Hagen-Poiseuille equation (Tyree and Ewers, 1991) as in Eqn 4:

$$SXHC = \frac{\pi\rho\sum_{i=1}^{n} D_i^4}{128\eta As} \quad \text{Eqn. 4}$$

where ρ is the density of water (998.2 kg m^{-3} at 20 °C), η is the water viscosity (1.002×10^{-9} MPa s at 20 °C) and A_s is the xylem cross-sectional area which measured directly with ImageJ in the microphotograph.

The remaining tissues fraction including fibres, fibre-tracheids and tracheids (FFT) was calculated as: 1-RAP-VF. For all traits, we then calculated the mean values for the three images for subsequent statistical analyses.

3.2.3 Measurement of xylem wood density

The outer bark was removed on one stem and one root sample from each tree. Wood density (WD) was then measured by soaking samples in water for 24 h. The fresh volume was determined using the water displacement method (Pérez-Harguindeguy *et al.*, 2016). After determining the fresh volume, samples were dried in a well-ventilated oven at 105 °C for more than 24 h and then the dry mass was weighed. Wood density used here is defined as oven-dry mass divided by fresh volume (Pérez-Harguindeguy *et al.*, 2016).

3.2.4 Measurement of xylem NSC content

Immediately on returning to the laboratory (on the same day the samples were collected), samples were heated in a microwave oven (90 s at 700 W) to stop enzymatic activity (Popp *et al.*, 1996) and then oven-dried at 40 °C until a constant weight was obtained. Dried samples were ground into powder using a ball mill (Retsch MM400, Retsch, Haan, Germany) and the ground samples were stored in sealed plastic tubes until chemical analyses. Due to the large number of samples (n = 360), we used the near infra-red spectroscopy (NIRS, Batten *et al.*, 1993) method to develop a model for predicting NSC contents in different organs (Zhang *et al.*, 2022b). The NIRS method has been used successfully in plant ecology for predicting NSC

content in different tissue types of a broad range of tree species (Ramirez *et al.*, 2015; Rosado *et al.*, 2019).

As this study is part of a larger study, where NIRS was used to develop a model for predicting NSC in organs of 90 tree species (Zhang *et al*., 2022b), we were able to create robust models using this larger dataset. Briefly, Near infrared spectra were obtained for all samples on powders previously stabilized in a conditioning room at a temperature of 20 ± 2 °C and air humidity of 65 ± 5%. A Bruker Vector 22/N spectrometer was used in reflectance mode. Data were measured for wavelengths between 1000 nm to 2500 nm with a resolution of 3 nm. The spectra set was thus composed by 501 wavelengths of reflectance values. NIRS spectra were first transformed (Naes *et al*., 2004) with a Standard Normal Variate (SNV) correction to reduce the effect of irregularities of surface and the intra spectrum variability (correction of the light dispersion). The second derivative was then computed using the algorithm of Savitzky Golay (Savitzky and Golay, 1964). The use of this derivative allowed for separating peaks that overlap and for correcting the baseline deviation of spectra. Then, the range of NIRS values was examined and 113 samples of stem and 140 samples of root were selected, for which values represented a broad range of data. Soluble sugars (SS) were extracted from 10 to 15 mg powder mixed in with 0.5 ml of 80% ethanol and incubated for 20 min at 80 °C. The extraction was repeated twice and the three supernatants were collected in a tube and dried under vacuum (Refrigerated CentriVap Vacuum Concentrators, Labconco). The resulting soluble sugar extract was solubilized in 1.5 ml ultrapure water by sonication and agitation and then stored at -20 °C. Total SS content was determined by a spectrophotometer at 620 nm (UV-visible DU 640 B, Beckman Coulter, USA) using anthrone reagent and glucose as standard (Van Handel, 1965). Starch was extracted from the dried pellets in 1.5 ml of 0.2 M KOH solution incubated for 20 min at 80 °C. Then hydrolysis of starch into glucose was carried out in 0.1 M sodium acetate buffer solution at pH 4.75 with amyloglucosidase

(EC 3.2.1.3. from Aspergillus niger Sigma A1602). The obtained glucose was determined colorimetrically using an enzymatic glucose oxidase (EC 1.1.3.4, Sigma G6125) / peroxidase (EC 1.11.1.7, Sigma P8125) and o-dianisidine dihydrochloride (Sigma D3252) reagent. After 10 min, 6N hydrochloric acid was added and absorbance was measured at 530 nm, using glucose as a standard (Chow and Landhäusser, 2004). Soluble sugar and starch contents were expressed as mg g^{-1} dry mass (DM) and their sum is referred to as the total NSC content.

Partial least squares regression (PLSR) was used to develop calibrations for the predictions of SS and starch content for stem and root samples separately (Zhang *et al*., 2022b). The calibration R^2, standard error and root mean square error of cross validation values are shown in Table S3.2.

3.2.5 Statistical analysis

In this study, the minimum, maximum, mean, standard deviation and coefficient of variation of each trait were calculated. The studied species contained 45 diffuse porous, nine ring porous and six semi-ring porous species. Since diffuse porous species were very different from semi-ring and ring porous species, and there was little variation between the latter, we grouped semi-ring and ring porous data for analyses (denoted hereafter as semi/ring porous). Due to the non-normality of the data, we used non-parametric tests to determine the variation of xylem traits between organs (stem and root), AP arrangements (paratracheal and apotracheal), porosity (diffuse and semi/ring porous) and among climates (temperate, Mediterranean and tropical). The Wilcoxon signed-rank test was used to examine differences in xylem traits between two categories. Kruskal-Wallis and pairwise Wilcoxon tests were conducted to determine differences in xylem traits among climates for stem and root samples separately.

In order to examine the correlations among all 13 xylem traits, we performed Spearman correlation analysis for both stem and root data. Linear regression analyses were also used to determine relationships between xylem traits. We also performed principal component analysis (PCA) to investigate if an overall xylem trait coordination existed. To detect the influence of phylogenetic trends on xylem traits, we implemented Spearman correlation analysis and PCA with phylogenetically independent contrasts (PICs) at the species level. We constructed a phylogenetic tree (Fig. S3.3) with all 60 species using PHYLOMATIC v.3 (Webb and Donoghue, 2005), which is based on the APG III classification of angiosperms and all species names were confirmed by the World Flora Online (http://www.worldfloraonline.org/). We calculated Blomberg's K-value to evaluate the strength of phylogenetic signals for each xylem trait (Blomberg *et al.*, 2003). In order to infer the potential connections between xylem traits and related functions, we also conducted a simple structural equation model (SEM), based on our hypotheses and pairwise trait correlations. The overall model fit was assessed with several tests, including a non-significant chi-square (X^2) test ($p > 0.05$), a comparative fit index (CFI > 0.95) and a standardized root mean square residual (SRMR < 0.08) (Malaeb *et al.*, 2000; Ali *et al.*, 2016). When performing PCA, linear regression analyses and SEM, the data were transformed using natural log for all traits except for WD which the data were normally distributed.

All statistical analyses were performed in R version 4.0.2 (R Development Core Team 2020), using the packages *vegan* (Dixon, 2003), *ape* (Paradis *et al.*, 2004), *picante* (Kembel *et al.*, 2010) and *lavaan* (Rosseel, 2012).

3.3 RESULTS

Across the 60 tree species, all xylem traits showed marked interspecific variation (Table 3.2, Fig. S3.4, S3.5). The coefficient of variation (CV) of SXHC was the largest, ranging from

0.81 to 460.05 kg m^{-1} MPa^{-1} s^{-1} for stem xylem with 151.7% of CV, and 0.45 to 459.18 kg m^{-1} MPa^{-1} s^{-1} for root xylem with 142.2% of CV. The proportion of FFT and WD showed relatively small interspecies variation. In stem xylem, FFT ranged from 0.47 to 0.88 with 11.9% of CV and for root xylem, FFT ranged from 0.27 to 0.88 with 16.3% of CV (Table 3.2). In stems, WD ranged from 0.24 to 0.85 g cm^{-3} with 21.9% of CV and in roots, from 0.23 to 0.88 g cm^{-3} with 24.9% of CV (Table 3.2). Regardless of the climate zone, certain xylem traits were significantly different between stems and roots: WD, VF, and VD were all significantly greater in stem compared to root xylem, while AP, RAP, SS, starch and NSC were all significantly lower in stem xylem than in root xylem. Other traits (RP, FFT, VMD, MHD and SXHC) were not significantly different between stem and root xylem (Table 3.2).

3.3.1 Effects of phylogeny on xylem traits in stem and root

Among all the xylem traits, stem WD, VF, VMD, VD, MHD, SXHC, starch and NSC had significant phylogenetic signals, whereas in roots, the traits WD, AP, RP, RAP, VMD, VD, MHD, SXHC, starch and NSC had significant phylogenetic signals (Table 3.3). When PICs were included in the Spearman correlations, we found the patterns of correlations among stem and root xylem traits did not show significant changes (Mantel test, Fig. 3.1B, D, Table S3.3). Similarly, when PICs were included in the PCA, the patterns of correlations among stem and root xylem traits were also consistent (Fig. 3.2B, D), further confirming that phylogeny was not the main factor affecting the correlation patterns among xylem traits.

3.3.2 Patterns of xylem traits in stem and root

Temperate species had lower WD in both stems and roots compared to Mediterranean and tropical species (Fig. 3.3). RAP and AP in both stems and roots were also lower in temperate species, whereas RP did not vary among the three climates (Fig. 3.3). VF in both stems and roots was greatest in temperate species, whereas VMD in stems and roots was highest in

tropical species. In contrast, the VD of both stems and roots was lowest in tropical species (Fig. 3.3). The SXHC of both stems and roots was lower in Mediterranean species compared to temperate and tropical species (Fig. 3.3). Mediterranean species had more stem SS but lower stem starch compared to temperate and tropical species, while stem NSC were not significantly different. However, tropical species possessed lower SS, starch and NSC in roots compared to temperate and Mediterranean species (Fig. 3.3).

Wood density, VF, VD, SXHC, SS and NSC were lower (but AP and VMD was greater) in stems of diffuse porous species compared to semi/ring porous species, whereas most xylem traits were not significantly different between diffuse porous and semi/ring porous species (Fig. 3.4). However, when comparing the differences in traits between diffuse porous and semi/ring porous species (excluding tropical species), we found that AP and VMD were not significantly different, while diffuse porous species did have lower SXHC and NSC than that of semi/ring porous species (Fig. S3.6). When dividing species in apotracheal AP and paratracheal AP species according to AP arrangement, species with apotracheal AP had higher RP in both stems and roots and higher WD in stems compared to species with paratracheal AP. In addition, species with paratracheal AP had larger vessels and greater SXHC in stems (Fig. S3.7). When focusing on temperate and Mediterranean species, neither apotracheal AP nor paratracheal AP showed a significant difference between diffuse-porous species and semi/ring porous species in stems, but semi/ring porous species did possess more apotracheal AP in roots (Fig. S3.6).

3.3.3 Multiple trade-offs in stem and root xylem

We found strong coordination patterns among traits both in stem and root xylem across all 60 species (Spearman, Fig. 3.1A, C). In particular, WD showed significant and positive correlations with RP, AP and RAP in stem xylem, but only with AP and RAP in root xylem,

while negative correlations with VF, VMD and SXHC were found in both stems and roots (Fig. 3.1A, C). Surprisingly, we did not find a significant correlation between WD and FFT, nor NSC, in either stem or root xylem (Fig. 3.1A, C). NSC and SS were significantly and positively correlated with RP, AP, and RAP, while starch was only positively correlated with RP and RAP in stem xylem (Fig. 3.1A). NSC and SS were positively related to RP and RAP, but starch was not correlated with RP, AP and RAP in roots (Fig. 3.1C). Additionally, NSC and starch were both significantly and positively associated with SXHC in stem xylem, whereas in roots, negative correlations were found between NSC, ST and SXHC (Fig. 3.1A, C). RAP and RP were significantly and negatively related to SXHC in stems, but in roots, AP showed a contrasting trend to RP (Fig. 3.1A, C).

PCAs were also conducted to elucidate multivariate relationships among stem and root xylem traits simultaneously (Fig. 3.2). For stem xylem, the first axis explained 34.2% of the variation, associating with VMD, MHD, SXHC, ST, VD and RP, while the second axis explained 20.5% of the variation, associating with AP, FFT, WD, SS and VF (Fig. 3.2A). For root xylem, the first axis described 35.0% of the variation, showing loadings for VMD, MHD, SXHC, FFT, SS, ST and RP, whereas the second axis described 17.0% of the variation, showing loads for VF, AP, WD and VD (Fig. 3.2C).

The result of SEM confirmed that there were trade-offs between WD and SXHC in both stem and root xylem, and the correlation patterns between SXHC and NSC were contrasting (Fig. 3.5). Additionally, both AP and RP were positively related with NSC in stems (Fig. 3.5A), while only RP was positively related with NSC in roots (Fig. 3.5B). The framework constructed by the SEM showed that WD was not related to NSC in both stems and roots (Fig. 3.5).

Relationships between certain xylem traits were different among climates and between the category of vessel porosity. There were significant correlations between WD and RAP of both stems and roots in temperate and Mediterranean species, but not for tropical species (Fig. 3.6B). Wood density in the stem was significantly related to stem RAP only in diffuse porous species (Fig. 3.6C). Similarly, stem WD was only correlated with stem SXHC in diffuse porous species (Fig. 3.7C). Root WD was only correlated with root SXHC in temperate and Mediterranean species (Fig. 3.7E). Moreover, the significant correlations between stem NSC and stem SXHC were only found in temperate and semi/ring porous species (Fig. 3.8B, C). We did not find any significant correlations between stem NSC and stem RAP in temperate and semi/ring porous species (Fig. S3.8B, C). Additionally, there were also no significant correlations between root NSC and root RAP in Mediterranean and tropical species (Fig. S3.8E). There were no significant correlations between WD and NSC in both stems and roots with all species pooled together, but significant relationships appeared in Mediterranean species (Fig. S3.9E).

3.4 DISCUSSION

We show that there is a trade-off among xylem traits that reflects the dominant functions provided by stems and roots, and that this trade-off is influenced by climate. Phylogenetic trends affected xylem traits, but was not the main factor impacting the coordination of trade-offs, corroborating our first hypothesis. Species with diffuse porous xylem (when excluding tropical tree species) generally had less NSC and lower hydraulic conductivity, compared to ring- and semi- porous species. However, we found no relationship between stem apotracheal and paratracheal AP design and porosity (diffuse, ring- and semi- porous species) in species from temperate and Mediterranean climates, refuting our second hypothesis. In agreement with our third hypothesis, we found that wood density was positively related to parenchyma

fraction in both stems and roots, but was negatively correlated with vessel fraction and hydraulic conductivity. The total parenchyma fractions were more abundant in roots than in stems in all species examined, providing roots with a greater capacity to store NSC.

3.4.1 Effect of phylogenetic trends on xylem traits and the coordination of trade-offs

Among the 60 angiosperm species in our study, wood density, vessel traits, hydraulic conductivity and NSC showed clear phylogenetic signals in the stem, while together with the traits mentioned above, parenchyma fractions in root also showed similar signals. Our results were consistent with Preston *et al.* (2006) who also found wood density and vessel traits exhibited significant phylogenetic signals in the stems of 51 angiosperm species. The phylogenetic conservatism of wood density in stems means that more closely related species would have similar wood density than less closely related species (Swenson and Enquist, 2007; Chave *et al.*, 2009). Additionally, the clear phylogenetic signals in vessel traits underline the major trends of secondary xylem evolution established by the Bailey school (Bailey, 1944), which further illustrates the effect of phylogenetic trends in wood anatomy. Sanchez-Martinez *et al.* (2020) also found a clear pattern of phylogenetic conservatism for hydraulic traits including stem hydraulic conductivity, which indicated that the legacy of traits existing in the evolutionary ancestors of species is thought to be an important determinant of traits in extant species. Although these xylem traits reflect their phylogenetic significance, the associations among traits in our study did not change much according to the PIC analyses. This result suggests that shared ancestry cannot explain correlation patterns among xylem traits, revealing that the tightly linked evolutionary relationship and co-evolution among xylem traits, can be partly interpreted as a result of ecological adaptations for water transport and mechanical support (Sperry, 2003).

3.4.2 Variations in xylem traits in stems and roots across climates

We showed that wood density in both the stems and root xylem of temperate species was lower than that in species from other climates. However, the variability in data from tropical species was high and the range of density values was large, as also found by Wiemann and Williamson (2002). The total parenchyma and axial parenchyma fraction were more abundant in roots than in stems in all species examined, providing roots with a greater capacity to store NSC (Plavcová *et al*., 2016; Zhang *et al*., 2022a). In agreement with Morris *et al.* (2016), we also found that the total parenchyma fraction was greater in tropical species than in temperate and Mediterranean species, which was mainly due to the increase in axial rather than radial parenchyma. Tropical species had larger vessels in both stems and roots, increasing hydraulic conductivity. However, vessels were less numerous than in species from other climates. In contrast, Mediterranean species had the lowest hydraulic conductivity in stem and root xylem, due mainly to smaller vessels, even though vessel density was greater than in trees from the other climates. As water is a limiting factor for tree growth in the Mediterranean region (Nardini *et al*., 2014), reduced hydraulic conductivity will decrease the likelihood of drought-induced embolism (Gleason *et al*., 2016). The climate in tropical French Guyana is moist and warm, therefore, the risk of drought- or freeze/thaw- induced embolism is negligible, and vessel size can be maximal for enhanced water uptake.

Root NSC content was always higher than that in the stem, as also found by Martínez-Vilalta *et al*., (2016), Smith *et al*., (2018b) and Furze *et al*., (2020). A high NSC content in roots allows for fast root growth in the spring, improving the supply of water and nutrients necessary for budburst or leafing out (Abramoff and Finzi, 2015). Mediterranean species had more NSC in roots, that will aid the recovery of hydraulic conductivity if embolism occurs (Yoshimura *et al.*, 2016; Kono *et al.*, 2019), especially during long dry periods. In agreement

with Martínez-Vilalta *et al.*, (2016), we did not find a significant difference among the three climates with regard to total NSC in stems. However, tropical species had less NSC in roots, possibly because they allocate more carbon for growth and respiration, resulting in a lower overall NSC (Körner, 2003; Martínez-Vilalta *et al.*, 2016).

The inherent xylem design (ring, semi- and diffuse porous; apotracheal and paratracheal AP) also impacted xylem traits. For example, species with diffuse porous xylem (when excluding tropical tree species) had less NSC and lower hydraulic conductivity, compared to semi/ring porous species. Most tropical species had diffuse porous xylem with wide vessels throughout the xylem, while semi/ring porous species had large vessels in the earlywood only, enhancing hydraulic efficiency after winter dormancy (Boura and De Franceschi, 2007). The radial distribution of stem NSC can be influenced by vessel porosity (Barbaroux and Bréda, 2002; Furze *et al*., 2020) and the seasonal fluctuation of NSC deeper in the sapwood may explain why NSC patterns differ between diffuse and semi/ring porous species (Furze *et al*., 2020). Additionally, ring porous species need high levels of NSC to assure the production of new and large earlywood vessels, especially as the previous year's vessels may have been embolized by frost events during the winter. Diffuse porous species are less sensitive to winter embolism and thus the recovery of hydraulic conductivity is less dependent on stored carbon (Barbaroux and Bréda, 2002). We found that tropical diffuse porous species always had more axial parenchyma in stems, confirming the close relationship with vessel diameter (Morris *et al*., 2018). However, in diffuse porous and semi/ring porous species from temperate and Mediterranean climates, we found no differences in stem apotracheal and paratracheal AP design, refuting our second hypothesis. Surprisingly, species with apotracheal AP usually had more radial parenchyma compared to those with paratracheal AP, therefore increasing radial strength and providing a connective pathway between isolated apotracheal cells and vessels (da Costa *et al*., 2020). Species with paratracheal AP had wider vessels in the stem, revealing

the roles of paratracheal AP in xylem water transport, as also found in other studies (Morris *et al*., 2018; Aristsara *et al*., 2021).

3.4.3 Association among xylem traits and structure-function trade-offs in stems and roots

Wood density is an indicator of the mechanical integrity of xylem and is linked to multiple anatomical traits (Jacobsen *et al.*, 2007; Martínez-Cabrera *et al.*, 2009; Ziemińska *et al.*, 2013). In both stems and roots, we found that wood density was positively correlated with total parenchyma fraction, but not with fibre (including fibre-tracheids and tracheids) fractions. Previous studies have showed that wood density was not related to total fibre fraction, but was positively correlated with fibre wall fraction and negatively with fibre lumen fraction (Ziemińska *et al.*, 2013; Janssen *et al.*, 2020). Positive relationships between wood density and parenchyma content have also been shown in previous studies (Woodrum *et al.*, 2003; Martínez-Cabrera *et al.*, 2009; Rana *et al.*, 2009; Zhang *et al*., 2022a). Additionally, xylem axial parenchyma are relatively thin-walled tissues and would influence wood density depending on the axial parenchyma fraction relative to fibre lumen fraction, which means wood with a high proportion of axial parenchyma would have narrow fiber lumen (Martínez-Cabrera *et al.*, 2009). Another possible explanation for the positive relationship between wood density and total parenchyma fraction is that radial parenchyma is usually strongly lignified and high lignin content increases wood density (Rana *et al.*, 2009; Zhang *et al*., 2022a). However, this positive relationship was only found in temperate and Mediterranean species, possibly because both wood density and RAP of tropical species are highly variable compared to species from other climates. As expected from our third hypothesis, we also found negative relationships between wood density and vessel fraction, vessel mean diameter and SXHC in both stems and roots, implying that there is a trade-off between mechanical integrity and hydraulic conductivity, as also found by several authors (Smith and Ennos, 2003; Christensen-

Dalsgaard *et al.*, 2007a,b; McCulloch *et al.*, 2011; Janssen *et al.*, 2020). Wood density could be used as a proxy for the hydraulic properties of xylem (Markesteijn *et al.*, 2011; Hoeber *et al.*, 2014), as hydraulic conductivity is proportional to vessel diameter to the fourth power, thus species with wide vessels have high SXHC and reduced wood density. Similarly, dense wood should have denser cell packing with narrower vessel lumens and low SXHC (Markesteijn *et al.*, 2011; Zanne *et al.*, 2010). It is also assumed that dense tissues reduce hydraulic efficiency of xylem containing narrow vessels with thick walls, because thicker walls will increase the path length through the pits where sap flows between vessels (Lens *et al.*, 2011; Pratt *et al.*, 2021a). However, the trade-off between wood density and hydraulic conductivity does not seem to be universally valid as other studies failed to find any trade-off (Pratt *et al.*, 2007; Martínez-Cabrera *et al.*, 2009; Poorter *et al.*, 2010a; Schuldt *et al.*, 2013), which was also the case in our study, when examining stems within each climate type. The possible explanation may be that compared to vessel traits, other properties that could drive wood density such as fibre wall thickness may not directly affect hydraulic conductivity (Hoeber *et al.*, 2014; Ziemińska *et al.*, 2013; Badel *et al.*, 2015).

As expected, we confirmed that both radial and axial parenchyma fractions were positively correlated with NSC content in the stem (Plavcová *et al.*, 2016; Kawai *et al.*, 2021; Zhang *et al.*, 2022a). However, we did not find significant relationships between axial parenchyma and NSC in roots, suggesting that either NSC stores were depleted in roots due to seasonal growth, or that axial parenchyma performs other functions, such as hydraulic transport and hydraulic optimization (Morris *et al.*, 2018; Aritsara *et al.*, 2021). When evaluating the relationships between stem NSC and RAP in each climate, we found no relationships in temperate species, which was contrary to our expectations, and again may be explained by the seasonal variation of NSC stocks (Smith *et al.*, 2018a; Furze *et al.*, 2020). Additionally, NSC could be involved in the reversal of embolism, especially for trees growing in temperate regions that are

susceptible to freeze–thaw induced xylem embolism (Nardini *et al*., 2011; Sala *et al*., 2012). The use of NSC for growth and reproduction could also lead to variations in NSC (Wiley *et al*., 2013; Klein and Hoch, 2015), resulting in a weakened relationship with RAP. Multiple sampling should be performed over several years to fully appreciate NSC fluctuations in diverse conditions. Furthermore, partially in agreement with our third hypothesis, we found contrary patterns between NSC and SXHC in stems and roots, which indicated that a greater NSC storage capacity was associated with high hydraulic conductivity in stems, but with low hydraulic conductivity in roots. This opposing strategy may be related to the different functions performed by radial parenchyma and axial parenchyma in the root and stem (Zheng and Martínez-Cabrera, 2013; Secchi *et al.*, 2017; Aritsara *et al.*, 2021). In agreement with Morris *et al.* (2018), our results confirmed that a large axial parenchyma fraction was associated with wider vessels, revealing the important role of axial parenchyma in xylem water transport. In contrast, radial parenchyma was negatively correlated with vessel mean diameter and hydraulic conductivity, demonstrating the functional differentiation of axial and radial parenchyma in xylem hydraulic efficiency (Zheng and Martínez-Cabrera, 2013). Therefore, in stems, both radial and axial parenchyma contribute to NSC storage, while in roots, axial parenchyma serves more a supportive role for support hydraulic functioning.

3.5 CONCLUSION

We evaluated the coordination in trade-offs among xylem traits across 60 angiosperm tree species in three distinct climates. By examining the changes in the design of the xylem space in stems and roots of the same individuals, we found that Mediterranean species tend to have smaller vessels and lower hydraulic conductivity but greater wood density, while temperate and tropical species usually had lower wood density but greater hydraulic conductivity, suggesting that the major functions of each cell within the xylem space changes depending on

climate. Semi/ring porous species had large vessels associated with axial parenchyma in the earlywood, enhancing hydraulic efficiency. Wood density was positively correlated with parenchyma fractions in both stems and roots across climates, but was negatively correlated with vessel size and fractions, revealing a trade-off between mechanical integrity and hydraulic conductivity. Additionally, NSC storage capacity in stems was positively associated to hydraulic conductivity, but negatively in roots due to the different roles of radial and axial parenchyma. Furthermore, our study provides strong evidence of phylogenetic trends in wood density, vessel traits, hydraulic conductivity and NSC quantity, whereas the coordination among these different traits was not affected by evolutionary history.

TABLES

Table 3.1 Summary of previous studies on trade-offs between xylem structure and function.

Study site	Plant form	Stage	Organ	Hydraulic function	Mechanical function	Storage function	Species number	References
Michigan	Tree	Adult	Branch	√	√		5	Woodrum et al., 2003
New Zealand, New Caledonia, USA, Bahamas	Tree	Adult	Branch, Root	√	√		18	Pittermann et al., 2006
California	Tree	Adult	Branch	√	√		51	Preston et al., 2006
French Guiana	Tree	Adult	Root	√	√		2	Christensen-Dalsgaard et al.,2007a
French Guiana	Tree	Adult	Stem, Root	√	√		5	Christensen-Dalsgaard et al.,2007b
South Africa	Shrub	Adult	Stem	√	√		17	Jacobsen et al., 2007
California	Shrub	Adult	Stem, Root	√	√	√	9	Pratt et al., 2007
Germany	Tree	Seedling	Stem	√	√		1	Rosner et al., 2007
North and South America	Shrub	Adult	Stem	√	√		61	Martínez-Cabrera et al., 2009
Philippines	Tree	Seedling	Stem	√	√		5	Rana et al., 2009
Panama, Oregon, Minnesota	Tree	Seedling	Branch Stem	√			16	McCulloh et al., 2010
Bolivia	Tree	Adult	Stem	√	√		42	Poorter et al., 2010a
Global	Angiosperms	Adult	Stem	√	√		2230	Zanne et al., 2010
Bolivia	Tree	Seedling	Stem	√	√		40	Markesteijin et al., 2011
Argentina, Mexico, USA	Tree, Shrub	Adult	Stem	√	√		200	Martínez-Cabrera et al., 2011
China	Tree	Adult	Woody tissue	√	√		316	Zhang et al., 2013
China	Tree	Adult	Stem	√	√		800	Zheng and Martínez-Cabrera 2013
Australia	Tree, Shrub	Adult	Branch	√	√		24	Ziemińska et al., 2013
French Guiana	Tree	Adult	Branch, Root	√	√		113	Fortunel et al., 2014
Costa Rica	Tree	Seedling	Stem	√	√		8	Hoeber et al., 2014

Indonesia	Tree	Adult	Stem, Root	√	√		6	Kotowaka et al., 2015
Global	Angiosperms, Gymnosperms	Adult	Branch	√	√		424	Gleason et al., 2016
California	Shrub	Adult	Branch	√	√		8	Jacobsen et al., 2016
Germany	Tree	Adult	Branch, Root	√			5	Jupa et al., 2016
Argentina	Tree	Adult	Branch	√	√		1	Barotto et al., 2018
China	Tree	Adult	Branch	√		√	1	Wang et al., 2018b
Germany	Tree	Adult	Stem, Root	√	√	√	9	Plavová et al., 2019
Italy	Tree	Adult	Branch	√		√	12	Trifilò et al.,2019
China	Tree	Adult	Branch	√		√	19	Chen et al., 2020
Amazon Basin, Guianas, Central America	Tree	Adult	Branch, Stem	√	√		3909	Janssen et al., 2020
Massachusetts	Tree	Adult	Branch	√	√		30	Ziemińska et al., 2020
Madagasar	Tree, Liana	Adult	Branch	√	√		28	Aritsara et al., 2021
China	Shrub	Adult	Stem	√		√	24	Jiang et al., 2021
Japan	Tree	Adult	Branch	√		√	15	Kawai et al., 2021
French Guiana	Tree	Adult	Branch	√	√		42	Levionnois et al., 2021
California	Shrub	Adult	Branch	√	√	√	29	Pratt et al., 2021a
California	Shrub	Adult	Branch	√		√	36	Pratt et al., 2021b

Table 3.2 Comparison of stem and root xylem traits from 180 individual trees across 60 species.

			Stem					Root					
Trait	Abbrev.	Unit	Min	Max	Mean	SD	CV	Min	Max	Mean	SD	CV	*P-value*
Wood density	WD	g cm^{-3}	0.239	0.846	0.560	0.122	21.87	0.235	0.883	0.507	0.126	24.94	***P*<0.001**
Radial parenchyma fraction	RP	-	0.039	0.288	0.127	0.051	40.15	0.049	0.366	0.138	0.062	44.98	*P*>0.05
Axial parenchyma fraction	AP	-	0.007	0.213	0.055	0.039	70.71	0.010	0.457	0.085	0.084	99.26	***P*<0.01**
Total Parenchyma fraction	RAP	-	0.053	0.395	0.181	0.064	35.38	0.075	0.648	0.223	0.101	45.14	***P*<0.001**
Fiber with tracheids fraction	FFT	-	0.474	0.877	0.691	0.083	11.94	0.267	0.883	0.667	0.108	16.28	*P*>0.05
Vessel fraction	VF	-	0.019	0.391	0.128	0.075	58.71	0.016	0.327	0.110	0.069	62.18	***P*<0.05**
Vessel mean diameter	VMD	μm	16.43	216.36	75.43	41.72	55.30	20.00	218.32	73.74	34.02	46.13	*P*>0.05
Vessel density	VD	n mm^{-2}	1.300	451.77	57.96	71.01	122.51	2.302	270.51	33.71	33.10	98.18	***P*<0.05**
Vessel mean hydraulic diameter	MHD	μm	17.11	233.03	87.12	45.31	52.00	20.87	230.84	82.88	38.52	46.48	*P*>0.05
Specific xylem hydraulic conductivity	SXHC	kg m^{-1} MPa^{-1} s^{-1}	0.812	460.05	48.47	73.53	151.73	0.452	459.18	37.11	52.77	142.19	*P*>0.05
Soluble sugars content	SS	mg g^{-1}	1.219	43.35	16.38	7.98	48.73	2.837	106.37	29.91	16.99	56.82	***P*<0.001**
Starch content	ST	mg g^{-1}	0.376	110.93	32.37	20.25	62.55	7.149	360.26	105.96	67.60	63.81	***P*<0.001**
Total NSC content	NSC	mg g^{-1}	7.581	120.91	49.06	22.61	46.11	21.34	376.39	135.12	74.25	54.96	***P*<0.001**

Note: Abbrev. is abbreviation, Min is minimum, Max is maximum, SD is standard deviation, CV is coefficient of variation, *P-value* indicates the difference between stem and root xylem traits and the significance level was set as $P<0.05$.

Table 3.3 Blomberg's K values for 13 xylem traits of stem and root across 60 species.

	Stem		Root	
Xylem trait	Blomberg's K	*P-value*	Blomberg's K	*P-value*
WD	0.08	**0.018**	0.09	**0.027**
RP	0.07	0.073	0.08	**0.013**
AP	0.06	0.105	0.08	**0.014**
RAP	0.06	0.113	0.07	**0.017**
FF	0.06	0.182	0.05	0.440
VF	0.09	**0.004**	0.06	0.386
VMD	0.09	**0.001**	0.12	**0.001**
VD	0.09	**0.001**	0.08	**0.007**
MHD	0.10	**0.003**	0.13	**0.001**
SXHC	0.10	**0.013**	0.10	**0.004**
SS	0.05	0.461	0.05	0.732
ST	0.10	**0.038**	0.08	**0.004**
NSC	0.09	**0.020**	0.07	**0.044**

Note: The significance level was set at $P<0.05$, and shown in bold. See table 3.2 for trait abbreviation.

FIGURES

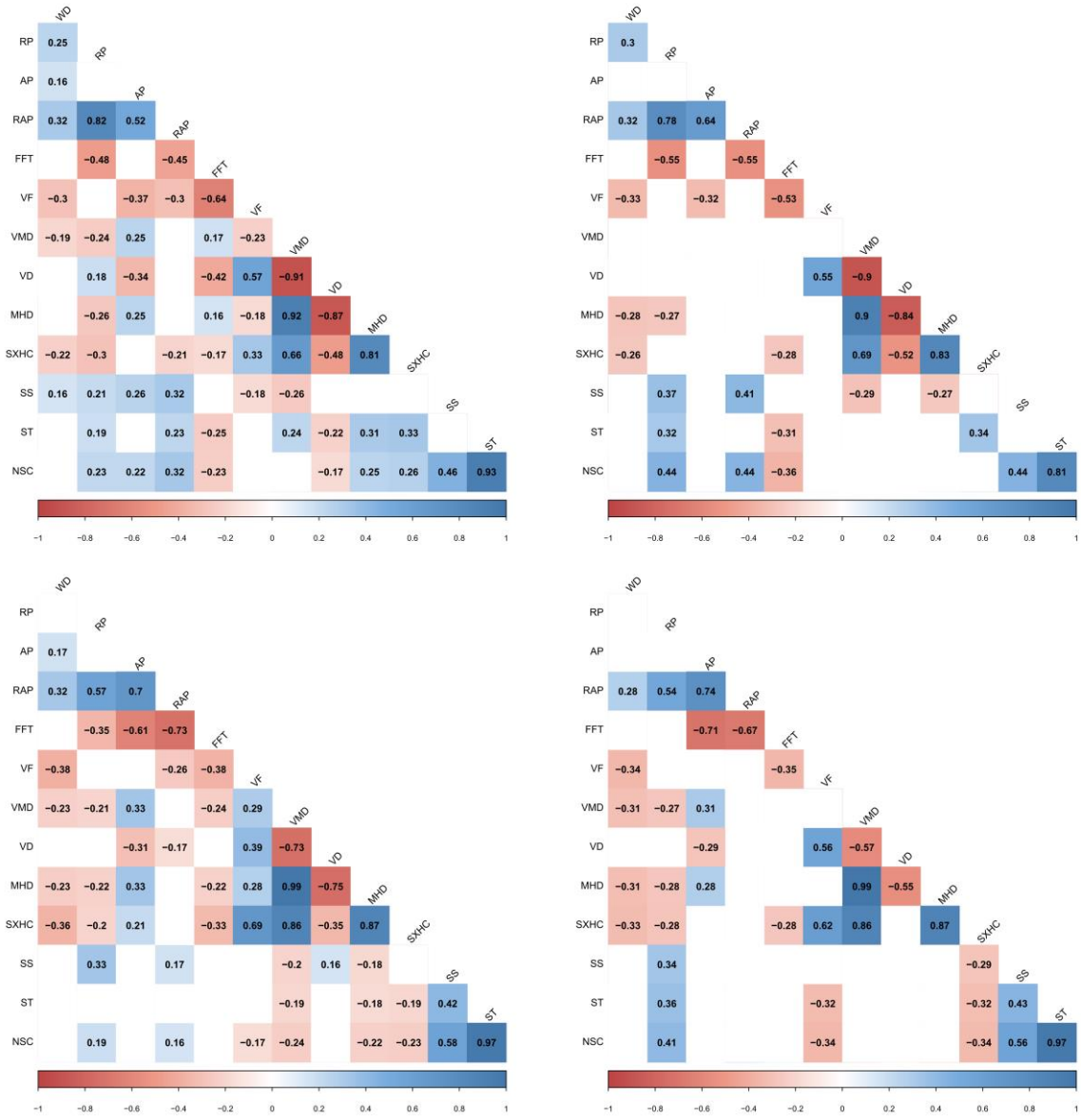

Fig. 3.1 Spearman correlations without and with phylogenetically independent contrasts (PICs) of xylem traits among 60 species for (A, B) stem and (C, D) root. Colored squares indicate significant correlation (blue, positive correlation; red, negative correlation). See Table 3.2 for trait abbreviation.

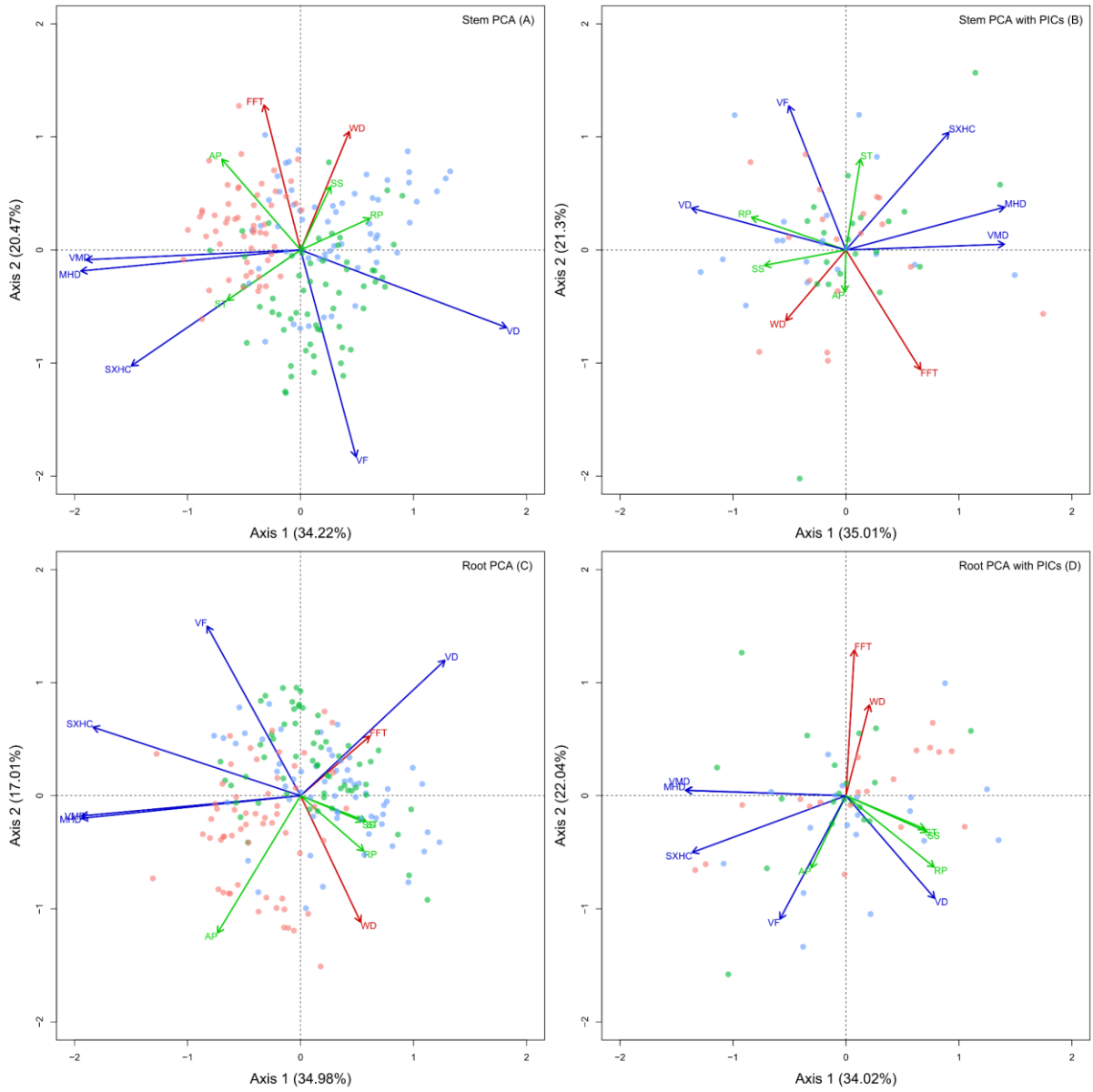

Fig. 3.2 Principal component analysis (PCA) without and with phylogenetically independent contrasts (PICs) of xylem traits among 60 species for (A, B) stem and (C, D) root. Colored dots indicate tree species from different climates (green, temperate species; blue, Mediterranean species; red, tropical species). See Table 3.2 for trait abbreviation.

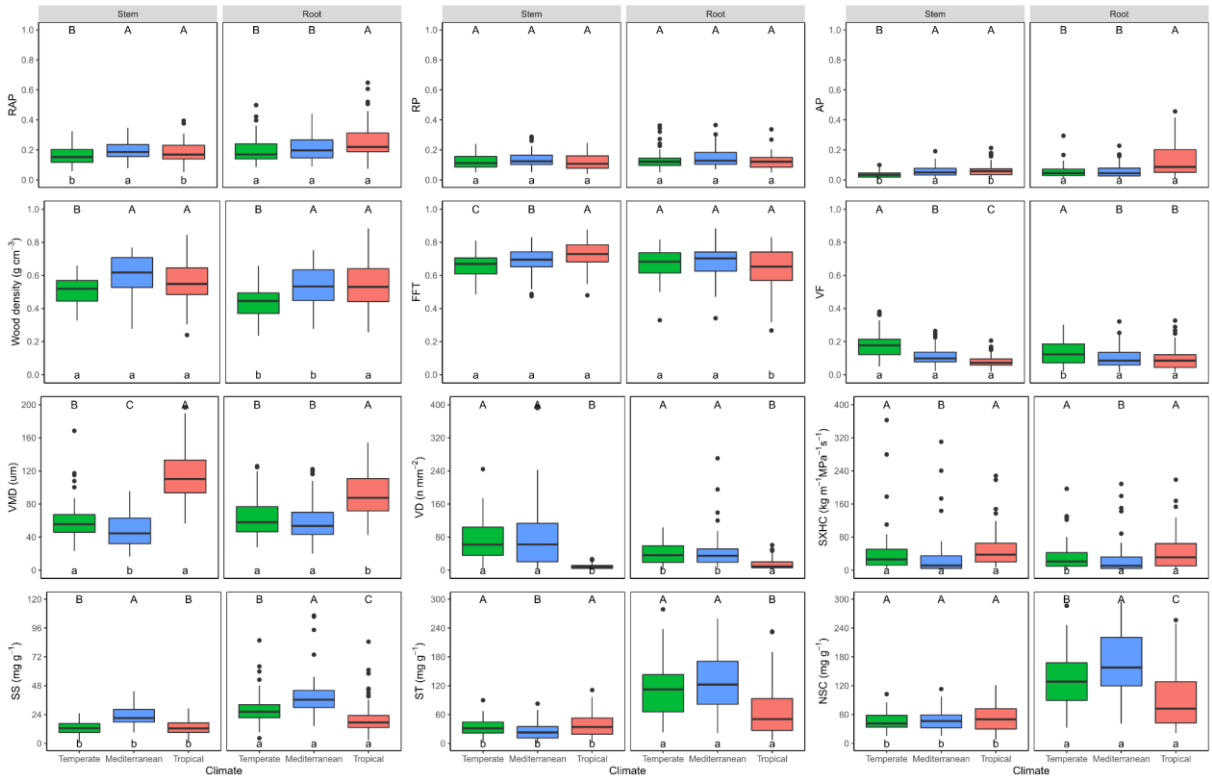

Fig. 3.3 Boxplot of stem and root xylem traits across three climates. The line in the box indicates the median; the whiskers above and below the box indicate the 75th and 25th percentiles. Different uppercase letters indicate significant differences between climates for a given xylem trait in the same organ. Different lowercase letters indicate significant differences between organs for a given xylem trait in the same climate. Colors indicate three climates (green, temperate climate; blue, Mediterranean climate; red, tropical climate). See Table 3.2 for trait abbreviation.

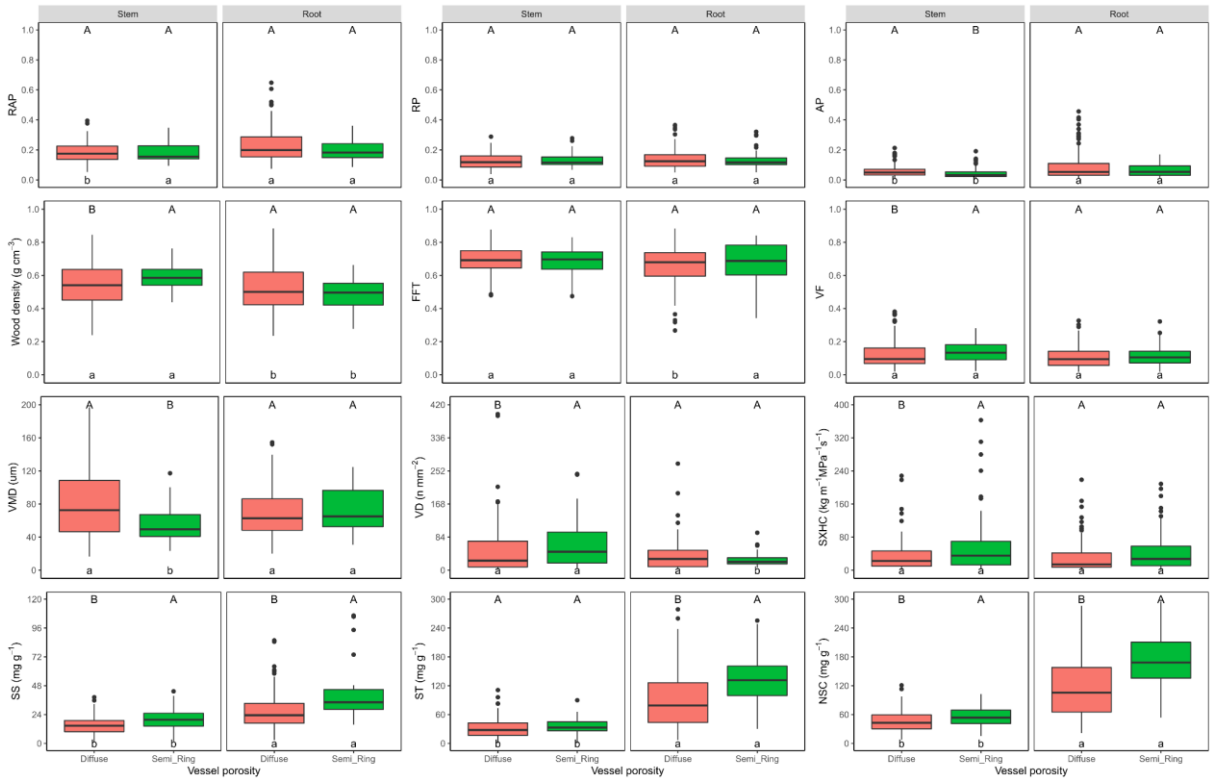

Fig. 3.4 Boxplot of stem and root xylem traits between diffuse-porous and Semi-Ring-porous species. The line in the box indicates the median; the whiskers above and below the box indicate the 75th and 25th percentiles. Different uppercase letters indicate significant differences between the two porosity groups for a given xylem trait in the same organ. Different lowercase letters indicate significant differences between organs for a given xylem trait in the same porosity group. Colors indicate two porosity groups (red, diffuse-porous species; green, Semi-Ring-porous species). See Table 3.2 for trait abbreviation.

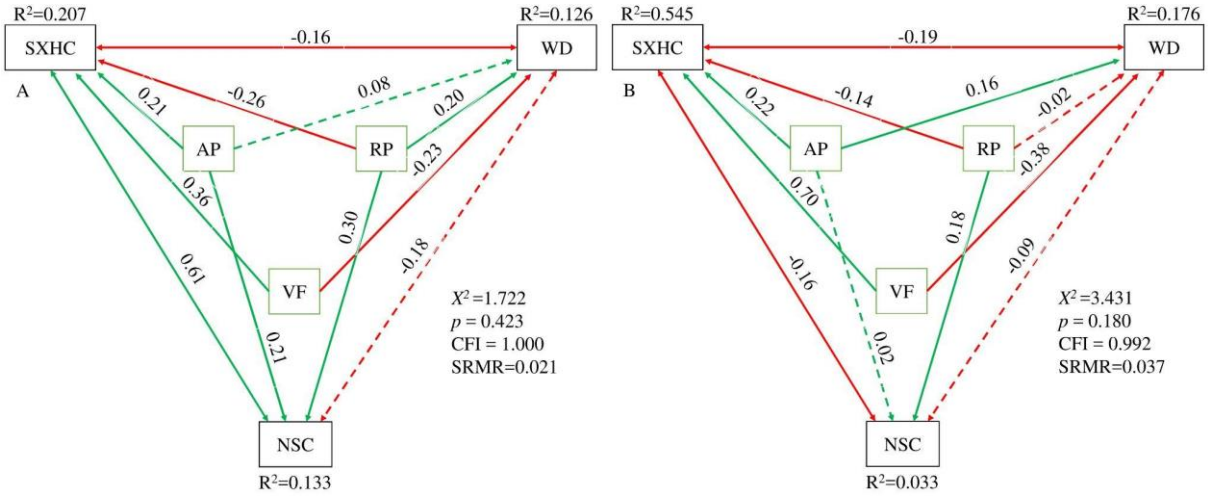

Fig. 3.5 Structural equation model (SEM) for displaying trade-offs among xylem traits of stem (A) and root (B) across 60 species. Solid arrows represent significant paths ($p < 0.05$), while dotted arrows represent non-significant paths. The red lines indicate negative correlations, and the green lines indicate positive correlations. For each path, the standardized regression coefficient is shown. The variance explained (R^2) is shown for SXHC, WD and NSC. Several model-fit statistics are shown, including chi-square (X^2), p value, the comparative fit index (CFI) and standardized root mean square residual (SRMR). See Table 3.2 for trait abbreviation.

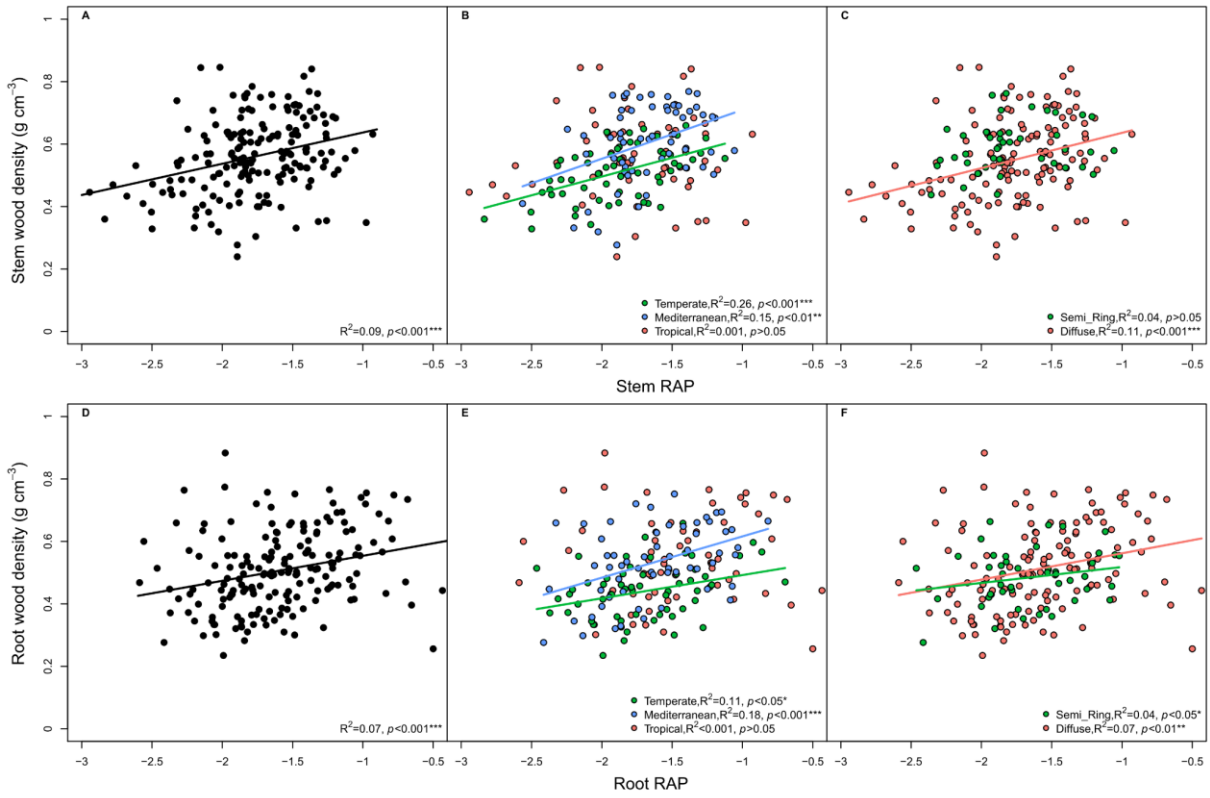

Fig. 3.6 Relationships between wood density and RAP fractions in stems (A, B, C) and roots (D, E, F) with all species pooled and across climates and vessel porosity. Diffuse means the category of porosity is diffuse porous. Semi_Ring means the category of porosity is semi/ring porous. See Table 3.2 for trait abbreviation.

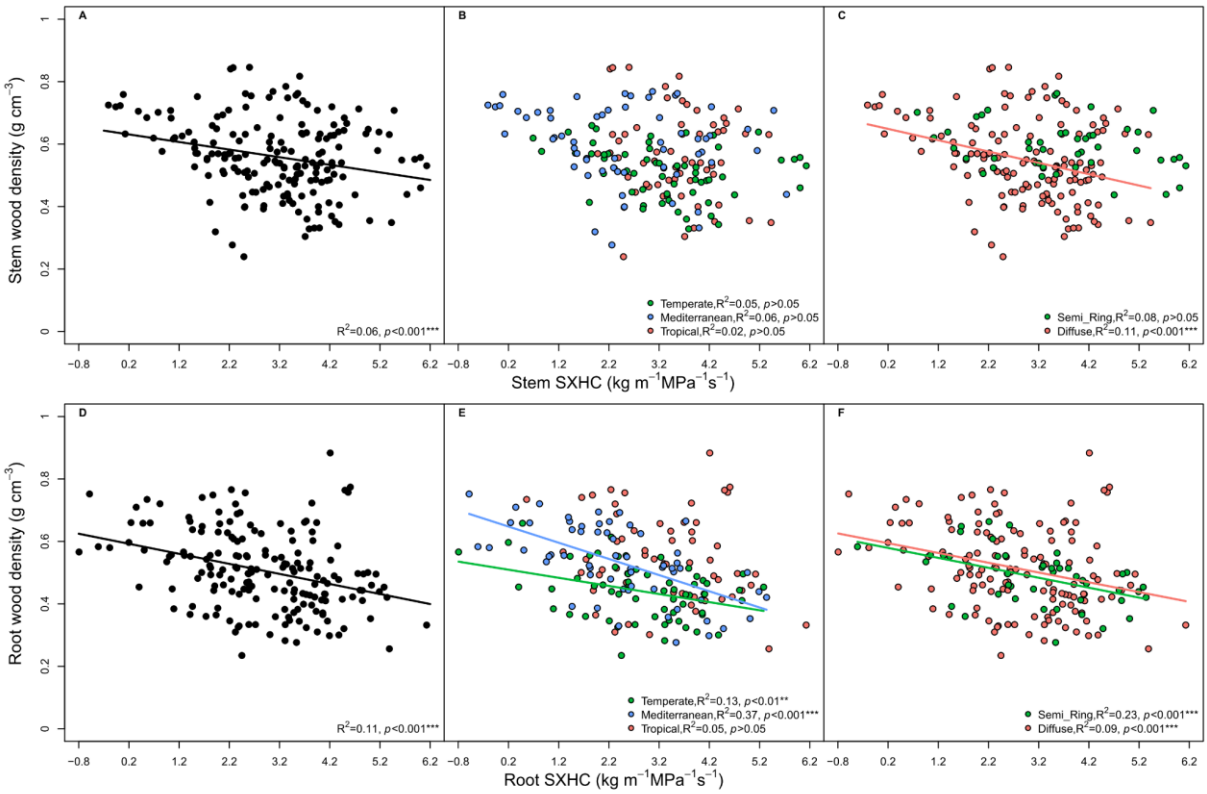

Fig. 3.7 Relationships between wood density and SXHC in stems (A, B, C) and roots (D, E, F) with all species pooled and across climates and vessel porosity. Diffuse means the category of porosity is diffuse porous. Semi_Ring means the category of porosity is semi/ring porous. See Table 3.2 for trait abbreviation.

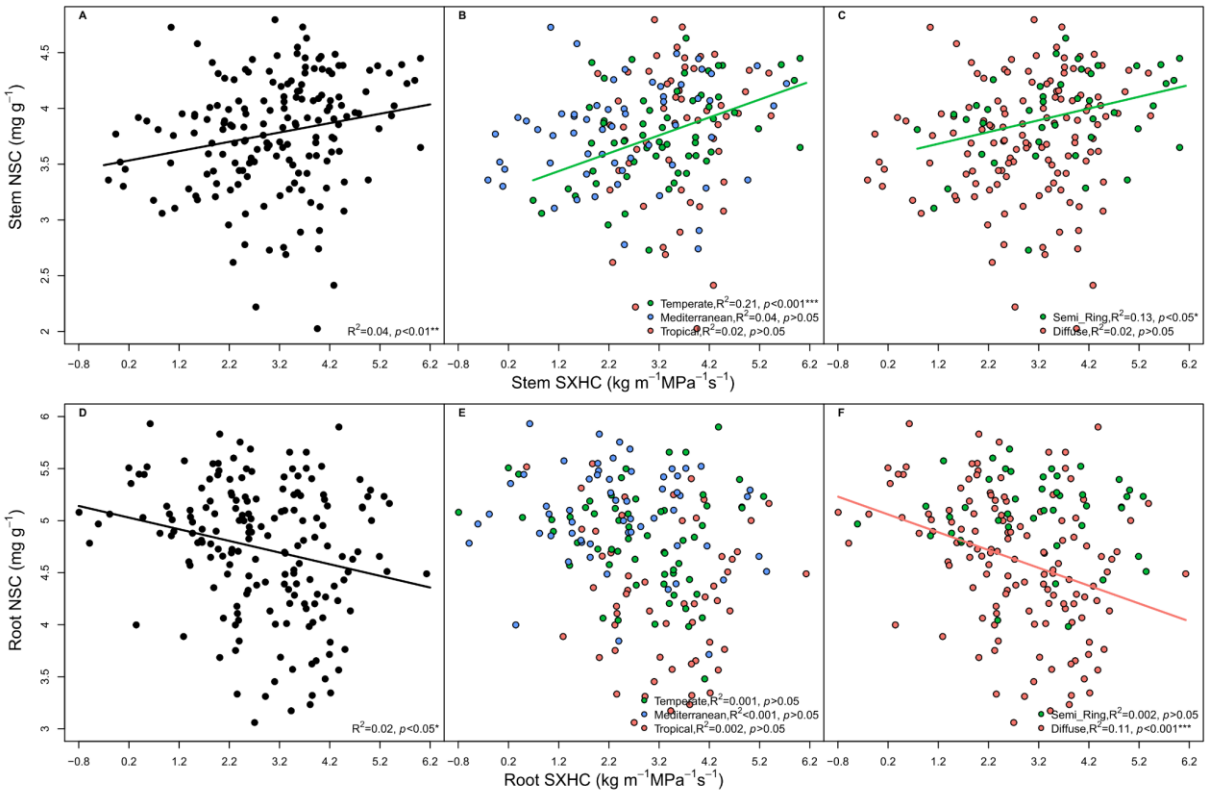

Fig. 3.8 Relationships between NSC and SXHC in stems (A, B, C) and roots (D, E, F) with all species pooled and across climates and vessel porosity. Diffuse means the category of porosity is diffuse porous. Semi_Ring means the category of porosity is semi/ring porous. See Table 3.2 for trait abbreviation.

SUPPLEMENTARY MATERIALS

Table S3.1 Tree species list with diameter at breast height (DBH), GPS coordinate and categories.

Family	Genus	Species	Tree number	DBH (cm)	Latitude	Longitude	Climate	AP arrangement	Porosity
Betulaceae	Alnus	Alnus glutinosa	1	17.3	43.1378	0.0592	Temperate	Apotracheal	Diffuse
Betulaceae	Alnus	Alnus glutinosa	2	15.8	43.1388	0.0556	Temperate	Apotracheal	Diffuse
Betulaceae	Alnus	Alnus glutinosa	3	33.6	43.1384	0.0554	Temperate	Apotracheal	Diffuse
Betulaceae	Alnus	Alnus incana	1	21.5	42.9896	-0.0742	Temperate	Apotracheal	Diffuse
Betulaceae	Alnus	Alnus incana	2	27.5	42.9881	-0.0735	Temperate	Apotracheal	Diffuse
Betulaceae	Alnus	Alnus incana	3	15.1	42.9881	-0.0736	Temperate	Apotracheal	Diffuse
Sapindaceae	Acer	Acer pseudoplatanus	1	16.6	42.9508	-0.0699	Temperate	Apotracheal	Diffuse
Sapindaceae	Acer	Acer pseudoplatanus	2	20.7	42.9858	-0.0724	Temperate	Apotracheal	Diffuse
Sapindaceae	Acer	Acer pseudoplatanus	3	10.7	42.9851	-0.0724	Temperate	Apotracheal	Diffuse
Buetulaceae	Betula	Betula pendula	1	15.0	43.1392	0.0544	Temperate	Apotracheal	Diffuse
Buetulaceae	Betula	Betula pendula	2	36.2	43.1396	0.0540	Temperate	Apotracheal	Diffuse
Buetulaceae	Betula	Betula pendula	3	34.2	43.1398	0.0542	Temperate	Apotracheal	Diffuse
Fagaceae	Castanea	Castanea sativa	1	38.8	43.1384	0.0570	Temperate	Apotracheal	Semi_ring
Fagaceae	Castanea	Castanea sativa	2	28.7	43.1386	0.0576	Temperate	Apotracheal	Semi_ring
Fagaceae	Castanea	Castanea sativa	3	31.7	43.1382	0.0566	Temperate	Apotracheal	Semi_ring
Oleaceae	Fraxinus	Fraxinus excelsior	1	18.3	43.1380	0.0590	Temperate	Paratracheal	Ring
Oleaceae	Fraxinus	Fraxinus excelsior	2	33.9	43.1380	0.0575	Temperate	Paratracheal	Ring
Oleaceae	Fraxinus	Fraxinus excelsior	3	28.1	43.1394	0.0528	Temperate	Paratracheal	Ring
Fagaceae	Fagus	Fagus sylvatica	1	31.8	42.9418	-0.0645	Temperate	Apotracheal	Diffuse
Fagaceae	Fagus	Fagus sylvatica	2	15.6	42.9420	-0.0656	Temperate	Apotracheal	Diffuse
Fagaceae	Fagus	Fagus sylvatica	3	16.8	42.9419	-0.0654	Temperate	Apotracheal	Diffuse
Aquifoliaceae	Ilex	Ilex aquifolium	1	10.0	43.1390	0.0562	Temperate	Apotracheal	Diffuse
Aquifoliaceae	Ilex	Ilex aquifolium	2	11.4	43.1389	0.0562	Temperate	Apotracheal	Diffuse
Aquifoliaceae	Ilex	Ilex aquifolium	3	8.8	43.1386	0.0561	Temperate	Apotracheal	Diffuse
Juglandaceae	Juglans	Juglans nigra	1	21.8	42.9861	-0.0725	Temperate	Apotracheal	Diffuse
Juglandaceae	Juglans	Juglans nigra	2	17.3	42.9860	-0.0725	Temperate	Apotracheal	Diffuse
Juglandaceae	Juglans	Juglans nigra	3	20.2	42.9854	-0.0724	Temperate	Apotracheal	Diffuse
Rosaceae	Prunus	Prunus avium	1	15.8	43.1397	0.0541	Temperate	Apotracheal	Diffuse

Rosaceae	Prunus	Prunus avium	2	18.2	43.1410	0.0530	Temperate	Apotracheal	Diffuse
Rosaceae	Prunus	Prunus avium	3	19.8	43.1410	0.0535	Temperate	Apotracheal	Diffuse
Rosaceae	Pyrus	Pyrus communis	1	12.0	43.1368	0.0600	Temperate	Paratracheal	Diffuse
Rosaceae	Pyrus	Pyrus communis	2	16.6	43.1370	0.0600	Temperate	Paratracheal	Diffuse
Rosaceae	Pyrus	Pyrus communis	3	15.9	43.1378	0.0590	Temperate	Paratracheal	Diffuse
Salicaceae	Populus	Populus nigra	1	39.1	42.9899	-0.0745	Temperate	Paratracheal	Diffuse
Salicaceae	Populus	Populus nigra	2	28.9	42.9879	-0.0734	Temperate	Paratracheal	Diffuse
Salicaceae	Populus	Populus nigra	3	41.4	42.9878	-0.0735	Temperate	Paratracheal	Diffuse
Rosaceae	Prunus	Prunus spinosa	1	11.1	43.0434	0.0470	Temperate	Apotracheal	Diffuse
Rosaceae	Prunus	Prunus spinosa	2	16.6	43.0434	0.0470	Temperate	Apotracheal	Diffuse
Rosaceae	Prunus	Prunus spinosa	3	10.9	43.0433	0.0471	Temperate	Apotracheal	Diffuse
Salicaceae	Populus	Populus tremula	1	23.8	43.1397	0.0559	Temperate	Paratracheal	Diffuse
Salicaceae	Populus	Populus tremula	2	35.2	43.1399	0.0538	Temperate	Paratracheal	Diffuse
Salicaceae	Populus	Populus tremula	3	19.4	43.1394	0.0538	Temperate	Paratracheal	Diffuse
Fagaceae	Quercus	Quercus petraea	1	17.0	42.9420	-0.0656	Temperate	Apotracheal	Semi_ring
Fagaceae	Quercus	Quercus petraea	2	18.3	42.9464	-0.0629	Temperate	Apotracheal	Semi_ring
Fagaceae	Quercus	Quercus petraea	3	26.0	42.9465	-0.0629	Temperate	Apotracheal	Semi_ring
Fagaceae	Quercus	Quercus robur	1	34.4	43.1386	0.0574	Temperate	Apotracheal	Semi_ring
Fagaceae	Quercus	Quercus robur	2	50.0	43.1381	0.0566	Temperate	Apotracheal	Semi_ring
Fagaceae	Quercus	Quercus robur	3	34.9	43.1383	0.0566	Temperate	Apotracheal	Semi_ring
Salicaceae	Salix	Salix alba	1	34.5	43.1387	0.0550	Temperate	Paratracheal	Diffuse
Salicaceae	Salix	Salix alba	2	36.3	43.1388	0.0551	Temperate	Paratracheal	Diffuse
Salicaceae	Salix	Salix alba	3	39.7	43.1389	0.0543	Temperate	Paratracheal	Diffuse
Salicaceae	Salix	Salix caprea	1	31.7	43.1389	0.0532	Temperate	Paratracheal	Diffuse
Salicaceae	Salix	Salix caprea	2	18.0	43.1393	0.0541	Temperate	Paratracheal	Diffuse
Salicaceae	Salix	Salix caprea	3	25.5	43.1390	0.0541	Temperate	Paratracheal	Diffuse
Adoxaceae	Sambucus	Sambucus nigra	1	14.0	43.1393	0.0524	Temperate	Paratracheal	Ring
Adoxaceae	Sambucus	Sambucus nigra	2	15.9	43.1387	0.0545	Temperate	Paratracheal	Ring
Adoxaceae	Sambucus	Sambucus nigra	3	14.9	43.1386	0.0556	Temperate	Paratracheal	Ring
Ulmaceae	Ulmus	Ulmus glabra	1	16.4	42.9419	-0.0650	Temperate	Paratracheal	Ring
Ulmaceae	Ulmus	Ulmus glabra	2	14.1	42.9427	-0.0656	Temperate	Paratracheal	Ring
Ulmaceae	Ulmus	Ulmus glabra	3	20.9	42.9427	-0.0656	Temperate	Paratracheal	Ring
Sapindaceae	Acer	Acer campestre	1	18.5	43.6494	3.8660	Mediterranean	Paratracheal	Diffuse
Sapindaceae	Acer	Acer campestre	2	16.9	43.6494	3.8660	Mediterranean	Paratracheal	Diffuse
Sapindaceae	Acer	Acer campestre	3	13.7	43.6494	3.8660	Mediterranean	Paratracheal	Diffuse
Sapindaceae	Acer	Acer monspessulanum	1	13.2	43.7133	4.0130	Mediterranean	Paratracheal	Diffuse
Sapindaceae	Acer	Acer monspessulanum	2	17.4	43.6718	3.7603	Mediterranean	Paratracheal	Diffuse

Sapindaceae	Acer	Acer monspessulanum	3	12.4	43.6719	3.7605	Mediterranean	Paratracheal	Diffuse
Ericaceae	Arbutus	Arbutus unedo	1	11.9	43.6718	3.7604	Mediterranean	Paratracheal	Semi_ring
Ericaceae	Arbutus	Arbutus unedo	2	10.4	43.6718	3.7604	Mediterranean	Paratracheal	Semi_ring
Ericaceae	Arbutus	Arbutus unedo	3	9.9	43.6718	3.7604	Mediterranean	Paratracheal	Semi_ring
Buxaceae	Buxus	Buxus sempervirens	1	5.1	43.6804	3.7563	Mediterranean	Apotracheal	Diffuse
Buxaceae	Buxus	Buxus sempervirens	2	5.1	43.6804	3.7563	Mediterranean	Apotracheal	Diffuse
Buxaceae	Buxus	Buxus sempervirens	3	5.4	43.6800	3.7562	Mediterranean	Apotracheal	Diffuse
Cannabaceae	Celtis	Celtis australis	1	19.6	43.7135	4.0127	Mediterranean	Paratracheal	Ring
Cannabaceae	Celtis	Celtis australis	2	10.4	43.7140	4.0128	Mediterranean	Paratracheal	Ring
Cannabaceae	Celtis	Celtis australis	3	8.2	43.7147	4.0112	Mediterranean	Paratracheal	Ring
Cornaceae	Cornus	Cornus mas	1	11.5	43.7131	4.0133	Mediterranean	Apotracheal	Diffuse
Cornaceae	Cornus	Cornus mas	2	8.9	43.7136	4.0132	Mediterranean	Apotracheal	Diffuse
Cornaceae	Cornus	Cornus mas	3	8.5	43.7136	4.0132	Mediterranean	Apotracheal	Diffuse
Rosaceae	Crataegus	Crataegus monogyna	1	9.5	43.7115	4.0126	Mediterranean	Apotracheal	Diffuse
Rosaceae	Crataegus	Crataegus monogyna	2	7.5	43.7115	4.0126	Mediterranean	Apotracheal	Diffuse
Rosaceae	Crataegus	Crataegus monogyna	3	7.3	43.7114	4.0127	Mediterranean	Apotracheal	Diffuse
Fagaceae	Cercis	Cercis siliquastrum	1	13.4	43.6720	3.7611	Mediterranean	Paratracheal	Ring
Fagaceae	Cercis	Cercis siliquastrum	2	12.9	43.6720	3.7609	Mediterranean	Paratracheal	Ring
Fagaceae	Cercis	Cercis siliquastrum	3	23.4	43.6720	3.7606	Mediterranean	Paratracheal	Ring
Oleaceae	Fraxinus	Fraxinus angustifolia	1	14.5	43.7116	4.0125	Mediterranean	Paratracheal	Ring
Oleaceae	Fraxinus	Fraxinus angustifolia	2	13.7	43.7116	4.0125	Mediterranean	Paratracheal	Ring
Oleaceae	Fraxinus	Fraxinus angustifolia	3	8.7	43.7115	4.0126	Mediterranean	Paratracheal	Ring
Oleaceae	Fraxinus	Fraxinus ornus	1	12.7	43.6492	3.8667	Mediterranean	Paratracheal	Ring
Oleaceae	Fraxinus	Fraxinus ornus	2	14.3	43.6492	3.8665	Mediterranean	Paratracheal	Ring
Oleaceae	Fraxinus	Fraxinus ornus	3	10.2	43.6493	3.8664	Mediterranean	Paratracheal	Ring
Lauraceae	Laurus	Laurus nobilis	1	17.2	43.6482	3.8739	Mediterranean	Paratracheal	Diffuse
Lauraceae	Laurus	Laurus nobilis	2	19.1	43.6482	3.8740	Mediterranean	Paratracheal	Diffuse
Lauraceae	Laurus	Laurus nobilis	3	8.6	43.6482	3.8742	Mediterranean	Paratracheal	Diffuse
Salicaceae	Populus	Populus alba	1	10.2	43.6489	3.8673	Mediterranean	Paratracheal	Diffuse
Salicaceae	Populus	Populus alba	2	12.4	43.6489	3.8672	Mediterranean	Paratracheal	Diffuse
Salicaceae	Populus	Populus alba	3	20.1	43.6484	3.8743	Mediterranean	Paratracheal	Diffuse
Oleaceae	Phillyrea	Phillyrea latifolia	1	9.2	43.6718	3.7604	Mediterranean	Apotracheal	Diffuse
Oleaceae	Phillyrea	Phillyrea latifolia	2	7.9	43.6717	3.7603	Mediterranean	Apotracheal	Diffuse
Oleaceae	Phillyrea	Phillyrea latifolia	3	7.2	43.6717	3.7604	Mediterranean	Apotracheal	Diffuse
Rosaceae	Prunus	Prunus mahaleb	1	7.5	43.6720	3.7604	Mediterranean	Apotracheal	Semi_ring
Rosaceae	Prunus	Prunus mahaleb	2	11.8	43.6720	3.7607	Mediterranean	Apotracheal	Semi_ring
Rosaceae	Prunus	Prunus mahaleb	3	9.3	43.6804	3.7560	Mediterranean	Apotracheal	Semi_ring

Anacardiaceae	Pistacia	Pistacia terebinthus	1	7.6	43.7139	4.0132	Mediterranean	Paratracheal	Semi_ring
Anacardiaceae	Pistacia	Pistacia terebinthus	2	8.9	43.7139	4.0132	Mediterranean	Paratracheal	Semi_ring
Anacardiaceae	Pistacia	Pistacia terebinthus	3	8.3	43.7140	4.0128	Mediterranean	Paratracheal	Semi_ring
Fagaceae	Quercus	Quercus ilex	1	21.7	43.7110	4.0135	Mediterranean	Apotracheal	Diffuse
Fagaceae	Quercus	Quercus ilex	2	8.4	43.7148	4.0122	Mediterranean	Apotracheal	Diffuse
Fagaceae	Quercus	Quercus ilex	3	16.6	43.7149	4.0122	Mediterranean	Apotracheal	Diffuse
Fagaceae	Quercus	Quercus pubescens	1	18.4	43.7113	4.0130	Mediterranean	Apotracheal	Ring
Fagaceae	Quercus	Quercus pubescens	2	21.3	43.7109	4.0135	Mediterranean	Apotracheal	Ring
Fagaceae	Quercus	Quercus pubescens	3	13.3	43.7145	4.0122	Mediterranean	Apotracheal	Ring
Malvaceae	Tilia	Tilia cordata	1	14.0	43.6482	3.8754	Mediterranean	Apotracheal	Diffuse
Malvaceae	Tilia	Tilia cordata	2	21.6	43.6485	3.8752	Mediterranean	Apotracheal	Diffuse
Malvaceae	Tilia	Tilia cordata	3	13.7	43.6490	3.8762	Mediterranean	Apotracheal	Diffuse
Adoxaceae	Viburnum	Viburnum tinus	1	25.1	43.6481	3.8726	Mediterranean	Apotracheal	Diffuse
Adoxaceae	Viburnum	Viburnum tinus	2	8.6	43.6481	3.8726	Mediterranean	Apotracheal	Diffuse
Adoxaceae	Viburnum	Viburnum tinus	3	24.2	43.6481	3.8726	Mediterranean	Apotracheal	Diffuse
Ulmaceae	Ulmus	Ulmus minor	1	18.0	43.7114	4.0126	Mediterranean	Paratracheal	Ring
Ulmaceae	Ulmus	Ulmus minor	2	22.9	43.7114	4.0127	Mediterranean	Paratracheal	Ring
Ulmaceae	Ulmus	Ulmus minor	3	8.9	43.7061	4.0115	Mediterranean	Paratracheal	Ring
Moraceae	Brosimum	Brosimum rubescens	1	13.6	5.2798	-52.9242	Tropical	Paratracheal	Diffuse
Moraceae	Brosimum	Brosimum rubescens	2	17.7	5.2761	-52.9253	Tropical	Paratracheal	Diffuse
Moraceae	Brosimum	Brosimum rubescens	3	8.4	5.2760	-52.9249	Tropical	Paratracheal	Diffuse
Urticaceae	Cercropia	Cecropia obtusa	1	11.2	5.2799	-52.9175	Tropical	Paratracheal	Diffuse
Urticaceae	Cercropia	Cecropia obtusa	2	7.6	5.2799	-52.9174	Tropical	Paratracheal	Diffuse
Urticaceae	Cercropia	Cecropia obtusa	3	9.5	5.2800	-52.9174	Tropical	Paratracheal	Diffuse
Meliaceae	Carapa	Carapa surinamensis	1	10.3	5.2754	-52.9244	Tropical	Paratracheal	Diffuse
Meliaceae	Carapa	Carapa surinamensis	2	8.4	5.2754	-52.9246	Tropical	Paratracheal	Diffuse
Meliaceae	Carapa	Carapa surinamensis	3	11.3	5.2756	-52.9242	Tropical	Paratracheal	Diffuse
Lecythidaceae	Eschweilera	Eschweilera coriacea	1	8.5	5.2765	-52.9241	Tropical	Apotracheal	Diffuse
Lecythidaceae	Eschweilera	Eschweilera coriacea	2	11.4	5.2757	-52.9225	Tropical	Apotracheal	Diffuse
Lecythidaceae	Eschweilera	Eschweilera coriacea	3	8.8	5.2711	-52.9238	Tropical	Apotracheal	Diffuse
Goupiaceae	Goupia	Goupia glabra	1	17.4	5.2753	-52.9241	Tropical	Apotracheal	Diffuse
Goupiaceae	Goupia	Goupia glabra	2	11.4	5.2747	-52.9241	Tropical	Apotracheal	Diffuse
Goupiaceae	Goupia	Goupia glabra	3	21.4	5.2741	-52.9241	Tropical	Apotracheal	Diffuse
Humiriaceae	Humiria	Humiria balsamifera	1	10.3	5.2482	-52.9075	Tropical	Paratracheal	Diffuse
Humiriaceae	Humiria	Humiria balsamifera	2	11.6	5.2484	-52.9079	Tropical	Paratracheal	Diffuse
Humiriaceae	Humiria	Humiria balsamifera	3	13.5	5.2483	-52.9076	Tropical	Paratracheal	Diffuse
Moraceae	Helicostylis	Helicostylis pedunculata	1	18.1	5.2757	-52.9228	Tropical	Paratracheal	Diffuse

Moraceae	Helicostylis	Helicostylis pedunculata	2	8.8	5.2761	-52.9239	Tropical	Paratracheal	Diffuse
Moraceae	Helicostylis	Helicostylis pedunculata	3	9.3	5.2723	-52.9223	Tropical	Paratracheal	Diffuse
Myristicaceae	Iryanthera	Iryanthera hostmannii	1	11.2	5.2792	-52.9260	Tropical	Apotracheal	Diffuse
Myristicaceae	Iryanthera	Iryanthera hostmannii	2	12.0	5.2793	-52.9260	Tropical	Apotracheal	Diffuse
Myristicaceae	Iryanthera	Iryanthera hostmannii	3	11.3	5.2791	-52.9260	Tropical	Apotracheal	Diffuse
Myristicaceae	Iryanthera	Iryanthera sagotiana	1	8.9	5.2773	-52.9242	Tropical	Apotracheal	Diffuse
Myristicaceae	Iryanthera	Iryanthera sagotiana	2	13.7	5.2614	-52.9280	Tropical	Apotracheal	Diffuse
Myristicaceae	Iryanthera	Iryanthera sagotiana	3	10.8	5.2765	-52.9250	Tropical	Apotracheal	Diffuse
Bignoniaceae	Jacaranda	Jacaranda copaia	1	11.4	5.2719	-52.9227	Tropical	Paratracheal	Diffuse
Bignoniaceae	Jacaranda	Jacaranda copaia	2	12.0	5.2688	-52.9243	Tropical	Paratracheal	Diffuse
Bignoniaceae	Jacaranda	Jacaranda copaia	3	11.6	5.2469	-52.9068	Tropical	Paratracheal	Diffuse
Apocynaceae	Lacmellea	Lacmellea aculeata	1	12.6	5.2749	-52.9226	Tropical	Apotracheal	Diffuse
Apocynaceae	Lacmellea	Lacmellea aculeata	2	10.7	5.2618	-52.9276	Tropical	Apotracheal	Diffuse
Apocynaceae	Lacmellea	Lacmellea aculeata	3	10.0	5.2757	-52.9251	Tropical	Apotracheal	Diffuse
Melastomataceae	Miconia	Miconia acuminata	1	16.2	5.2720	-52.9227	Tropical	Paratracheal	Diffuse
Melastomataceae	Miconia	Miconia acuminata	2	13.7	5.2721	-52.9227	Tropical	Paratracheal	Diffuse
Melastomataceae	Miconia	Miconia acuminata	3	10.2	5.2725	-52.9229	Tropical	Paratracheal	Diffuse
Euphorbiaceae	Maprounea	Maprounea guianensis	1	11.1	5.2481	-52.9071	Tropical	Apotracheal	Diffuse
Euphorbiaceae	Maprounea	Maprounea guianensis	2	10.9	5.2482	-52.9074	Tropical	Apotracheal	Diffuse
Euphorbiaceae	Maprounea	Maprounea guianensis	3	9.6	5.2483	-52.9074	Tropical	Apotracheal	Diffuse
Sapotaceae	Micropholis	Micropholis guyanensis	1	8.9	5.2794	-52.9256	Tropical	Apotracheal	Diffuse
Sapotaceae	Micropholis	Micropholis guyanensis	2	14.3	5.2765	-52.9251	Tropical	Apotracheal	Diffuse
Sapotaceae	Micropholis	Micropholis guyanensis	3	9.7	5.2791	-52.9257	Tropical	Apotracheal	Diffuse
Annonaceae	Oxandra	Oxandra asbeckii	1	14.1	5.2762	-52.9238	Tropical	Apotracheal	Diffuse
Annonaceae	Oxandra	Oxandra asbeckii	2	10.7	5.2762	-52.9238	Tropical	Apotracheal	Diffuse
Annonaceae	Oxandra	Oxandra asbeckii	3	13.6	5.2765	-52.9242	Tropical	Apotracheal	Diffuse
Burseraceae	Protium	Protium subserratum	1	12.6	5.2762	-52.9239	Tropical	Apotracheal	Diffuse
Burseraceae	Protium	Protium subserratum	2	9.9	5.2763	-52.9239	Tropical	Apotracheal	Diffuse
Burseraceae	Protium	Protium subserratum	3	9.9	5.2765	-52.9241	Tropical	Apotracheal	Diffuse
Anacardiaceae	Tapirira	Tapirira guianensis	1	22.8	5.2669	-52.9245	Tropical	Paratracheal	Diffuse
Anacardiaceae	Tapirira	Tapirira guianensis	2	17.6	5.2680	-52.9269	Tropical	Paratracheal	Diffuse
Anacardiaceae	Tapirira	Tapirira guianensis	3	23.2	5.2683	-52.9268	Tropical	Paratracheal	Diffuse
Fabaceae	Tachigali	Tachigali melinonii	1	19.4	5.2755	-52.9242	Tropical	Paratracheal	Diffuse
Fabaceae	Tachigali	Tachigali melinonii	2	15.9	5.2713	-52.9234	Tropical	Paratracheal	Diffuse
Fabaceae	Tachigali	Tachigali melinonii	3	15.3	5.2712	-52.9233	Tropical	Paratracheal	Diffuse
Fabaceae	Vouacapoua	Vouacapoua americana	1	10.4	5.2763	-52.9239	Tropical	Paratracheal	Diffuse
Fabaceae	Vouacapoua	Vouacapoua americana	2	10.4	5.2766	-52.9236	Tropical	Paratracheal	Diffuse

Fabaceae	Vouacapoua	Vouacapoua americana	3	11.6	5.2774	-52.9236	Tropical	Paratracheal	Diffuse
Hypericaceae	Vismia	Vismia sessilifolia	1	16.9	5.2726	-52.9230	Tropical	Apotracheal	Diffuse
Hypericaceae	Vismia	Vismia sessilifolia	2	11.9	5.2484	-52.9073	Tropical	Apotracheal	Diffuse
Hypericaceae	Vismia	Vismia sessilifolia	3	12.8	5.2485	-52.9074	Tropical	Apotracheal	Diffuse

Table S3.2 Model parameters of near-infrared spectroscopy (NIRS) calibration for contents of soluble sugars and starch.

Organ	NSC	No.	R^2c	SEC	RMSECV	R^2p	RMSEP
Stem	Soluble sugars	113	0.82	4.1	5.2	0.68	5.2
	Starch	113	0.75	12.9	13.2	0.74	11.3
Root	Soluble sugars	140	0.85	8.2	11.6	0.71	11.0
	Starch	140	0.95	17.5	21.6	0.89	22.7

Note: NSC is non-structural carbohydrates, No. is numbers of samples for calibration, R^2c is coefficient of determination in calibration, SEC is standard error of calibration, RMSECV is root mean square error of cross validation, R^2p is coefficient of determination in prediction, RMSEP is root mean square error of prediction.

Table S3.3 Comparison of pairwise xylem trait correlation matrices between Spearman's test with and without phylogenetically independent contrasts (PICs).

Stem	Spearman's test without PICs		Root	Spearman's test without PICs	
	Mantel statistic R	Significance		Mantel statistic R	Significance
Spearman's test with PICs	0.9566	*P*<0.001	Spearman's test with PICs	0.9684	*P*<0.001

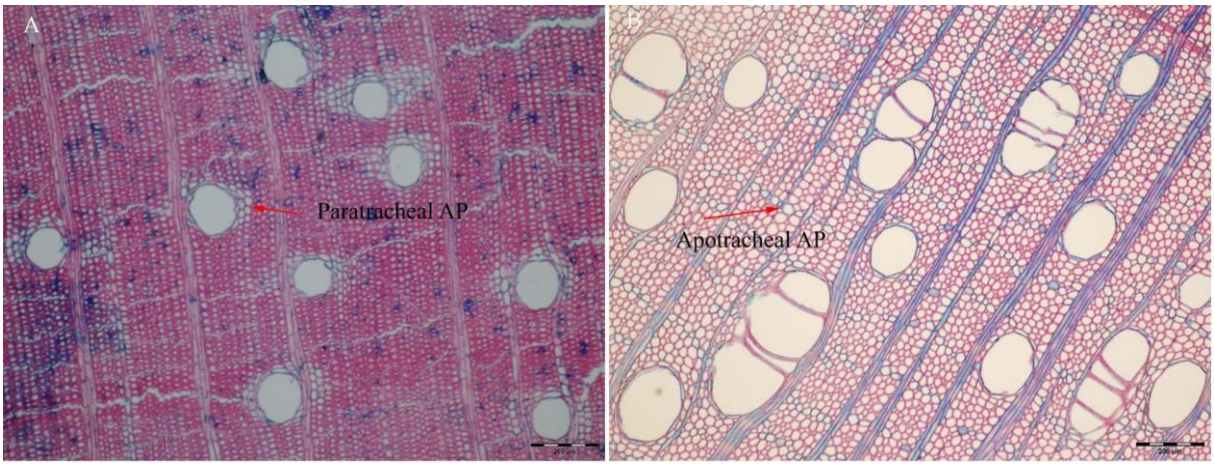

Fig. S3.1 Light microscopy images of transverse sections of (A) *Helicostylis pedunculata* with paratracheal axial parenchyma and (B) *Juglans nigra* with apotracheal axial parenchyma. All bars, 200 µm. Abbreviations: AP: axial parenchyma

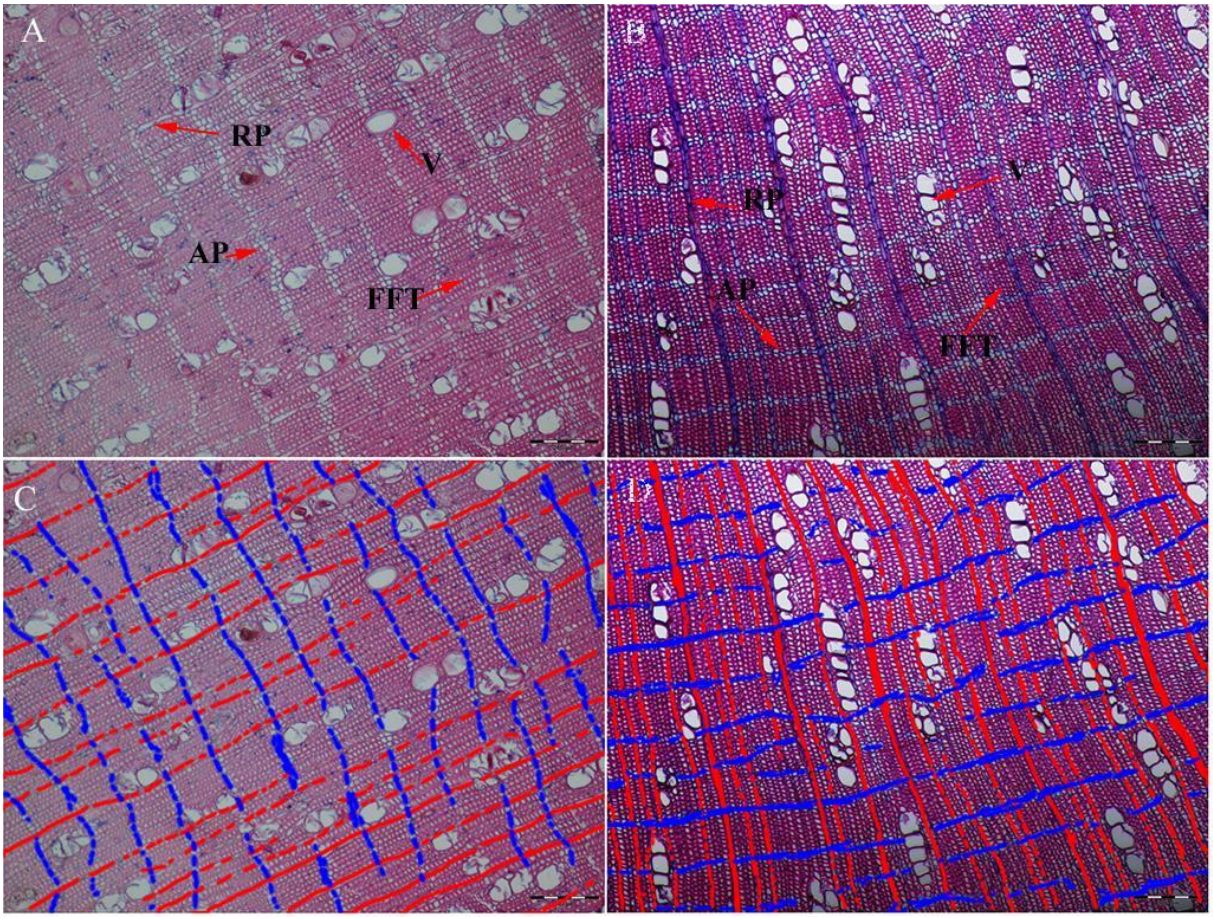

Fig. S3.2 Light microscopy images of transverse sections of *Micropholis guyanensis*. (A) original stem transverse section image, (B) original root transverse section image, (C) and D image colored using Photoshop, the blue area is axial parenchyma, the red area is radial parenchyma. All bars, 200 µm. Abbreviations: AP: axial parenchyma; RP: radial parenchyma; V: vessel; FFT: fibres, fibre-tracheids and tracheids.

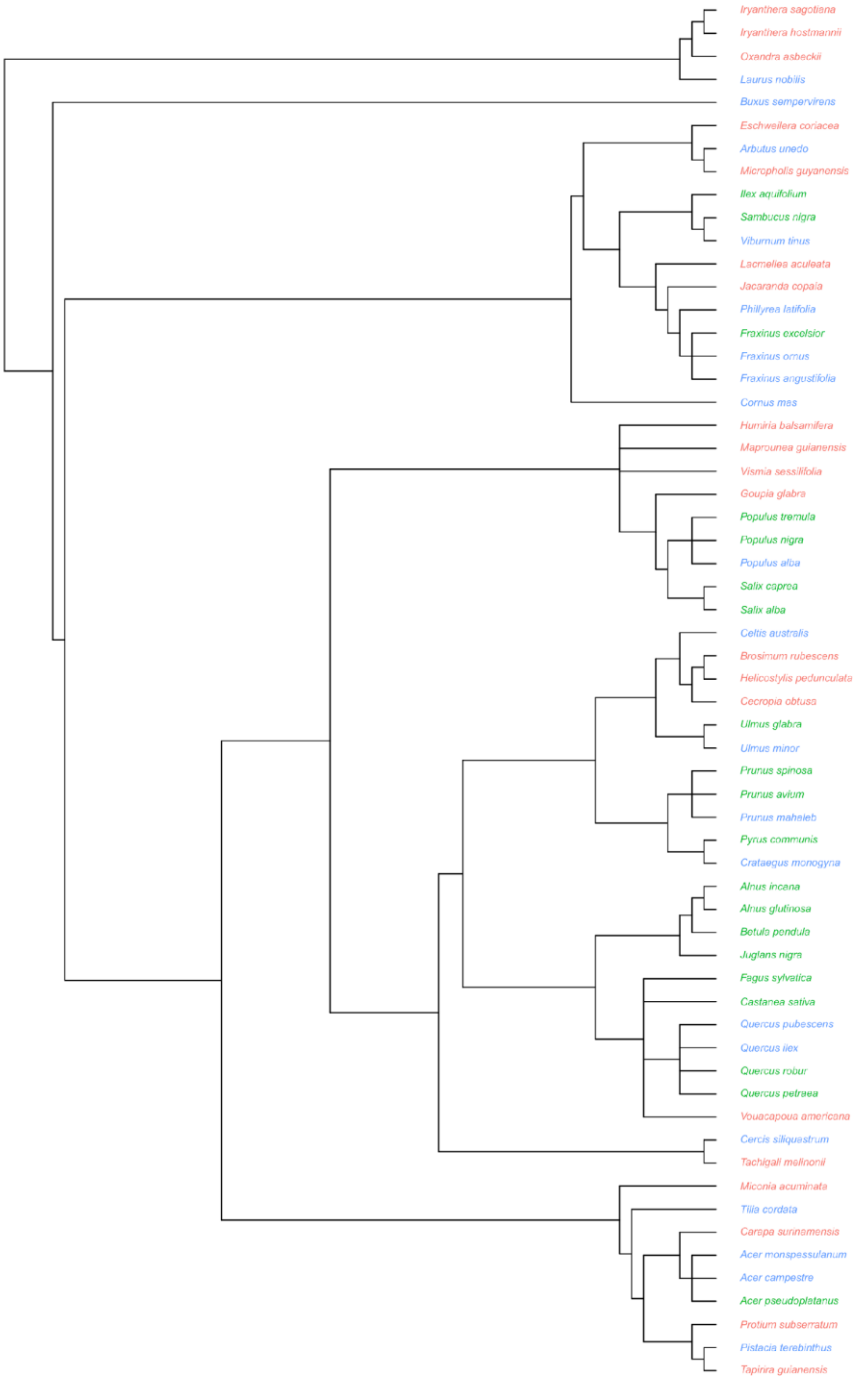

Fig. S3.3 Phylogenetic relationship of the 60 tree species. The backbone is based on Angiosperm Phylogeny Group (APG) III classification. Colors indicate species in three climates (green, temperate species; blue, Mediterranean species; red, tropical species).

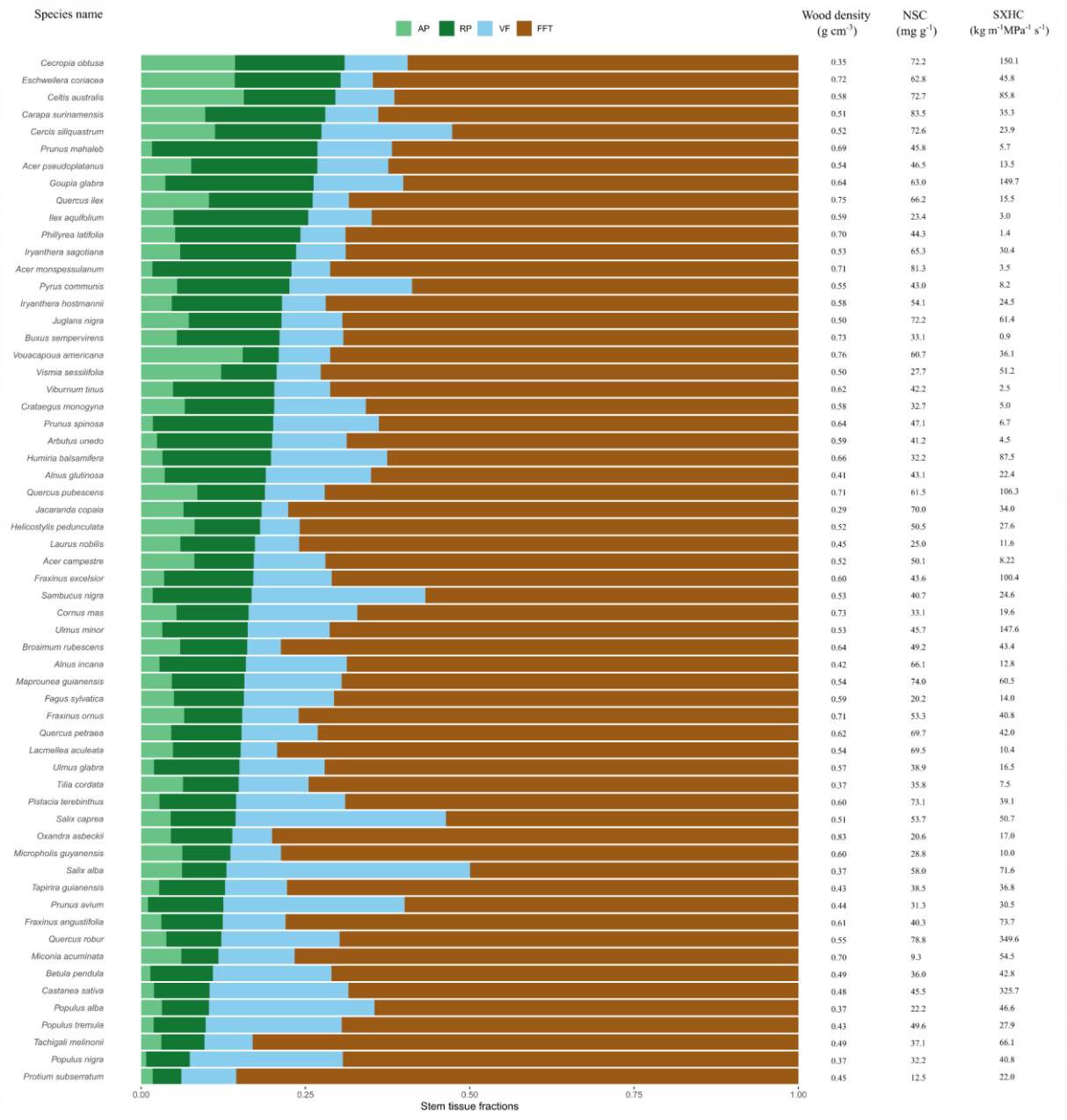

Fig. S3.4 Stack bar graph of stem tissue fractions across 60 species. Each bar represents an individual species. Species are sorted in order of decreasing total parenchyma fraction (axial + radial parenchyma). Numbers on the right side indicate wood density, NSC and SXHC of a given species. See Table 3.2 for trait abbreviation.

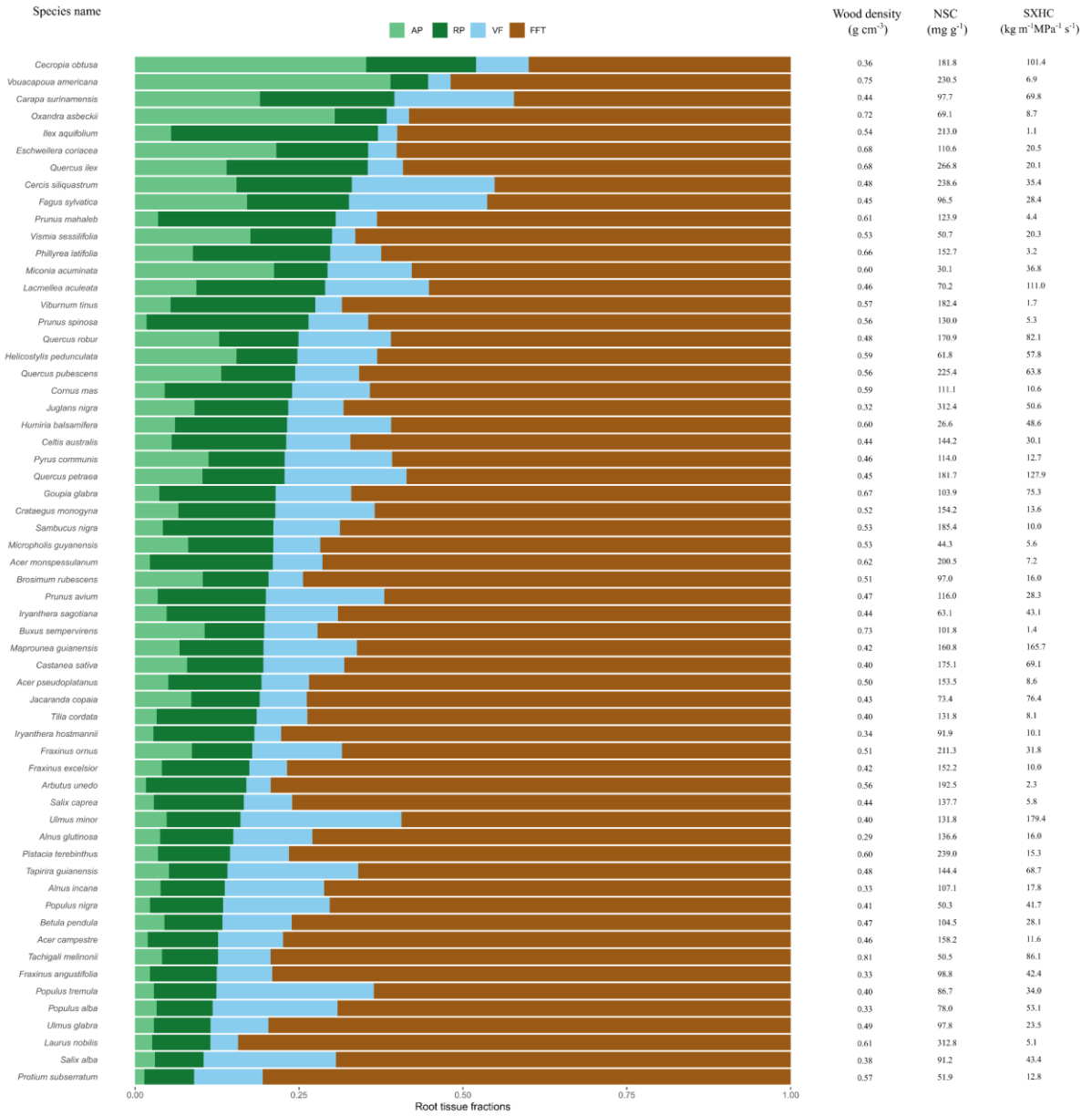

Fig. S3.5 Stack bar graph of root tissue fractions across 60 species. Each bar represents an individual species. Species are sorted in order of decreasing total parenchyma fraction (axial + radial parenchyma). Numbers on the right side indicate wood density, NSC and SXHC of a given species. See Table 3.2 for trait abbreviation.

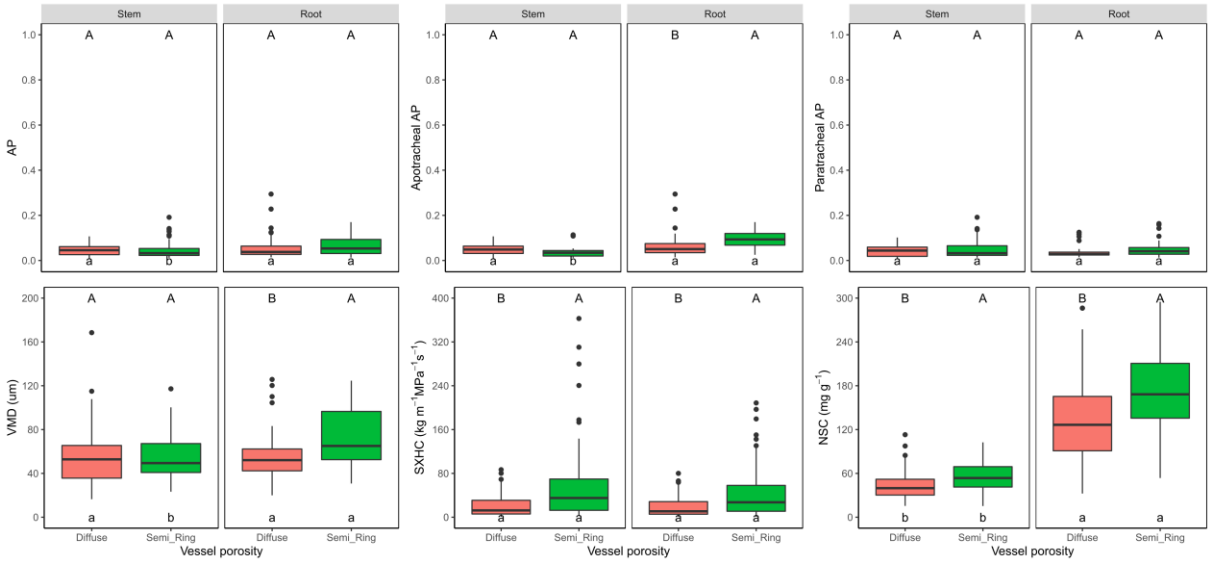

Fig. S3.6 Boxplot of stem and root xylem traits in stem and root between diffuse-porous and Semi-Ring-porous species when focusing on temperate and Mediterranean species. The line in the box indicates the median; the whiskers above and below the box indicate the 75th and 25th percentiles. Different uppercase letters indicate significant differences between the two porosity groups for a given xylem trait in the same organ. Different lowercase letters indicate significant differences between organs for a given xylem trait in the same porosity group. Colors indicate two porosity groups (red, diffuse-porous species; green, Semi-Ring-porous species). See Table 3.2 for trait abbreviation.

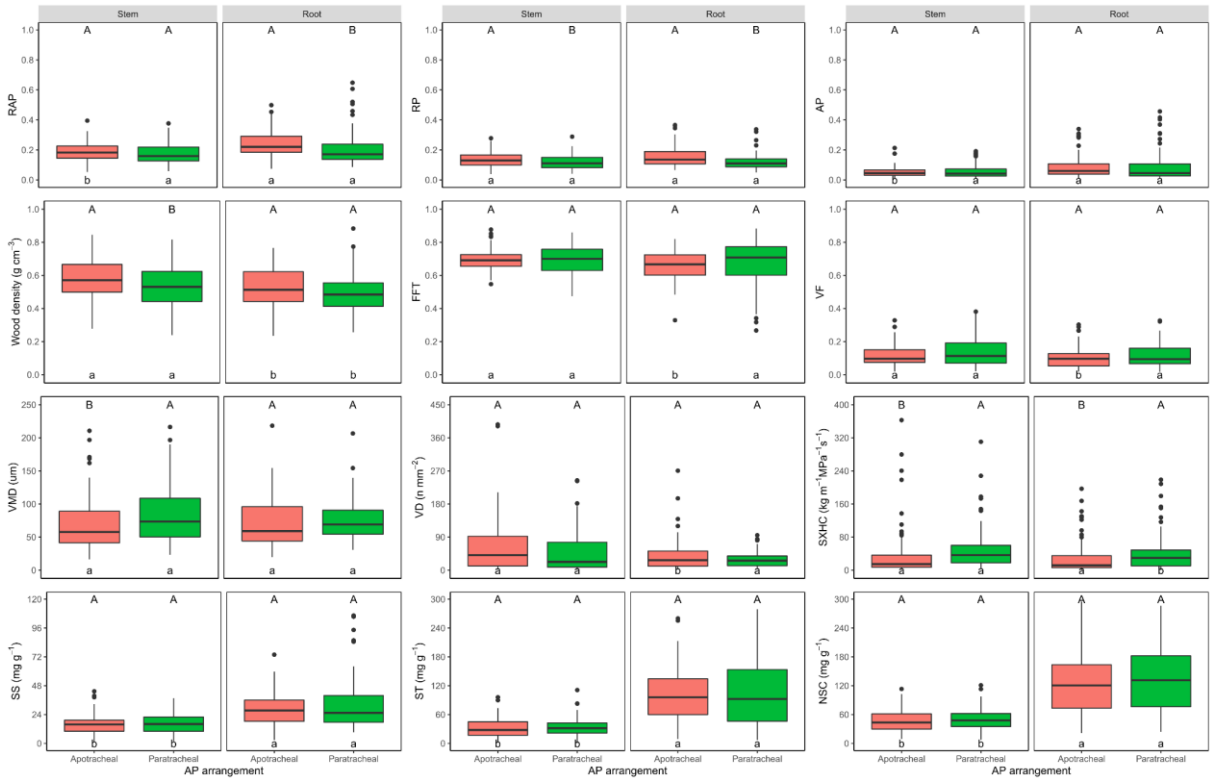

Fig. S3.7 Boxplot of stem and root xylem traits between apotracheal AP and paratracheal AP species. The line in the box indicates the median; the whiskers above and below the box indicate the 75th and 25th percentiles. Different uppercase letters indicate significant differences between apotracheal AP and paratracheal AP species for a given xylem trait in the same organ. Different lowercase letters indicate significant differences between organs for a given xylem trait in the same AP arrangement species. Colors indicate two AP arrangement groups (red, apotracheal AP species; green, paratracheal AP species). See Table 3.2 for trait abbreviation.

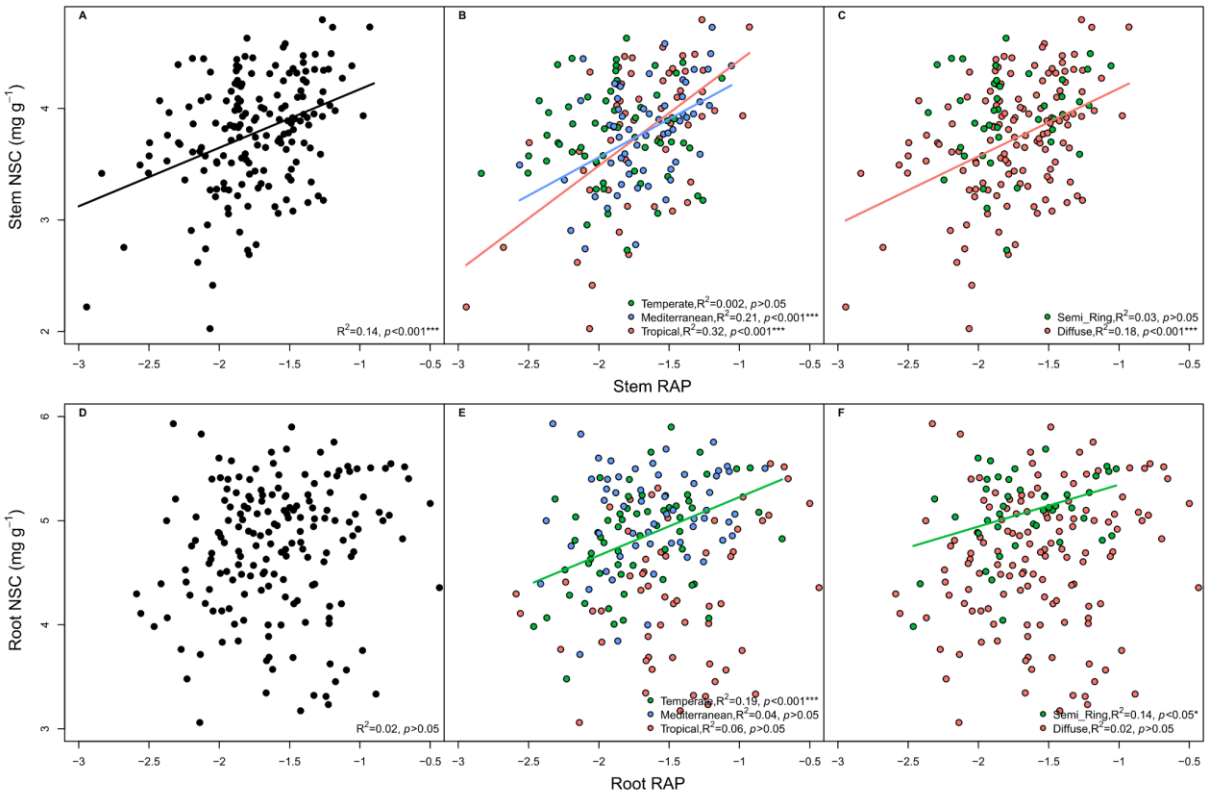

Fig. S3.8 Relationships between NSC and RAP fractions in stems (A, B, C) and roots (D, E, F) with all species pooled and across climates and vessel porosity. Diffuse means the category of porosity is diffuse porous. Semi_Ring means the category of porosity is semi/ring porous. See Table 3.2 for trait abbreviation.

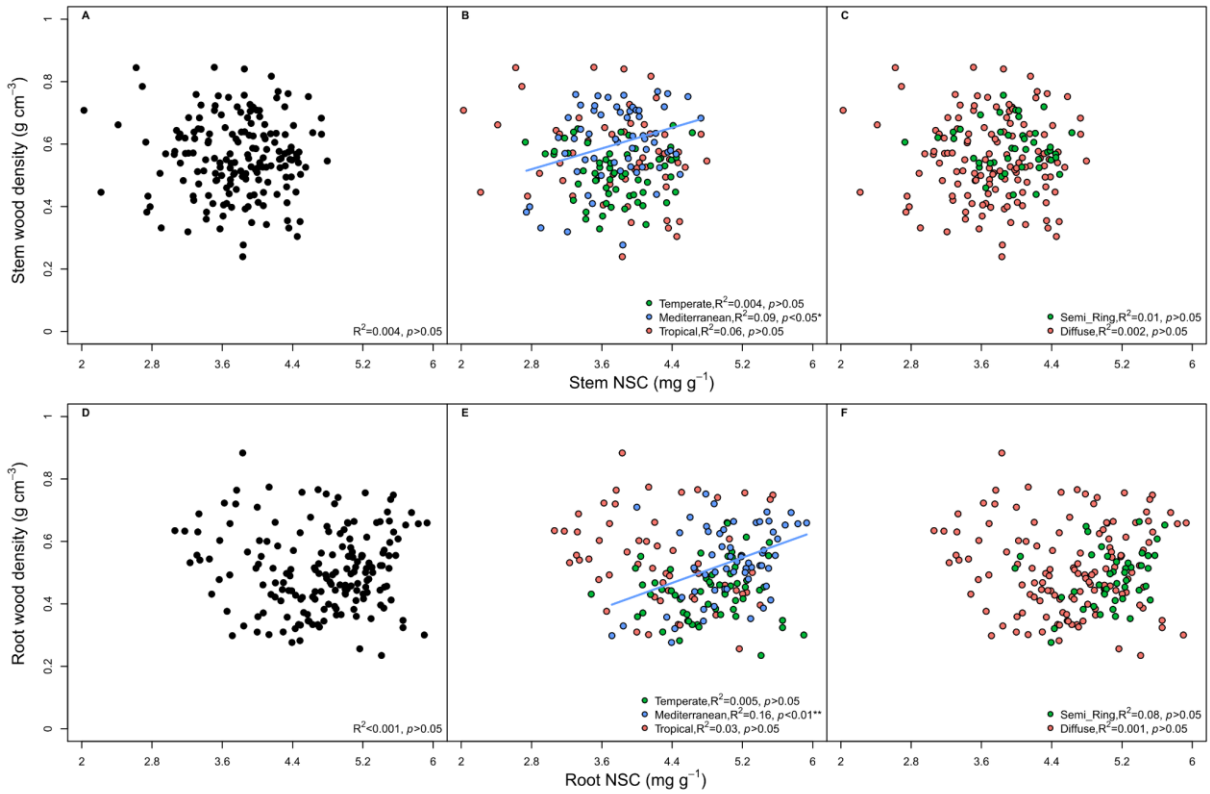

Fig. S3.9 Relationships between wood density and NSC in stems (A, B, C) and roots (D, E, F) with all species pooled and across climates and vessel porosity. Diffuse means the category of porosity is diffuse porous. Semi_Ring means the category of porosity is semi/ring porous. See Table 3.2 for trait abbreviation.

CHAPTER 4: Not all sweetness and light – non-structural carbohydrates and the tree economics spectrum across climates

Guangqi Zhang[1], Zhun Mao[1], Pascale Maillard[2], Loic Brancheriau[3], Bastien Gérard[2], Julien Engel[1], Claire Fortunel[1], Jean-Luc Maeght[1], Jordi Martínez-Vilalta[4,5], Alexia Stokes[1]

1 AMAP, Université de Montpellier, CIRAD, CNRS, INRAE, IRD, 34000 Montpellier, France
2 SILVA, INRAE, Université de Lorraine, Agroparistech, Centre de Recherche Grand-Est Nancy, 54280 Champenoux, France
3 CIRAD, Université de Montpellier, UR BioWooEB, 34000 Montpellier, France
4 CREAF, E08193 Bellaterra (Cerdanyola del Vallès), Catalonia, Spain
5 Universitat Autònoma Barcelona, E08193 Bellaterra (Cerdanyola del Vallès), Catalonia, Spain

In preparation for submission to *Functional Ecology*

ABSTRACT

Premise: The attribution of functional traits to plant species has been used for the assessment of ecological strategies. As an important functional trait, non-structural carbohydrate (NSC) is considered as an indicator of balance between carbon sources and sinks and reflects the adaptive strategies of trees, especially in harsh environmental conditions. However, little is known about whether NSC in different organs coordinates with other leaf or xylem traits, including those linked to the economics spectrum, such as leaf mass per area, nitrogen content and xylem density.

Methods: NSC content and functional traits in leaves, stem and coarse root xylem of 90 angiosperm trees were measured in temperate, Mediterranean and tropical climates. By performing principal component analysis (PCA) and standardized major axis (SMA) regression, we explored the relationships between NSC and functional traits, as well as the economics spectrum depending on climate and leaf habit (deciduous or evergreen).

Results: Our results revealed there was a covariation between leaf NSC content and leaf economics traits, whereas the variation between NSC in woody organs, especially stem NSC content, and economics traits were largely decoupled. Additionally, leaf functional traits and root xylem traits were closely integrated, while most stem xylem traits were independent of the leaf economics spectrum. Tree ecological strategies were influenced by climate and depended on leaf habit, that exhibited different resource strategies: deciduous species tended to gather on the acquisitive side, whereas evergreen species gathered more on the conservative side.

Conclusions: We conclude that xylem NSC content was weakly coordinated with resource-use traits, while leaf NSC content could contribute to global variation in plant ecological strategies, structured by climate and leaf habit. Our study provides further insight about trade-offs in resource allocation along economics spectrum from a whole-tree perspective, and thus develop predictions for how ecosystems respond to global change.

Key words: climates, deciduous species, economics spectrum, evergreen species, functional traits, non-structural carbohydrates

4.1 INTRODUCTION

Functional traits that impact plant fitness indirectly via their effects on growth, reproduction and survival are considered a widely accepted tool for studying ecological strategies (Grime, 1977; Díaz *et al.*, 2004; Violle *et al.*, 2007; Díaz *et al.*, 2016). Ecologists often group plants based on similar ecological strategies or on taxonomic criteria which form different plant functional groups. The attribution of functional traits to single species or broad groups of species has allowed functional groups to be used in the assessment of ecological status. The patterns in traits have been described using various concepts, with the “economics spectrum”

currently being one of the most popular models to describe the relationship between trait characteristics and functional groups (Wright *et al.*, 2004; Reich, 2014). For example, the leaf economics spectrum described plant resource trade-offs based on the functional traits of leaves, which revealed that fast-growing species have high leaf nutrient concentrations, low leaf mass per area and low leaf life span, allowing a better acquisition of resources, while in slow-growing species, a contrary pattern of traits is found, as species' strategies tend towards the conservation of resources (Wright *et al.*, 2004; Osnas *et al.*, 2013; Pan *et al.*, 2020). These changes demonstrate the differences in resource use and life history strategy among plants during succession, and reflect the important fundamental niche axes along which the species are differentiated (Westoby *et al.*, 2002; Violle and Jiang, 2009). Therefore, the resource investment in organs of large plants such as trees, should indicate important trade-offs and be a major factor determining their position along the economics spectrum.

As an important functional trait, non-structural carbohydrates (NSC) are the primary substrates and the key energy source for plant metabolic processes, which play a vital role in plant multiple functions such as osmoregulation, growth, defence and survival (Kozlowski, 1992; Sala *et al.*, 2012; Dietze *et al.*, 2014; Hartmann and Trumbore, 2016). NSC produced by photosynthesis can be quickly used for immediate functions or stored for reserves and defence (Myers and Kitajima, 2007; Wiley *et al.*, 2013; Klein and Hoch, 2015; Weber *et al.*, 2019), which suggest an allocation-based trade-off between carbon demand and supply. Thus, the content of NSC and allocation patterns in leaves, stems and roots are considered as indicators of balance between carbon sources and sinks in plants and reflect the adaptive strategies of plants (Chapin *et al.*, 1990; Hoch *et al.*, 2003; Körner, 2003; Würth *et al.*, 2005; Martínez-Vilalta *et al.*, 2016). For example, species with a higher specific leaf area or lower leaf mass per area (LMA) tend to have higher light capture potential and higher net photosynthetic rate, which may result in an increase of photosynthates then transported as

NSC for rapid growth of a plant (Wright *et al.*, 2002; Li *et al.*, 2016). Additionally, in trees, species with tough leaves, higher LMA and dense wood usually have more carbon investment in reserves and defence, allowing trees to persist when carbon demand is higher than supply (e.g., under severe drought stress) (Poorter and Kitajima, 2007; Poorter *et al.*, 2010a; Anderegg and Anderegg, 2013). However, few studies have directly examined the relationship between NSC and the economic spectrum in trees, and whether NSC in different organs coordinates with economic traits that design ecological strategies.

In analogy with the "leaf economic spectrum", several studies have reported the resource economics trade-off in different tissues, i.e., wood (Chave *et al.*, 2009), root (Prieto *et al.*, 2015; Roumet *et al.*, 2016) tissues, as well as at the whole-plant level (Freschet *et al.*, 2010; de la Riva *et al.*, 2016; Zhao *et al.*, 2017; Li *et al.*, 2022). These studies demonstrated that the traits of leaves, stems and roots are coordinated and thus provide a useful framework for exploring the trade-off between acquisition and conservation of resources at the whole plant level (Reich, 2014). Although so many studies have confirmed the whole plant trait covariation, there are still studies that have put forward different views. For example, Baraloto *et al.* (2010) argued that the leaf and stem economics spectra are largely decoupled in tropical rain forests. The leaf and root functional traits were also not always coordinated with economics spectrum, and Fortunel *et al.* (2012) conclude that woody root traits coordinated with stem traits rather than leaf traits in tropical trees. In addition, Isaac *et al.* (2017) found fine root economics traits were strongly orthogonal with respect to leaf traits in coffee (*Coffea arabica* L.) plants (see also Kramer-Walter *et al.*, 2016; Weemstra *et al.*, 2016; Kurze *et al.*, 2021). These studies suggest that the economics spectrum model is not ubiquitous at a whole tree level and across climates. Additionally, in tree xylem, vessel, parenchyma and fibre cell size and distribution are recognized as critical functional traits as they perform basic functions linked to transport and storage. However, studies that explore the economics spectrum,

seldom touch on the traits of wood structure, although they have received increasing attention in studies investigating plant ecological strategies (Pratt *et al.*, 2007; Ziemińska *et al.*, 2013; Fortunel *et al.*, 2014; Janssen *et al.*, 2020). Therefore, more studies are needed that test the coordination among multiple traits, including the design of xylem space, to reveal the existence and nature of a whole tree economics spectrum.

Studies of functional traits across biomes would advance our understanding of plant function. Due to the divergence of functional traits in temperate, Mediterranean and tropical climates, as well as wet versus dry conditions, differentiated ecological strategies are likely to occur. For example, wood density, which results from the interaction of different xylem properties, and is considered to play an important role in ecological strategy, varies across environmental gradients (Chave *et al.*, 2009). Although the average wood density of tropical and temperate tree species is not significantly different, a broader variation in density occurs in tropical species compared to temperate species (Wiemann and Williamson, 2002), reflecting the high taxonomical diversity. Many tropical species are also evergreen, and so could also display different strategies to temperate species, that comprise deciduous and evergreen species. Wright *et al.* (2004) reported that when trait means were considered, species with different leaf habit (evergreen or deciduous) would be differentiated along the leaf economics spectrum, as evergreen trees have longer mean leaf lifespan and higher leaf mass per area than deciduous trees. In addition, evergreen and deciduous species have different ways of using and storing carbon. Deciduous species must have enough carbon accumulation during the growing season to support the physiological activities over the dormant period and ensure carbon supply for next year's flushing of new leaves, while evergreen species could maintain a whole year of physiological activities to provide energy for the various functions of plants (Gough *et al.*, 2009; Fajardo *et al.*, 2013; Klein *et al.*, 2016; Ramirez *et al.*, 2021). Zhao *et al.* (2017) and Li *et al.* (2022) both reported that deciduous species tend to perform resource

acquisitive strategies, whereas evergreen species have conservative strategies, but their studies were limited to tree species in subtropical regions. Whether these strategies occur across climates is still not clear. Furthermore, determining the impact of evolutionary history on the economics spectrum is also important to reveal the resource trade-off among leaves, stems and roots. However, few studies have explored the impact of phylogeny on the economic spectrum of trees, although de la Riva *et al.* (2016) found that the most significant correlations were still consistent between economic traits after considering phylogenetically independent contrasts.

In this study, we explored the coordination of functional traits along with economics spectrum linking leaf habit by measuring suites of similar traits representing leaf, stem and root across 90 angiosperm species from temperate, Mediterranean and tropical forests. We sought to answer three main questions and made the following associated hypotheses: (Q1) Is NSC content in leaf, stem and coarse roots coordinated with functional traits associated with acquisitive and conservative resource strategies? We hypothesize that (H1): leaf NSC content would coordinate with functional economics traits, while stem and root NSC content would be independent of acquisitive and conservative resource strategy spectrum. (Q2) Do leaf, stem and root traits covary and are integrated along the economics spectrum? We hypothesize that (H2): leaf, stem and coarse root traits would be correlated towards a whole tree economic spectrum. (Q3) Is the plant economics spectrum structured by climatic zones and leaf habits? We hypothesize that (H3): the economics spectrum is influenced by climate and that deciduous species would have an acquisitive resource strategy, whereas evergreen species would possess a conservative resource strategy across climates.

4.2 MATERIALS AND METHODS

4.2.1 Study sites and species

This study was conducted in a temperate forest (Luz-Saint-Sauveur, France; 43°08'N, 0°03'E), a Mediterranean forest (Montpellier, France; 43°42'N, 4°00'E) and a tropical forest (Paracou, French Guiana; 5°15'N, 52°55'W). The Luz-Saint-Sauveur site has a temperate mountain climate, with the heaviest rainfall in first half of a year. The mean annual precipitation (MAP) is 1217 mm and the mean annual temperature (MAT) is 11.8 ℃. The Montpellier site has a typical Mediterranean climate with hot dry summers and cool wet winters. The MAP is 588 mm with about 80% of the annual rainfall occurring between September and April. The MAT is 15.4 ℃. The Paracou site has a typical tropical rainforest climate with distinct dry season from mid-August to mid-November and long rainy season often interrupted by a short drier period between March and April. The MAP is 3035 mm with a minimum in September and maximum in May and the MAT is 26.9 ℃. The temperature and precipitation data were calculated using mean monthly data from the past 31 years (Figure S4.1: data are from Meteo-France).

A total of 90 species of angiosperm trees was selected, with 20 species each in temperate and Mediterranean climates and 50 species in the tropical climate, spanning 27 deciduous species and 63 evergreen species (Table S4.1). For each species, three healthy, adult, single-stemmed trees were identified, with a distance of at least 20 m between them. We collected leaf and stem samples for each tree, and collected root samples for 60 tree species with 20 species in each climate. Stems chosen were between 0.05 m and 0.4 m wide at a height of 1.3 m. For Mediterranean and tropical trees, samples were collected at the end of August and September 2019, and for temperate trees, samples were collected in September 2020. During this period, NSC storage should be close to its seasonal maximum. We sampled all trees between 7 am

and midday, to reduce variability in NSC content linked to photosynthate production. Fully expanded leaves were collected from the canopy with a telescopic ratchet pulley pole pruner. In French Guyana, only the lower leaves were accessible due to the high stem density and resulting high crowns in this primary tropical forest. Therefore, we chose to sample shade leaves from the lower canopy of all 90 species, so that all trees were sampled similarly. Leaves were chosen from the same side of the tree where stem and root samples were taken and divided in two groups. At a height of 1.3 m, three 0.05 m long cores were extracted from tree stems with a 4.3 mm diameter increment borer. To collect samples of roots, we excavated a single lateral root (0.02 – 0.05 m in diameter) and at a distance of 0.3 – 0.5 m from the base of the tree, we extracted three increment cores or removed three 0.02 m long segments of root, depending on accessibility. We also collected one stem core for temperate and Mediterranean trees in March 2021 (before bud burst) to capture variability in seasonal dynamics of NSC. However, we found that stem NSC content did not show any significant differences between the two sampling times ($P > 0.05$). Therefore, the following analyses were based on the autumnal NSC data, since they may be a better indicator of the current year's growth-storage trade-offs (Martínez-Vilalta *et al.*, 2016). All samples were immediately placed in moist paper, put in a cooler box and taken to the laboratory prior to midday, where they were kept in a fridge at 4°C. In total, 540 leaf samples, 930 stem cores and 540 root segments were collected and 25 functional traits were measured for each individual tree (Table 4.1).

4.2.2 Measurement of NSC, carbon and nitrogen content

Immediately on returning to the laboratory (on the same day the samples were collected), one of the three replicate increment cores/root sections and stem cores sampled in spring were trimmed and a 0.02 m long section was taken from the outer sapwood. Then, these stem and root samples and one of two groups of leaf samples were heated in a microwave oven (90 s at

700 W) to stop enzymatic activity (Popp *et al*., 1996) and oven-dried at 40 °C until a constant weight was obtained. Dried samples were ground into powder using a ball mill (Retsch MM400, Retsch, Haan, Germany) and the ground samples were stored in sealed plastic tubes until chemical analyses were performed.

As there was a total of 270 leaf samples, 390 stem samples and 180 root samples, it was not possible to perform time-consuming analytical methods on all samples, therefore, we used the near infra-red spectroscopy (NIRS) method to predict NSC content. The NIRS method has been used successfully for determining NSC, C, and N contents in different tissue types of a broad range of tree species (Gillon *et al*., 1999; Ramirez *et al.*, 2015; Wang *et al.*, 2018a; Rosado *et al.*, 2019). Near infrared spectra were first obtained for all samples on powders previously stabilized in a conditioning room at a temperature of 20 ± 2 °C and air humidity of 65 ± 5% (methods described in Zhang *et al*. (2022b). The NSC content was determined at the SILVATECH platform (Silvatech, INRAE Champenoux, France): a colorimetric method was performed on all leaf samples (n = 270), and a sub-sample of stems (n = 113) and roots (n = 140). For the remaining samples, stem and root samples, NSC content was predicted using the NIRS method (methods described in Zhang et al. (2022b). Soluble sugar and starch content were expressed as dry weight (mg g^{-1}) and their sum is referred to as the total NSC content.

The C and N contents in each organ were measured in a subsample of leaves (n = 110), stems (n = 113) and in all root samples (n = 180). For the remaining samples, the C and N contents were predicted by the NIRS method. The C and N contents per unit mass (%) were determined using an elemental analyzer (CHN model EA 1108, Carlo Erba instruments, Milan, Italy).

Partial least squares regression (PLSR) was used to develop calibrations for the prediction of soluble sugar and starch contents (Table S4.2) and C and N contents (Table S4.3), for stems,

roots and leaves separately. We removed outliers when present in the prediction results. The performance and the robustness of the models were computed using the cross-validation (leave-one-out) method (Mevik and Cederkvist, 2004) and in prediction by splitting the data set into a calibration set (3/4 of the samples) and a prediction set (1/4). R^2 values of calibration ranged between 0.75 and 0.95 for soluble sugars and starch, and between 0.87 and 0.92 for C and N, respectively.

4.2.3 Measurement of other functional traits

Another group of fresh leaf samples (n=270) were scanned using Epson scanner (Epson V39, Epson Inc., Nagano, Japan) and the leaf area determined by image analyses with ImageJ software (https://imagej.nih.gov/ij/). The leaves were then dried at 40 ℃ in an oven until constant weight and the weight used to determine LMA (leaf dry mass divided by leaf area, g m^{-2}). We used the mean LMA value obtained from leaves of the same tree as the mean value for each tree. Stem (n=270) and root (n=180) samples (with outer bark removed) were selected for stem wood density (SWD) and root wood density (RWD) measurements. Stem and root samples were soaked in water for 24 h and the fresh volume was determined using the water displacement method. After determining the fresh volume, samples were dried in a well-ventilated oven at 105 ℃ for more than 24 h and then the dry mass was weighed. Wood density used here is defined as oven-dry mass divided by fresh volume (g cm^{-3}) (Pérez-Harguindeguy *et al.*, 2016).

Stem (n=270) and root (n=180) sections were placed in a 50% solution of alcohol and water. These sections were kept for the analysis of xylem anatomical traits (methods described in Zhang et al. (2022b). Increment cores were embedded in paraffin individually after dehydration through immersion in a sequence of alcohol solution, whereas samples of root were just clamped in the microtome. We used a sliding microtome to cut 15-20 μm thick

cross-sections. Cross-sections were stained with a mixture of safranin and alcian blue (0.35 g safranin in 35ml 50% alcohol with 0.65 g alcian blue in 65 ml deionized water) and dehydrated using an ethanol series (50, 75, 95 and 100%). Finally, sections were mounted on glass slides and observed under a light microscope (Olympus BX 60F; Olympus Co. Ltd, Japan). Three microphotographs of transversal sections for each stem and root sample were taken (one or two microphotographs were taken for very few sections) with an APO x5 lens using a digital camera (Canon EOS 500D; Canon Inc., Tokyo, Japan). Radial parenchyma (RP) and axial parenchyma (AP) were manually colored using Photoshop (Adobe Systems Incorporated, USA). Then, the proportion of total radial and axial parenchyma (RAP, i.e., the sum of RP and AP, %), was then estimated using ImageJ 1.52 software (https://imagej.nih.gov/ij/). Using the same image, vessel fraction (VF, i.e., the total vessel area divided by xylem cross-section area) was also determined. The remaining tissues fraction including fibres, fibre-tracheids and tracheids (FFT) was calculated as: 1-RAP-VF.

4.2.4 Statistical analyses

To examine the trait-by-trait correlations among all 25 traits, we performed a Pearson correlation test. Data were transformed using natural logarithms to correct for deviations from normality except for SWD and RWD, that were normally distributed. In order to test the influence of species' evolutionary histories on the observed relationships, we further performed Pearson correlation analysis with phylogenetically independent contrasts (PICs, Felsenstein, 1985) at the species level. We constructed a phylogenetic tree (Fig. S4.2) including all 90 species using R package V.PhyloMaker (Jin and Qian, 2019), with the GBOTB phylogeny as the backbone (Smith and Brown, 2018). All species names were confirmed by the World Flora Online (http://www.worldfloraonline.org/).

We performed principal components analysis (PCA) using LMA, leaf nitrogen and leaf carbon to show the classical resource economics spectrum defining leaf tissues (Fig. S4.3). To examine the degree of associations between leaf, stem and root traits and the classical leaf resource economics spectrum, we used the standardized major axis (SMA) regression method (Warton *et al.*, 2006) to determine the scaling relationships among leaf economics spectrum PC1 (LESPC1) and organ functional traits (e.g., NSC, wood density, chemical and anatomical traits). We also performed PCA on each organ and whole-plant level to examine overall traits coordination. In addition, an independent-samples t-test was carried out on the PC1 score of leaf, stem, root and whole-plant to evaluate the significant different among climates and between deciduous and evergreen species. We also used two-way ANOVA to examine the effect of leaf habits (deciduous and evergreen), and climates (temperate, Mediterranean and tropical) on individual values of NSC, LMA, stem and root wood density. Tukey honestly significant differences (HSD) post hoc tests were then performed to identify variation among these groups.

All statistical analyses were performed in R version 4.0.2 (R Development Core Team 2020), using the packages *ape* (Paradis *et al.*, 2004), *vegan* (Dixon, 2003), and *smatr* (Warton *et al.*, 2012).

4.3 RESULTS

4.3.1 Relationships between leaf economics traits, NSC content and wood traits

According to the Pearson correlation analysis, we found most functional traits were significantly correlated with one another (Fig. 4.1A). The LMA was significantly and positively correlated with leaf and root C content, but negatively related to leaf and root N content. Species with high values of stem wood density also tended to have denser root wood. Only root wood density was negatively correlated with leaf N content and positively

correlated with LMA. The NSC content in leaves was positively correlated with leaf N content and negatively with LMA, while stem NSC content was not correlated with any leaf trait. Root NSC content was positively correlated with leaf N content, and negatively related to leaf C content. We also found that leaf NSC content was not correlated with either stem or root NSC content, but stem NSC content was significantly correlated to root NSC content (Fig. 4.1A). Both stem and root RAP were negatively related with leaf N content, and only stem RAP was positively related with LMA. Both stem and root VF were negatively related with LMA, and only stem VF was positively related with leaf N content. Although leaf N content was negatively correlated with stem FFT, the correlations between the remaining leaf traits and FFT were not significant. When PICs were included in the Pearson correlations, the matrices of pairwise correlations among traits were similar according to the Mantel test (R_{Mantel}=0.37, P<0.001) and patterns of correlation among leaf, stem and root traits were conserved (Fig. 4.1B).

The results of the leaf economics spectrum PCA for 90 tree species are shown in Fig. S4.3. The first axis accounted for 56.3% of variation with leaf N content demonstrating an acquisitive resource strategy whereas LMA was associated with a conservative resource strategy. The SMA regressions showed that there was a significant and negative correlation between leaf economics spectrum PC1 (LESPC1) and leaf NSC content when all species were pooled together. When focusing on climates and leaf habits, significant and positive correlations between LESPC1 and leaf NSC were found in tropical and evergreen species (Fig. 4.2A). As with leaf NSC content, there was also a significant and negative correlation between LESPC1 and root NSC content, but not with stem NSC content, when all species were pooled together. Additionally, a positive correlation was found between LESPC1 and stem NSC content in deciduous species, and root NSC content was positively related to LESPC1 in Mediterranean species (Fig. 4.2B, C). With all species pooled together, LESPC1

was not related with stem C, N content and wood density (Fig. 4.3A-C), but was positively associated to root C content and wood density and negatively with N content (Fig. 4.3D-F). When focusing on climates and leaf habits, significant and negative correlations were found between LESPC1 and stem N content in temperate, tropical and evergreen species and between LESPC1 and root N content in Mediterranean, tropical and evergreen species (Fig. 4.3B, E). Significant and positive correlations were found between LESPC1 and stem and root wood density in Mediterranean species, but negative correlations between LESPC1 and root wood density in tropical species (Fig. 4.3C, F). There were significant and positive correlations between LESPC1 and stem and root RAP with all species pooled together and in Mediterranean species, while significant and negative correlations between LESPC1 and stem and root VF were found with all species pooled together (Fig. 4.4A, B, D, E). Negative correlations between LESPC1 and root VF were also found in temperate and Mediterranean species, while the opposite trend was found in tropical species (Fig. 4.4E). There were no significant relationships between LESPC1 and FFT in either stems or roots, except for the significant and negative correlation between LESPC1 and stem FFT that existed in deciduous species (Fig. 4.4C, F).

Our results also showed that functional traits exhibited major variation across organs, climates and leaf habits (Figs. S4.4-4.7). Root organs had highest NSC content, while stems had lowest NSC content. Both leaf and root NSC content were higher in temperate, Mediterranean and deciduous species than that of tropical and evergreen species, whereas stem NSC content was not significantly different among climates and between deciduous and evergreen species (Fig. S4.4-4.5). Moreover, the LMA of tropical and evergreen species was higher than that of temperate, Mediterranean and deciduous species, whereas the wood density of stems and roots were lower in temperate and deciduous species than that of Mediterranean, tropical and evergreen species (Fig. S4.6-4.7).

4.3.2 Scaling relationships among leaf, stem, root and whole-plant resource economics strategies

When we performed PCAs for leaf, stem, root and the whole-tree, we found that relationships between NSC content and functional traits differed in each organ (Fig. 4.5A-D). In leaves, the variations explained by PC1 and PC2 were 44.0% and 23.7%, respectively, with the first PCA axis loading by LMA, leaf C and N content, and the second PCA axis loading by leaf NSC content (Fig. 4.5A, Table 4.2). In stems, the first PCA axis was defined by stem NSC content, RAP, and N content, which explained 29.1% of the variation and the second axis was defined by stem C content, VF, FFT and wood density, which explained 21.7% of the variation (Fig. 4.5B, Table 4.2). In roots, the first PCA axis was defined by root N content, VF, wood density and RAP, while the second axis was defined by root NSC content, FFT and C content, with the two axes explaining the variations of 26.5% and 25.9% respectively (Fig. 4.5C, Table 4.2). When we performed PCA at the whole-tree level, including leaf, stem and root traits, PC1 and PC2 explained 20.0% and 15.9% of the trait variation, respectively (Fig. 4.5D). Additionally, the first PCA axis was defined by leaf and root N content, VF, leaf NSC content, C content, LMA and stem and root wood density, while the second PCA axis was defined by stem and root NSC content, RAP, FFT, stem N and root C content. Stem C content was not strongly correlated with either axis (Fig. 4.5D).

We could clearly see that tree species in different climates and with different leaf habits showed different resource allocation strategies (Figs. 4.5-4.7). The score on the first PCA axis of temperate, Mediterranean and deciduous species was significantly lower than that of tropical and evergreen species at the leaf, stem and root level, with deciduous species having high leaf and root N content and low LMA (indicating an acquisitive resource strategy). Evergreen species had higher leaf C, LMA and wood density (indicating a conservative

resource strategy) (Fig. 4.6A-C, Fig. 4.7A-C). At the whole-tree level, the score on the first PCA axis of temperate and Mediterranean and deciduous species was significantly greater than that of tropical and evergreen species (Fig. 4.6D, Fig. 4.7D).

4.4 DISCUSSION

4.4.1 The link between NSC content and traits related to the economic spectrum

In agreement with our first hypothesis, we found there was a covariation between leaf and root NSC content and leaf economic traits. However, the relationship between stem NSC content and leaf economic traits was largely decoupled. Our results were partly consistent with those found by Ramirez *et al.* (2021), who showed that the position of tree species along the plant acquisition and conservative strategy spectrum was a predictor of NSC content in leaves, but not in stems and woody roots. Surprisingly, we also showed that leaf NSC content augmented with increasing leaf N content and decreasing LMA, suggesting that species with an acquisitive resource strategy could accumulate more NSC in their leaves than those with a conservative resource strategy. Additionally, lower LMA and higher N content is usually associated net photosynthetic rate, and thus the increase in leaf NSC content with increasing N content possibly resulted from an elevated photosynthetic rate (Wright *et al.*, 2002; Li *et al.*, 2016). In addition to photosynthesis, part of the nutrients in leaves originates directly from roots, resulting in a close relationship between the root NSC content and leaf economic traits (Liu and Wang, 2021). However, although we found that root NSC content was associated with leaf economic traits, both stem and root NSC content displayed an orthogonal trend (along the first PCA axis) with other traits, from an acquisitive to a conservative resource strategy (Fig. 4.5D). Previous studies have also reported that there were no trade-offs between NSC content and the investment in reserves that lead to conservative traits (Lusk and Piper, 2007; Imaji and Seiwa, 2010; Piper, 2015). The underlying cause may be due to the different

functional roles that stems, leaves and roots play. Leaves and roots acquire resources that need rapidly transporting to organs located at the opposing extremities of the tree. The stem must provide a transport route that is efficient, whilst maintaining the display of branch and leaf organs. Therefore, the design of the xylem space must reflect an optimized route for nutrient transport, that takes into account seasonal demands for NSC (especially in deciduous species), as well as climatic constraints, such as prolonged dry and cold periods. As tree mechanical integrity is largely dependent on morphology (bending stiffness is proportional to the fourth power of the stem/branch radius), wood density therefore plays a small role in resisting lateral forces such as wind loading (Larjavaara and Muller-Landau, 2010). The design of the xylem space can therefore be decoupled from leaf and root traits, that are positioned along an acquisition-conservation spectrum.

We found that soluble sugars were more abundant in leaves than in root and stem xylem. Soluble sugars are mainly synthesized from newly assimilated carbon by daytime photosynthesis, creating an intermediate, ready-to-use pool of NSC to support daily metabolism. However, in xylem, we found that starch was primarily stored as a recalcitrant form of NSC (Table S4.4) which may serve as a long-term storage pool and contribute to regrowth after disturbance, providing carbohydrates to new organs (Vargas *et al.*, 2009; Clarke *et al.*, 2013; Dietze *et al.*, 2014; Hartmann and Trumbore, 2016). When carbon assimilation is insufficient to support metabolic activity, starch can be converted back to soluble sugars (Chapin et al., 1990; Gibon et al., 2009) and starch reserves are also fundamental for providing sugars to rebuild the foliage of deciduous tree species, after leaf fall (trees lose autotrophy ability and function using their carbon reserves) (El Zein *et al*., 2011; Gilson *et al*., 2014). In addition, the allocation of NSC in stem and root xylem could take several seasons or even years (Lacointe, 2000; Hartmann and Trumbore, 2016) and this "older" NSC could contribute to annual growth, especially in temperate deciduous species

(such as *Fagus* and *Quercus* sp), where storage of NSC occurs before the winter months and can be remobilised the following spring (Barbaroux and Bréda, 2002; El Zein *et al*., 2011). Therefore, stem NSC remains largely immobile and varies little unless a disturbance occurs, and so does not coordinate with functional traits associated with the economics spectrum. Furthermore, the decoupled relationship between xylem NSC and the economics spectrum may be because xylem NSC performs another role, such the repair of drought-induced embolism and maintenance of xylem transport. Previous studies suggest that embolism can be repaired by water influx from surrounding non embolized vessels, driven by an osmotic gradient established by importing sugars into embolized vessels (Brodersen *et al*., 2010).

4.4.2 Coordination of leaf, stem and root traits associated with whole-plant economics spectrum

We found that leaf functional traits, root chemical traits and wood density were closely integrated, partially supporting our second hypothesis. However, whereas most stem traits were independent of the leaf economics spectrum, there were some significant correlations between leaf economic traits, stem N content and wood density for several species in specific climates (Fig. 4.4A). A possible reason for the coupling of leaf and root traits is that the primary function of roots is more towards nutrient storage and fast water absorption from soil (Drew, 1987) than in stems. In addition, a negative relationship between wood density and hydraulic conductivity was found by several authors (McCulloch et al., 2011; Janssen et al., 2020), indicating that high wood density is a conservative strategy, as greater hydraulic conductivity means faster tree growth. Our results are also in accordance with previous studies that reported a decoupled relationship between leaf and stem economics in tropical woody species (Baraloto *et al.*, 2010), even when phylogenetic contrasts were considered with species-level data. Fortunel *et al.* (2012) also found there are two orthogonal axes of trait

variation between the leaf and wood economics spectra in Amazonian tree species, demonstrating that the different investment in leaf and wood tissues optimized tree growth and survival. These results indicate that certain combinations of leaf and wood economics traits have more opportunity to coexist in climates that have less marked seasonality (Méndez-Alonzo *et al.*, 2012). However, with regard to xylem anatomical traits, we found that leaf economic traits (such as leaf N contents and LMA) were significantly correlated with stem and root RAP and VF. A high VF reflected resource acquisition whereas high RAP indicated resource conservation. Vessel fraction is also positively associated with hydraulic conductivity (Zanne *et al.*, 2010), in line with the strategy of rapid acquisition. Parenchyma cells play multiple roles in xylem, including nutrient and water storage (Plavcová *et al.*, 2016; Zhang *et al.*, 2022a), defense and wound repair (Morris *et al.*, 2020) and the proportion of RAP is strongly related to NSC storage capacity (Zhang et al 2022a). A strong trade-off occurs between the RAP and VF fractions, therefore, it is not surprising that RAP was more inclined to the resource-conservative side of the economic spectrum. Recent studies have also shown that there are conspicuous patterns of integration for leaf and wood traits toward a whole-plant economics spectrum (Freschet *et al.*, 2010; de la Riva *et al.*, 2016; Zhao *et al.*, 2017; Li *et al.*, 2022). For example, de la Riva *et al.* (2016) revealed a high degree of coordination between the traits of different organs at both species and community levels in Mediterranean forests. Li *et al.* (2022) also found the existence of a robust whole-plant economics spectrum, which not only included the interactions between leaf and wood economics, but also included a bark economics spectrum. Overall, the inconsistent results regarding resource economics suggest that trait coordination may be contingent to the traits examined and the abiotic factors of the environment (Méndez-Alonzo *et al.*, 2012; Reich, 2014). Further studies related to empirical data and meta-analyses are still needed on plant strategies across both large and local scales (Freschet *et al.*, 2010).

4.4.3 Plant resource strategy is influenced by climates and is structured by leaf habits

In agreement with our third hypothesis, we also found tree resource strategy was influenced by climate, and dependent on leaf habit: temperate and Mediterranean or deciduous species tended to gather on the acquisitive side of the whole-tree spectrum, whereas tropical or evergreen species were found more on the conservative side. In addition, we also demonstrated that in tropical species, the relationships between leaf economic traits and leaf NSC content, root wood density and root VF opposed those when species from all climates were pooled together. In general, there is considerably greater species diversity in tropical forests than in temperate or Mediterranean forests (Grubb, 1977; Cunningham and Read, 2002). High taxonomic diversity means tree species could vary in their light requirements (e.g., shade-tolerant versus light-demanding species) which could mediate a trade-off between growth and survival. Also, in warm and wet climates, photosynthesis and growth can continue year-round, minimizing seasonal mismatches between carbon sources and sinks. Additionally, due to different phenologies (Lusk *et al.*, 2008), leaf life span (Westoby *et al.*, 2002; van Ommen Kloeke *et al.*, 2012) and nutrient use efficiency (Aerts, 1995; Aerts, 1999), species with different leaf habit could also lead to contrasting patterns of plant functional strategies. For example, deciduous species with thinner leaf cross-sections and greater stomatal conductance should have higher rates of photosynthesis per unit leaf mass, associated with high N content, compared to evergreen species (Givnish, 2002). Moreover, deciduousness is an adaptation enabling the reduction of transpiration under dry or cold conditions (Givnish, 2002; Zhao *et al.*, 2017). Thus, deciduous species tend to possess an acquisitive strategy for rapid growth after dormancy. In contrast, evergreen species with long leaf lifespan and high nutrient-use efficiency tend to have lower nutrient losses compared to deciduous species, and can also perform photosynthesis over a longer period, albeit at reduced rates (Aerts, 1995; Givnish, 2002), therefore compensating for the increased construction costs of evergreen

leaves (DeLucia *et al.*, 1989; Schlesinger *et al.*, 1989; Gower and Richards, 1990). Evergreen species therefore tend to possess a conservative strategy to maintain normal functioning.

4.5 CONCLUSION

We investigated the coordination of functional traits (including NSC content), that are associated with the economics spectrum, across 90 deciduous and evergreen angiosperm species growing in three contrasting climates. We found that leaf NSC content was coordinated with the leaf economic spectrum, while stem and coarse root xylem NSC content (particularly in stems), was independent of the leaf economics spectrum. In addition, we also found there was a decoupled relationship between leaf and stem economic traits, even though coarse root chemical and xylem traits were coordinated with leaf functional traits. Species evolutionary history did not influence the relationships among traits in different organs. We show that the whole tree economics spectrum was influenced by climate, with tropical species tending to be more conservative while temperate and Mediterranean species were more acquisitive. Deciduous and evergreen species had different resource allocation strategies at both the organ and whole tree level: deciduous trees possessed an acquisitive resource strategy and evergreen species had a conservative resource strategy. We conclude that stem xylem design and NSC storage capacity leads to a stem economics spectrum that is independent from leaf and root spectra. This decoupling reflects the dominant role that stems must play in the efficient transport of nutrients between organs that are primarily responsible for resource capture.

TABLES

Table 4.1 Summary of the 25 measured traits across 90 tree species for leaf and stem (coarse roots were measured in 60 tree species).

Organ	Trait	Abbreviation	Unit	Strategy
Leaf	Leaf carbon content	LC	%	Resource capture
	Leaf nitrogen content	LN	%	Resource capture
	Leaf mass per area	LMA	g m^2	Resource capture and defense
	Leaf soluble sugars	LSS	mg g^{-1}	Resource capture and defense
	Leaf starch	LST	mg g^{-1}	Resource capture and defense
	Leaf non-structural carbohydrates	LNSC	mg g^{-1}	Resource capture and defense
Stem	Stem carbon content	SC	%	Structure and defense
	Stem nitrogen content	SN	%	Structure and defense
	Stem wood density	SWD	g cm^{-3}	Transport, structure and defense
	Stem soluble sugars	SSS	mg g^{-1}	Storage, structure and defense
	Stem starch	SST	mg g^{-1}	Storage, structure and defense
	Stem non-structural carbohydrates	SNSC	mg g^{-1}	Storage, structure and defense
	Stem total parenchyma fractions	SRAP	-	Storage, structure and defense
	Stem vessel fractions	SVF	-	Transport, structure and defense
	Stem fiber (including tracheid) fractions	SFFT	-	Transport, structure and defense
Root	Root carbon content	RC	%	Structure and defense
	Root nitrogen content	RN	%	Structure and defense
	Root wood density	RWD	g cm^{-3}	Transport, structure and defense
	Root soluble sugars	RSS	mg g^{-1}	Storage, structure and defense
	Root starch	RST	mg g^{-1}	Storage, structure and defense
	Root non-structural carbohydrates	RNSC	mg g^{-1}	Storage, structure and defense
	Root wood density	RWD	g cm^{-3}	Transport, structure and defense
	Root total parenchyma fractions	RRAP	-	Storage, structure and defense
	Root vessel fractions	RVF	-	Transport, structure and defense
	Root fiber (including tracheid) fractions	RFFT	-	Transport, structure and defense

Table 4.2 Bivariate relationships between functional traits and the scores of the first and second principal component in leaf, stem (LPC1, 2 and SPC1, 2) across 90 species and in root and whole plant economic spectra (RPC1, 2 and WPC1, 2) across 60 tree species. The Pearson correlation coefficient (r) is given and the significance level is *p < 0.05, **p < 0.01, ***p < 0.001. See Table 4.1 for trait abbreviation.

Traits	Leaf		Stem		Root		Whole-plant	
	LPC1	LPC2	SPC1	SPC2	RPC1	RPC2	WPC1	WPC2
LC	0.58***	-0.56***					-0.44***	0.26**
LN	-0.73***	-0.24***					0.69***	0.27***
LMA	0.86***	-0.16					-0.60***	-0.21
LNSC	-0.38***	-0.74***					0.30***	-0.08
SC			0.08	0.21*			0.01	-0.10
SN			0.52***	-0.34***			0.03	0.41***
SWD			0.25***	-0.48***			-0.55***	0.33***
SNSC			0.65***	0.12			0.04	-0.48***
SRAP			0.88***	0.01			-0.42***	0.68***
SVF			-0.32***	0.80***			0.66***	-0.01
SFFT			-0.64***	-0.69***			-0.30***	-0.48***
RC					0.43***	-0.71***	-0.40***	-0.53***
RN					-0.45***	0.38***	0.45***	0.32***
RWD					0.56***	-0.05	-0.64***	0.17
RNSC					-0.22	0.78***	0.16	0.67***
RRAP					0.81***	0.50***	-0.57***	0.59***
RVF					-0.42***	0.05	0.55***	-0.08
RFFT					-0.53***	-0.55***	0.17	-0.51***

FIGURES

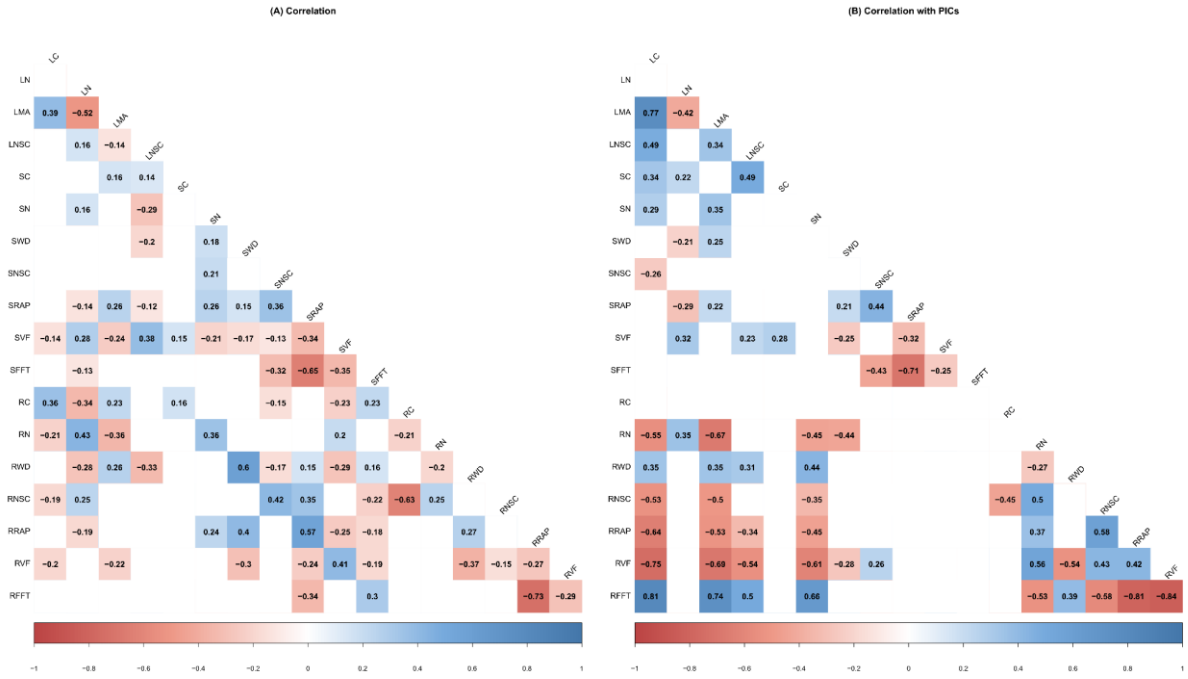

Fig. 4.1 Pearson correlations (A) without and (B) with phylogenetically independent contrasts (PICs) of leaf, stem among 90 species and root traits among 60 species. Different colored squares indicate different significant correlations: blue represents a positive correlation; red represents a negative correlation; white represents no significant correlation. See Table 4.1 for trait abbreviation.

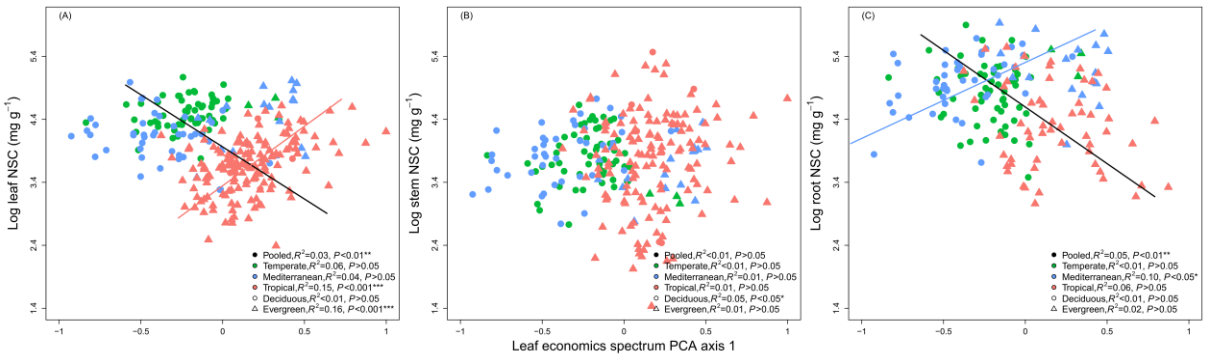

Fig. 4.2 Standardized major axis (SMA) regressions (A, B) between leaf economics spectrum PC1 and leaf and stem NSC for 90 species and (C) between leaf economics spectrum PC1 and root NSC for 60 tree species across climates and leaf habits. Different colors indicate tree species from different climates: green represents temperate species; blue represents Mediterranean species; red represents tropical species. Different dot shapes indicate different leaf habits: circles represent deciduous species; triangles represent evergreen species. Regression lines are shown only for species pooled together and different climates. NSC is non-structural carbohydrates.

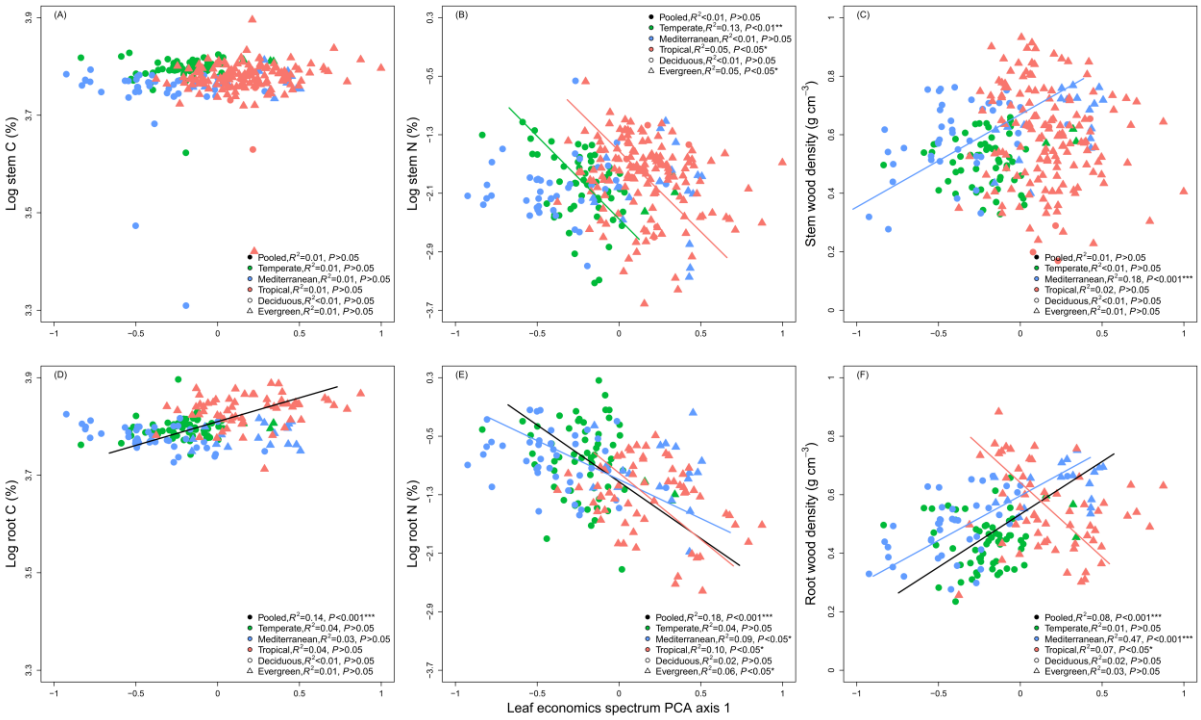

Fig. 4.3 Standardized major axis (SMA) regressions (A, B, C) between leaf economics spectrum PC1 and stem C, N and wood density for 90 species and (D, E, F) between leaf economics spectrum PC1 and root C, N and wood density for 60 tree species across climates and leaf habits. Different colors indicate tree species from different climates: green represents temperate species; blue represents Mediterranean species; red represents tropical species. Different dot shapes indicate different leaf habits: circles represent deciduous species; triangles represent evergreen species. Regression lines are shown only for species pooled together and different climates. C is carbon; N is nitrogen.

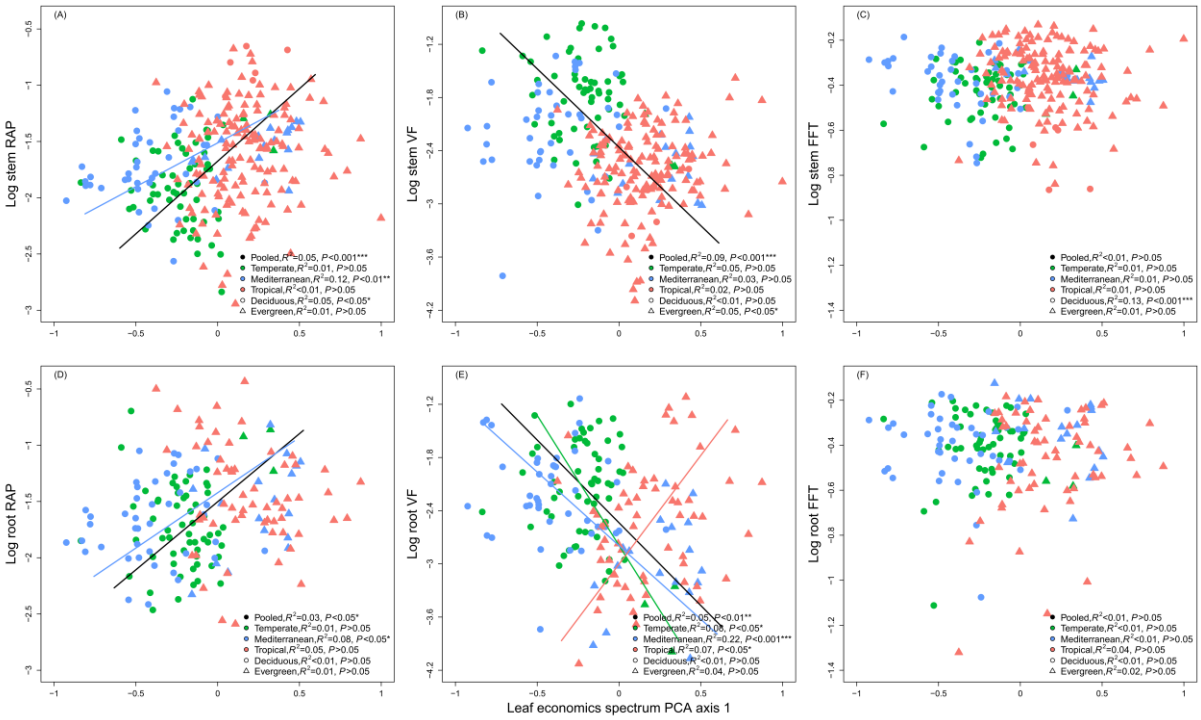

Fig. 4.4 Standardized major axis (SMA) regressions (A, B, C) between leaf economics spectrum PC1 and stem RAP, VF and FFT for 90 species and (D, E, F) between leaf economics spectrum PC1 and root RAP, VF and FFT for 60 tree species across climates and leaf habits. Different colors indicate tree species from different climates: green represents temperate species; blue represents Mediterranean species; red represents tropical species. Different dot shapes indicate different leaf habits: circles represent deciduous species; triangles represent evergreen species. Regression lines are shown only for species pooled together and different climates. FFT is fibre (including tracheid) fractions; RAP is total parenchyma fractions; VF is vessel fractions.

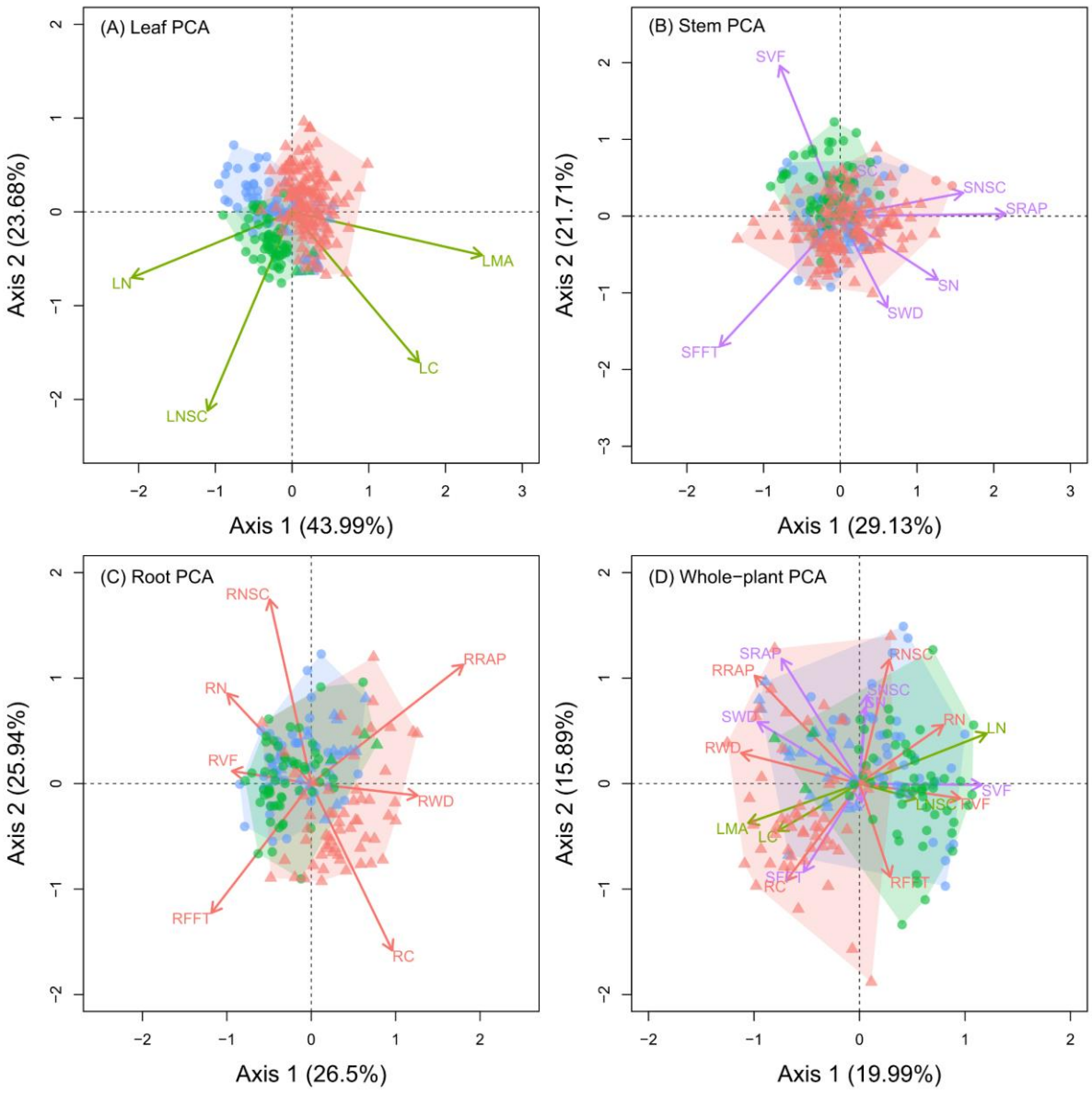

Fig. 4.5 Principal component analysis (PCA) of functional traits among 90 species for (A) leaf, (B) stem, and for (C) root and (D) whole-plant among 60 species. Different colored dots and area indicate tree species from different climates: green represents temperate species; blue represents Mediterranean species; red represents tropical species. Different dot shapes indicate different leaf habits: circles represent deciduous species; triangles represent evergreen species. Green, purple and red arrows represent leaf, stem and root traits, respectively. See Table 4.1 for trait abbreviation.

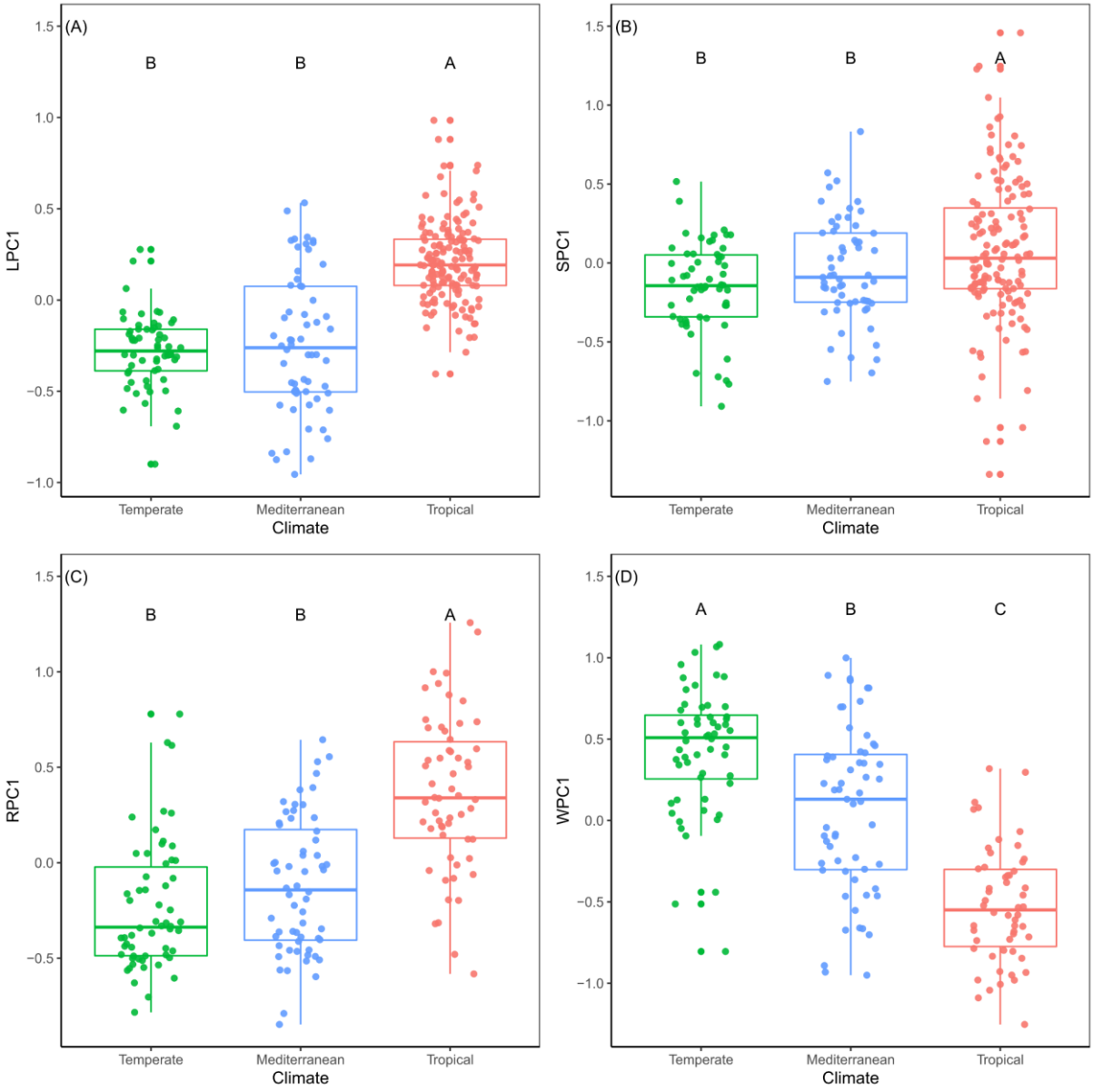

Fig. 4.6 Boxplot of (A) leaf PC1, (B) stem PC1 scores across 90 species and (C) root PC1 and (D) whole-plant PC1 scores across 60 tree species with different climates. The line in the box indicates the median; the whiskers above and below the box indicate the 75th and 25th percentiles. Different uppercase letters indicate significant differences among climates. Different colors indicate tree species from different climates: green represents temperate species; blue represents Mediterranean species; red represents tropical species. LPC1, SPC1, RPC1 and WPC1 represent leaf, stem, root and whole-plant principal component first axis, respectively.

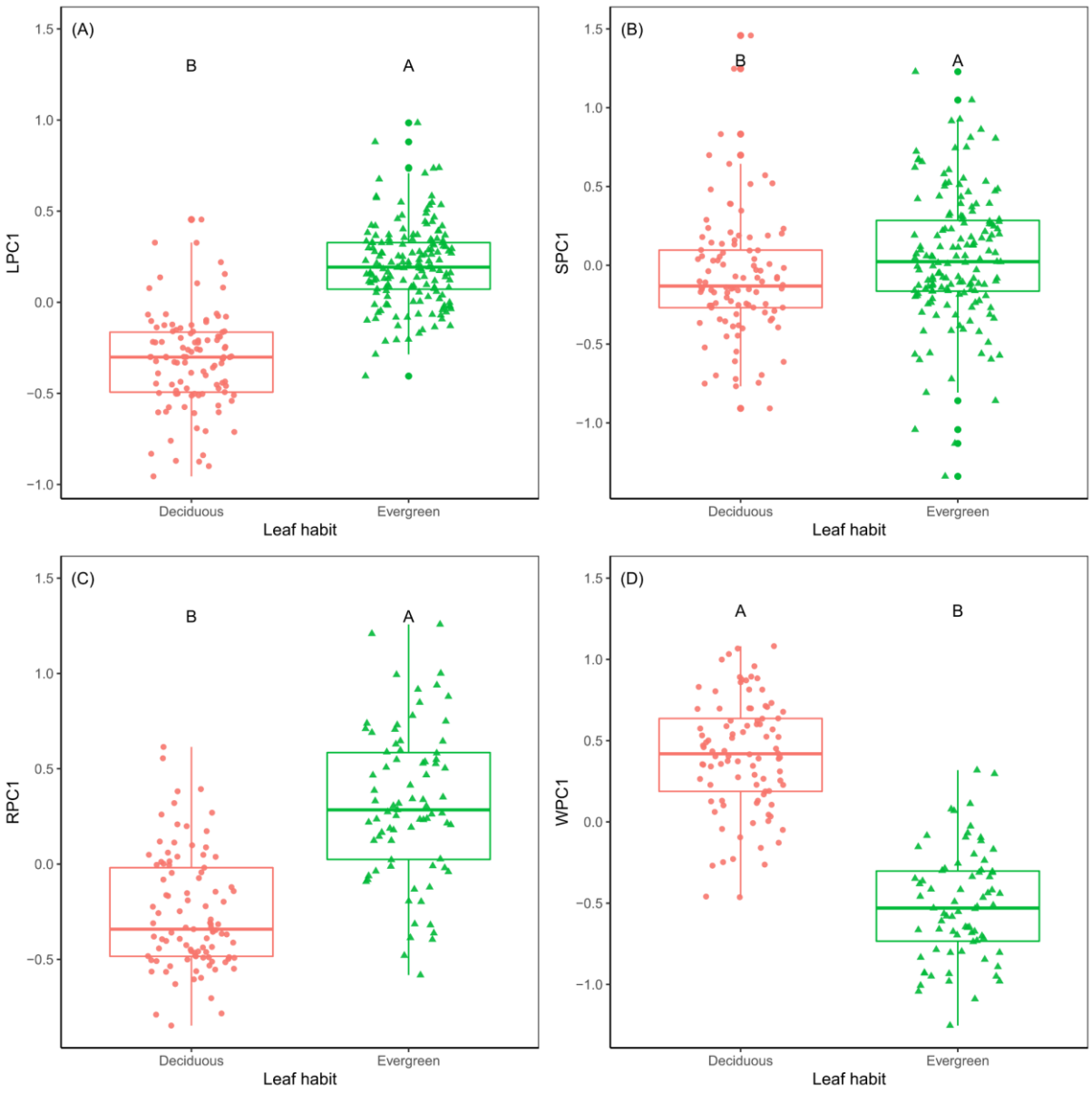

Fig. 4.7 Boxplot of (A) leaf PC1, (B) stem PC1 scores across 90 species and (C) root PC1 and (D) whole-plant PC1 scores across 60 tree species with different leaf habits. The line in the box indicates the median; the whiskers above and below the box indicate the 75th and 25th percentiles. Different uppercase letters indicate significant differences between deciduous and evergreen species. Different colored and shaped dots indicate different leaf habits: red and circle represent deciduous species; green and triangle represent evergreen species. LPC1, SPC1, RPC1 and WPC1 represent leaf, stem, root and whole-plant principal component first axis, respectively.

SUPPLEMENTARY MATERIALS

Table S4.1 List of 90 species from three climates.

Family	Genus	Species	Climate	Leaf habit
Sapindaceae	Acer	*Acer campestre*	Mediterranean	Deciduous
Sapindaceae	Acer	*Acer monspessulanum*	Mediterranean	Deciduous
Ericaceae	Arbutus	*Arbutus unedo*	Mediterranean	Evergreen
Buxaceae	Buxus	*Buxus sempervirens*	Mediterranean	Evergreen
Cannabaceae	Celtis	*Celtis australis*	Mediterranean	Deciduous
Fabaceae	Cercis	*Cercis siliquastrum*	Mediterranean	Deciduous
Cornaceae	Cornus	*Cornus mas*	Mediterranean	Deciduous
Rosaceae	Crataegus	*Crataegus monogyna*	Mediterranean	Deciduous
Oleaceae	Fraxinus	*Fraxinus angustifolia*	Mediterranean	Deciduous
Oleaceae	Fraxinus	*Fraxinus ornus*	Mediterranean	Deciduous
Lauraceae	Laurus	*Laurus nobilis*	Mediterranean	Evergreen
Oleaceae	Phillyrea	*Phillyrea latifolia*	Mediterranean	Evergreen
Anacardiaceae	Pistacia	*Pistacia terebinthus*	Mediterranean	Deciduous
Salicaceae	Populus	*Populus alba*	Mediterranean	Deciduous
Rosaceae	Prunus	*Prunus mahaleb*	Mediterranean	Deciduous
Fagaceae	Quercus	*Quercus ilex*	Mediterranean	Evergreen
Fagaceae	Quercus	*Quercus pubescens*	Mediterranean	Deciduous
Malvaceae	Tilia	*Tilia cordata*	Mediterranean	Deciduous
Ulmaceae	Ulmus	*Ulmus minor*	Mediterranean	Deciduous
Adoxaceae	Viburnum	*Viburnum tinus*	Mediterranean	Evergreen
Sapindaceae	Acer	*Acer pseudoplatanus*	Temperate	Deciduous
Betulaceae	Alnus	*Alnus glutinosa*	Temperate	Deciduous
Betulaceae	Alnus	*Alnus incana*	Temperate	Deciduous
Betulaceae	Betula	*Betula pendula*	Temperate	Deciduous
Fagaceae	Castanea	*Castanea sativa*	Temperate	Deciduous
Fagaceae	Fagus	*Fagus sylvatica*	Temperate	Deciduous
Oleaceae	Fraxinus	*Fraxinus excelsior*	Temperate	Deciduous
Aquifoliaceae	Ilex	*Ilex aquifolium*	Temperate	Evergreen
Juglandaceae	Juglans	*Juglans nigra*	Temperate	Deciduous
Salicaceae	Populus	*Populus nigra*	Temperate	Deciduous
Salicaceae	Populus	*Populus tremula*	Temperate	Deciduous
Rosaceae	Prunus	*Prunus avium*	Temperate	Deciduous
Rosaceae	Prunus	*Prunus spinosa*	Temperate	Deciduous
Rosaceae	Pyrus	*Pyrus communis*	Temperate	Deciduous
Fagaceae	Quercus	*Quercus petraea*	Temperate	Deciduous
Fagaceae	Quercus	*Quercus robur*	Temperate	Deciduous
Salicaceae	Salix	*Salix alba*	Temperate	Deciduous
Salicaceae	Salix	*Salix caprea*	Temperate	Deciduous
Adoxaceae	Sambucus	*Sambucus nigra*	Temperate	Deciduous
Ulmaceae	Ulmus	*Ulmus glabra*	Temperate	Deciduous
Fabaceae	Bocoa	*Bocoa prouacensis*	Tropical	Evergreen
Moraceae	Brosimum	*Brosimum rubescens*	Tropical	Evergreen
Meliaceae	Carapa	*Carapa surinamensis*	Tropical	Evergreen
Malvaceae	Catostemma	*Catostemma fragrans*	Tropical	Evergreen
Urticaceae	Cercropia	*Cecropia obtusa*	Tropical	Evergreen
Urticaceae	Cecropia	*Cecropia sciadophylla*	Tropical	Evergreen
Cordiaceae	Cordia	*Cordia sagotii*	Tropical	Evergreen
Sapindaceae	Cupania	*Cupania rubiginosa*	Tropical	Evergreen
Fabaceae	Dicorynia	*Dicorynia guianensis*	Tropical	Evergreen
Fabaceae	Eperua	*Eperua falcata*	Tropical	Evergreen
Fabaceae	Eperua	*Eperua grandiflora*	Tropical	Evergreen
Vochysiaceae	Erisma	*Erisma uncinatum*	Tropical	Evergreen

Lecythidaceae	Eschweilera	*Eschweilera coriacea*	Tropical	Evergreen
Lecythidaceae	Eschweilera	*Eschweilera sagotiana*	Tropical	Evergreen
Goupiaceae	Goupia	*Goupia glabra*	Tropical	Evergreen
Lecythidaceae	Gustavia	*Gustavia hexapetala*	Tropical	Evergreen
Linaceae	Hebepetalum	*Hebepetalum humiriifolium*	Tropical	Evergreen
Moraceae	Helicostylis	*Helicostylis pedunculata*	Tropical	Evergreen
Simaroubaceae	Homalolepis	*Homalolepis cedron*	Tropical	Evergreen
Humiriaceae	Humiria	*Humiria balsamifera*	Tropical	Evergreen
Fabaceae	Hymenolobium	*Hymenolobium flavum*	Tropical	Deciduous
Fabaceae	Inga	*Inga alba*	Tropical	Evergreen
Myristicaceae	Iryanthera	*Iryanthera hostmannii*	Tropical	Evergreen
Myristicaceae	Iryanthera	*Iryanthera sagotiana*	Tropical	Evergreen
Bignoniaceae	Jacaranda	*Jacaranda copaia*	Tropical	Evergreen
Apocynaceae	Lacmellea	*Lacmellea aculeata*	Tropical	Evergreen
Salicaceae	Laetia	*Laetia procera*	Tropical	Evergreen
Lecythidaceae	Lecythis	*Lecythis poiteaui*	Tropical	Evergreen
Chrysobalanaceae	Licania	*Licania alba*	Tropical	Evergreen
Fabaceae	Limadendron	*Limadendron hostmannii*	Tropical	Evergreen
Euphorbiaceae	Maprounea	*Maprounea guianensis*	Tropical	Evergreen
Melastomataceae	Miconia	*Miconia acuminata*	Tropical	Evergreen
Sapotaceae	Micropholis	*Micropholis guyanensis*	Tropical	Evergreen
Annonaceae	Oxandra	*Oxandra asbeckii*	Tropical	Evergreen
Chrysobalanaceae	Parinari	*Parinari campestris*	Tropical	Evergreen
Peraceae	Pogonophora	*Pogonophora schomburgkiana*	Tropical	Evergreen
Rubiaceae	Posoqueria	*Posoqueria latifolia*	Tropical	Evergreen
Sapotaceae	Pradosia	*Pradosia cochlearia*	Tropical	Evergreen
Burseraceae	Protium	*Protium opacum subsp rabelianum*	Tropical	Evergreen
Burseraceae	Protium	*Protium subserratum*	Tropical	Evergreen
Vochysiaceae	Qualea	*Qualea rosea*	Tropical	Evergreen
Malvaceae	Sterculia	*Sterculia pruriens*	Tropical	Deciduous
Clusiaceae	Symphonia	*Symphonia globulifera*	Tropical	Evergreen
Fabaceae	Tachigali	*Tachigali melinonii*	Tropical	Evergreen
Anacardiaceae	Tapirira	*Tapirira guianensis*	Tropical	Evergreen
Dichapetalaceae	Tapura	*Tapura capitulifera*	Tropical	Evergreen
Myristicaceae	Virola	*Virola michelii*	Tropical	Evergreen
Hypericaceae	Vismia	*Vismia sessilifolia*	Tropical	Evergreen
Fabaceae	Vouacapoua	*Vouacapoua americana*	Tropical	Evergreen
Annonaceae	Xylopia	*Xylopia nitida*	Tropical	Evergreen

Table S4.2 Model parameters of near-infrared spectroscopy (NIRS) calibration for soluble sugars and starch.

Organ	NSC	No.	R^2c	SEC	RMSECV	R^2p	RMSEP
Stem	Soluble sugars	113	0.82	4.1	5.2	0.68	5.2
	Starch	113	0.75	12.9	13.2	0.74	11.3
Root	Soluble sugars	140	0.85	8.2	11.6	0.71	11.0
	Starch	140	0.95	17.5	21.6	0.89	22.7

Note: NSC is non-structural carbohydrates, No. is number of samples for calibration, R^2c is coefficient of determination in calibration, SEC is standard error of calibration, RMSECV is root mean square error of cross validation, R^2p is coefficient of determination in prediction, RMSEP is root mean square error of prediction.

Table S4.3 Model parameters of near-infrared spectroscopy (NIRS) calibration for carbon and nitrogen.

Organ	Trait	No.	R^2c	SEC	RMSECV	R^2p	RMSEP
Leaf	Carbon	110	0.92	0.84	1.04	0.78	1.47
	Nitrogen	110	0.90	0.17	0.19	0.89	0.20
Stem	Carbon	113	0.92	0.28	0.38	0.85	0.32
	Nitrogen	113	0.87	0.02	0.04	0.87	0.03

Note: No. is numbers of samples for calibration, R^2c is coefficient of determination in calibration, SEC is standard error of calibration, RMSECV is root mean square error of cross validation, R^2p is coefficient of determination in prediction, RMSEP is root mean square error of prediction.

Table S4.4 The mean value of soluble sugars and starch in leaf, stem and root across total, deciduous, evergreen, temperate, Mediterranean and tropical species, respectively. Different lowercase letters indicate significant differences between soluble sugars and starch in the same organ.

NSC	Total species			Deciduous species			Evergreen species		
	Leaf	Stem	Root	Leaf	Stem	Root	Leaf	Stem	Root
Sugars	56.14 a	15.85 b	29.91 b	74.11 a	16.98 b	31.28 b	44.70 a	15.14 b	28.27 b
Starch	4.09 b	35.91 a	105.91 a	4.53 b	35.28 a	116.22 a	3.81 b	36.33 a	93.01 a
NSC	Temperate species			Mediterranean species			Tropical species		
	Leaf	Stem	Root	Leaf	Stem	Root	Leaf	Stem	Root
Sugars	86.58 a	12.95 b	28.78 b	66.86 a	22.97 a	39.46 b	39.67 a	14.11 b	21.46 b
Starch	5.47 b	34.17 a	112.82 a	6.00 b	25.45 a	133.33 a	2.78 b	41.03 a	70.41 a

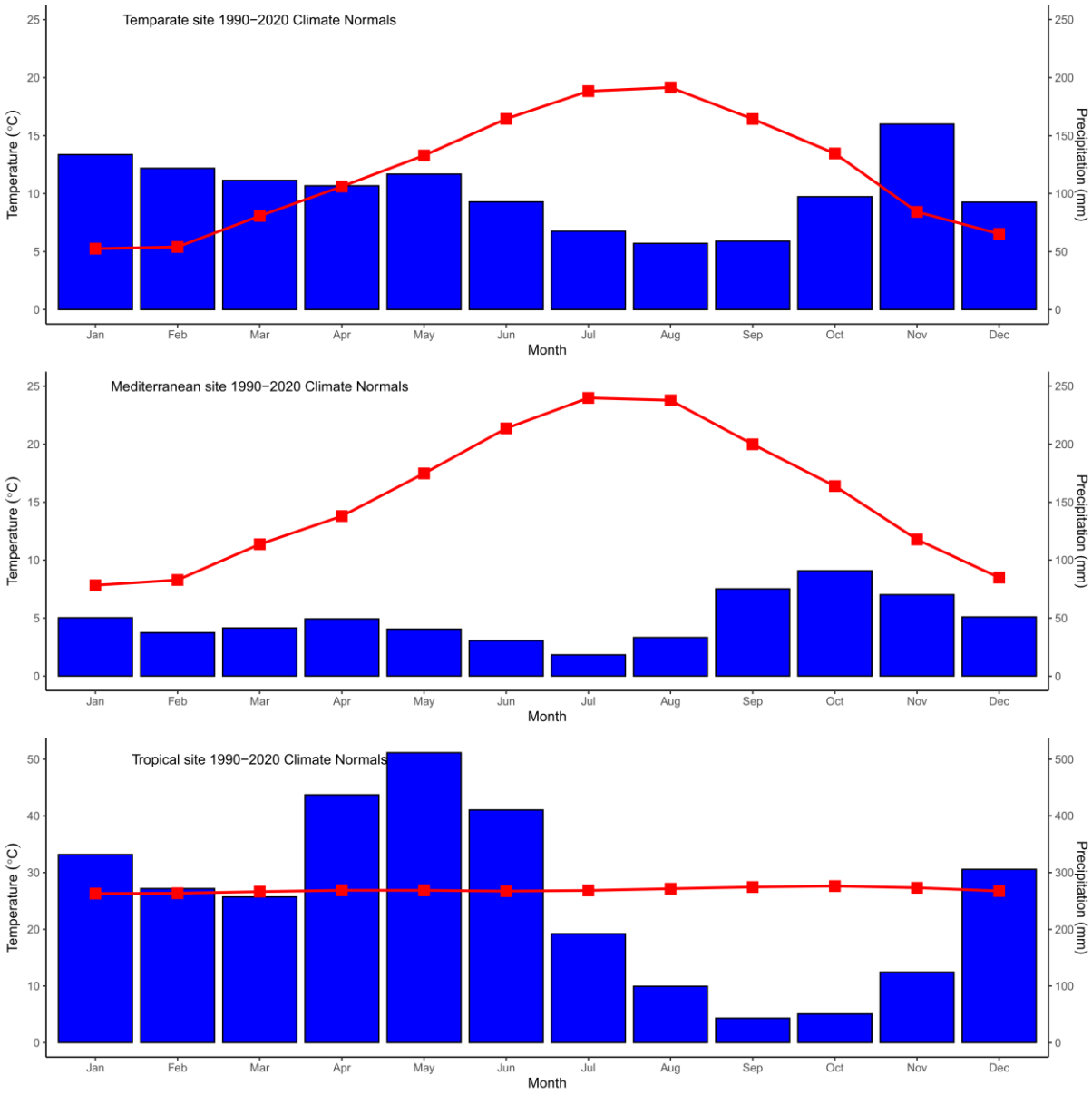

Fig. S4.1 1990 – 2020 climate normal in three climate sites. The red line represents the monthly average temperature and the blue bars represent the monthly average precipitation.

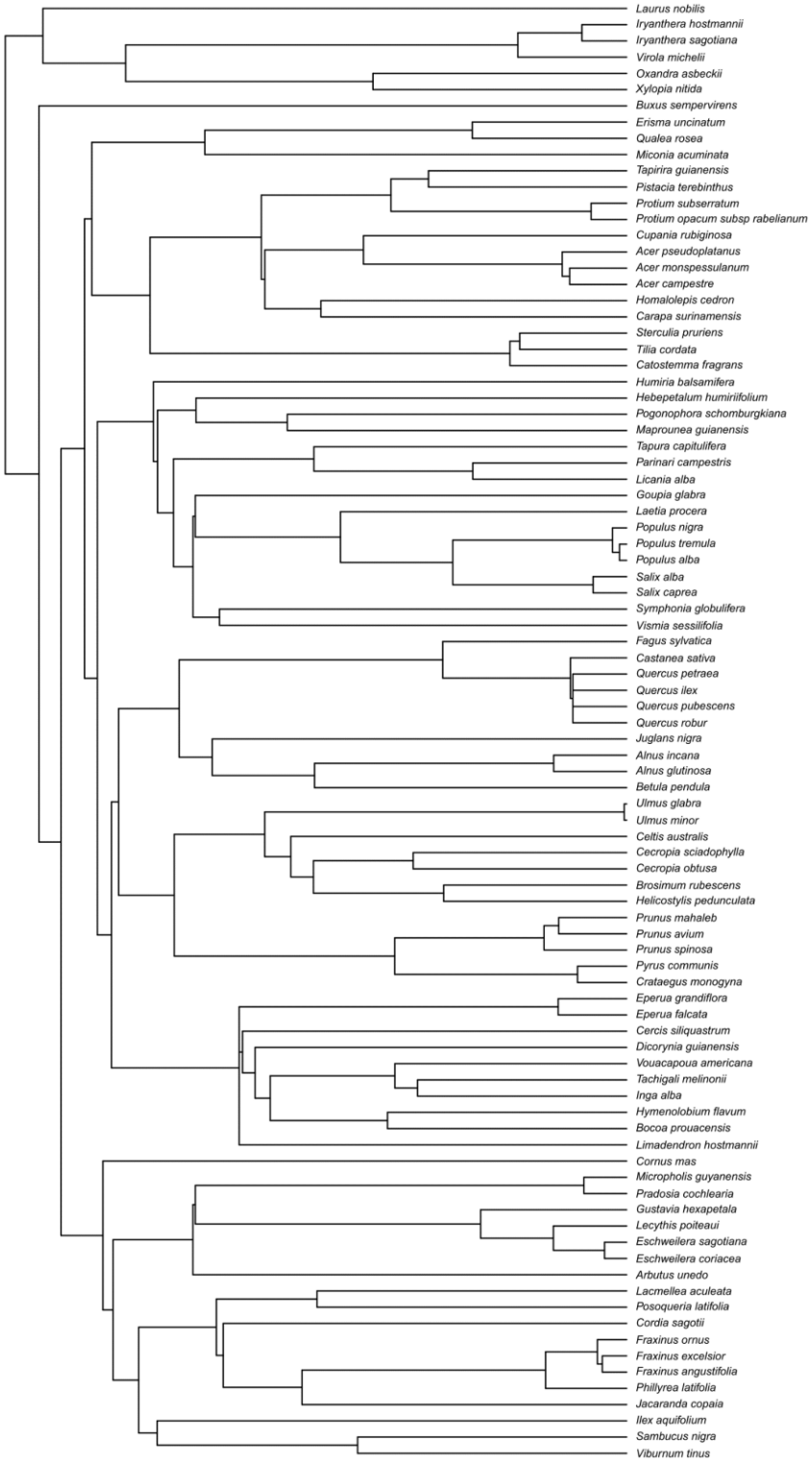

Fig. S4.2 Phylogenetic tree of the 90 tree species. The backbone is based on GBOTB (GenBank and phylogenetic data from the Open Tree of Life, version 9.1)

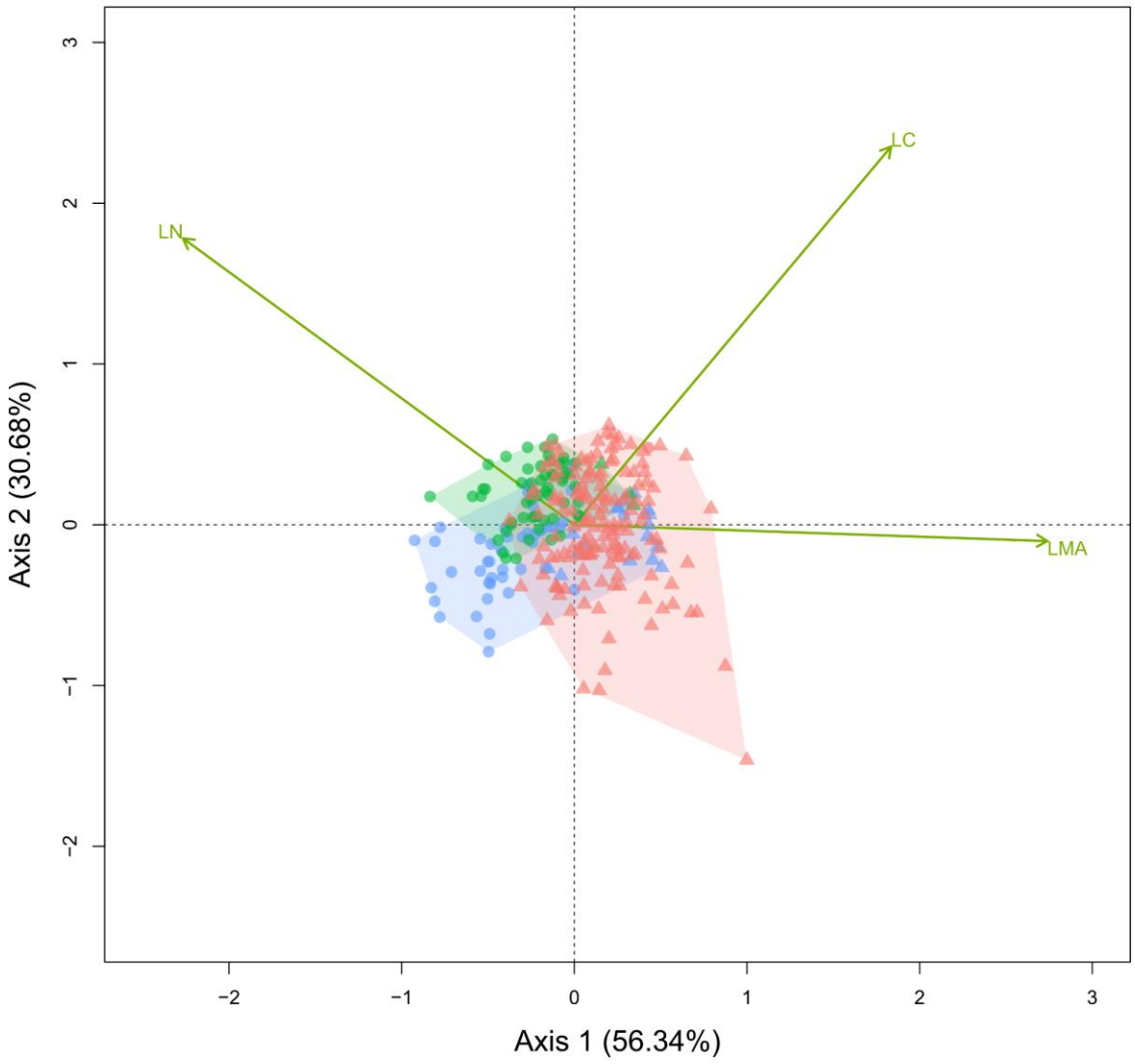

Fig. S4.3 Principal component analysis (PCA) of LMA, leaf nitrogen (LN) and leaf carbon (LC) across 90 species to show the classical leaf resource economics spectrum. Different colored dots and area indicate tree species from different climates: green represents temperate species; blue represents Mediterranean species; red represents tropical species. Different dot shapes indicate different leaf habits: circles represent deciduous species; triangles represent evergreen species.

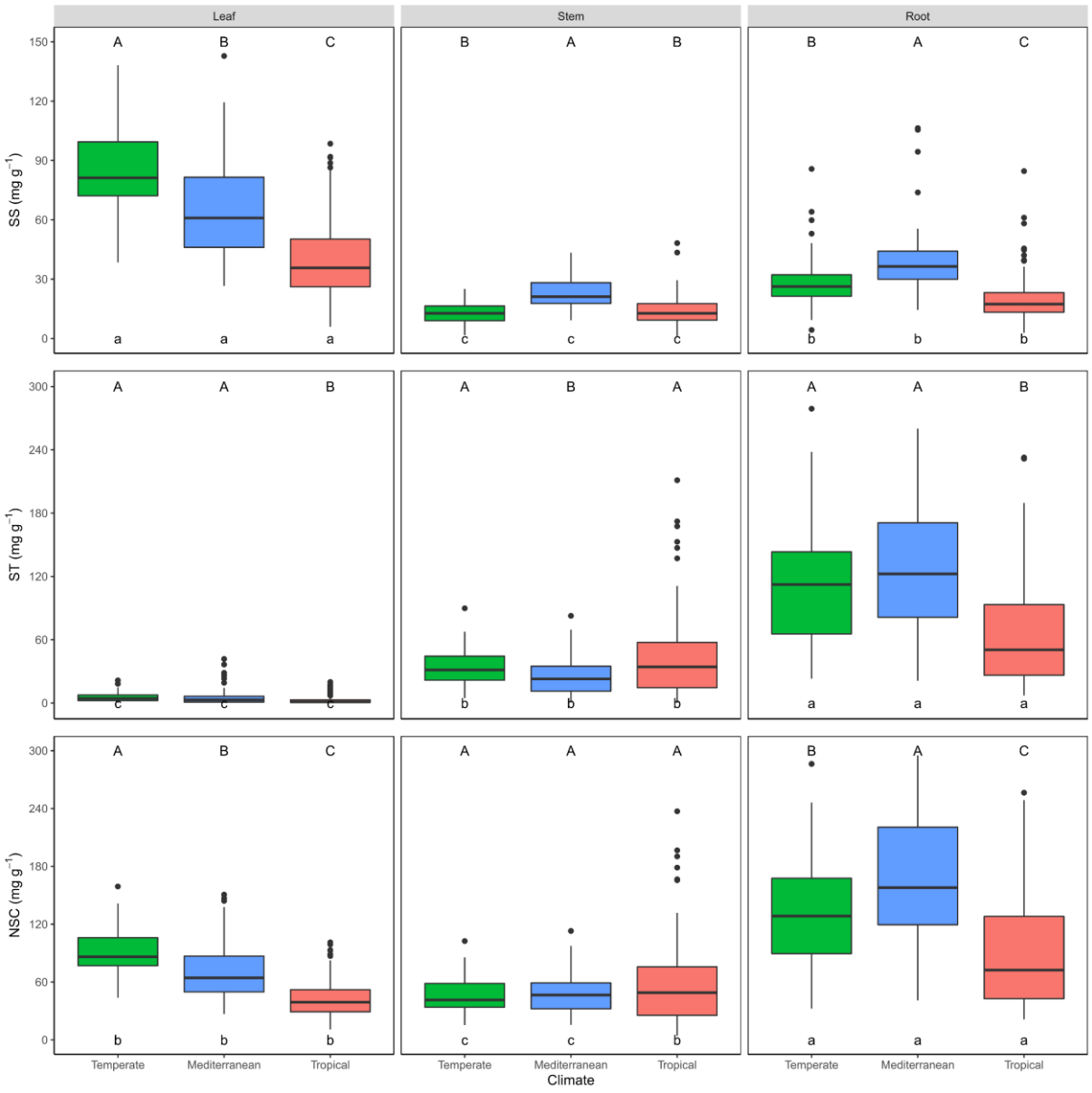

Fig. S4.4 Boxplot of leaf, stem NSC content across 90 tree species and root NSC content across 60 tree species with different climates. The line in the box indicates the median; the whiskers above and below the box indicate the 75th and 25th percentiles. Different uppercase letters indicate significant differences among climates in the same organ. Different lowercase letters indicate significant differences among organs in the same climate. Different colors indicate tree species from different climates: green represents temperate species; blue represents Mediterranean species; red represents tropical species. NSC is non-structural carbohydrates.

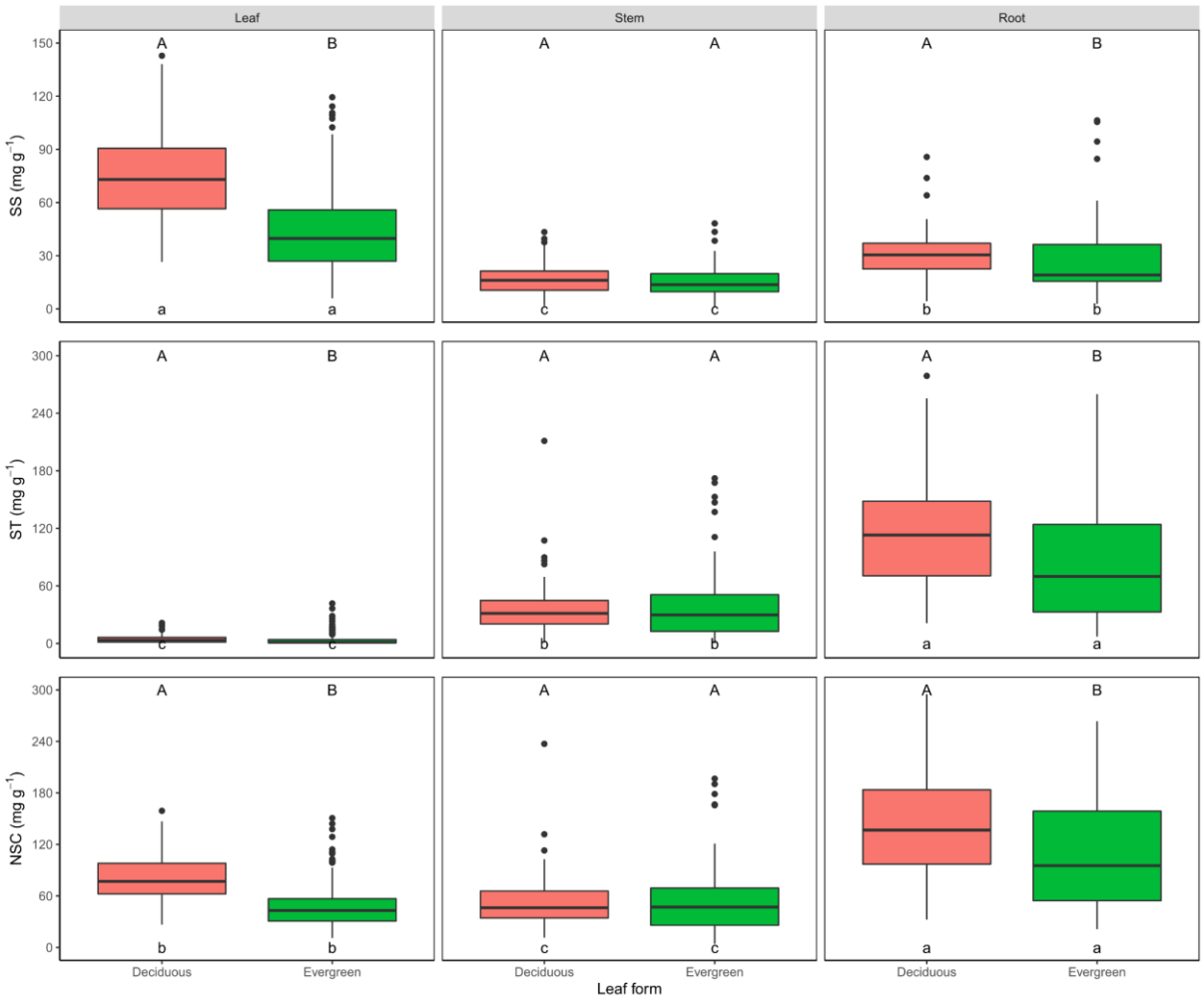

Fig. S4.5 Boxplot of leaf, stem NSC content across 90 tree species and root NSC content across 60 tree species with different leaf habits. The line in the box indicates the median; the whiskers above and below the box indicate the 75th and 25th percentiles. Different uppercase letters indicate significant differences between deciduous and evergreen species in the same organ. Different lowercase letters indicate significant differences between organs in the same leaf habit. Different colors indicate different leaf habits: red represents deciduous species; green represents evergreen species. NSC is non-structural carbohydrates.

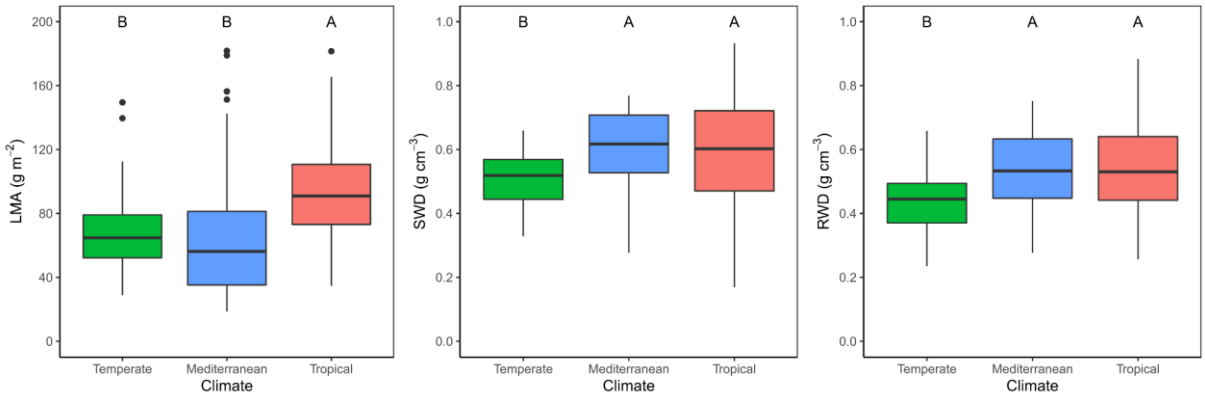

Fig. S4.6 Boxplot of LMA and stem wood density across 90 tree species and root wood density across 60 tree species with different climates. The line in the box indicates the median; the whiskers above and below the box indicate the 75th and 25th percentiles. Different uppercase letters indicate significant differences among climates. Different colors indicate tree species from different climates: green represents temperate species; blue represents Mediterranean species; red represents tropical species. LMA is leaf mass per area; SWD is stem wood density and RWD is root wood density.

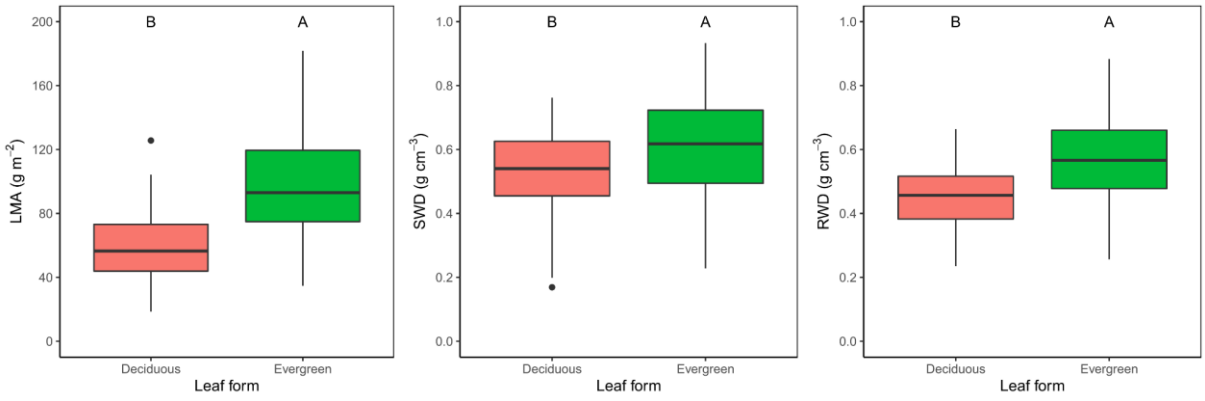

Fig. S4.7 Boxplot of LMA and stem wood density across 90 tree species and root wood density across 60 tree species with different leaf habits. The line in the box indicates the median; the whiskers above and below the box indicate the 75th and 25th percentiles. Different uppercase letters indicate significant differences between deciduous and evergreen species. Different colors indicate different leaf habits: red represents deciduous species; green represents evergreen species. LMA is leaf mass per area; SWD is stem wood density and RWD is root wood density.

CHAPTER 5: General discussion

The overarching aim of the study presented in my thesis was to provide foundational knowledge about the trade-offs in resource allocation from a whole-plant perspective, and to better quantify xylem structure and function related to water transportation, mechanical support and storage. In Chapter 2, I carried out a systematic review by compiling a database which included NSC, RAP, wood density and maximum tree height data for 68 tree species to explore the relationships among these traits, especially the relationship between NSC and parenchyma fraction. In Chapter 3 and 4, I collected leaves, stems and roots xylem from 90 species grown under three climates and measured functional traits including NSC, carbon, nitrogen, leaf mass per area, stem and root wood density and xylem anatomical traits to disentangle how NSC and xylem traits are linked to tree physiological processes and ecological strategies and explore the trade-off of xylem structure and function. My findings deepen our understanding about how parenchyma fractions affect NSC storage and the role of NSC as well as the design of xylem space in tree physiological processes, especially across a broad range of species and climates. In this chapter, I summarize the key results from each paper chapter and then discuss the broader insights that have been gained about the trade-offs of NSC and xylem traits in different forest trees. At the end, I discuss the implications of what has been learned and provide some recommendations for further research.

5.1 SUMMARY OF KEY RESULTS

In Chapter 2, with the systematic review, we confirmed that trees with large RAP fractions had more NSC contents in stem, underlining the important role of parenchyma cells in NSC storage. In addition, we did not find higher NSC in denser wood, although the radial parenchyma (but not axial parenchyma) fraction was positively related to wood density, but NSC and RAP were more abundant in tropical species. These findings were also be confirmed

in Chapter 3, which we investigated stem and root xylem traits (including NSC and anatomical traits) of 60 tree species from temperate, Mediterranean and tropical climates. In addition, we also found that all xylem traits showed marked interspecific variation and certain xylem traits were also significantly different between stems and roots: wood density, vessel fraction and vessel density were higher in stem, while axial parenchyma fractions, RAP fractions, NSC contents were higher in roots. And xylem traits also varied significantly across climates and xylem arrangement types. By examining how the design of xylem space coordinate with multifunctionality, we revealed a trade-off between xylem mechanical support and hydraulic conductivity as there was negative correlation between specific xylem hydraulic conductivity (SXHC) and wood density. Additionally, NSC contents were significantly and positively associated with SXHC in stem xylem, whereas negative correlations were found between NSC contents and SXHC in roots, indicating hydraulic-storage strategies differed between stems and roots, with more closer ties existing in the stem.

In Chapter 4, we investigated coordination of functional traits along with plant economics spectrum of leaf, stem and root across 90 angiosperm species from temperate, Mediterranean and tropical forests to explore the functional role of NSC content in plant resource acquisitive and conservative strategies. Our findings revealed that leaf NSC content was coordinated with leaf economics traits, as species with higher leaf NSC tend to exhibit resource acquisitive strategy. The variation between NSC content in woody organs, especially in stems, and economics traits were largely decoupled. Moreover, leaf functional traits were closely related with xylem anatomical traits and root traits, while most of stem traits were independent of leaf economics spectrum. Plant ecological strategies were influenced by climates and species with different leaf habit exhibiting different resource strategies: temperate, Mediterranean and deciduous species tend to gather on acquisitive side, whereas tropical and evergreen species tend to gather on conservative side.

5.2 ADVANCES IN KNOWLEDGE

5.2.1 Traits matters: with focusing on NSC content and parenchyma fractions

The use of trait-based approaches is widespread in ecology and evolutionary research and functional traits are considered the widely accepted tool for studying the plant strategies (Violle *et al*., 2007). Relative to other functional traits, NSC and xylem anatomical traits are less widely used in the study of ecological strategies, although they are increasingly recognized as core functional traits in plants recently. The importance of NSC storage for tree growth and functioning have been known for many decades (Kozlowski, 1992; Morin *et al.*, 2007; Sala *et al.*, 2012; Klein and Hoch, 2015; Furze *et al.*, 2019). The storage of NSC is arguably one of the most widely accepted functions of RAP and put in contrast with the main role of vessels in facilitating water conduction and the role of fibers in providing the mechanical support. Regarding if parenchyma fractions that can directly affect NSC storage pool size is still limited understood, although studies found positive correlations between NSC contents and RAP fractions in woody stem and branches with limited number of species (Plavcová *et al.*, 2016; Chen *et al.*, 2020; Kawai *et al.*, 2021). Our systematic review in Chapter 2 confirmed the important role of stem parenchyma in NSC storage across a broad range of tree species. However, when considering tree evolution subdivisions (angiosperms vs. gymnosperms), we did not find significant relationships between NSC contents and RAP fractions in gymnosperms. The distinct differences in wood structure and function between angiosperms and gymnosperms could mask effect. Angiosperms have a wide range of ray types and dimensions, whereas gymnosperms usually only have uni/bi-seriate rays. The amount of NSC was also greater in angiosperms than in gymnosperms, which translated in different associations between NSC contents and RAP fractions. Also, the proportion of axial

parenchyma in conifers that constitutes secondary xylem is usually much lower than that of angiosperms (Spicer, 2014; Morris *et al.*, 2016; Aritsara *et al.*, 2021).

Besides the total amount of parenchyma fractions, their partitioning into axial parenchyma and radial parenchyma fractions is of importance. According to the findings of Chapter 2, we found a positive relationship between NSC contents and radial parenchyma across 68 species, but no relationships with axial parenchyma, which indicate that radial parenchyma may play a greater role in NSC storage than axial parenchyma. Although total parenchyma fractions were not correlated with hydraulic properties (Jacobsen *et al.*, 2007; Poorter *et al.*, 2010a; Fortunel *et al.*, 2014), it has been suggested that the axial parenchyma can influence hydraulic capacitance in angiosperms by releasing water into vessels in periods of drought (Morris *et al.*, 2018b). Additionally, vessel to axial parenchyma connectivity would facilitate xylem hydraulic optimization, suggesting that plants may need axial parenchyma to surround and service vessels (Ziemińska *et al.*, 2020; Aritsara *et al.*, 2021). However, inconsistent with our results is that Chen *et al.* (2020) found that xylem NSC contents were positively related to axial parenchyma fractions, but not related to the radial parenchyma fractions in branches of 19 temperate tree species. The possible reason is that the physiological function of both types of parenchyma could be very different between woody organs, calling for a careful consideration of xylem structure for a better understanding of tree ecological strategies.

Furthermore, in Chapter 3, we also examined how RAP patterns affected NSC contents by measuring stem xylem traits acorss 60 species. We confirmed that both radial and axial parenchyma fractions are positively correlated with NSC in the stem, which evidenced that parenchyma fractions could act as a proxy for NSC storage capacity. These findings are timely and relevant in the study focus on storage function, especially for the measurement of NSC is not easy at large-scale stuies due to the seasonality in NSC fluxes. The direct links

between NSC content and parenchyma fractions could provide a new outlook and further insight on studies focus on carbon storage under changed envrionment, especially in long term drought responses.

5.2.2 Multifunctionality matters: trade-offs between xylem structure and function

The xylem of woody organs mainly provides three types of functions: hydraulic functioning, carbohydrate storage and mechanical support, which linked three cell types: vessels (sometimes tracheids), parenchyma and fibers. However, trees have evolved in response to a multitude of diverse environmental signals, that have led to trade-offs in structure and function within the xylem space (Pratt *et al.*, 2007; Grubb, 2016; Pratt *et al.*, 2021a). The resulting design of the xylem space actively influences physiological processes occurring within trees, potentially driving survival or failure when local environmental conditions change. Understanding the trade-offs between structure and function therefore, will allow us to identify strategies that contribute to tree survival in different climates. A number of studies have explored the interrelations between hydraulic efficiency and mechanical support, with inconsistent results. Our study findings from the Chapter 3 revealed a negative relationship between wood density and SXHC in both stem and root across 60 tree species, which implied that there is a trade-off between mechanical strength and hydraulic conductivity, as well as shown in previous studies (Christensen-Dalsgaard *et al.*, 2007a; Christensen-Dalsgaard *et al.*, 2007b; McCulloh *et al.*, 2011; Janssen *et al.*, 2020). In species showing a relatively large fraction of vessels and mean vessel diameters, hydraulic conductivity should be correlated negatively with wood density as wood density is often influenced by the allocation of xylem volume (Markesteijn *et al.*, 2011; Hoeber *et al.*, 2014). Following the Hagen-Poiseuille law, xylem hydraulic conductivity is proportional to vessel diameter to the fourth power (Tyree and Ewers, 1991), thus species with large vessel diameter tend to have higher SXHC and thus

reduced wood density. Similarly, dense wood should have denser cell packing with narrower vessel lumens and thus lower SXHC (Markesteijn *et al.*, 2011; Zanne *et al.*, 2010). It is assumed that denser tissues would affect the efficiency between vessels with narrower diameter and thicker walls, because thicker walls will increase the path length through the pits where sap flows in between vessels, which would reduce hydraulic efficiency (Lens *et al.*, 2011; Pratt *et al.*, 2021a). However, the trade-off between wood density and hydraulic conductivity does not seem to be universally valid as other studies failed to find any trade-off (Pratt *et al.*, 2007; Martínez-Cabrera *et al.*, 2009; Poorter *et al.*, 2010a; Schuldt *et al.*, 2013). The possible explanation may be that compared to vessel characters, other properties that could drive wood density such as fiber wall thickness and non-lumen tissues may not directly affect hydraulic conductivity (Ziemińska *et al.*, 2013; Hoeber *et al.*, 2014; Badel *et al.*, 2015). Additionally, the relationships between wood properties and tree hydraulics may also depend on the biogeographic origin or drought adaptation strategies of the species studied, since converging environmental factors (such as water availability) are known to contribute to the variation of functional wood anatomical properties (Swenson and Enquist, 2007; Richardson *et al.*, 2013b).

The hydraulic efficiency versus safety trade-off is one of the most frequently studied relationships, although this trade-off still remains poorly understood (Badel *et al.*, 2015; Gleason *et al.*, 2016; Pratt and Jacobsen, 2017). Hydraulic efficiency usually refers to specific xylem hydraulic conductivity and is commonly expressed as the rate of water transport through a given area of sapwood across a given pressure gradient, while hydraulic safety refers to resistance to embolism and is expressed as the negative pressure for a given percentage loss of maximum efficiency (Gleason *et al.*, 2016; Pratt *et al.*, 2021a). In line with our results form Chapter 3, the commonly observed negative relationship between vessel diameter and vessel density could be associated with the hydraulic trade-off (Sperry *et al.*,

2008; Zanne *et al.*, 2010). Wide vessel diameters are important for achieving the greater hydraulic efficiency, while high vessel density is important for safety as it reduces the overall impact of cavitation in a single vessel (Tyree and Ewers, 1991; Ewers *et al.*, 2007). A recent meta-analysis assessed the hydraulic efficiency and safety trade-off and found that there is a negative but weak correlation between these two traits, supporting the idea of hydraulic trade-off (Gleason *et al.*, 2016). Besides, most of species tend to have low efficiency and low safety, which was interpreted as being due to the influence of both ecological and evolutionary factors (Pratt and Jacobsen, 2017). Another recent study explained that both the climatic conditions during the growth season and seasonality were inportant factors affecting the co-optimization of hydraulic efficiency and safety for both angiosperms and gymnosperms (Liu *et al.*, 2021).

The economics spectrum theory is widely used to describe functional traits patterns which define plant ecological strategies (Wright *et al.*, 2004; Chave *et al.*, 2009; Reich, 2014; Díaz *et al.*, 2016). The trade-offs between acquisition and conservation of resources is the main argument of economics spectrum, and species with a acquisitive resource-use strategy tend to have higher photosynthetic rates, higher leaf nitrogen and lower leaf mass per area, while species with contrasting traits associated with conservative resource-use strategy. Woody organs contain parenchyma which is primarily storage tissue (Plavcová *et al.*, 2016; Zhang *et al.*, 2022a) and it could be expected that species with more parenchyma fractions tend to have acquisitive strategy as greater storage may align with presence in a resource-rich environment (Lubbe *et al.*, 2021). However, our results in Chapter 4 revealed that parenchyma fractions were positively correlated with LMA and negatively correlated with leaf N content, which means parenchyma fractions increases with a more conservative strategy. This could be caused by a trade-off between carbon allocation to growth and allocation to storage and defense. Allocation to storage and defense has a low opportunity cost because of the low

growth potential in low light (Poorter and Kitajima, 2007; Piper, 2015). In addition, parenchyma cells have multiple functional roles in woody xylem except for nutrient storage, including defense and wound repair (Morris *et al.*, 2020) and mechanical support (Burgert and Eckstein, 2001; Rana *et al.*, 2009). Vessel fraction has been linked to hydraulic efficiency (Zanne *et al.*, 2010) and thus could be part of the resource acquisitive strategy, which is consistent with what we have observed.

5.2.3 Organ matters: different organs with different traits performance

In general, the growth of trees depends not only on the acquisition of above-ground resources, but also on the acquisition of underground resources and the condition of transportation and storage in the xylem. The combined study of leaf, stem and root traits may explain the growth of trees better than the study of individual organ. Simultaneously, different organs also have different traits use which jointly shape species performance and distribution. For example, when studying the relationship between NSC and RAP in stem and root, we did not find significant relationships between axial parenchyma and NSC in root (Chapter 3), which implied axial parenchyma might perform other functions in root, such as hydraulic transport and optimization (Morris *et al.*, 2018a; Aritsara *et al.*, 2021). Another potential reason would be that axial parenchyma in root was higher than that in stem and exhibited greater variation (Morris *et al.*, 2016; Spicer, 2014). In addition, our findings from Chapter 3 also revealed contrary correlation patterns between NSC and SXHC in stem and root, which indicated high NSC storage capacity was associated with high hydraulic conductivity in stem, but with low hydraulic conductivity in root. This opposite strategy may be related to the different functions performed by radial parenchyma and axial parenchyma, as well as the utilization of parenchyma in the root and stem (Zheng and Martínez-Cabrera, 2013; Secchi *et al.*, 2017; Aritsara *et al.*, 2021). In agreement with previous study (Morris *et al.*, 2018a), our results

confirmed that higher axial parenchyma was associated with larger vessel mean diameter, which revealed the important role of axial parenchyma in xylem water transport. In contrast, radial parenchyma was negatively associated with vessel mean diameter and hydraulic conductivity, showing the functional differentiation of axial and radial parenchyma in xylem hydraulic efficiency (Zheng and Martínez-Cabrera, 2013). As mentioned above, in stem, both radial and axial parenchyma contributed to the NSC storage, while in root axial parenchyma was more inclined hydraulic function, which explains why relationships between NSC storage and hydraulic conductivity in stem and root exhibit different patterns. Additionally, it should be noted that roots tend to play a greater role in carbohydrate storage but with fewer mechanical demands than do stems, which could also lead to different trade-off strategies in different woody organs (Plavcová *et al.*, 2019).

Our results from Chatper 4 suggested that there was a covariation between leaf and root NSC content and leaf economics traits indicating species with higher leaf NSC content tend to have higher N content and lower LMA, whereas stem NSC content was largely decoupled with leaf economics spectrum when all species pooled togehter. Lower LMA and higher N content is usually associated net photosynthetic rate, and thus the observed increase in leaf NSC content with increasing N content possibly resulted from the higher photosynthetic rate (Wright *et al.*, 2002; Li *et al.*, 2016). Although we found that root NSC content was associated with leaf economic traits, in terms of whole-plant PCA, both stem and root NSC content showed an orthogonal trend with other traits along with the first PCA axis from acquisitive resource strategy to conservative resource strategy. The underlying cause may be the age difference between leaf NSC and stem or root NSC, as the carbon accumulation of leaf and woody organs act on different time scales (Carbone *et al.*, 2013; Richardson *et al.*, 2015). According to the distance and osmotic gradient between carbon source and sink, the allocation of NSC in stem and root could take several seasons or even years (Hartmann and Trumbore, 2016). The

NSC stored recently in leaves can be used quickly and support daily metabolism, whereas older NSC stored in stems and roots may serve as long-term storage pool and contribute to regrowth after disturbance (Vargas *et al.*, 2009; Clarke *et al.*, 2013). Therefore, stem and root NSC content probably remain sequestered and may not vary considerably before a disturbance and thus may not coordinate with functional traits associated with plant economics spectrum.

5.2.4 Climate matters: traits and functions were affected by climates

Studies of functional traits across biomes would advance our understanding of plant function. Due to the divergence of functional traits in temperate, Mediterranean and tropical climates as well as wet versus dry conditions, there is likely to perform differentiated plant ecological strategies. Our results revealed that tropical species have higher wood density than temperate species in both stem and root, even if the wood density of tropical species with greater ranges and variances (Chapter 3), which is different from the result of Wiemann and Williamson (2002) who found a similar wood density between temperate and tropical species. we also found that the total parenchyma fraction was higher in tropical species than that in temperate species, which is mainly due to the increase in axial parenchyma rather than radial parenchyma (Chapter 2, 3). When evaluating the relationship between NSC and RAP in each climate, we found there was no significant correlation between NSC and RAP in temperate species which is contrary to our expectation (Chapter 3). This is probably because NSC content would vary greatly with environment and seasonal changes, especially in temperate climate (Smith *et al.*, 2018a; Furze *et al.*, 2020). Multiple seasonal sampling should be considered in future studies, including NSC measurements under drought conditions.

The plant resource strategy is also influenced by climates. When focus on NSC storage with resource allocation strategy in each climate, a special pattern between leaf NSC and leaf economics traits showed in tropical species when compared with other climates. That is in

tropical forest, species which allocate more carbohydrates to reserves may have a conservative carbon use strategy (Poorter and Kitajima, 2007). Many species persist in the understory of forests with light-limited photosynthesis which performing slow-growth, high-survival strategy (i.e., shade tolerance species). Theoretical models suggests carbon investment in storage is a beneficial strategy in habitats often stressed and disturbed (Iwasa and Kubo, 1997) and carbon allocation to storage improves plant survival as it allows the plant to overcome periods of stress and disturbance (Poorter and Kitajima, 2007). In addition, the photosynthesis and growth can continue year-round in the tropics, minimizing seasonal mismatches between carbon sources and sinks. Additionally, in this study, tropical tree species were mostly composed of evergreen species, while Mediterranean, especially temperate species, were mostly composed of deciduous species. Due to different phenology, leaf life span and nutrient use efficiency, deciduous and evergreen species could exhibit different resource strategy.

5.3 PERSPECTIVE OF FURTHER RESEARCH

Carbon fixed during photosynthesis is exported from leaves towards sink organs as NSC, that are a key energy source for metabolic processes in trees. In xylem, NSC are stocked in the live ray and axial parenchyma cells, therefore the size of the parenchyma fraction drives the capacity for NSC storage in trees. Our research provided preliminary but clear evidence that RAP fractions and NSC storage capacity are closely related, underlining the important role of stem parenchyma cells in NSC storage. By investigating xylem anatomical and related functional traits, we also revealed complicated trade-offs between xylem structure and functions in stems and roots. The findings presented in this thesis has not only broadened the scope of our knowledge about the storage and physiology of NSC in trees, but also provided insight on functional strategies related design of xylem space in angiosperms. Nevertheless,

scientific research is never-ending, and further comprehensive studies are necessary to explore the NSC storage and utilization and the understanding of xylem structure and function strategies. Here, based on our results, several recommendations can be made for future studies:

1) Although our study has included a relatively large number of tree species and three distinct climate zones, research on larger scales and ranges, and more tree species can facilitate a comprehensive of understanding of the tree ecological strategies across terrestrial ecosystems. Additionally, species structure and function differ not only in plant growth form (e.g., tree, shrub, vine, liana) but also in geographically location (even in same climate, e.g., America tropical, Asia tropical, Africa tropical). To obtain a conclusive result about wood functional strategies, more parallel studies at different plant types and locations are need.

2) The seasonal changes in xylem NSC reflect the balance carbon supply by photosynthesis and carbon use for various physiological needs such as growth, reproduction and defense. Thus, the seasonal dynamics of NSC content and its partitioning between soluble sugars and starch should receive more attention, especially when focus on the relationships between NSC contents and parenchyma fractions. Assuming that the storage capacity of parenchymal cells is fully utilized during this period, total parenchymal volume should be the parameter most closely related to seasonal maxima of NSC content. Moreover, in the tropical climate, there are dry and wet seasons, even if there is no obvious seasonal change. The patterns of NSC content appear more variable in a seasonally dry tropical forest. Therefore, wet and dry season changes should be considered in studies on tropical tree species NSC.

3) Nitrogen (N) is a crucial element for plant growth and reproduction and plays an important role in photosynthesis as integral to the proteins. N is also a growth-limiting factor for trees in natural forest ecosystems with low anthropogenic N input. In the general theory of leaf economics spectrum, leaf N is one of the important features to describe the utilization strategy

of leaf resources. Species with high leaf N content normally tent to perform acquisitive resource strategy. However, the direct relationships between xylem N content and structural functions are rarely mentioned. It is necessary to explore the role of N content in xylem resource allocation strategies and the trade-off between structure and function.

4) Embolism are gas bubbles that form in conduits that block transport during drought or following freeze-thaw events. Increased embolism resistance is linked to reduced hydraulic efficiency, which led to the trade-off between hydraulic safety and efficiency. Although the relationship between vessel diameter and vessel density reflects the trade-off to some extent, the measured traits of the water potential associated with 50% loss in hydraulic conductivity could more directly reflect the hydraulic safety and efficiency trade-off. In addition, the influence of fiber and parenchyma on embolism resistance should also be considered.

5) Stem respiration plays an important role in species coexistence and forest dynamics. The consumption of assimilated carbon in stem respiration makes it an important part of the carbon budget of tree and ecosystems. The relationships between NSC contents stored in parenchyma cells as well as nitrogen concentration (which affects cell respiratory potential) and stem respiration should be a topic worthy of study, as the weighted rate of stem respiration per unit surface area depends on the amount of living cells and their activity

REFERENCES

Abramoff RZ, Finzi AC. 2015. Are above-and below-ground phenology in sync? *New Phytologist* **205**: 1054–1061.

Aerts R. **1995**. The advantages of being evergreen. *Trends in Ecology & Evolution* **10**: 402–407.

Aerts R. **1999**. Interspecific competition in natural plant communities: mechanisms, trade-offs and plant-soil feedbacks. *Journal of Experimental Botany* **50**: 29–37.

Adams HD, Zeppel MJB, Anderegg WRL, Hartmann H, Landhäusser SM, Tissue DT, Huxman TE, et al. 2017. A multi-species synthesis of physiological mechanisms in drought-induced tree mortality. *Nature Ecology & Evolution* **1**: 1285–1291.

Ali A, Yan ER, Chen HYH, Chang SX, Zhao YT, Yang XD, Xu M-S. 2016. Stand structural diversity rather than species diversity enhances aboveground carbon storage in secondary subtropical forests in Eastern China. *Biogeosciences* **13**: 4627–4635.

Allard V, Ourcival JM, Rambal S, Joffre R, Rocheteau A. 2008. Seasonal and annual variation of carbon exchange in an evergreen Mediterranean forest in southern France. *Global Change Biology* **14**: 714–725.

Anderegg WRL, Anderegg LDL. **2013**. Hydraulic and carbohydrate changes in experimental drought-induced mortality of saplings in two conifer species. *Tree Physiology* **33**: 252–260.

Aritsara ANA, Razakandraibe VM, Ramananantoandro T, Gleason SM, Cao K-F. **2021**. Increasing axial parenchyma fraction in the Malagasy Magnoliids facilitated the co-optimisation of hydraulic efficiency and safety. *New Phytologist* **229**: 1467–1480.

Badel E, Ewers FW, Cochard H, Telewski FW. **2015**. Acclimation of mechanical and hydraulic functions in trees: impact of the thigmomorphogenetic process. *Frontiers in Plant Science* **6**: 266.

Bailey IW. **1944**. The development of vessels in angiosperms and its significance in morphological research. *American Journal of Botany* **31**: 421–428.

Barotto AJ, Monteoliva S, Gyenge J, Martinez-Meier A, Fernandez ME. **2018**. Functional relationships between wood structure and vulnerability to xylem cavitation in races of Eucalyptus globulus differing in wood density. *Tree Physiology* **38**: 243–251.

Baraloto C, Hardy OJ, Paine CET, Dexter KG, Cruaud C, Dunning LT, Gonzalez MA, et al. 2012. Using functional traits and phylogenetic trees to examine the assembly of tropical tree communities. *Journal of Ecology* **100**: 690–701.

Baraloto C, Timothy Paine CE, Poorter L, Beauchene J, Bonal D, Domenach A-M, Hérault B, Patiño S, Roggy JC, Chave J. **2010**. Decoupled leaf and stem economics in rain forest trees. *Ecology Letters* **13**: 1338–1347.

Barbaroux C, Bréda N. 2002. Contrasting distribution and seasonal dynamics of carbohydrate reserves in stem wood of adult ring-porous sessile oak and diffuse-porous beech trees. *Tree physiology* **22**: 1201–1210.

Batten GD, Blakeney AB, McGrath VB, Ciavarella S. **1993**. Non-structural carbohydrate: Analysis by near infrared reflectance spectroscopy and its importance as an indicator of plant growth. *Plant and Soil* **155**: 243–246.

Beeckman H. **2016**. Wood anatomy and trait-based ecology. *IAWA Journal* **37**: 127–151.

Biggs A. 1987. Occurrence and location of suberin in wound reaction zones in xylem of 17 tree species. *Phytopathology* **77**: 718–725.

Blomberg SP, Garland T, Ives AR. **2003**. Testing for phylogenetic signal in comparative data: behavioral traits are more labile. *Evolution* **57**: 717–745.

Boura A, De Franceschi D. **2007**. Is porous wood structure exclusive of deciduous trees? *Comptes Rendus Palevol* **6**: 385–391.

Brodersen CR, McElrone AJ, Choat B, Matthews MA, Shackel KA. **2010**. The dynamics of embolism repair in xylem: in vivo visualizations using high-resolution computed tomography. *Plant Physiology* **154**: 1088–1095.

Bucci SJ, Scholz FG, Goldstein G, Meinzer FC, Sternberg LDSL. **2003**. Dynamic changes in hydraulic conductivity in petioles of two savanna tree species: factors and mechanisms contributing to the refilling of embolized vessels. *Plant, Cell & Environment* **26**: 1633–1645.

Burgert I, Eckstein D. **2001**. The tensile strength of isolated wood rays of beech (*Fagus sylvatica* L.) and its significance for the biomechanics of living trees. *Trees* **15**: 168–170.

Cadotte MW, Cardinale BJ, Oakley TH. 2008. Evolutionary history and the effect of biodiversity on plant productivity. *Proceedings of the National Academy of Sciences* **105**: 17012–17017.

Cadotte MW, Dinnage R, Tilman D. 2012. Phylogenetic diversity promotes ecosystem stability. *Ecology* **93**: S223–S233.

Carbone MS, Czimczik CI, Keenan TF, Murakami PF, Pederson N, Schaberg PG, Xu X, Richardson AD. **2013**. Age, allocation and availability of nonstructural carbon in mature red maple trees. *New Phytologist* **200**: 1145–1155.

Carlquist S. 2001. Comparative wood anatomy: systematic, ecological, and evolutionary aspects of dicotyledon wood. Springer-Verlag, Berlin, Germany.

Carlquist S. 2014. Fibre dimorphism: cell type diversification as an evolutionary strategy in angiosperm woods. *Botanical Journal of the Linnean Society* **174**: 44–67.

Carnicer J, Barbeta A, Sperlich D, Coll M, Penuelas J. 2013. Contrasting trait syndromes in angiosperms and conifers are associated with different responses of tree growth to temperature on a large scale. *Frontiers in Plant Science* **4**: 409.

Cavender-Bares J, Ackerly DD, Baum DA, Bazzaz FA. 2004. Phylogenetic overdispersion in Floridian oak communities. *The American Naturalist* **163**: 823–843.

Chapin FS, Schulze ED, Mooney HA. 1990. The ecology and economics of storage in plants. *Annual Review of Rcology and Systematics* **21**: 423–447.

Chave J, Muller-Landau HC, Baker TR, Easdale TA, ter Steege H, Webb CO. 2006. Regional and phylogenetic variation of wood density across 2456 neotropical tree species. *Ecological Applications* **16**: 2356–2367.

Chave J, Coomes D, Jansen S, Lewis SL, Swenson NG, Zanne AE. **2009**. Towards a worldwide wood economics spectrum. *Ecology Letters* **12**: 351–366.

Chen Z, Zhu S, Zhang Y, Luan J, Li S, Sun P, Wan X, Liu S. **2020**. Tradeoff between storage capacity and embolism resistance in the xylem of temperate broadleaf tree species. *Tree Physiology* **40**: 1029–1042.

Chow PS, Landhäusser SM. **2004**. A method for routine measurements of total sugar and starch content in woody plant tissues. *Tree Physiology* **24**: 1129–1136.

Christensen-Dalsgaard KK, Ennos AR, Fournier M. **2007a**. Changes in hydraulic conductivity, mechanical properties, and density reflecting the fall in strain along the lateral roots of two species of tropical trees. *Journal of Experimental Botany* **58**: 4095–4105.

Christensen-Dalsgaard KK, Fournier M, Ennos AR, Barfod AS. **2007b**. Changes in vessel anatomy in response to mechanical loading in six species of tropical trees. *New Phytologist* **176**: 610–622.

Chuste PA, Maillard P, Bréda N, Levillain J, Thirion E, Wortemann R, Massonnet C. 2020. Sacrificing growth and maintaining a dynamic carbohydrate storage are key processes for promoting beech survival under prolonged drought conditions. *Trees* **34**: 381–394.

Clarke A, Gaston KJ. **2006**. Climate, energy and diversity. *Proceedings of the Royal Society B: Biological Sciences* **273**: 2257–2266.

Clarke PJ, Lawes MJ, Midgley JJ, Lamont BB, Ojeda F, Burrows GE, Enright NJ, Knox KJE. **2013**. Resprouting as a key functional trait: how buds, protection and resources drive persistence after fire. *New Phytologist* **197**: 19–35.

Clough BJ, Curzon MT, Domke GM, Russell MB, Woodall CW. **2017**. Climate-driven trends in stem wood density of tree species in the eastern United States: Ecological impact and implications for national forest carbon assessments. *Global Ecology and Biogeography* **26**: 1153–1164.

da Costa H de JA, Gurgel ESC, Dantas do Amaral D, Vasconcelos LV, Rebelo LGB, Teodoro GS. **2020**. CSR ecological strategies, functional traits and trade-offs of woody species in Amazon sandplain forest. *Flora* **273**: 151710.

Coomes DA, Heathcote S, Godfrey ER, Shepherd JJ, Sack L. 2008. Scaling of xylem vessels and veins within the leaves of oak species. *Biology Letters* **4**: 302–306.

Cunningham S, Read J. **2002**. Comparison of temperate and tropical rainforest tree species: photosynthetic responses to growth temperature. *Oecologia* **133**: 112–119.

DeLucia EH, Schlesinger WH, Billings WD. **1989**. Edaphic limitations to growth and photosynthesis in Sierran and Great Basin vegetation. *Oecologia* **78**: 184–190.

Díaz S, Kattge J, Cornelissen JHC, Wright IJ, Lavorel S, Dray S, Reu B, Kleyer M, Wirth C, Colin Prentice I, *et al.* 2016. The global spectrum of plant form and function. *Nature* **529**: 167–171.

Dietze MC, Sala A, Carbone MS, Czimczik CI, Mantooth JA, Richardson AD, Vargas R. **2014**. Nonstructural carbon in woody plants. *Annual Review of Plant Biology* **65**: 667–687.

Dixon P. 2003. VEGAN, a package of R functions for community ecology. *Journal of Vegetation Science* **14**: 927–930.

Donovan LA, Maherali H, Caruso CM, Huber H, de Kroon H. **2011**. The evolution of the worldwide leaf economics spectrum. *Trends in Ecology & Evolution* **26**: 88–95.

Drew MC. 1987. Function of root tissues in nutrient and water transport. Root development and function. Cambridge University Press, Cambridge, 71–101.

El Zein R, Maillard P, Bréda N, Marchand J, Montpied P, Gérant D. 2011. Seasonal changes of C and N non-structural compounds in the stem sapwood of adult sessile oak and beech trees. *Tree physiology* **31**: 843–854.

Enquist BJ, West GB, Charnov EL, Brown JH. 1999. Allometric scaling of production and life-history variation in vascular plants. *Nature* **401**: 907–911.

Ewers FW, Ewers JM, Jacobsen AL, López-Portillo J. **2007**. Vessel redundancy: modeling safety in numbers. *IAWA Journal* **28**: 373–388.

Fajardo A, Piper FI, Hoch G. **2013**. Similar variation in carbon storage between deciduous and evergreen treeline species across elevational gradients. *Annals of Botany* **112**: 623–631.

Fahn A. 1967. Plant Anatomy. Pergamon Press Ltd., Oxford. pp.514.

Felsenstein J. 1985. Phylogenies and the comparative method. *The American Naturalist* **125**: 1–15.

Fick SE, Hijmans RJ. 2017. WorldClim 2: new 1-km spatial resolution climate surfaces for global land areas. *International Journal of Climatology* **37**: 4302–4315.

Fortunel C, Fine PVA, Baraloto C. **2012**. Leaf, stem and root tissue strategies across 758 Neotropical tree species. *Functional Ecology* **26**: 1153–1161.

Fortunel C, Ruelle J, Beauchêne J, Fine PVA, Baraloto C. **2014**. Wood specific gravity and anatomy of branches and roots in 113 Amazonian rainforest tree species across environmental gradients. *New Phytologist* **202**: 79–94.

Fortunel C, Valencia R, Wright SJ, Garwood NC, Kraft NJB. 2016. Functional trait differences influence neighbourhood interactions in a hyperdiverse Amazonian forest. *Ecology Letters* **19**: 1062–1070.

Freckleton RP, Harvey PH, Pagel M. 2002. Phylogenetic analysis and comparative data: A test and review of evidence. *The American Naturalist* **160**: 712–726.

Freschet GT, Cornelissen JHC, Logtestijn RSPV, Aerts R. **2010**. Evidence of the 'plant economics spectrum' in a subarctic flora. *Journal of Ecology* **98**: 362–373.

Furze ME, Huggett BA, Aubrecht DM, Stolz CD, Carbone MS, Richardson AD. **2019**. Whole-tree nonstructural carbohydrate storage and seasonal dynamics in five temperate species. *New Phytologist* **221**: 1466–1477.

Furze ME, Huggett BA, Chamberlain CJ, Wieringa MM, Aubrecht DM, Carbone MS, Walker JC, Xu X, Czimczik CI, Richardson AD. **2020**. Seasonal fluctuation of nonstructural carbohydrates reveals the metabolic availability of stemwood reserves in temperate trees with contrasting wood anatomy. *Tree Physiology* **40**: 1355–1365.

Galiano L, Martínez-Vilalta J, Lloret F. 2011. Carbon reserves and canopy defoliation determine the recovery of Scots pine 4 yr after a drought episode. *New Phytologist* **190**: 750–759.

Gardner WR. 1965. Dynamic aspects of soil-water availability to plants. *Annual Review of Plant Physiology* **16**: 323–342.

Gibon Y, Pyl ET, Sulpice R, Lunn JE, Höhne M, Günther M, Stitt M. **2009**. Adjustment of growth, starch turnover, protein content and central metabolism to a decrease of the carbon

supply when Arabidopsis is grown in very short photoperiods. *Plant, Cell & Environment* **32**: 859–874.

Gillon D, Houssard C, Joffre R. 1999. Using near-infrared reflectance spectroscopy to predict carbon, nitrogen and phosphorus content in heterogeneous plant material. *Oecologia* **118**: 173–182.

Gilson A, Barthes L, Delpierre N, Dufrêne É, Fresneau C, Bazot S. 2014. Seasonal changes in carbon and nitrogen compound concentrations in a Quercus petraea chronosequence. *Tree Physiology* **34**: 716–729.

Givnish T. **2002**. Adaptive significance of evergreen vs. deciduous leaves: solving the triple paradox. *Silva Fennica* **36**: 703–743.

Gleason SM, Butler DW, Ziemińska K, Waryszak P, Westoby M. **2012**. Stem xylem conductivity is key to plant water balance across Australian angiosperm species. *Functional Ecology* **26**: 343–352.

Gleason SM, Westoby M, Jansen S, Choat B, Hacke UG, Pratt RB, Bhaskar R, Brodribb TJ, Bucci SJ, Cao K-F, *et al.* 2016. Weak tradeoff between xylem safety and xylem-specific hydraulic efficiency across the world's woody plant species. *New Phytologist* **209**: 123–136.

Godfrey JM, Riggio J, Orozco J, Guzmán-Delgado P, Chin ARO, Zwieniecki MA. **2020**. Ray fractions and carbohydrate dynamics of tree species along a 2750 m elevation gradient indicate climate response, not spatial storage limitation. *New Phytologist* **225**: 2314–2330.

Gough CM, Flower CE, Vogel CS, Curtis PS. **2010**. Phenological and temperature controls on the temporal non-structural carbohydrate dynamics of *Populus grandidentata* and *Quercus rubra*. *Forests* **1**: 65–81.

Gower ST, Richards JH. **1990**. Larches: deciduous conifers in an evergreen world. *BioScience* **40**: 818–826.

Gravel D, Bell T, Barbera C, Combe M, Pommier T, Mouquet N. **2012**. Phylogenetic constraints on ecosystem functioning. *Nature Communications* **3**: 1117.

Grime JP. **1977**. Evidence for the existence of three primary strategies in plants and its relevance to ecological and evolutionary theory. *The American Naturalist* **111**: 1169–1194.

Grubb PJ. **2016**. Trade-offs in interspecific comparisons in plant ecology and how plants overcome proposed constraints. *Plant Ecology & Diversity* **9**: 3–33.

Hacke U, Sauter JJ. 1996. Xylem dysfunction during winter and recovery of hydraulic conductivity in diffuse-porous and ring-porous trees. *Oecologia* **105**: 435–439.

Hacke UG, Sperry JS, Wheeler JK, Castro L. **2006**. Scaling of angiosperm xylem structure with safety and efficiency. *Tree Physiology* **26**: 689–701.

Hartmann H, Trumbore S. **2016**. Understanding the roles of nonstructural carbohydrates in forest trees – from what we can measure to what we want to know. *New Phytologist* **211**: 386–403.

He W, Liu H, Qi Y, Liu F, Zhu X. **2020**. Patterns in nonstructural carbohydrate contents at the tree organ level in response to drought duration. *Global Change Biology* **26**: 3627–3638.

Herrera-Ramírez D, Muhr J, Hartmann H, Römermann C, Trumbore S, Sierra CA. **2020**. Probability distributions of nonstructural carbon ages and transit times provide insights into carbon allocation dynamics of mature trees. *New Phytologist* **226**: 1299–1311.

Hoeber S, Leuschner C, Köhler L, Arias-Aguilar D, Schuldt B. **2014**. The importance of hydraulic conductivity and wood density to growth performance in eight tree species from a tropical semi-dry climate. *Forest Ecology and Management* **330**: 126–136.

Hoch G, Körner C. **2009**. Growth and carbon relations of tree line forming conifers at constant vs. variable low temperatures. *Journal of Ecology* **97**: 57–66.

Hoch G, Richter A, Korner Ch. **2003**. Non-structural carbon compounds in temperate forest trees. *Plant, Cell and Environment* **26**: 1067–1081.

Hoeber S, Leuschner C, Köhler L, Arias-Aguilar D, Schuldt B. **2014**. The importance of hydraulic conductivity and wood density to growth performance in eight tree species from a tropical semi-dry climate. *Forest Ecology and Management* **330**: 126–136.

Hothorn T, Bretz F, Westfall P. **2008**. Simultaneous inference in general parametric models. *Biometrical Journal* **50**: 346–363.

Imaji A, Seiwa K. **2010**. Carbon allocation to defense, storage, and growth in seedlings of two temperate broad-leaved tree species. *Oecologia* **162**: 273–281.

Isaac ME, Martin AR, de Melo Virginio Filho E, Rapidel B, Roupsard O, Van den Meersche K. **2017**. Intraspecific trait variation and coordination: root and leaf economics spectra in coffee across environmental gradients. *Frontiers in Plant Science* **8**: 1196.

Iwasa Y, Kubo T. **1997**. Optimal size of storage for recovery after unpredictable disturbances. *Evolutionary Ecology* **11**: 41–65.

Jacobsen AL, Ewers FW, Pratt RB, Paddock WA, Davis SD. **2005**. Do xylem fibers affect vessel cavitation resistance? *Plant Physiology* **139**: 546–556.

Jacobsen AL, Agenbag L, Esler KJ, Pratt RB, Ewers FW, Davis SD. **2007**. Xylem density, biomechanics and anatomical traits correlate with water stress in 17 evergreen shrub species of the Mediterranean-type climate region of South Africa. *Journal of Ecology* **95**: 171–183.

Jacobsen AL, Tobin MF, Toschi HS, Percolla MI, Pratt RB. **2016**. Structural determinants of increased susceptibility to dehydration-induced cavitation in post-fire resprouting chaparral shrubs. *Plant, Cell & Environment* **39**: 2473–2485.

Jagels R, Equiza MA, Maguire DA, Cirelli D. **2018**. Do tall tree species have higher relative stiffness than shorter species? *American Journal of Botany* **105**: 1617–1630.

Janssen TAJ, Hölttä T, Fleischer K, Naudts K, Dolman H. **2020**. Wood allocation trade-offs between fiber wall, fiber lumen, and axial parenchyma drive drought resistance in neotropical trees. *Plant, Cell & Environment* **43**: 965–980.

Jiang P, Meinzer FC, Fu X, Kou L, Dai X, Wang H. **2021**. Trade-offs between xylem water and carbohydrate storage among 24 coexisting subtropical understory shrub species spanning a spectrum of isohydry. *Tree Physiology* **41**: 403–415.

Jin Y, Qian H. 2019. V. PhyloMaker: an R package that can generate very large phylogenies for vascular plants. *Ecography* **42**: 1353–1359.

Jupa R, Plavcová L, Gloser V, Jansen S. **2016**. Linking xylem water storage with anatomical parameters in five temperate tree species. *Tree Physiology* **36**: 756–769.

Kattge J, Díaz S, Lavorel S, Prentice IC, Leadley P, Bönisch G, Garnier E, Westoby M, Reich PB, Wright IJ, *et al.* 2011. TRY – a global database of plant traits. *Global Change Biology* **17**: 2905–2935.

Kawai K, Minagi K, Nakamura T, Saiki S-T, Yazaki K, Ishida A. **2021**. Parenchyma underlies the interspecific variation of xylem hydraulics and carbon storage across 15 woody species on a subtropical island in Japan. *Tree Physiology*: tpab100.

Kembel SW, Cowan PD, Helmus MR, Cornwell WK, Morlon H, Ackerly DD, Blomberg SP, Webb CO. **2010**. Picante: R tools for integrating phylogenies and ecology. *Bioinformatics* **26**: 1463–1464.

Klein T, Hoch G. **2015**. Tree carbon allocation dynamics determined using a carbon mass balance approach. *New Phytologist* **205**: 147–159.

Klein T, Vitasse Y, Hoch G. **2016**. Coordination between growth, phenology and carbon storage in three coexisting deciduous tree species in a temperate forest. *Tree Physiology* **36**: 847–855.

Kono Y, Ishida A, Saiki S-T, Yoshimura K, Dannoura M, Yazaki K, Kimura F, Yoshimura J, Aikawa S. **2019**. Initial hydraulic failure followed by late-stage carbon starvation leads to drought-induced death in the tree Trema orientalis. *Communications Biology* **2**: 1–9.

Kotowska MM, Hertel D, Rajab YA, Barus H, Schuldt B. **2015**. Patterns in hydraulic architecture from roots to branches in six tropical tree species from cacao agroforestry and their relation to wood density and stem growth. *Frontiers in Plant Science* **6**: 191.

Körner C. **2003**. Carbon limitation in trees. *Journal of Ecology* **91**: 4–17.

Kozlowski T. **1992**. Carbohydrate sources and sinks in woody plants. *The Botanical Review* **58**: 107–222.

Kramer-Walter KR, Bellingham PJ, Millar TR, Smissen RD, Richardson SJ, Laughlin DC. **2016**. Root traits are multidimensional: specific root length is independent from root tissue density and the plant economic spectrum. *Journal of Ecology* **104**: 1299–1310.

Kurze S, Engelbrecht BMJ, Bilton MC, Tielbörger K, Álvarez-Cansino L. **2021**. Rethinking the plant economics spectrum for annuals: A multi-species study. *Frontiers in Plant Science* **12**: 454.

Kuznetsova A, Brockhoff PB, Christensen RH. 2017. lmerTest package: tests in linear mixed effects models. *Journal of Statistical Software* **82**: 1-26.

Lacointe A. **2000**. Carbon allocation among tree organs: A review of basic processes and representation in functional-structural tree models. *Annals of Forest Science* **57**: 521–533.

Larjavaara M, Muller-Landau HC. 2010. Rethinking the value of high wood density. *Functional Ecology* **24**: 701-705.

Lachenbruch B, McCulloh KA. 2014. Traits, properties, and performance: how woody plants combine hydraulic and mechanical functions in a cell, tissue, or whole plant. *New Phytologist* **204**: 747–764.

Lens F, Sperry JS, Christman MA, Choat B, Rabaey D, Jansen S. **2011**. Testing hypotheses that link wood anatomy to cavitation resistance and hydraulic conductivity in the genus Acer. *New Phytologist* **190**: 709–723.

Levionnois S, Salmon C, Alméras T, Clair B, Ziegler C, Coste S, Stahl C, González-Melo A, Heinz C, Heuret P. **2021**. Anatomies, vascular architectures, and mechanics underlying the leaf size-stem size spectrum in 42 Neotropical tree species. *Journal of Experimental Botany* **72**: 7957–7969.

Lewis AM. **1992**. Measuring the hydraulic diameter of a pore or conduit. *American Journal of Botany* **79**: 1158–1161.

Li N, He N, Yu G, Wang Q, Sun J. **2016**. Leaf non-structural carbohydrates regulated by plant functional groups and climate: Evidences from a tropical to cold-temperate forest transect. *Ecological Indicators* **62**: 22–31.

Li J, Chen X, Niklas KJ, Sun J, Wang Z, Zhong Q, Hu D, Cheng D. **2022**. A whole-plant economics spectrum including bark functional traits for 59 subtropical woody plant species. *Journal of Ecology* **110**: 248–261.

Liu R, Wang D. 2021. C: N: P stoichiometric characteristics and seasonal dynamics of leaf-root-litter-soil in plantations on the loess plateau. *Ecological Indicators* **127**: 107772.

Liu H, Ye Q, Gleason SM, He P, Yin D. **2021**. Weak tradeoff between xylem hydraulic efficiency and safety: climatic seasonality matters. *New Phytologist* **229**: 1440–1452.

Loepfe L, Martinez-Vilalta J, Piñol J, Mencuccini M. **2007**. The relevance of xylem network structure for plant hydraulic efficiency and safety. *Journal of Theoretical Biology* **247**: 788–803.

Lubbe FC, Klimeš A, Doležal J, Jandová V, Mudrák O, Janeček Š, Bartušková A, Klimešová J. **2021**. Carbohydrate storage in herbs: the forgotten functional dimension of the plant economic spectrum. *Annals of Botany* **127**: 813–825.

Lusk CH, Piper FI. **2007**. Seedling size influences relationships of shade tolerance with carbohydrate-storage patterns in a temperate rainforest. *Functional Ecology* **21**: 78–86.

Lusk CH, Reich PB, Montgomery RA, Ackerly DD, Cavender-Bares J. **2008**. Why are evergreen leaves so contrary about shade? *Trends in Ecology & Evolution* **23**: 299–303.

Markesteijn L, Poorter L, Bongers F, Paz H, Sack L. **2011**. Hydraulics and life history of tropical dry forest tree species: coordination of species' drought and shade tolerance. *New Phytologist* **191**: 480–495.

Martínez-Cabrera HI, Jones CS, Espino S, Schenk HJ. **2009**. Wood anatomy and wood density in shrubs: Responses to varying aridity along transcontinental transects. *American Journal of Botany* **96**: 1388–1398.

Martínez-Cabrera HI, Schenk HJ, Cevallos-Ferriz SRS, Jones CS. **2011**. Integration of vessel traits, wood density, and height in angiosperm shrubs and trees. *American Journal of Botany* **98**: 915–922.

Martínez-Vilalta J, Mencuccini M, Vayreda J, Retana J. 2010. Interspecific variation in functional traits, not climatic differences among species ranges, determines demographic rates across 44 temperate and Mediterranean tree species: Determinants of demographic rates across species. *Journal of Ecology* **98**: 1462–1475.

Martínez-Vilalta J, Sala A, Asensio D, Galiano L, Hoch G, Palacio S, Piper FI, Lloret F. **2016**. Dynamics of non-structural carbohydrates in terrestrial plants: a global synthesis. *Ecological Monographs* **86**: 495–516.

McCulloh K, Sperry JS, Lachenbruch B, Meinzer FC, Reich PB, Voelker S. **2010**. Moving water well: comparing hydraulic efficiency in twigs and trunks of coniferous, ring-porous, and diffuse-porous saplings from temperate and tropical forests. *New Phytologist* **186**: 439–450.

McCulloh KA, Meinzer FC, Sperry JS, Lachenbruch B, Voelker SL, Woodruff DR, Domec J-C. **2011**. Comparative hydraulic architecture of tropical tree species representing a range of successional stages and wood density. *Oecologia* **167**: 27–37.

McDowell N, Pockman WT, Allen CD, Breshears DD, Cobb N, Kolb T, Plaut J, et al. 2008. Mechanisms of plant survival and mortality during drought: why do some plants survive while others succumb to drought? *New Phytologist* **178**: 719–739.

Mei L, Xiong Y, Gu J, Wang Z, Guo D. **2015**. Whole-tree dynamics of non-structural carbohydrate and nitrogen pools across different seasons and in response to girdling in two temperate trees. *Oecologia* **177**: 333–344.

Méndez-Alonzo R, Paz H, Zuluaga RC, Rosell JA, Olson ME. **2012**. Coordinated evolution of leaf and stem economics in tropical dry forest trees. *Ecology* **93**: 2397–2406.

Mevik BH, Cederkvist HR. 2004. Mean squared error of prediction (MSEP) estimates for principal component regression (PCR) and partial least squares regression (PLSR). *Journal of Chemometrics* **18**: 422–429.

Moles AT, Perkins SE, Laffan SW, Flores-Moreno H, Awasthy M, Tindall ML, Sack L, Pitman A, Kattge J, Aarssen LW, *et al.* 2014. Which is a better predictor of plant traits: temperature or precipitation? *Journal of Vegetation Science* **25**: 1167–1180.

Morin X, Ameglio T, Ahas R, Kurz-Besson C, Lanta V, Lebourgeois F, Miglietta F, Chuine I. **2007**. Variation in cold hardiness and carbohydrate concentration from dormancy induction to bud burst among provenances of three European oak species. *Tree Physiology* **27**: 817–825.

Morris H. **2016**. The structure and function of ray and axial parenchyma in woody seed plants. PhD thesis, Ulm University, Ulm, Germany, 171p.

Morris H, Jansen S. **2016**. Secondary xylem parenchyma – from classical terminology to functional traits. *IAWA Journal* **37**: 1–15.

Morris H, Gillingham MAF, Plavcová L, Gleason SM, Olson ME, Coomes DA, Fichtler E, Klepsch MM, Martínez-Cabrera HI, McGlinn DJ, *et al.* 2018a. Vessel diameter is related to amount and spatial arrangement of axial parenchyma in woody angiosperms. *Plant, Cell & Environment* **41**: 245–260.

Morris H, Plavcová L, Cvecko P, Fichtler E, Gillingham MAF, Martínez-Cabrera HI, McGlinn DJ, Wheeler E, Zheng J, Ziemińska K, *et al.* 2016. A global analysis of parenchyma tissue fractions in secondary xylem of seed plants. *New Phytologist* **209**: 1553–1565.

Morris H, Plavcová L, Gorai M, Klepsch MM, Kotowska M, Jochen Schenk H, Jansen S. **2018b**. Vessel-associated cells in angiosperm xylem: Highly specialized living cells at the symplast-apoplast boundary. *American Journal of Botany* **105**: 151–160.

Morris H, Hietala AM, Jansen S, Ribera J, Rosner S, Salmeia KA, Schwarze FWMR. **2020**. Using the CODIT model to explain secondary metabolites of xylem in defence systems of temperate trees against decay fungi. *Annals of Botany* **125**: 701–720.

Muller-Landau HC. 2004. Interspecific and inter-site variation in wood specific gravity of tropical trees. *Biotropica* **36**: 20–32.

Myers JA, Kitajima K. **2007**. Carbohydrate storage enhances seedling shade and stress tolerance in a neotropical forest. *Journal of Ecology* **95**: 383–395.

Nabais C, Hansen JK, David-Schwartz R, Klisz M, López R, Rozenberg P. 2018. The effect of climate on wood density: What provenance trials tell us? *Forest Ecology and Management* **408**: 148–156.

Naes T, Isaksson T, Fearn T, Davies T. 2004. A User-friendly guide to Multivariate calibration and classification. NIR Publications UK, pp. 344.

Nardini A, Lo Gullo MA, Salleo S. **2011**. Refilling embolized xylem conduits: Is it a matter of phloem unloading? *Plant Science* **180**: 604–611.

Nardini A, Lo Gullo MA, Trifilò P, Salleo S. 2014. The challenge of the Mediterranean climate to plant hydraulics: responses and adaptations. *Environmental and Experimental Botany* **103**: 68–79.

Newell EA, Mulkey SS, Wright JS. **2002**. Seasonal patterns of carbohydrate storage in four tropical tree species. *Oecologia* **131**: 333–342.

O'Brien MJ, Leuzinger S, Philipson CD, Tay J, Hector A. 2014. Drought survival of tropical tree seedlings enhanced by non-structural carbohydrate levels. *Nature Climate Change* **4**: 710–714.

Olson ME, Anfodillo T, Gleason SM, McCulloh KA. 2021. Tip-to-base xylem conduit widening as an adaptation: causes, consequences, and empirical priorities. *New Phytologist* **229**: 1877–1893.

Olson ME, Rosell JA. **2013**. Vessel diameter–stem diameter scaling across woody angiosperms and the ecological causes of xylem vessel diameter variation. *New Phytologist* **197**: 1204–1213.

van Ommen Kloeke AEE, Douma JC, Ordoñez JC, Reich PB, van Bodegom PM. **2012**. Global quantification of contrasting leaf life span strategies for deciduous and evergreen species in response to environmental conditions. *Global Ecology and Biogeography* **21**: 224–235.

Orme D, Freckleton R, Thomas G, Petzoldt T, Fritz S, Isaac N, Pearse W. 2018. The caper package: comparative analysis of phylogenetics and evolution in R. *R package version* **5**: 1–36 (https://CRAN.R-project.org/package=caper).

Osazuwa-Peters OL, Wright SJ, Zanne AE. 2017. Linking wood traits to vital rates in tropical rainforest trees: Insights from comparing sapling and adult wood. *American Journal of Botany* **104**: 1464–1473.

Osnas JLD, Lichstein JW, Reich PB, Pacala SW. **2013**. Global leaf trait relationships: mass, area, and the leaf economics spectrum. *Science* **340**: 741–744.

Pan Y, Cieraad E, Armstrong J, Armstrong W, Clarkson BR, Colmer TD, Pedersen O, Visser EJW, Voesenek LACJ, van Bodegom PM. **2020**. Global patterns of the leaf economics spectrum in wetlands. *Nature Communications* **11**: 4519.

Paradis E, Claude J, Strimmer K. 2004. APE: Analyses of phylogenetics and evolution in R language. *Bioinformatics* **20**: 289–290.

Patten AM, Vassão DG, Wolcott MP, Davin LB, Lewis NG. 2010. Trees: a remarkable biochemical bounty. *In* L. Mander and H. W. Liu [eds.], Comprehensive natural products chemistry II, 1173-1296. Elsevier Press, Oxford, UK.

Pérez-Harguindeguy N, Díaz S, Garnier E, Lavorel S, Poorter H, Jaureguiberry P, Bret-Harte MS, Cornwell WK, Craine JM, Gurvich DE, *et al.* 2016. Corrigendum to: New handbook for standardised measurement of plant functional traits worldwide. *Australian Journal of Botany* **64**: 715–716.

Piispanen R, Saranpää P. **2001**. Variation of non-structural carbohydrates in silver birch (*Betula pendula* Roth) wood. *Trees* **15**: 444–451.

Piper FI. **2015**. Patterns of carbon storage in relation to shade tolerance in southern South American species. *American Journal of Botany* **102**: 1442–1452.

Piper FI, Hoch G, Fajardo A. **2019**. Revisiting the relative growth rate hypothesis for gymnosperm and angiosperm species co-occurrence. *American Journal of Botany* **106**: 101–112.

Pittermann J, Sperry JS, Wheeler JK, Hacke UG, Sikkema EH. 2006. Mechanical reinforcement of tracheids compromises the hydraulic efficiency of conifer xylem. *Plant, Cell & Environment* **29**: 1618–1628.

Plavcová L, Gallenmüller F, Morris H, Khatamirad M, Jansen S, Speck T. **2019**. Mechanical properties and structure–function trade-offs in secondary xylem of young roots and stems. *Journal of Experimental Botany* **70**: 3679–3691.

Plavcová L, Hoch G, Morris H, Ghiasi S, Jansen S. **2016**. The amount of parenchyma and living fibers affects storage of nonstructural carbohydrates in young stems and roots of temperate trees. *American Journal of Botany* **103**: 603–612.

Poorter H, Niklas KJ, Reich PB, Oleksyn J, Poot P, Mommer L. **2012**. Biomass allocation to leaves, stems and roots: meta-analyses of interspecific variation and environmental control. *New Phytologist* **193**: 30–50.

Poorter L, Kitajima K. **2007**. Carbohydrate storage and light requirements of tropical moist and dry forest tree species. *Ecology* **88**: 1000–1011.

Poorter L, McDonald I, Alarcón A, Fichtler E, Licona J-C, Peña-Claros M, Sterck F, Villegas Z, Sass-Klaassen U. **2010a**. The importance of wood traits and hydraulic conductance for the performance and life history strategies of 42 rainforest tree species. *New Phytologist* **185**: 481–492.

Poorter L, Kitajima K, Mercado P, Chubiña J, Melgar I, Prins HHT. **2010b**. Resprouting as a persistence strategy of tropical forest trees: relations with carbohydrate storage and shade tolerance. *Ecology* **91**: 2613–2627.

Poorter L, Wright SJ, Paz H, Ackerly DD, Condit R, Ibarra-Manríquez G, Harms KE, Licona JC, Martínez-Ramos M, Mazer SJ, *et al.* 2008. Are functional traits good predictors of demographic rates? Evidence from five Neotropical forests. *Ecology* **89**: 1908–1920.

Popp M, Lied W, Meyer AJ, Richter A, Schiller P, Schwitte H. **1996**. Sample preservation for determination of organic compounds: microwave versus freeze-drying. *Journal of Experimental Botany* **47**: 1469–1473.

Pratt RB, Jacobsen AL. **2017**. Conflicting demands on angiosperm xylem: Tradeoffs among storage, transport and biomechanics. *Plant, Cell & Environment* **40**: 897–913.

Pratt RB, Jacobsen AL, Ewers FW, Davis SD. **2007**. Relationships among xylem transport, biomechanics and storage in stems and roots of nine Rhamnaceae species of the California chaparral. *New Phytologist* **174**: 787–798.

Pratt RB, Jacobsen AL, Percolla MI, Guzman MED, Traugh CA, Tobin MF. **2021a**. Trade-offs among transport, support, and storage in xylem from shrubs in a semiarid chaparral environment tested with structural equation modeling. *Proceedings of the National Academy of Sciences* **118**: e2104336118.

Pratt RB, Tobin MF, Jacobsen AL, Traugh CA, Guzman MED, Hayes CC, Toschi HS, MacKinnon ED, Percolla MI, Clem ME, *et al.* 2021b. Starch storage capacity of sapwood is related to dehydration avoidance during drought. *American Journal of Botany* **108**: 91–101.

Preston KA, Cornwell WK, DeNoyer JL. **2006**. Wood density and vessel traits as distinct correlates of ecological strategy in 51 California coast range angiosperms. *New Phytologist* **170**: 807–818.

Prieto I, Roumet C, Cardinael R, Dupraz C, Jourdan C, Kim JH, Maeght JL, Mao Z, Pierret A, Portillo N, *et al.* 2015. Root functional parameters along a land-use gradient: evidence of a community-level economics spectrum. *Journal of Ecology* **103**: 361–373.

Rahman, MM, Fujiwara S, Kanagawa Y. 2005. Variations in volume and dimensions of rays and their effect on wood properties of teak. *Wood and Fiber Science* **37**: 497–504.

Ramirez JA, Craven D, Posada JM, Reu B, Sierra CA, Hoch G, Handa IT, Messier C. **2021**. Non-structural carbohydrate concentrations in woody organs, but not leaves, of temperate and tropical tree angiosperms are independent of the 'fast-slow' plant economic spectrum. *BioRxiv* **doi**: https://doi.org/10.1101/2021.04.20.440698.

Ramírez, JA, Handa IT, Posada JM, Delagrange S, Messier C. 2018. Carbohydrate dynamics in roots, stems, and branches after maintenance pruning in two common urban tree species of North America. *Urban Forestry & Urban Greening* **30**: 24–31.

Ramirez JA, Posada JM, Handa IT, Hoch G, Vohland M, Messier C, Reu B. **2015**. Near-infrared spectroscopy (NIRS) predicts non-structural carbohydrate concentrations in different tissue types of a broad range of tree species. *Methods in Ecology and Evolution* **6**: 1018–1025.

Rana R, Langenfeld-Heyser R, Finkeldey R, Polle A. **2009**. Functional anatomy of five endangered tropical timber wood species of the family Dipterocarpaceae. *Trees* **23**: 521–529.

Reich PB. **2014**. The world-wide 'fast-slow' plant economics spectrum: a traits manifesto. *Journal of Ecology* **102**: 275–301.

Richardson AD, Carbone MS, Keenan TF, Czimczik CI, Hollinger DY, Murakami P, Schaberg PG, Xu X. **2013a**. Seasonal dynamics and age of stemwood nonstructural carbohydrates in temperate forest trees. *New Phytologist* **197**: 850–861.

Richardson SJ, Allen RB, Buxton RP, Easdale TA, Hurst JM, Morse CW, Smissen RD, Peltzer DA. **2013b**. Intraspecific relationships among wood density, leaf structural traits and environment in four co-occurring species of Nothofagus in New Zealand. *PLoS One* **8**: e58878.

Richardson AD, Carbone MS, Huggett BA, Furze ME, Czimczik CI, Walker JC, Xu X, Schaberg PG, Murakami P. **2015**. Distribution and mixing of old and new nonstructural carbon in two temperate trees. *New Phytologist* **206**: 590–597.

de la Riva EG, Tosto A, Pérez-Ramos IM, Navarro-Fernández CM, Olmo M, Anten NPR, Marañón T, Villar R. **2016**. A plant economics spectrum in Mediterranean forests along environmental gradients: is there coordination among leaf, stem and root traits? *Journal of Vegetation Science* **27**: 187–199.

Rius D, Galop D, Doyen E, Millet L, Vannière B. 2014. Biomass burning response to high-amplitude climate and vegetation changes in Southwestern France from the Last Glacial to the early Holocene. *Vegetation history and Archaeobotany* **23**: 729–742.

Roderick ML. **2000**. On the measurement of growth with applications to the modelling and analysis of plant growth. *Functional Ecology* **14**: 244–251.

Rodríguez-Calcerrada J, López R, Salomón R, Gordaliza GG, Valbuena-Carabaña M, Oleksyn J, Gil L. **2015**. Stem CO2 efflux in six co-occurring tree species: underlying factors and ecological implications. *Plant, Cell & Environment* **38**: 1104–1115.

Rosado LR, Takarada LM, Araújo ACC de, Souza KRD de, Hein PRG, Rosado SC da S, Gonçalves FMA. **2019**. Near infrared spectroscopy: rapid and accurate analytical tool for prediction of non-structural carbohydrates in wood. *Cerne* **25**: 84–92.

Rosner S, Klein A, Müller U, Karlsson B. **2007**. Hydraulic and mechanical properties of young Norway spruce clones related to growth and wood structure. *Tree Physiology* **27**: 1165–1178.

Rosseel Y. **2012**. lavaan: an R package for structural equation modeling. *Journal of Statistical Software* **48**: 1–36.

Roumet C, Birouste M, Picon-Cochard C, Ghestem M, Osman N, Vrignon-Brenas S, Cao K, Stokes A. **2016**. Root structure-function relationships in 74 species: evidence of a root economics spectrum related to carbon economy. *New Phytologist* **210**: 815–826.

Rowland L, da Costa ACL, Galbraith DR, Oliveira RS, Binks OJ, Oliveira A a. R, Pullen AM, Doughty CE, Metcalfe DB, Vasconcelos SS, *et al.* 2015. Death from drought in tropical forests is triggered by hydraulics not carbon starvation. *Nature* **528**: 119–122.

Rüger N, Comita LS, Condit R, Purves D, Rosenbaum B, Visser MD, Wright SJ, Wirth C. **2018**. Beyond the fast–slow continuum: demographic dimensions structuring a tropical tree community. *Ecology Letters* **21**: 1075–1084.

Ryan MG, Asao S. **2014**. Phloem transport in trees. *Tree Physiology* **34**: 1–4.

Sala A, Woodruff DR, Meinzer FC. **2012**. Carbon dynamics in trees: feast or famine? *Tree Physiology* **32**: 764–775.

Sanchez-Martinez P, Martínez-Vilalta J, Dexter KG, Segovia RA, Mencuccini M. 2020. Adaptation and coordinated evolution of plant hydraulic traits. *Ecology Letters* **23**: 1599–1610.

Sapes G, Demaree P, Lekberg Y, Sala A. **2021**. Plant carbohydrate depletion impairs water relations and spreads via ectomycorrhizal networks. *New Phytologist* **229**: 3172–3183.

Sapes G, Roskilly B, Dobrowski S, Maneta M, Anderegg WRL, Martinez-Vilalta J, Sala A. **2019**. Plant water content integrates hydraulics and carbon depletion to predict drought-induced seedling mortality. *Tree Physiology* **39**: 1300–1312.

Savitzky A, Golay MJE. 1964. Smoothing and differentiation of data by simplified least squares procedures. *Analytical Chemistry* **36**: 1627–1639.

Schädel C, Blöchl A, Richter A, Hoch G. **2009**. Short-term dynamics of nonstructural carbohydrates and hemicelluloses in young branches of temperate forest trees during bud break. *Tree Physiology* **29**: 901–911.

Schiestl-Aalto P, Ryhti K, Mäkelä A, Peltoniemi M, Bäck J, Kulmala L. **2019**. Analysis of the NSC storage dynamics in tree organs reveals the allocation to belowground symbionts in the framework of whole tree carbon balance. *Frontiers in Forests and Global Change* **2**: 17.

Schlesinger WH, DeLucia EH, Billings WD. **1989**. Nutrient-use efficiency of woody plants on contrasting soils in the western great basin, Nevada. *Ecology* **70**: 105–113.

Scholz A, Klepsch M, Karimi Z, Jansen S. **2013**. How to quantify conduits in wood? *Frontiers in Plant Science* **4**: 56.

Schuldt B, Leuschner C, Brock N, Horna V. **2013**. Changes in wood density, wood anatomy and hydraulic properties of the xylem along the root-to-shoot flow path in tropical rainforest trees. *Tree Physiology* **33**: 161–174.

Schweiger AK, Cavender-Bares J, Townsend PA, Hobbie SE, Madritch MD, Wang R, Tilman D, Gamon JA. **2018**. Plant spectral diversity integrates functional and phylogenetic components of biodiversity and predicts ecosystem function. *Nature Ecology & Evolution* **2**: 976–982.

Secchi F, Pagliarani C, Zwieniecki MA. **2017**. The functional role of xylem parenchyma cells and aquaporins during recovery from severe water stress. *Plant, Cell & Environment* **40**: 858–871.

Signori-Müller, C., R. S. Oliveira, J. Valentim Tavares, F. Carvalho Diniz, M. Gilpin, F. de V. Barros, M. J. Marca Zevallos, et al. 2021. Variation of non-structural carbohydrates across the fast–slow continuum in Amazon Forest canopy trees. *Functional Ecology* **36**: 341–355.

Šímová I, Violle C, Svenning J-C, Kattge J, Engemann K, Sandel B, Peet RK, Wiser SK, Blonder B, McGill BJ, *et al.* 2018. Spatial patterns and climate relationships of major plant traits in the New World differ between woody and herbaceous species. *Journal of Biogeography* **45**: 895–916.

Slik JWF, Franklin J, Arroyo-Rodríguez V, Field R, Aguilar S, Aguirre N, Ahumada J, Aiba S-I, Alves LF, K A, *et al.* 2018. Phylogenetic classification of the world's tropical forests. *Proceedings of the National Academy of Sciences* **115**: 1837–1842.

Smith VC, Ennos AR. **2003**. The effects of air flow and stem flexure on the mechanical and hydraulic properties of the stems of sunflowers *Helianthus annuus* L. *Journal of Experimental Botany* **54**: 845–849.

Smith MG, Miller RE, Arndt SK, Kasel S, Bennett LT. **2018a**. Whole-tree distribution and temporal variation of non-structural carbohydrates in broadleaf evergreen trees. *Tree Physiology* **38**: 570–581.

Smith MG, Arndt SK, Miller RE, Kasel S, Bennett LT. 2018b. Trees use more non-structural carbohydrate reserves during epicormic than basal resprouting. *Tree physiology* **38**: 1779–1791.

Smith SA, Btown JW. 2018. Constructing a broadly inclusive seed plant phylogeny. *American Journal of Botany* **105**: 302–314.

Sperry JS, Hacke UG, Pittermann J. **2006**. Size and function in conifer tracheids and angiosperm vessels. *American Journal of Botany* **93**: 1490–1500.

Sperry JS, Meinzer FC, McCULLOH KA. **2008**. Safety and efficiency conflicts in hydraulic architecture: scaling from tissues to trees. *Plant, Cell & Environment* **31**: 632–645.

Spicer R. **2014**. Symplasmic networks in secondary vascular tissues: parenchyma distribution and activity supporting long-distance transport. *Journal of Experimental Botany* **65**: 1829–1848.

Stokes A, Guitard D. **1997**. Tree root response to mechanical stress. In: Altman A, Waisel Y, eds. Biology of root formation and development. Boston, MA: Springer US, 227–236.

Swenson NG, Enquist BJ. **2007**. Ecological and evolutionary determinants of a key plant functional trait: wood density and its community-wide variation across latitude and elevation. *American Journal of Botany* **94**: 451–459.

Taylor FW. 1969. The effect of ray tissue on the specific gravity of wood. *Wood and Fiber Science* **1**: 142–145.

Thomas SC. 1996. Asymptotic height as a predictor of growth and allometric characteristics in malaysian rain forest trees. *American Journal of Botany* **83**: 556–566.

Tomasella M, Petrussa E, Petruzzellis F, Nardini A, Casolo V. **2020**. The possible role of non-structural carbohydrates in the regulation of tree hydraulics. *International Journal of Molecular Sciences* **21**: 144.

Trifilò P, Kiorapostolou N, Petruzzellis F, Vitti S, Petit G, Lo Gullo MA, Nardini A, Casolo V. **2019**. Hydraulic recovery from xylem embolism in excised branches of twelve woody species: Relationships with parenchyma cells and non-structural carbohydrates. *Plant Physiology and Biochemistry* **139**: 513–520.

Tyree MT, Ewers FW. **1991**. The hydraulic architecture of trees and other woody plants. *New Phytologist* **119**: 345–360.

Utsumi Y, Sano Y, Fujikawa S, Funada R, Ohtani J. 1998. Visualization of cavitated vessels in winter and refilled vessels in spring in diffuse-porous trees by cryo-scanning electron microscopy. *Plant Physiology* **117**: 1463–1471.

Van Handel E. **1965**. Estimation of glycogen in small amounts of tissue. *Analytical Biochemistry* **11**: 256–265.

Vargas R, Trumbore SE, Allen MF. **2009**. Evidence of old carbon used to grow new fine roots in a tropical forest. *New Phytologist* **182**: 710–718.

Violle C, Jiang L. 2009. Towards a trait-based quantification of species niche. *Journal of Plant Ecology* **2**: 87–93.

Violle C, Navas ML, Vile D, Kazakou E, Fortunel C, Hummel I, Garnier E. 2007. Let the concept of trait be functional! *Oikos* **116**: 882–892.

von Arx G, Arzac A, Fonti P, Frank D, Zweifel R, Rigling A, Galiano L, et al. 2017. Responses of sapwood ray parenchyma and non-structural carbohydrates of *Pinus sylvestris* to drought and long-term irrigation. *Functional Ecology* **31**: 1371–1382.

Wang A-Y, Han S-J, Zhang J-H, Wang M, Yin X-H, Fang L-D, Yang D, Hao G-Y. 2018b. The interaction between nonstructural carbohydrate reserves and xylem hydraulics in Korean pine trees across an altitudinal gradient. *Tree Physiology* **38**: 1792–1804.

Wang Y, Mao Z, Bakker MR, Kim JH, Brancheriau L, Buatois B, Leclerc R, Selli L, Rey H, Jourdan C, *et al.* 2018a. Linking conifer root growth and production to soil temperature and carbon supply in temperate forests. *Plant and Soil* **426**: 33–50.

Warton DI, Wright IJ, Falster DS, Westoby M. 2006. Bivariate line-fitting methods for allometry. *Biological Reviews* **81**: 259–291.

Webb CO, Donoghue MJ. 2005. Phylomatic: tree assembly for applied phylogenetics. *Molecular Ecology Notes* **5**: 181–183.

Weber R, Gessler A, Hoch G. 2019. High carbon storage in carbon-limited trees. *New Phytologist* **222**: 171–182.

Weemstra M, Mommer L, Visser EJW, Ruijven J, Kuyper TW, Mohren GMJ, Sterck FJ. 2016. Towards a multidimensional root trait framework: a tree root review. *New Phytologist* **211**: 1159–1169.

Westoby M. 1998. A leaf-height-seed (LHS) plant ecology strategy scheme. *Plant and soil* **199**: 213–227.

Westoby M, Falster DS, Moles AT, Vesk PA, Wright IJ. 2002. Plant ecological strategies: some leading dimensions of variation between species. *Annual Review of Ecology and Systematics* **33**: 125–159.

Wheeler JK, Sperry JS, Hacke UG, Hoang N. **2005**. Inter-vessel pitting and cavitation in woody Rosaceae and other vesselled plants: a basis for a safety versus efficiency trade-off in xylem transport. *Plant, Cell & Environment* **28**: 800–812.

Wheeler EA, Baas P, Rodgers S. **2007**. Variations in dieot wood anatomy: a global analysis based on the insidewood database. *IAWA Journal* **28**: 229–258.

Wiemann MC, Williamson GB. **2002**. Geographic variation in wood specific gravity: effects of latitude, temperature, and precipitation. *Wood and Fiber Science* **34**: 96-107.

Wiley E, Helliker B. 2012. A re-evaluation of carbon storage in trees lends greater support for carbon limitation to growth. *New Phytologist* **195**: 285–289.

Wiley E, Huepenbecker S, Casper BB, Helliker BR. **2013**. The effects of defoliation on carbon allocation: can carbon limitation reduce growth in favour of storage? *Tree Physiology* **33**: 1216–1228.

Williamson GB, Wiemann MC. 2010. Measuring wood specific gravity… correctly. *American Journal of Botany* **97**: 519–524.

Woodrum CL, Ewers FW, Telewski FW. **2003**. Hydraulic, biomechanical, and anatomical interactions of xylem from five species of *Acer* (Aceraceae). *American Journal of Botany* **90**: 693–699.

Wright IJ, Westoby M, Reich PB. **2002**. Convergence towards higher leaf mass per area in dry and nutrient-poor habitats has different consequences for leaf life span. *Journal of Ecology* **90**: 534–543.

Wright IJ, Reich PB, Westoby M, Ackerly DD, Baruch Z, Bongers F, Cavender-Bares J, Chapin T, Cornelissen JHC, Diemer M, *et al.* 2004. The worldwide leaf economics spectrum. *Nature* **428**: 821–827.

Wright IJ, Reich PB, Cornelissen JHC, Falster DS, Groom PK, Hikosaka K, Lee W, Lusk CH, Niinemets Ü, Oleksyn J, *et al.* 2005. Modulation of leaf economic traits and trait relationships by climate. *Global Ecology and Biogeography* **14**: 411–421.

Würth MKR, Peláez-Riedl S, Wright SJoseph, Körner C. **2005**. Non-structural carbohydrate pools in a tropical forest. *Oecologia* **143**: 11–24.

Yamada Y, Awano T, Fujita M, Takabe K. **2011**. Living wood fibers act as large-capacity "single-use" starch storage in black locust (*Robinia pseudoacacia*). *Trees* **25**: 607–616.

Yoshimura K, Saiki S-T, Yazaki K, Ogasa MY, Shirai M, Nakano T, Yoshimura J, Ishida A. **2016**. The dynamics of carbon stored in xylem sapwood to drought-induced hydraulic stress in mature trees. *Scientific Reports* **6**: 24513.

Yu R, Huang J, Xu Y, Ding Y, Zang R. **2020**. Plant functional niches in forests across four climatic zones: Exploring the periodic table of niches based on plant functional traits. *Frontiers in Plant Science* **11**: 841.

Zanne AE, Lopez-Gonzalez G, Coomes DA, Ilic J, Jansen S, Lewis SL, Miller RB, et al. 2009. Data from: Towards a worldwide wood economics spectrum, Dryad, Dataset, https://doi.org/10.5061/dryad.234.

Zanne AE, Westoby M, Falster DS, Ackerly DD, Loarie SR, Arnold SEJ, Coomes DA. **2010**. Angiosperm wood structure: Global patterns in vessel anatomy and their relation to wood density and potential conductivity. *American Journal of Botany* **97**: 207–215.

Zhang G, Mao Z, Fortunel C, Martínez-Vilalta J, Viennois G, Maillard P, Stokes A. **2022a**. Parenchyma fractions drive the storage capacity of non-structural carbohydrates across a broad range of tree species. *American Journal of Botany* **4**: 535–549.

Zhang G, Maillard P, Mao Z, Brancheriau L, Engel J, Gerard B, Fortunel C, Maeght JL, Martínez-Vilalta J, Ramel M, Nourissier-Mountou S, Fourtier S, Stokes A. 2022b. Non-structural carbohydrates and morphological traits of leaves, stems and roots from tree species in different climates. *BMC Research Notes* **15**: 251.

Zhang SB, Cao KF, Fan ZX, Zhang JL. **2013**. Potential hydraulic efficiency in angiosperm trees increases with growth-site temperature but has no trade-off with mechanical strength. *Global Ecology and Biogeography* **22**: 971–981.

Zhao YT, Ali A, Yan ER. **2017**. The plant economics spectrum is structured by leaf habits and growth forms across subtropical species. *Tree Physiology* **37**: 173–185.

Zheng J, Martínez-Cabrera HI. **2013**. Wood anatomical correlates with theoretical conductivity and wood density across China: evolutionary evidence of the functional differentiation of axial and radial parenchyma. *Annals of Botany* **112**: 927–935.

Zheng J, Zhao X, Morris H, Jansen S. **2019**. Phylogeny best explains latitudinal patterns of xylem tissue fractions for woody angiosperm species across China. *Frontiers in Plant Science* **10**: 556.

Ziemińska K, Butler DW, Gleason SM, Wright IJ, Westoby M. **2013**. Fibre wall and lumen fractions drive wood density variation across 24 Australian angiosperms. *AoB Plants* **5**: plt046.

Ziemińska K. **2014**. Anatomical variation in twig wood across Australian angiosperm. PhD thesis, Macquarie University, Sydney, Australia, 244p.

Ziemińska K, Westoby M, Wright IJ. **2015**. Broad anatomical variation within a narrow wood density range—a study of twig wood across 69 Australian angiosperms. *PloS One* **10**: e0124892.

Ziemińska K, Rosa E, Gleason SM, Holbrook NM. **2020**. Wood day capacitance is related to water content, wood density, and anatomy across 30 temperate tree species. *Plant, Cell & Environment* **43**: 3048–3067.

Zwieniecki MA, Holbrook NM. **2009**. Confronting Maxwell's demon: biophysics of xylem embolism repair. *Trends in Plant Science* **14**: 530–534.

ANNEX I: Non-structural carbohydrates and morphological traits measured of leaves, stems and roots from tree species in different climates

Guangqi Zhang[1*], Pascale Maillard[2], Zhun Mao[1], Loic Brancheriau[3], Julien Engel[1], Bastien Gérard[2], Claire Fortunel[1], Jean-Luc Maeght[1], Jordi Martínez-Vilalta[4,5], Merlin Ramel[1], Sophie Nourissier-Mountou[1], Stéphane Fourtier[1], Alexia Stokes[1]

1 AMAP, Université de Montpellier, CIRAD, CNRS, INRAE, IRD, 34000 Montpellier, France
2 SILVA, INRAE, Université de Lorraine, Agroparistech, Centre de Recherche Grand-Est Nancy, 54280 Champenoux, France
3 CIRAD, Université de Montpellier, UR BioWooEB, 34000 Montpellier, France
4 CREAF, E08193 Bellaterra (Cerdanyola del Vallès), Catalonia, Spain
5 Universitat Autònoma Barcelona, E08193 Bellaterra (Cerdanyola del Vallès), Catalonia, Spain
*Corresponding author: zh.guangqi@gmail.com

Published in *BMC Research Notes*, https://doi.org/10.1186/s13104-022-06136-7

ABSTRACT

Objectives: Carbon fixed during photosynthesis is exported from leaves towards sink organs as non-structural carbohydrates (NSC), that are a key energy source for metabolic processes in trees. In xylem, NSC are mostly stored as soluble sugars and starch in radial and axial parenchyma. The multi-functional nature of xylem means that cells possess several functions, including water transport, storage and mechanical support. Little is known about how NSC impacts xylem multi-functionality, nor how NSC vary among species and climates. We collected leaves, stem and root xylem from tree species growing in three climates and estimated NSC in each organ. We also measured xylem traits linked to hydraulic and mechanical functioning.

Data description: The paper describes functional traits in leaves, stems and roots, including NSC, carbon, nitrogen, specific leaf area, stem and root wood density and xylem traits. Data are provided for up to 90 angiosperm species from temperate, Mediterranean and tropical

climates. These data are useful for understanding the trade-offs in resource allocation from a whole-plant perspective, and to better quantify xylem structure and function related to water transportation, mechanical support and storage. Data will also give researchers keys to understanding the ability of trees to adjust to a changing climate.

Keywords: angiosperms, non-structural carbohydrates, fibers, functional traits, Mediterranean, parenchyma, root, temperate, tropical, vessels

OBJECTIVE

Non-structural carbohydrates (NSC) are essential substrates for metabolic processes in trees, including respiration, osmoregulation, growth, reproduction and defense [1, 2, 3, 4], as well as having major consequences for downstream processes such as microbial activity in the rhizosphere [5]. NSC is a product of photosynthesis and comprises mainly soluble sugars involved in transport or immediate functions, and starch stored in different plant organs for future use and maintaining functionality when carbon demand is higher than supply (e.g., under severe drought stress) [6, 7, 8, 9]. Therefore, understanding how patterns of NSC vary in trees will enable us to better evaluate the role of NSC in tree physiological processes and ecological strategies, especially across a broad range of species and climates [10].

The secondary xylem of angiosperms is generally composed of three specialized cell types including parenchyma, vessels and fibers (tracheids and fiber-tracheids may also be present), that perform storage, hydraulic and mechanical functions [11, 12, 13]. NSC are mainly stored in the live radial and axial parenchyma cells, therefore the size of the parenchyma fraction drives the capacity for NSC storage in trees [14, 15, 16]. In an attempt to disentangle how NSC and xylem traits are linked to tree physiological processes and ecological strategies, we collated data on stem and root NSC and xylem cell patterns, as well as leaf traits, from 90 tree species in temperate, Mediterranean and tropical climates. Our data will allow researchers to

explore the direct relationships between leaf, stem and root NSC contents with patterns in xylem cell composition. To our knowledge, this dataset represents the largest freely available collection of data for NSC xylem and leaf traits measured simultaneously in adult trees from diverse climates. Detailed information on materials and methods can be found in the accompanying Excel file (Table 1).

DATA DESCRIPTION

Study sites and species

This study was conducted in a temperate forest (Luz-Saint-Sauveur, France), a Mediterranean forest (Montpellier, France) and a tropical forest (Paracou, French Guiana). A total 90 angiosperm species were collected which are commonly found in local forests, with 20 species in both temperate and Mediterranean climates and 50 species in the tropical climate (Table 1, file 1). For each species, we chose three, healthy, adult trees that usually had a stem diameter of between 0.05 - 0.4 m at a height of 1.3 m. We collected leaf and stem samples for all trees, as well as coarse root samples for 60 species (n = 20 in each climate). Samples were collected at the end of August and early September 2019 for Mediterranean and tropical species and September 2020 for temperate species, when NSC storage should be close to its seasonal maximum [17, 18, 19]. We sampled all trees between 7am and midday, to reduce variability linked to photosynthate production. At a height of 1.3 m, three 0.05 m long cores were extracted from tree stems with a 4.3 mm diameter increment borer. To collect samples of roots, we excavated a single lateral root (0.02 - 0.05 m in diameter) and at a distance of 0.3-0.5 m from the base of the tree and extracted three increment cores or removed three 0.02 m long segments of root. We also collected one stem core from each tree in temperate and Mediterranean climates in March 2021 (before bud burst). In total, 540 leaf samples, 930 stem cores and 540 root segments were collected.

Measurement of leaf and xylem functional traits

A total of 270 leaf samples, 390 stem samples and 180 root samples were used to determine NSC, carbon (C) and nitrogen (N) measurements. For NSC content, a colorimetric method [20] was performed on all leaf samples, and a subsample of stems (n = 113) and roots (n = 140). C and N content were measured in a sub-sample of leaves (n = 110), stems (n = 113) and all root samples, using an elemental analyzer (CHN model EA 1108, Milan, Italy). Then, near infra-red spectroscopy (NIRS) [21] was performed on all samples and calibration models developed using data obtained from the analytical methods to predict soluble sugars, starch, C and N in the three organs (Table 1, file 1).

Cross-sections of 15-20 µm thick for stem (n=270) and root (n=180) samples were cut with a sliding microtome and stained with a mixture of safranin and alcian blue. Microphotographs of transversal sections were taken where radial and axial parenchyma fractions, vessel fractions, mean vessel area, mean vessel diameter, vessel density, mean vessel hydraulic diameter and theoretical specific xylem hydraulic conductivity were determined [22] (Table 1, file 1).

Specific leaf area (n=270) was determined using leaf area and dry mass. Stem wood density (n=270) and root wood density (n=180) were defined as oven-dry mass divided by fresh volume which measured by water displacement method (Table 1, file 1).

LIMITATIONS

Root NSC data were only collected for 60 species (n = 20 in each climate type). It was not possible to collect NSC in samples from tropical trees over two different seasons within a 12-month time period because of travel restrictions linked to the COVID pandemic. However, there is significantly less seasonal variability in NSC in tropical trees [10], compared to

Mediterranean and temperate species, therefore we do not consider this limitation as detrimental to the quality of data.

ABBREVIATIONS

NSC: non-structural carbohydrates

C: carbon

N: nitrogen

NIRS: near infra-red spectroscopy

DECLARATIONS

Ethics approval and consent to participate

Not applicable.

Consent for publication

Not applicable.

Availability of data and materials

The data and methods described in this Data note can be freely and openly accessed on Portail Data INRAE under https://doi.org/10.15454/MU0HXX. Please see table 1 and references [23] for details and links to the data.

Competing interests

The authors declare that they have no competing interests.

Funding

This study was supported by China Scholarship Council (PhD bursary for GZ) and a grant from Investissement d'Avenir grants of the ANR, France (CEBA: ANR-10-LABX-25-01).

Authors' contributions

GZ and AS prepared the manuscript. GZ, AS, PM, ZM, JE, CF, JLM, JMV, MR, SNM, SF conducted fieldwork. GZ, AS, LB, BG performed laboratory analyses. GZ, ZM, AS analyzed data. All the authors contributed critically to the drafts and gave final approval for publication.

Acknowledgments

We are grateful to N. Boutahar (CIRAD) and J. Cazal (INRAE) for their help with field and laboratory work. We thank G. Derroire and A. Dourdain for their aid with logistical arrangements and field authorizations in French Guyana. The collecting of genetic resources in French Guyana was authorized by the French Government (APA No. 1371201). We kindly thank to managers of state-owned land for their collaboration and to B. Dupin (Eco-Altitude) for permission to sample trees on private property at Luz-Saint-Sauveur, France. The authors would like to thank SILVATECH (doi: 10.15454/1.5572400113627854E12) from UMR 1434 SILVA, 1136 IAM, 1138 BEF and 4370 EA LERMAB from the research center INRAE Grand-Est Nancy for its contribution to NSC analyses. The SILVATECH facility is supported by the French National Research Agency through the Laboratory of Excellence ARBRE (ANR-11-LABX-0002-01).

REFERENCES

1. Kozlowski T. Carbohydrate sources and sinks in woody plants. Bot. Rev. 1992;58: 107–222.

2. Morin X, Ameglio T, Ahas R, Kurz-Besson C, Lanta V, Lebourgeois F, et al. Variation in cold hardiness and carbohydrate concentration from dormancy induction to bud burst among provenances of three European oak species. Tree Physiol. 2007;27:817–25.

3. Sala A, Woodruff DR, Meinzer FC. Carbon dynamics in trees: feast or famine? Tree Physiol. 2012;32:764–75.

4. Morris H, Hietala AM, Jansen S, Ribera J, Rosner S, Salmeia KA, Schwarze FW. Using the CODIT model to explain secondary metabolites of xylem in defence systems of temperate trees against decay fungi. Ann. Bot. 2020;125:701–720.

5. Schiestl-Aalto P, Ryhti K, Mäkelä A, Peltoniemi M, Bäck J, Kulmala L. Analysis of the NSC storage dynamics in tree organs reveals the allocation to belowground symbionts in the framework of whole tree carbon balance. Front. For. Glob. Change. 2019;2:17.

6. Anderegg WRL, Anderegg LDL. Hydraulic and carbohydrate changes in experimental drought-induced mortality of saplings in two conifer species. Tree Physiol. 2013;33:252–60.

7. Wiley E, Huepenbecker S, Casper BB, Helliker BR. The effects of defoliation on carbon allocation: can carbon limitation reduce growth in favour of storage? Tree Physiol. 2013;33:1216–28.

8. Klein T, Hoch G. Tree carbon allocation dynamics determined using a carbon mass balance approach. New Phytol. 2015;205:147–59.

9. Furze ME, Huggett BA, Aubrecht DM, Stolz CD, Carbone MS, Richardson AD. Whole-tree nonstructural carbohydrate storage and seasonal dynamics in five temperate species. New Phytol. 2019;221:1466–77.

10. Martínez-Vilalta J, Sala A, Asensio D, Galiano L, Hoch G, Palacio S, et al. Dynamics of non-structural carbohydrates in terrestrial plants: a global synthesis. Ecol. Monogr. 2016;86:495–516.

11. Pratt RB, Jacobsen AL. Conflicting demands on angiosperm xylem: Tradeoffs among storage, transport and biomechanics. Plant Cell Environ. 2017;40:897–913.

12. Chen Z, Zhu S, Zhang Y, Luan J, Li S, Sun P, et al. Tradeoff between storage capacity and embolism resistance in the xylem of temperate broadleaf tree species. Tree Physiol. 2020;40:1029–42.

13. Plavcová L, Gallenmüller F, Morris H, Khatamirad M, Jansen S, Speck T. Mechanical properties and structure–function trade-offs in secondary xylem of young roots and stems. J. Exp. Bot. 2019;70:3679–91.

14. Plavcová L, Hoch G, Morris H, Ghiasi S, Jansen S. The amount of parenchyma and living fibers affects storage of nonstructural carbohydrates in young stems and roots of temperate trees. Am. J. Bot. 2016;103:603–12.

15. Zhang G, Mao Z, Fortunel C, Martínez-Vilalta J, Viennois G, Maillard P, et al. Parenchyma fractions drive the storage capacity of non-structural carbohydrates across a broad range of tree species. Am. J. Bot. 2022;109:535–549.

16. Rodríguez-Calcerrada J, López R, Salomón R, Gordaliza GG, Valbuena-Carabaña M, Oleksyn J, Gil L. Stem CO2 efflux in six co-occurring tree species: Underlying factors and ecological implications. Plant Cell Environ. 2015;38:1104–1115.

17. Palacio S, Camarero JJ, Maestro M, Alla AQ, Lahoz E, Montserrat-Martí G. Are storage and tree growth related? Seasonal nutrient and carbohydrate dynamics in evergreen and deciduous Mediterranean oaks. Trees. 2018;32:777–790.

18. Würth MK, Pelaez-Riedl S, Wright SJ, Körner C. Non-structural carbohydrate pools in a tropical forest. Oecologia. 2005;143:11–24.

19. Richardson AD, Carbone MS, Keenan TF, Czimczik CI, Hollinger DY, Murakami P, et al. Seasonal dynamics and age of stemwood nonstructural carbohydrates in temperate forest trees. New Phytol. 2013;197:850–861.

20. Black M, Corbineau F, Grzesik M, Guy P, Come D. Carbohydrate metabolism in the developing and maturing wheat embryo in relation to its desiccation tolerance. J. Exp. Bot. 1996;47:161–9.

21. Ramirez JA, Posada JM, Handa IT, Hoch G, Vohland M, Messier C, Reu B. Near-infrared spectroscopy (NIRS) predicts non-structural carbohydrate concentrations in different tissue types of a broad range of tree species. Methods Ecol. Evol. 2015;6:1018–1025.

22. Scholz A, Klepsch M, Karimi Z, Jansen S. How to quantify conduits in wood? Front. Plant Sci. 2013;4.

23. Zhang G, Stokes A. Xylem_Stem_Root_Leaf_Trait data. Portail Data INRAE https://doi.org/10.15454/MU0HXX (2022).

TABLE

Table 1: Overview of data files/data sets.

Label	**Name of data file/data set**	**File types (file extension)**	**Data repository and identifier (DOI or accession number)**
Data file 1	Xylem_Stem_Root_Leaf_Trait data	MS Excel file (.xlsx)	Portail Data INRAE https://doi.org/10.15454/MU0HXX [23]

ANNEX II: Root topological order governs intra- and interspecific variations of tree root hydraulic features

Guangqi Zhang[1,2], Claire Fortunel[2], Shan Niu[1], Juan Zuo[3,4], Jean-luc Maeght[2], Xiaodong Yang[1], Shangwen Xia[1*], Zhun Mao[2*]

1 Key Laboratory of Tropical Forest Ecology, Xishuangbanna Tropical Botanical Garden, Chinese Academy of Sciences, Menglun, Mengla, Yunnan 666303, China
2 AMAP, Univ Montpellier, INRAE, CIRAD, CNRS, IRD, 34000 Montpellier, France
3 Key Laboratory of Aquatic Botany and Watershed Ecology, Wuhan Botanical Garden, Chinese Academy of Sciences, Wuhan, 430074, China
4 Center of Plant Ecology, Core Botanical Gardens, Chinese Academy of Sciences, Wuhan, 430074, China
*Corresponding authors: Zhun Mao zhun.mao@inrae.fr, Shangwen Xia xsw@xtbg.org.cn

In preparation for submission to *New Phytologist*

ABSTRACT

Premise: Root traits reflect key plant functions such as water absorption, transportation and use, mechanical strength and storage in roots. Despite their importance in plant function, we have a limited understanding of the ecological and evolutionary drivers of root traits. In particular, we still know little about variation in root traits along fine root orders, especially in tropical tree species.

Methods: Here, we sampled five fine root orders in 20 tree species in a tropical forest in southwestern China. We measured 11 traits relating to hydraulics, structure and morphology in each root order. We tested intra- and inter-specific traits relationships across and within root orders.

Results: We found high intraspecific variability across root orders for most traits. Species specific xylem hydraulic conductivity increased with root order, associated with greater vessel

mean area and lower vessel density. Conversely, we detected no significant difference among root orders for vessel fraction of most species which had a positive correlation with hydraulic conductivity, but had no correlations with other vessel traits. Interspecific correlations between traits varied across root orders: they were weak in low-order roots, but high in high order roots. We found no effect of species evolutionary history on trait correlations.

Conclusion: Our study provides evidence on the changes and associations of root traits and hydraulic-related variables across species and root orders. We demonstrated the patterns of root trait variation, covariation and evolution. These findings highlight the important roles of root topology in driving root ecological and evolutionary processes in tropical forest.

Key words: anatomy, fine root, hydraulic conductivity, topology, vessel, root traits

INTRODUCTION

Root hydraulic conductivity, defined as the root's intrinsic ability to conduct water from root surface to the stem xylem (Eissenstat 1997), is essential for plant water absorption, transportation and use. Root hydraulic conductivity consists of both radial and axial conductivity, which differ in water movement speed and concerned root organs (Cuneo *et al*., 2016). Epidermis and cortex are the first pathways allowing water radially traverses from soil to stele (Steudle and Peterson, 1998). In stele, water is then axially transported via vessels in xylem toward aboveground compartment (Esau, 1960). Root hydraulic conductivity greatly matters plant nutrient uptake, reproduction and strategies to environmental stimuli (Passioura, 1988; Tyree and Ewers, 1991; Huang and Eissenstat, 2000). However, hydraulic conductivity is disproportionately less well studied for roots, especially for distal and fine roots, than for stems, partially due to the technical difficulties in directly measurement of root hydraulic indicators.

Anatomical traits are commonly used as proxies to represent root hydraulic conductivity, (Tyree and Ewers, 1991; Rieger and Litvin, 1999; Poorter *et al*., 2010; Schuldt *et al*., 2013). A series of size-related metrics, including cordial thickness and stele diameter, as well as their relative sizes, are conventionally measured anatomical traits as rough characterization of root hydraulic functions (Rieger and Litvin 1999). For example, increasing proportion of stele in roots can enhance axial hydraulic conductivity (Oliveras *et al*., 2003; Rodríguez-Gamir *et al*, 2010; Wang *et al*., 2016); species having higher cordial thickness is found to have lower axial conductivity, according to a study on five temperate tree species (Rieger and Litvin 1999).

Root vessels are main channels for axial water transport in plants and their traits greatly affect the flow rate of water, maintenance of water potential gradient and vulnerability to xylem cavitation (Wheeler *et al*., 2005). Vessel fraction, defended as the portion of sapwood occupied by vessel lumens, is found be closely related to wood mechanical robustness and hydraulic conductivity (Scholz *et al*., 2013). Vessel sizes (e.g., diameter) in a root are directly used to calculate both mean hydraulic dimeter (MHD, i.e., the actual conductance of conduits) and root specific xylem hydraulic conductivity (SXHC, i.e., conductance per unit root surface area), two fundamental hydraulic variables widely used in literature (Tyree and Ewers, 1991; Poorter *et al*., 2010, Fortunel *et al*., 2014). A higher mean vessel diameter favors conducting efficiency, but may decrease conducting safety due to the increasing risk of vessel implosion and cavitation (Loepfe *et al*., 2007). Therefore, for a given total vessel fraction in a root, mean vessel size shall be closely related to vessel density, thereby affecting the plant's hydraulic strategy in water use (Hacke *et al*., 2006). Furthermore, few studies have focused on vessel variability. Since vessel variability is certainly not the same between different tree species or among root orders, whether it would affect hydraulic conductivity is still poorly understood. So far, data on these above vessel traits for fine roots are still scanty. In the sporadic studies on fine root vessel traits, e.g., Wang *et al*. (2016) and Zhou *et al*. (2020), only vessel size and

density were measured, but neither vessel fraction nor their trade-off relationships were investigated. Moreover, they only focus on absorptive roots, i.e., either on the first order roots (Wang *et al*., 2016) or on mixed roots of the first two orders (Zhou *et al*., 2020), but lack a holistic understanding of how these vessel traits (i.e., MHD and SXHC) vary and covary across multiple root topological orders.

Root topological orders (Fitter, 1987) have been increasingly used as a gradient to understand plant functionality and shown to be a better predictor of numerous root traits compared with root diameter, which was, conventionally, based on the arbitrary use of 2 mm cut-off (McCormack *et al*., 2015). With increasing root orders of a species, root diameter, total non-structural carbohydrate, cellulose concentrations and mechanical strength tend to increase, whereas specific root length, nitrogen and lignin concentrations, mycorrhizal colonization, and root turnover tend to decrease (Guo *et al*., 2004, 2008a; Fan and Guo, 2010; Ouimette *et al*., 2013; Xiong *et al*., 2013; Mao *et al*., 2018). Therefore, it is scientifically meaningful to examine the variation patterns of root hydraulic traits, especially vessel traits, following the root order gradient. Like nutrients, it is reported that roots' water absorptive capacity decreases and transport capacity increases with increasing root order of a species (McCormack *et al*., 2015). For several root anatomical traits that are related to water use, e.g., stele diameter, cortex thickness and their relative size, their variation patterns along root order gradient are well-known (Guo *et al*., 2008b; Gu *et al*., 2014). We argue that how root hydraulic conductivity, in particular axial conductivity, vary along root orders still lacks a trait-based evidence support. To our best knowledge, no studies have ever examined the intraspecific variation of vessel traits and their derived hydraulic variables (i.e., MHD and SXHC), as well as their relationships, along multiple root orders.

Examining interspecific variation of hydraulic traits can help us better understand trade-off or synergy between water use strategies (e.g., efficiency versus safety) and between water use and other functions (e.g., mechanical robustness) among species. Based on aboveground vessel traits, previous studies have evidenced that species could either favor hydraulic efficiency (i.e., high water transport capacity with large vessel size) or favor hydraulic safety (i.e., strong cavitation resistance with small vessel size or high vessel density) (Loepfe *et al*., 2007; Martínez-Vilalta *et al*., 2012). It is little known whether such a pattern works on belowground too. Fortunel *et al*. (2014) working on woody roots of >1 cm in diameter of Amazonian rainforest tree species found that species with higher mean vessel size tended to have lower vessel density, thus supporting the existence of such an interspecific tradeoff pattern for large coarse roots. Whether such a pattern can be further extrapolated to finer roots is a lacuna. Existing studies examining fine roots' hydraulic traits are quite preliminary and only concentrate on stele and cortex sizes. For example, Guo *et al*. (2008b) measured stele and cortical sizes along a root order gradient among 23 Chinese temperate tree species and found that gymnosperms had higher root stele : diameter ratio than angiosperms, suggesting a higher water transport capacity in gymnosperms. So far, no study has ever examined the interspecific variation of fine root vessel traits and how the patterns shift along root orders. In particular, root stele : diameter ratio was found to be a good proxy of root mechanical strength at both intra- and interspecific levels (Chimungu *et al*., 2015; Mao *et al*., 2018). Associating stele : diameter ratio with vessel traits may provide us insights on plants' resource allocation strategies between hydraulic transport and mechanical support, but is, again, little explored in literature.

Considering evolutionary history in the study of plant functional traits help us better understand plants' strategies facing natural selection. First, simple trait relationships observed across species do not necessarily reflect coordinated evolutionary changes (Felsenstein, 1985).

Exploring phylogenetically independent trait relationships could provide us a more genuine insight for correlated evolutionary shifts and trait variation (Maherali *et al*., 2004). Second, for root anatomical traits, it remains unclear whether their evolutionary changes are congruent or not. Although it is challenging to study the evolutionary history of root anatomical traits due to scarce root fossils (Raven and Edwards, 2001), it becomes possible to study root traits by identifying evolutionary traces along divergent time series (Wikström *et al*., 2001). Previous studies have shown that root diameter of extent species was significantly related to the divergence time at the family level (Chen *et al*., 2013; Ma *et al*., 2018) and cortical thickness, number of cortical cell layers and stele diameter showed similar variation pattern with root diameter (Gu *et al*., 2014). However, whether root vessels traits also have the similar trends and how they shift among different root orders is totally unexplored.

In the present study, we characterized root hydraulic conductivity by determining a series of root morphological and anatomical traits for cortex, stele and vessel across five root topological orders for 20 tree species in an Asian tropical forest in southwestern China. In particular, vessel traits include three anatomical traits (vessel fraction, vessel density and mean vessel area) and two hydraulic variables (MHD and SHXC) that reflect axial hydraulic conductivity. We ask:

(1) at the intraspecific level, how the anatomical traits and hydraulic variables change along root order gradient? Following Guo *et al*. (2008b), we expect a lower relative size of cortex, but a higher relative stele size with increasing root order (Hypothesis 1A, H1A). For vessel traits, we expect an increase in axial hydraulic conductivity, due to the increase in vessel fraction and mean diameter, with increasing root order (H1B), as higher order roots are assumed to be more apt to transport water and nutrient according to McCormak *et al*. (2015). When mixing all the data belonging to different root orders together for each species, we

predict that the coordination of traits and variables is fixed and comparable among the species, rather than diversified, following the hypothesis that the ability of root order in reflecting the shifts in plant functionality is generic among species in a common community (H1C).

(2) at the interspecific level, what are relationships among the traits for different root orders? First of all, we assume that root topology would contribute to explaining interspecific variation (H2A). Specifically, we expect the correlations among hydraulic traits would be stronger in high-order roots than in low-order roots, as low-order roots are considered to be absorptive roots, while high-order roots are transport roots (H2B). Then, we expect that species with high SXHC would exhibit high vessel fraction, vessel mean area, vessel variability but low vessel density (H2C). Finally, we expect a positive relationship between vessel traits and stele: root diameter ratio (H2D), implying a synergy in water transport and mechanical support.

(3) whether evolutionary history affect the values and interdependences of the root anatomical traits for different root orders? We expect that root morphology trait (i.e., diameter) and non-vessel anatomical traits (i.e., cortex and epidermis thickness) would be affected by evolution history (H3A), while vessel traits tend to be conserved in all root orders (H3B). We also expect that there is no effect of species evolutionary history on the correlation patterns among root anatomical traits and hydraulic variables (H3C).

METERIALS AND METHODS

Study site and species selection

The study site was located in a tropical and naturally regenerated forest near the village of Bubeng (21°36'42" N,101°34'26" E), Yunnan Province, China. The region has a tropical monsoon climate with distinct rainy season from May to October and dry season from

November to April. The mean annual temperature is 21.7 ℃ with a monthly temperature of 25.7 ℃ for the warmest month (June) and 15.9 ℃ for the coldest month (January). The mean annual precipitation is 1493 mm, of which 84% occurred during the rainy season (Liu *et al*., 2004; Cao *et al*., 2006). The soil is lateritic and developed from siliceous rocks (Cao *et al*. 2006). In this study, we selected 20 native species belonging to 12 families (Table 1). All the species are common in the natural forest. For each species, four healthy adult individual trees were randomly identified in the forest and to ensure sampling representativeness, trees for the same species within a distance of ⩽20 meters were avoided.

Root sampling and processing

For each selected tree, we carefully excavated root samples from the top 20 cm of soil, following same procedures as in Guo *et al*. (2008b) and Mao *et al*. (2018). Excavation started from the tree stem to lateral coarse roots to make sure that roots to sample are from the target tree. Root branches including at least five intact topological orders were cut from the main lateral roots. We followed the classical stream classification approach initiated by Fitter (1987) and then described by Pregitzer *et al*. (2002) and Guo *et al*. (2008) to determine the root topological orders of each root branch with the most distal roots were considered as first-order roots (Freschet *et al*. 2021). The only difference from Guo *et al*. (2008b) is that for the first-order roots, we deliberately avoided root tips from the pioneer roots that will be deem to become higher-order roots soon.

After excavation, these roots were wrapped in moist paper towels, quickly put into the ice box and then transported to the laboratory within 3 h for further processing. In laboratory, they were gently washed in deionized water. A subsample for anatomical analyses was cut and immediately fixed in Formalin-Aceto-Alcohol (FAA) solution (90 ml 50% ethanol, 5 ml 100%

glacial acetic acid, 5 ml 37% methanol). All the above field sampling and laboratory work was performed during late October and early November of 2018.

Determining anatomical traits and hydraulic variables

For each of the four trees, we selected one entire, healthy and size-representative root per order from the root segments in the FAA solution for dissection. In total, 400 roots (20 species × 4 trees (as replicates) × 5 orders) were analyzed. Cross-sections were then cut from the fresh root material and stained with acid fuchsin, dehydrated in a set of alcohol solutions, embedded in paraffin. First- and second-order roots were cut under a microscope (S8 APO, Leica, Germany). For each root order, one cross-section was chosen and slide of 8-um-thick was prepared (Guo *et al*., 2008b). Photographs of each slide were shoot using a microscope (DM 2000, Leica, Germany) which was connected to a computer and digital images analyses were conducted with public software ImageJ 1.52 (https://imagej.nih.gov/ij/) for determination of anatomical characteristics.

For each image, root diameter, outer tissue thickness, cortex thickness and stele diameter were measured in three directions and mean values were calculated. For roots with cortex, the outer tissue thickness represents the thickness of the outer part of cortex, and for roots without cortex, the outer tissue thickness represents the thickness of the outer part of stele. The ratios of stele diameter to root diameter, cortex thickness to root radius, outer tissue thickness to root radius were also calculated. Besides length metrics, we also estimated the area metrics of the above components. As root sections were not perfectly round, the sum of the area of measured stele diameter, cortex thickness and outer tissue thickness could not be exactly equal to the area calculated from the measured root diameter. Therefore, for each root, we first standardized stele diameter, cortex thickness and outer tissue thickness with the measured root

diameter. Then, we calculated the areas of stele, cortex and outer tissue with their standardized metrics based on the circular area formula.

We also determined vessel fraction (VF, total vessel area divided by xylem cross-section area), vessel density (Vd, vessel number divided by xylem cross-section area) and vessel mean area (VMA, total vessel area divided by vessel number). Vessel diameter (D, in) for a vessel *i* was calculated using the equation (Lewis, 1992) as:

$$D = \sqrt{\frac{2a^2b^2}{a^2+b^2}} \qquad \text{Eqn. 1}$$

where *a* is vessel major diameter and *b* is vessel minor diameter.

We calculated hydraulic variables from vessel traits. The vessel mean hydraulic diameter (MHD) was calculated (Scholz *et al.*, 2013) as:

$$MHD = \sqrt[4]{\frac{\sum_{i=1}^{n} D_i^4}{n}} \qquad \text{Eqn. 2}$$

where *n* is the number of vessels ($i \in [1, n]$). We also calculated the theorical specific xylem hydraulic conductivity (SXHC) using Hagen-Poiseuille equation (Tyree and Ewers, 1991) as:

$$SXHC = \frac{\pi\rho \sum_{i=1}^{n} D_i^4}{128\eta As} \qquad \text{Eqn. 3}$$

where ρ is the density of water (998.2 kg m^{-3} at 20 °C), η is the water viscosity (1.002×10^{-9} MPa s at 20 °C) and A_s is the xylem cross-sectional area.

We also determined an index of vessel inhomogeneity (VI) that can be considered as the coefficient of variation of SXHC. Because of the different sizes of vessels in the xylem, the SXHC calculated according to their diameters are also different. When the diameter of each vessel (D_m) in the xylem is the same, the calculated SXHC is the theoretical minimum value

($SXHC_m$). In the actual situation, the diameter of each vessel in the root xylem is different, so the calculated SXHC value would be larger than the $SXHC_m$ (i.e., the same diameter for each vessel). We calculated the VI index based on the relationship between the actual calculated SXHC and the $SXHC_m$. The ideal mean vessel diameter in xylem was calculated as:

$$D_m = \sqrt{\frac{4\sum_i^n \frac{\pi D_i^2}{4}}{\pi n}} \qquad \text{Eqn. 4}$$

Then, the $SXHC_m$ was calculated as:

$$SXHC_m = \frac{\pi \rho \sum D_m^4}{128 \eta As} \qquad \text{Eqn. 5}$$

Therefore, the index of vessel inhomogeneity (VI) was calculated as:

$$VI = \frac{SXHC - SXHC_m}{SXHC_m} \qquad \text{Eqn. 6}$$

Species phylogeny

We conducted phylogenetic analyses of our 20 species and confirmed species names using The Plant List (http://www.theplantlist.org/). A phylogenetic tree was constructed using the Phylomatic version 3 (Webb and Donoghue, 2005), which is based on Angiosperm Phylogeny Group Ⅲ classification of angiosperms (Fig. S1).

Statistical analysis

In this study, the minimum, maximum, mean and standard deviation were calculated at tree level for all anatomical traits and hydraulic-related variables. We also calculated Pagel's λ and Blomberg's K statistic to evaluate the strength of phylogenetic signal for each trait (Pagel 1999; Blomberg *et al*., 2003). Intra-specific variations in each anatomical trait among root order were analyzed using analysis of variance (ANOVA), by considering tree species (20

levels) and orders (5 levels) are independent qualitative variables, followed by multiple-comparison tests (i.e., Tukey's range test).

To test for multivariate correlations across root orders, vessel traits and hydraulic-related variables, principal component analysis (PCA) were performed for each species. In order to evaluate anatomical trait and hydraulic-related variable associations at interspecific level, we also performed Pearson's correlations and PCA among these traits for all orders mixed and for each root order, respectively. We conducted phylogenetic independent contrasts (PICs, Felsenstein, 1985) analyses to account for the effect of evolutionary histories among species and performed Mantel test between correlation matrices with and without PICs to determine whether correlation patterns differ when including PICs.

Linear regression analyses were used to determine the relationships between vessel traits and hydraulic-related variables for all orders mixed and for each root order, respectively. Variations of anatomical traits and hydraulic-related variables at family level in geological time and their correlations with divergence time were also determined by the linear regression analyses.

All statistical analyses were performed in R software (version 4.0.2, R Development Core Team, 2020), using ape package (Paradis *et al*., 2004) and phytools (Revell, 2012) for phylogeny analysis, vegan package (Dixon, 2003) for principal component analysis.

RESULTS

Intraspecific variations of root anatomical traits and hydraulic-related variables along root order gradient

For each of species, root anatomical traits (e.g., root tissue area, root diameter, VMA and Vd) and hydraulic-related variables (e.g., MHD and SXHC) showed great variability across root

orders (Fig. 1, Fig. S2, Table 2), while VF of most species showed no significant difference among root orders (Fig. S2). The relative area of outer tissue and cortex decreased with increasing root order in most species, while that of stele, xylem and vessel showed the opposite trend (Fig. 1). Cortex thickness decreased with the increase of root order and most of root cortex disappeared at higher root order, primarily from the fourth order (Fig. 1).

According to the PCAs over seven variables (including Vd, VMA, VF, SXHC, VI, stele : root diameter ratio and order) for each of the 20 species, the first two axes always explained more than 54% of the variability (Fig. 2). For most species, solely VF was associated with the second axis, while all the other variables were associated with the first axis. The exceptional cases occurred for *Chisocheton cumingianus*, *Dysoxylum gotadhora*, *Elaeocarpus varunua*, *Cleidion brevipetiolatum*, *Baccaurea ramiflora*, *Litsea dilleniifolia*, *Pseuduvaria trimera*, *Alphonsea monogyna* and *Knema tenuinervia*, for which VF tended to be more associated with the first axis. Vessel density (Vd) showed strong tradeoffs with all the other first-axis associated traits (i.e., VI, VMA, SXHC, stele : root diameter ratio and order). Stele : root diameter ratio and order were highly correlated with each other and both are comparable predictors of the traits along the first axis.

Interspecific variation of root anatomical traits and hydraulic-related variables along root order gradient

Linear regressions showed that SXHC was positively and significantly correlated with VF, VMA and VI, regardless of all root order pooled together or each root order separately (Fig. 3A, C, D, E, G, H, $P<0.001$). There was a significant and negative correlation between SXHC and Vd with all root order pooled together (Fig. 3B, $P<0.001$). In order 2 (i.e., the lowest root order for root vessel trait characterization), no significant correlation was found, but when root order increased, significant relationships appeared and were getting stronger (Fig. 3F,

P<0.01). There was a significant and positive correlation between VF and VMA with all root order included together (Fig. S4A, *P*<0.001). However, in order 2, no significant correlation was found but when root order increased, significant relationships appeared (Fig. S4C, *P*<0.05), despite the exception for order 5. There was a negative relationship between Vd and VMA with all root order pooled together and in each root order (Fig. S4B, D, *P*<0.001).

PCAs were also performed across species to evaluate how root vessel traits and hydraulic-related variables were associated with all root order pooled together and in each root order, respectively (Fig. S3). With all root orders pooled together across species, the PCA showed fairly similar patterns with those for each species: VMA, SXHC, Vd, VI, root order and stele : root diameter ratio were associated with the first axis (explaining 54.6% of the variation), while VF was associated with the second axis (explaining 17.8 % of the variation) (Fig. S3A). Within each root order, as the root order increased, stele : root diameter ratio transited from the second axis to the first axis and VF was always associated with the second axis. (Fig. S3B, C, D).

According to Pearson's correlations based on tree-level data, nearly all the trait correlations were significant with all the data included (Table S1): VMA, MHD and SXHC were strongly and positively correlated among themselves, but were all negatively correlated with Vd; VF was significantly and positively correlated with all above traits, but in a much weaker manner. Root order was strongly and positively correlated with root diameter (r=0.62), stele diameter (r=0.68), stele : root diameter ratio (r=0.76), VF (r=0.23), VMA (r=0.56), MHD (r=0.67), SXHC (r=0.51), VI (r=0.56) but was strongly and negatively with Vd (r=-0.56) and cortex thickness : root radius (r=-0.75) (Table S1). According to Pearson's correlations based on species-level data, VMA, MHD and SXHC were strongly and positively correlated among themselves for both the averaged metrics of all the orders (Table S2) and each order (Tables

S3-S6). Vessel density were usually negatively correlated with VMA, MHD and SXHC. VF had a positive correlation with SXHC, but had no correlations with VMA and MHD in most cases (Tables S2-S6).

According to linear regressions over tree-level data, all relationships between vessel traits and stele: root diameter ratio were significant when all the orders were mixed (Fig. 4A, B, C and D). However, once regressions were performed within each root order, all the relationships turned to be very poor (R^2 <0.12) and the tendencies were different, even opposite from those achieved when the orders were mixed (Fig. 4B versus Fig. 4F). With increasing stele: root diameter ratio, VF and Vd show almost no tendencies for each order, while VMA and SXHC increased significantly in roots of order 4 and 5, but not in lower order roots.

Phylogenetic variations in root anatomical traits and hydraulic-related variables along root order gradient

Phylogenetically independent contrasts showed that the patterns of correlations among root traits were generally conserved (Tables S2-S6). The matrices of Pearson correlations between root traits (n=20) determined with and without PICs were similar (R_{Mantel}=0.91, 0.91, 0.93, 0.85, 0.93; P<0.001), regardless of all root order pooled together or each root order separately. In addition, the traits including root diameter, epidermis thickness, cortex thickness, stele diameter and Vd displayed a clear phylogenetic signal (Pagel's λ and Blomberg's K value in Table 2).

DISSCUSION

Intraspecific variations and associations of root vessel traits and hydraulic conductivity among root orders

We found strong intraspecific variations of most studied traits across root orders. With increasing root orders, root diameter, stele diameter and stele: root ratio increased, but cortex thickness: root radius ratio decreased. These patterns are well consistent with our expectation (H1A) and with previous findings such as Guo *et al*. (2008b), Gu *et al*. (2014) and Mao *et al*. (2018). In addition, cortex is responsible for resource absorption, while the stele is served for resource transportation (Guo *et al.*, 2008b; Kong *et al.*, 2017). All these above findings support the existence of a functional shift from absorption to transport with increasing root order. In literature, the stronger transport ability in higher-order roots has been largely discussed for carbon and nutrient (McCormark *et al*. 2015). Here, with a series of vessel traits, we further confirm that this tendency is also valid for hydraulic functions, as we found strong increase in SXHC, VMA, MHD and VI with increasing root order (Fig. S2). Our result is consistence with Long *et al*. (2013), i.e., one of the very rare studies characterizing vessel size along root order for five tree species.

Interestingly, we found no relationship between vessel fraction and order for the great majority of tree species, thus rejecting our hypothesis H1B. This is due to the fact that both vessel (hollow) and non-vessel (solid) areas in xylem increased with order for most species (Fig. 1), rendering vessel fraction relatively stable. High-order roots (i.e., the 4^{th}- and 5^{th} orders) play a key mechanical role in stem stability and such a role is largely contributed by stele size (Mao *et al*., 2018). Higher vessel fraction signifies a higher capacity for axial water transport (Zanne *et al*., 2010), but can reduce its mechanical robustness due to the lower fraction of the support tissue (Jacobsen and Ewers, 2005; Scholz *et al*., 2013). As xylem takes a major portion of stele (usually >50%), with increasing order, keeping a relatively stable vessel fraction by increasing in both vessel and non-vessel areas is a “smart” option for trees to maintain both water transport and mechanical support.

With increasing root order, we found a net decrease in vessel density, indicating its strong and negative correlations with VMA and SXHC for every species (Fig. 2. Table S2). In literature, such a pattern has only been reported at interspecific level for stem and coarse roots, and was then interpreted as the existence of trade-off between hydraulic efficiency and hydraulic safety (Loepfe *et al.*, 2007; Sperry *et al.*, 2008). In general, species of larger the vessel sizes tend to show higher hydraulic efficiency, but more vulnerability to embolism (Pockman and Sperry, 2000; Martínez-Vilalta *et al.*, 2002). Similarly, species with many small vessels to reduce the risk of vessel cavitation and embolization (Poorter *et al.*, 2010). Provided such a hypothesis could to be extended to roots of different orders within a species, our results tend to suggest that higher order roots have higher hydraulic efficiency but lower hydraulic safety. While it is generally recognized that hydraulic efficiency can be measured by SXHC, hydraulic safety is more proxied by P_{50} rather than vessel density according to studies on stems or coarse roots (Sande *et al.*, 2019; Sanchez-Martinez *et al.*, 2020). So far, P_{50} is rarely measured for thin and distal roots due to technical barriers. Further data based controlled laboratory condition may be needed to confirm such an assumption.

The positive relationship among SXHC, VMA, and order and the negative relationship between all these traits and Vd were stable and non-exceptionally associated with the first axis of PCA for every species. Such pattern seems to be generalizable for a wide range of species and be more intrinsically related based on physical laws (e.g., larger vessel size tends to allow high water transport according to the Hagen-Poiseuille law) or allometry (e.g., higher root diameter tends to have higher vessel size). Yet, the coordination between vessel fraction and those above first axis traits were fairly diverse among species, suggesting the high specialized nature of vessel fraction depending on species. The exception of vessel fraction enables us to reject our hypothesis H1C.

Interspecific variations and associations of root vessel traits and hydraulic conductivity among root orders

Considering or not root orders could greatly change the interpretation of interspecific relationships among vessel traits (Fig. 3) or between vessel traits and stele: root diameter ratio (Fig. 4). For example, for the relationships of SXHC versus vessel density (Fig. 3B and 3E), vessel density versus stele: root diameter (Fig. 4B and 4F) and SXHC versus stele: root diameter ratio (Fig. 4D and 4H), provided that root orders were not considered, contrasted, even opposite diagnostics on the relationship among the traits would have been drawn. Therefore, our results validated our hypothesis H2A and highlight the primary importance of considering root order when exploring in interspecific variations of the traits related to hydraulic conductivity.

Partially against our expectation H2B, we found that in low-order roots (orders 2 and 3), the intraspecific relationship between certain traits, such as SXHC versus vessel mean area (Fig. 3C and 3G) could be as strong as in high-order roots. According to the Hagen-Poiseuille law, the hydraulic conductivity increases with the fourth power of the vessel diameter (Tyree and Ewers, 1991). Therefore, among the vessel traits we measured, vessel size is the most important trait that affect root SXHC and, accordingly, whether in low-order root or high-order root level, vessel mean area always showed a very high correlation with root SXHC.

Vessel fraction should theoretically affect the variation of root SXHC. Higher vessel fraction means that there is less space in xylem tissues outside the vessel and more vessel volume for water transportation, thus can potentially enhance hydraulic capacitance (Zanne *et al.*, 2010). Moreover, higher proportion of vessel area in xylem cross-section area should lead to greater inter-vessel connectivity (Pratt *et al.*, 2007) which should increase overall conductivity as larger vessel area enables a larger sap flow (Poorter *et al.*, 2010), although it may lead to a

higher risk of being embolized in vessels (Loepfe *et al.*, 2007). Indeed, we always found positive relationships of SXHC versus vessel fraction among species for roots of all the orders mixed and of each root order (Fig. 3A and 3E). Nevertheless, we found that vessel fraction played an increasingly important role (represented by increasing slope) with increasing root order (Fig. 3E), thereby partially supporting our expectation H2B. For the 2nd-order roots, SXHC was ubiquitously low for all the species because of the small proportion of stele area; while for the 5th-order roots, high SXHC requires high vessel mean area to maintain, then vessel fraction is bound to increase accordingly to satisfy such a need. Among the vessel traits, vessel fraction is the most overlooked one and relatively less characterized in previous studies (see Wang *et al*. 2016; Zhou *et al*.2020). Our study underlines the mechanistic importance of vessel fraction in contribution to SXHC in fine roots. In addition, we also found a significant correlation between SXHC and VI, which might mean that the greater the vessel variability, the higher the water conduction efficiency of the xylem, which needs to be clarified in further studies. The relationships between vessel density and SXHC seemed to be loose, although they also depended on root order (Fig. 3F). The possible explanation is that SXHC is more directly linked with vessel mean area rather than vessel density, whose variation among different root orders is simply a consequence of increasing vessel mean area.

When performing PCA analysis on all root vessel traits plus stele: root diameter across species based on roots of all orders mixed together and of each root order, we found that the pattern of trait coordination was largely fixed, but clearly moderated by root order (Fig. S3). On the one hand, regardless root orders, strong associations always occurred between SXHC and VMA due to the Hagen-Poiseuille law and strong oppositions always occurred between VMA and Vd, representing different strategies among species (favoring hydraulic efficiency versus favoring hydraulic safety). On the other hand, with increasing root order, stele : root diameter ratio shifted from the second axis (i.e., 2nd and 3rd order; Fig. S3B and S3C) to the

first axis (i.e., 4th and 5th order; Fig. S3D and S3E), showing, again, the key role of root order in elucidating interspecific variations of traits. Root order is served as a good proxy to distinguish root functional type (transport versus absorptive), but it remains unclear whether 2nd- or 3rd-order roots should be served as the threshold. 3rd-order roots were sometimes considered as absorptive roots (McCormack *et al*. 2015). Based on vessel traits, the difference between 2nd-order roots and 3rd-order roots observed in this study tends to support the use of 2nd-order roots as a conservative threshold to differentiate absorptive and transport roots.

The relationships between vessel mean area or SXHC and stele: root diameter ratio, were unclear or very weak in lower order roots (orders 2 and 3) than in higher order roots (orders 4 and 5). Therefore, such root order-dependent correlation patterns enable us to partially reject our hypothesis H2D. This phenomenon may simply be due to the fact that mechanical support and axial hydraulic conductivity are marginalized functions in lower-order roots that are more responsible for nutrient and water uptake and radial transport. For high-order roots (orders 4 and 5), species with higher stele: root diameter (i.e., a higher mechanical robustness) showed higher VMA and SXHC (i.e., a higher capacity for axial hydraulic conductivity). This suggests that the two major functions in transport roots are in strong synergy rather than trade-off.

We also expected a positive relationship between vessel fraction and stele: root diameter ratio (H2D), because species with higher vessel fraction may have higher capacity for axial hydraulic conductivity, but a lower mechanical robustness and the latter may be compensated by a higher stele: root diameter ratio. The observed relationships only weakly support this, as positive tendencies could only be found for the cases of all root orders mixed together (Fig. 4A, significant slope) and each root order (Fig. 4E, but significant slope only for order 3). For the 2nd, 4th and 5th- order roots, the slopes of the relationships were not significant, implying

the existence of strong disparity of root mechanical robustness among species. To test their how root mechanics and hydraulics covary among species, more direct metrics on root mechanical robustness, such as tensile strength, modulus of elasticity and tensile strain, should be characterized.

Evolutionary patterns of root anatomical traits and hydraulics among root orders

In order to estimate patterns of root anatomical trait evolution during species radiation in geological time, we performed phylogenetic analysis to root traits of extent species of different origins. Our results showed root morphology traits did not exhibit a strong phylogenetic signal which were consistent with the findings of previous studies (Chen *et al.*, 2013; Gu *et al.*, 2014; Ma *et al.*, 2018). Comas *et al*. (2012) and Chen *et al*. (2013) suggested that evolutionary trends of root morphology traits may be linked to long-term environmental and climatic changes in geological time. The diversity of root traits of angiosperms is an adaptation to the appearance of cold and dry climates in the Late Cretaceous (Comas *et al.*, 2012; Chen *et al.*, 2013). Moreover, the fact that epidermis and cortex are both located at a root's external part that are susceptible to environmental and climatic changes. Additionally, our study showed that except for vessel density, none of the other vessel traits showed strong phylogenetic signal according to the Pagel's λ and Blomberg's K value (Table 2), suggesting the general weak evolution. One possible reason may be that vessel is located in the xylem in root stele that is surrounded by cortex. The cortex could act as a buffer zone to prevent root stele from being affected by environmental stresses (Lux *et al.*, 2004) such as drought (Kondo *et al.*, 2000). In this case, vessel traits in root stele tend to be less sensitive to environmental changes and this could also explain why there was no significant correlation between root stele diameter and divergence time. Another potential reason may be that water is not the limiting factor of tree growth in our study as the tree species we studied are from tropical

regions with stable and sufficient water and heat conditions (Walker, 1986; Gu *et al*., 2008). Meanwhile, Carlquist and Hoekman (1985) also indicated that vessel density changes more rapidly or is more evolutionarily labile than other vessel traits which may be the reason for the strong phylogenetic signal of vessel density.

Given the generally weak effect of evolutionary history on root vessel traits, it is not surprising that relationships among root anatomical traits were found to be similar with and without phylogenetic independence contrasts analysis. This suggests that there seems to be no effect of species evolutionary trends on the correlation patterns among these root traits and indicated that the detected patterns reflect coordinated evolution regardless of all root order mixed together or each root order separately.

CONCLUSIONS

This present work is one of the first study to focus on changes and associations of root vessel traits and hydraulic-related variables among root orders. By quantifying a series of root morphological and anatomical traits, especially vessel traits, along five root orders for 20 Chinese tropical tree species, we demonstrated the patterns of trait variation, covariation and evolution. While we highlighted the primary importance of root order in explaining intra- and interspecific variations of the traits related to root hydraulic conductivity, we found that the traits as well as their covariation respond differently to root orders. At intraspecific level, with increasing root orders, root specific xylem hydraulic conductivity (SXHC), vessel mean diameter, and vessel inhomogeneity increased and vessel density decreased, while vessel fraction showed complex patterns depending on species (Fig. 5). At interspecific level, while the relationships between SXHC and vessel mean diameter were consistent among roots orders, those between SXHC and vessel fraction or between SXHC and vessel density exhibited contrasted patterns among roots orders. Our results support the existence of trade-

off between hydraulic efficiency and hydraulic safety at both intra- and interspecific levels. Regarding the relationships between vessel traits and stele : root diameter ratio (i.e., a proxy of root mechanical robustness), no or weak correlations were found for low order roots (2nd- and 3rd orders), but positive correlations for SXHC for high order roots (4th- and 5th orders). This suggests a synergy between root mechanical and hydraulic robustness at both intra- and interspecific levels for transport roots. Finally, we further pointed out that root vessel traits are different from root morphological traits, which are poorly affected by phylogeny and correlation patterns among root traits seem to be not affected by evolutionary history.

ACKNOWLEDGEMENTS

This study was financed by the project INIESTA, which is an open-founding of CAS Key Laboratory of Tropical Forest Ecology, Xishuangbanna Tropical Botanical Garden, Chinese Academy of Sciences. The study was also co-financed by a French-Chinese Xuguangqi program from Campus France (2019) that sponsored GZ, CF, ZM's visit to XTBG for academic exchanges in 2019 for conceiving this work. This study was supported by China Scholarship Council (PhD bursary for GZ). We are grateful to Mr. Xiaobao Deng, Mr. Hui Chen, Mr. Shengdong Yuan and all the staffs of Bubeng Ecological Station, Xishuangbanna, Chinese Academy of Sciences for their support with regard to the field sampling authorization or the use of the laboratory devices. Finally, we thank Mr. Defu Chen, Ms. Xiaoling Chen, Mr. Anjana J. Atapattu, Mr. Nuttaporn Luyprasert, Mr. Xiong Ma, Mr. Hongyun Sun, Mr. Jiangchao Yuan for field and laboratory work.

REFERENCES

Blomberg SP, Garland T, Ives AR. 2003. Testing for phylogenetic signal in comparative data: behavioral traits are more labile. *Evolution* **57**: 717–745.

Cao M, Zou X, Warren M, Zhu H. 2006. Tropical forests of Xishuangbanna, China. *Biotropica* **38**: 306–309.

Carlquist S, Hoekman DA. 1985. Ecological wood anatomy of the woody southern Californian flora. *IAWA Journal* **6**: 319–347.

Chen W, Zeng H, Eissenstat DM, Guo D. 2013. Variation of first-order root traits across climatic gradients and evolutionary trends in geological time. *Global Ecology and Biogeography* **22**: 846–856.

Chimungu, J. G., K. W. Loades, and J. P. Lynch. 2015. Root anatomical phenes predict root penetration ability and biomechanical properties in maize (Zea Mays). *Journal of Experimental Botany* **66**: 3151–3162.

Comas LH, Mueller KE, Taylor LL, Midford PE, Callahan HS, Beerling DJ. 2012. Evolutionary patterns and biogeochemical significance of angiosperm root traits. *International Journal of Plant Sciences* **173**: 584–595.

Cuneo, I. F., T. Knipfer, C. R. Brodersen, and A. J. McElrone. 2016. Mechanical failure of fine root cortical cells initiates plant hydraulic decline during drought. *Plant Physiology* 172: 1669–1678.

Dixon P. 2003. VEGAN, a package of R functions for community ecology. *Journal of Vegetation Science* **14**: 927–930.

Eissenstat, D. M. 1997. Trade-offs in root form and function. In: Jackson LE, ed. *Ecology in agriculture*. San Diego, Academic Press, 173–199.

Esau K. 1960. Anatomy of seed plants, *Soil Science* **90**:149.

Fan P, Guo D. 2010. Slow decomposition of lower order roots: a key mechanism of root carbon and nutrient retention in the soil. *Oecologia* **163**: 509–515.

Felsenstein J. 1985. Phylogenies and the comparative method. *The American Naturalist* **125**: 1–15.

Fitter AH. 1987. An architectural approach to the comparative ecology of plant root systems. *New Phytologist* **106**: 61–77.

Fortunel C, Ruelle J, Beauchêne J, Fine PVA, Baraloto C. 2014. Wood specific gravity and anatomy of branches and roots in 113 Amazonian rainforest tree species across environmental gradients. *New Phytologist* **202**: 79–94.

Freschet, G. T., L. Pagès, C. M. Iversen, L. H. Comas, B. Rewald, C. Roumet, J. Klimešová, et al. 2021. A starting guide to root ecology: strengthening ecological concepts and standardising root classification, sampling, processing and trait measurements. *New Phytologist* **232**: 973–1122.

Gu J, Xu Y, Dong X, Wang H, Wang Z. 2014. Root diameter variations explained by anatomy and phylogeny of 50 tropical and temperate tree species. *Tree Physiology* **34**: 415–425.

Gu Y, Pearsall DM, Xie S, Yu J. 2008. Vegetation and fire history of a Chinese site in southern tropical Xishuangbanna derived from phytolith and charcoal records from Holocene sediments. *Journal of Biogeography* **35**: 325–341.

Guo DL, Mitchell RJ, Hendricks JJ. 2004. Fine root branch orders respond differentially to carbon source-sink manipulations in a longleaf pine forest. *Oecologia* **140**: 450–457.

Guo D, Mitchell RJ, Withington JM, Fan PP, Hendricks JJ. 2008a. Endogenous and exogenous controls of root life span, mortality and nitrogen flux in a longleaf pine forest: root branch order predominates. *Journal of Ecology* **96**: 737–745.

Guo D, Xia M, Wei X, Chang W, Liu Y, Wang Z. 2008b. Anatomical traits associated with absorption and mycorrhizal colonization are linked to root branch order in twenty-three Chinese temperate tree species. *New Phytologist* **180**: 673–683.

Hacke UG, Sperry JS, Wheeler JK, Castro L. 2006. Scaling of angiosperm xylem structure with safety and efficiency. *Tree Physiology* **26**: 689–701.

Huang B, Eissenstat DM. 2000. Linking hydraulic conductivity to anatomy in plants that vary in specific root length. *Journal of the American Society for Horticultural Science* **125**: 260–264.

Jacobsen, A. L., F. W. Ewers, R. B. Pratt, W. A. Paddock III, and S. D. Davis. 2005. Do xylem fibers affect vessel cavitation resistance? *Plant Physiology* **139**: 546–556.

Kondo M, Aguilar A, Abe J, Morita S. 2000. Anatomy of nodal roots in tropical upland and lowland rice varieties. *Plant Production Science* **3**: 437–445.

Kong D, Wang J, Zeng H, Liu M, Miao Y, Wu H, Kardol P. 2017. The nutrient absorption–transportation hypothesis: optimizing structural traits in absorptive roots. *New Phytologist* **213**: 1569–1572.

Lewis AM. 1992. Measuring the hydraulic diameter of a pore or conduit. *American Journal of Botany* **79**: 1158–1161.

Liu W, Meng F-R, Zhang Y, Liu Y, Li H. 2004. Water input from fog drip in the tropical seasonal rain forest of Xishuangbanna, South-west China. *Journal of Tropical Ecology* **20**: 517–524.

Loepfe L, Martinez-Vilalta J, Piñol J, Mencuccini M. 2007. The relevance of xylem network structure for plant hydraulic efficiency and safety. *Journal of Theoretical Biology* **247**: 788–803.

Long Y, Kong D, Chen Z, Zeng H. 2013. Variation of the linkage of root function with root branch order. *PloS one* **8**: e57153.

Lux A, Luxová M, Abe J, Morita S. 2004. Root cortex: structural and functional variability and responses to environmental stress. *Root Research* **13**: 117–131.

Ma Z, Guo D, Xu X, Lu M, Bardgett RD, Eissenstat DM, McCormack ML, Hedin LO. 2018. Evolutionary history resolves global organization of root functional traits. *Nature* **555**: 94–97.

Maherali H, Pockman WT, Jackson RB. 2004. Adaptive variation in the vulnerability of woody plants to xylem cavitation. *Ecology* **85**: 2184–2199.

Mao Z, Wang Y, McCormack ML, Rowe N, Deng X, Yang X, Xia S, Nespoulous J, Sidle RC, Guo D, *et al.* 2018. Mechanical traits of fine roots as a function of topology and anatomy. *Annals of Botany* **122**: 1103–1116.

Martínez-Vilalta J, Prat E, Oliveras I, Piñol J. 2002. Xylem hydraulic properties of roots and stems of nine Mediterranean woody species. *Oecologia* **133**: 19–29.

Martínez-Vilalta J, Mencuccini M, Álvarez X, Camacho J, Loepfe L, Piñol J. 2012. Spatial distribution and packing of xylem conduits. *American Journal of Botany* **99**: 1189–1196.

McCormack ML, Dickie IA, Eissenstat DM, Fahey TJ, Fernandez CW, Guo D, Helmisaari H-S, Hobbie EA, Iversen CM, Jackson RB, *et al.* 2015. Redefining fine roots improves understanding of below-ground contributions to terrestrial biosphere processes. *New Phytologist* **207**: 505–518.

Oliveras I, Martínez-Vilalta J, Jimenez-Ortiz T, Lledó MJ, Escarré A, Piñol J. 2003. Hydraulic properties of *Pinus halepensis*, *Pinus pinea* and *Tetraclinis articulata* in a dune ecosystem of Eastern Spain. *Plant Ecology* **169**: 131–141.

Ouimette A, Guo D, Hobbie E, Gu J. 2013. Insights into root growth, function, and mycorrhizal abundance from chemical and isotopic data across root orders. *Plant and Soil* **367**: 313–326.

Pagel M. 1999. Inferring the historical patterns of biological evolution. *Nature* **401**: 877–884.

Paradis E, Claude J, Strimmer K. 2004. APE: Analyses of phylogenetics and evolution in R language. *Bioinformatics* **20**: 289–290.

Passioura JB. 1988. Water transport in and to roots. *Annual Review of Plant Physiology and Plant Molecular Biology* **39**: 245–265.

Pockman WT, Sperry JS. 2000. Vulnerability to xylem cavitation and the distribution of Sonoran Desert vegetation. *American Journal of Botany* **87**: 1287–1299.

Poorter L, McDonald I, Alarcón A, Fichtler E, Licona J-C, Peña-Claros M, Sterck F, Villegas Z, Sass-Klaassen U. 2010. The importance of wood traits and hydraulic conductance for the performance and life history strategies of 42 rainforest tree species. *New Phytologist* **185**: 481–492.

Pratt RB, Jacobsen AL, Ewers FW, Davis SD. 2007. Relationships among xylem transport, biomechanics and storage in stems and roots of nine Rhamnaceae species of the California chaparral. *New Phytologist* **174**: 787–798.

Pregitzer KS, DeForest JL, Burton AJ, Allen MF, Ruess RW, Hendrick RL. 2002. Fine root architecture of nine North American trees. *Ecological Monographs* **72**: 293–309.

R Core Team. 2020. R: A language and environment for statistical computing. R Foundation for Statistical Computing, Vienna, Austria. URL https://www.R-project.org/.

Raven JA, Edwards D. 2001. Roots: evolutionary origins and biogeochemical significance. *Journal of Experimental Botany* **52**: 381–401.

Revell LJ. 2012. phytools: an R package for phylogenetic comparative biology (and other things). *Methods in ecology and evolution* **3**: 217–223.

Rieger M, Litvin P. 1999. Root system hydraulic conductivity in species with contrasting root anatomy. *Journal of Experimental Botany* **50**: 201–209.

Rodríguez-Gamir J, Intrigliolo DS, Primo-Millo E, Forner-Giner MA. 2010. Relationships between xylem anatomy, root hydraulic conductivity, leaf/root ratio and transpiration in citrus trees on different rootstocks. *Physiologia plantarum* **139**: 159–169.

Sanchez-Martinez P, Martínez-Vilalta J, Dexter KG, Segovia RA, Mencuccini M. 2020. Adaptation and coordinated evolution of plant hydraulic traits. *Ecology Letters* **23**: 1599–1610.

Sande MT van der, Poorter L, Schnitzer SA, Engelbrecht BMJ, Markesteijn L. 2019. The hydraulic efficiency–safety trade-off differs between lianas and trees. *Ecology* **100**: e02666.

Schuldt B, Leuschner C, Brock N, Horna V. 2013. Changes in wood density, wood anatomy and hydraulic properties of the xylem along the root-to-shoot flow path in tropical rainforest trees. *Tree Physiology* **33**: 161–174.

Scholz A, Klepsch M, Karimi Z, Jansen S. 2013. How to quantify conduits in wood? *Frontiers in Plant Science* **4**: 56.

Sperry JS, Meinzer FC, McCULLOH KA. 2008. Safety and efficiency conflicts in hydraulic architecture: scaling from tissues to trees. *Plant, Cell & Environment* **31**: 632–645.

Steudle, E., and C. A. Peterson. 1998. How does water get through roots? *Journal of Experimental Botany* **49**: 775–788.

Tyree MT, Ewers FW. 1991. The hydraulic architecture of trees and other woody plants. *New Phytologist* **119**: 345–360.

Wang Y, Dong X, Wang H, Wang Z, Gu J. 2016. Root tip morphology, anatomy, chemistry and potential hydraulic conductivity vary with soil depth in three temperate hardwood species. *Tree physiology*, **36**: 99–108.

Walker D. 1986. Late pleistocene-early Holocene vegetational and climatic changes in Yunnan Province, Southwest China. *Journal of Biogeography* **13**: 477–486.

Webb CO, Donoghue MJ. 2005. Phylomatic: tree assembly for applied phylogenetics. *Molecular Ecology Notes* **5**: 181–183.

Wheeler JK, Sperry JS, Hacke UG, Hoang N. 2005. Inter-vessel pitting and cavitation in woody Rosaceae and other vesselled plants: a basis for a safety versus efficiency trade-off in xylem transport. *Plant, Cell & Environment* **28**: 800–812.

Wikström N, Savolainen V, Chase MW. 2001. Evolution of the angiosperms: calibrating the family tree. *Proceedings of the Royal Society of London. Series B: Biological Sciences* **268**: 2211–2220.

Xiong Y, Fan P, Fu S, Zeng H, Guo D. 2013. Slow decomposition and limited nitrogen release by lower order roots in eight Chinese temperate and subtropical trees. *Plant and Soil* **363**: 19–31.

Zanne AE, Westoby M, Falster DS, Ackerly DD, Loarie SR, Arnold SEJ, Coomes DA. 2010. Angiosperm wood structure: Global patterns in vessel anatomy and their relation to wood density and potential conductivity. *American Journal of Botany* **97**: 207–215.

Zhou M, Wenming B, Li Q, Guo Y, Zhang WH. 2020. Root anatomical traits determined leaf-level physiology and responses to precipitation change of herbaceous species in a temperate steppe. *New Phytologist* **229**: 1484–1491.

TABLES

Table 1 List of 20 focal species.

Species name	Abbreviation	Family
Parashorea chinensis Hsie Wang (望天树)	Pach	Dipterocarpaceae
Ficus langkokensis Drake (青藤公)	Fila	Moraceae
Ficus auriculata Lour. (大果榕)	Fiau	Moraceae
Chisocheton cumingianus (C.DC.) Harms (溪桫)	Chcu	Meliaceae
Dysoxylum gotadhora (Buch.-Ham.) Mabb. (红果樫木)	Dygo	Meliaceae
Garcinia cowa Roxb. Ex Choisy (云树)	Gaco	Clusiaceae
Garcinia lancilimba C.Y.Wu ex Y.H.Li (长裂藤黄)	Gala	Clusiaceae
Elaeocarpus varunua Buch.-Ham. Ex Mast. (美脉杜英)	Elva	Elaeocarpaceae
Castanopsis hystrix Hook. f. & Thomson ex A. DC. (红锥)	Cahy	Fagaceae
Cleidion brevipetiolatum Pax & K.Hoffm. (棒柄花)	Clbr	Euphorbiaceae
Trigonostemon thyrsoideus Stapf (长梗三宝木)	Trth	Euphorbiaceae
Baccaurea ramiflora Lour. (木奶果)	Bara	Phyllanthaceae
Diospyros nigrocortex C.Y.Wu (黑皮柿)	Dini	Ebenaceae
Litsea verticillata Hance (轮叶木姜子)	Live	Lauraceae
Litsea dilleniifolia P.Y. Pai & P.H. Huang (五桠果叶木姜子)	Lidi	Lauraceae
Pseuduvaria trimera (W. G. Craib) Y.C.F. Su & R.M.K. Saunders (金钩花)	Pstr	Annonaceae
Alphonsea monogyna Merr. & Chun (藤春)	Almo	Annonaceae
Pittosporopsis kerrii Craib (假海桐)	Pike	Icacinaceae
Knema tenuinervia W.J. de Wilde (红光树)	Knte	Myristicaceae
Myristica yunnanensis Y.H. Li (云南肉豆蔻)	Myyu	Myristicaceae

Table 2 List of 11 studied root anatomical traits.

Traits	Abbreviation	Unit	Minimum	Maximum	Mean	Standard deviation	Bomberg's K	Pagel's λ
Vessel fraction	VF	-	0.0167	0.2980	0.1253	0.0570	0.19	<0.001
Vessel density	Vd	n mm^{-2}	15.708	3691.261	380.594	431.423	**0.27**	0.56
Vessel mean area	VMA	um^2	46.70	5608.80	791.18	943.04	0.13	<0.001
Mean hydraulic diameter	MHD	um	7.728	97.743	29.249	16.847	0.14	<0.001
Specific xylem hydraulic conductivity	SXHC	kg m^{-1} MPa^{-1} s^{-1}	0.0501	76.3000	5.9204	9.1276	0.13	<0.001
Vessel inhomogeneity	VI	-	0.0026	1.2283	0.3033	0.2183	0.17	0.34
Root diameter	RD	um	130.01	4742.31	1088.50	848.16	**0.32**	0.51
Cortex thickness	CT	um	0.00	730.42	150.75	134.40	**0.24**	0.36
Stele diameter	SD	um	35.75	4312.70	638.39	722.97	**0.27**	0.38
Stele : root diameter ratio	S-R	-	0.122	0.932	0.511	0.217	**0.30**	0.74
Cortex thickness : root radius ratio	C-R	-	0.00	0.746	0.355	0.237	**0.35**	0.81

Note: Trait abbreviation, unit, maximum, minimum, mean and standard deviation are indicated. Significant phylogenetic signal (Blomberg's K value) is indicated in bold ($P < 0.05$); a large (close to the upper bound of 1.0) Pagel's λ value indicates high phylogenetic conservatism.

FIGURES

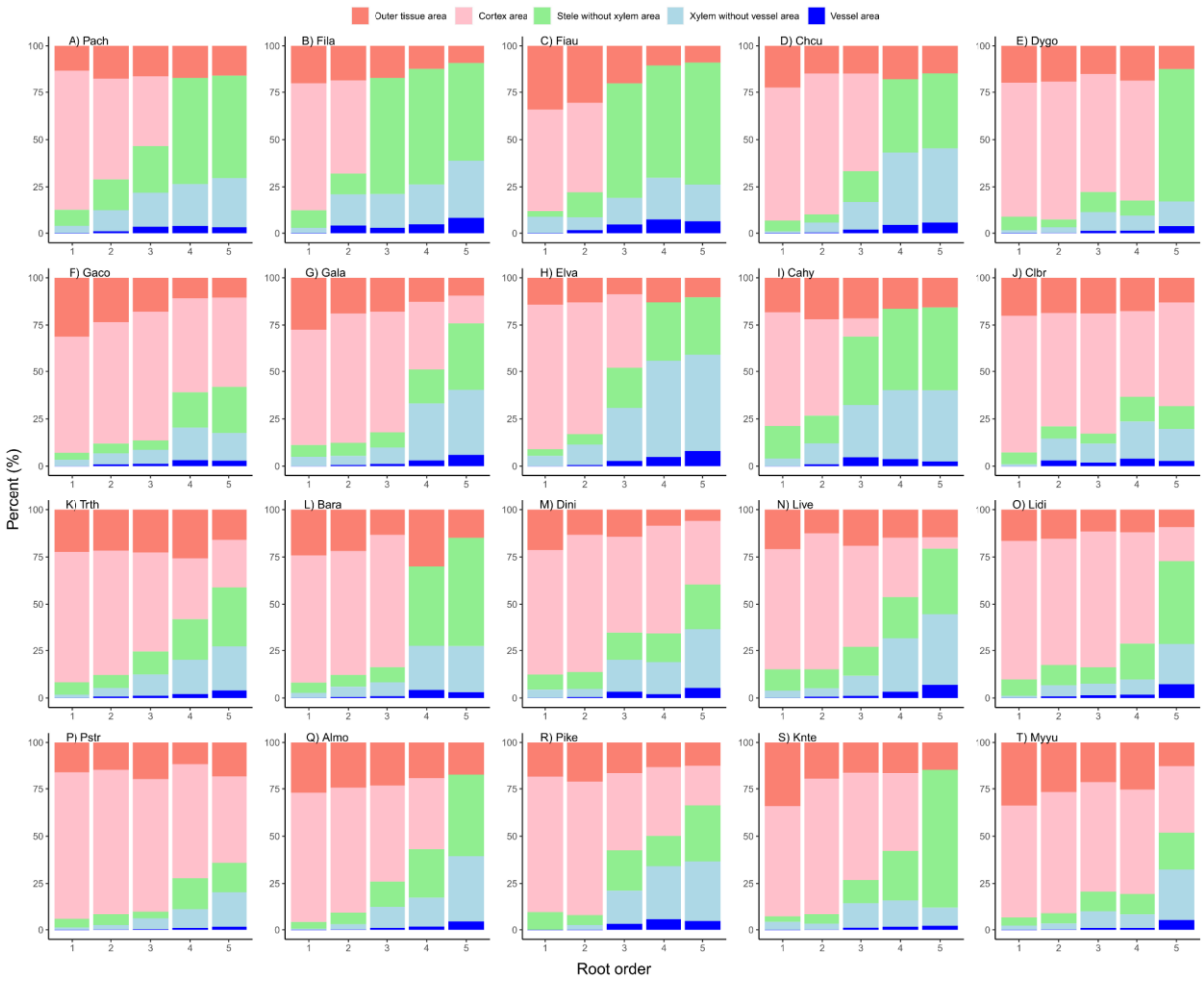

Fig. 1 Percentage of tissue area in different root topological orders in 20 Chinese tropical tree species. See Table 1 for species abbreviations.

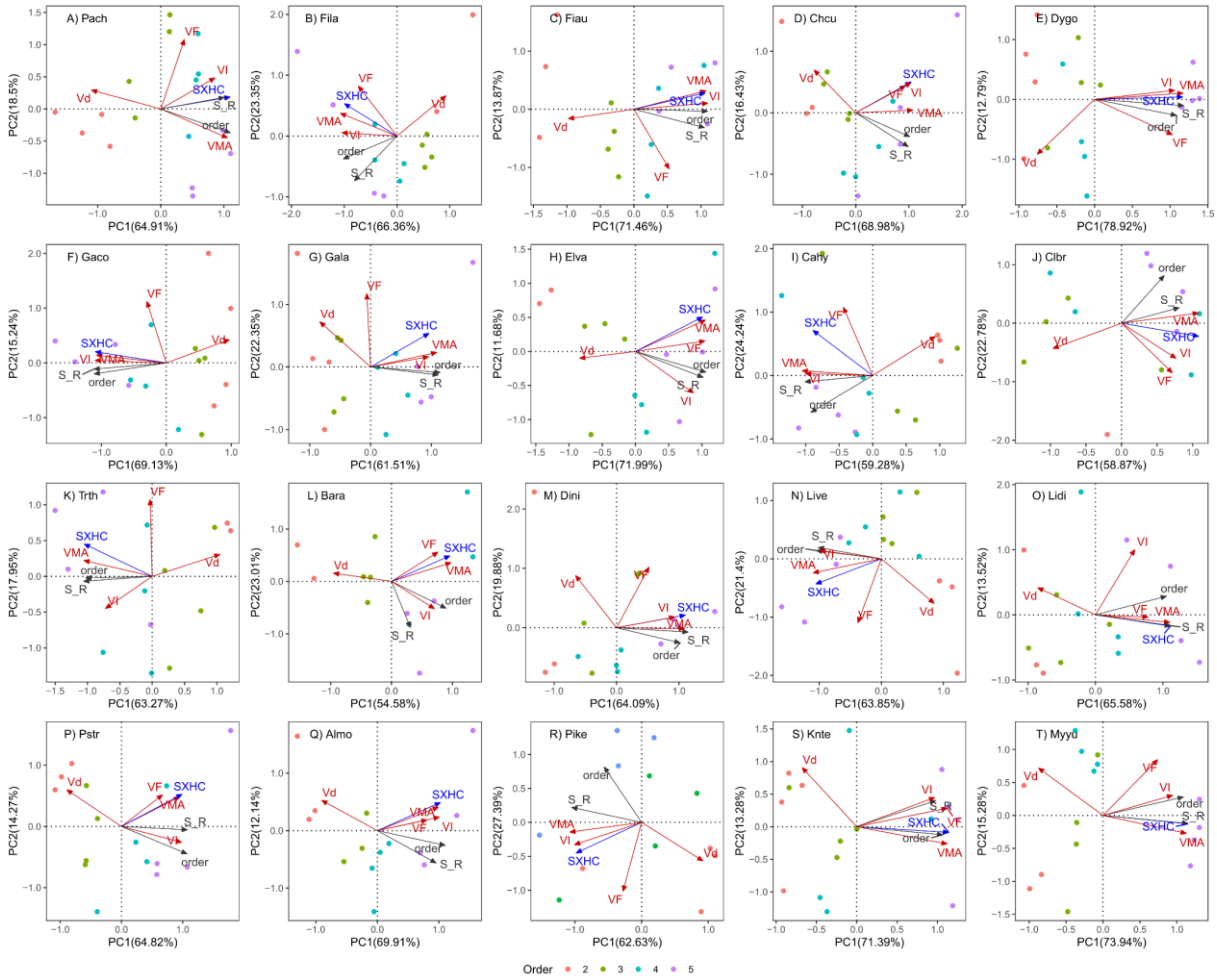

Fig. 2 Principal components analysis (PCA) on root orders and vessels traits in 20 Chinese tropical tree species. See Tables 1 and 2 for species and trait abbreviations, respectively. Colored points represent different root orders: red – 2nd order; green – 3rd order; light blue – 4th order; purple – 5th order. Color of arrows: red – vessel traits; blue – variable calculated from vessel traits, grey – morphological or architectural trait.

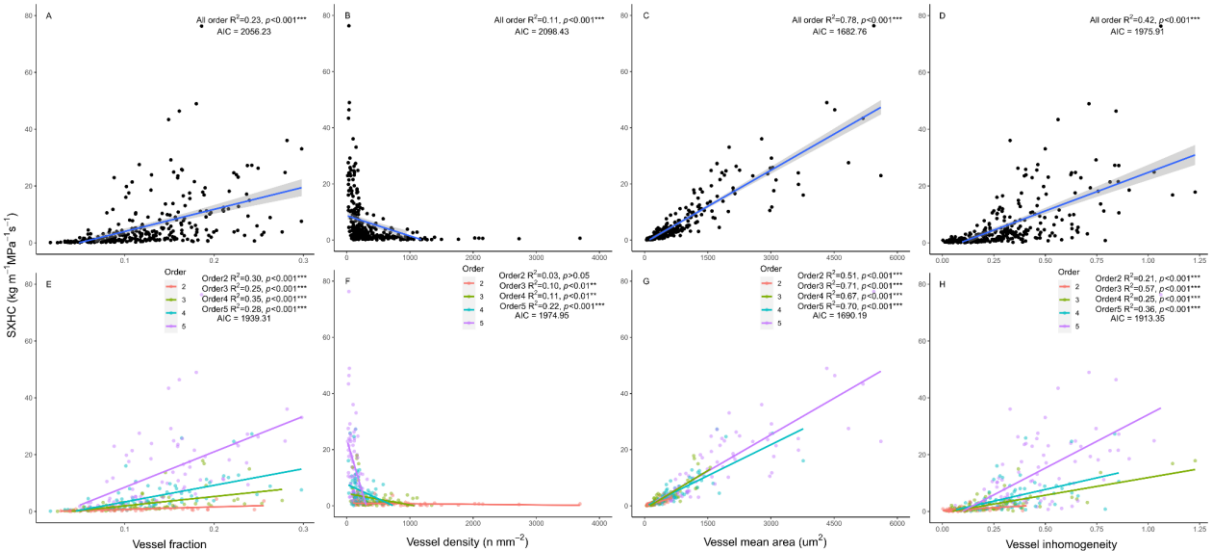

Fig. 3 Interspecific relationships between specific xylem hydraulic conductivity (SXHC) and vessel fraction (A, E), vessel density (B, F), vessel mean area (C, G) and vessel inhomogeneity (D, H), across all root orders mixed together (A, B, C and D) or by root order (E, F, G and H). AIC stands for model evaluation without (A, B, C and D) and with (E, F, G and H) the effect of root order, respectively. Colored dots represent different root orders.

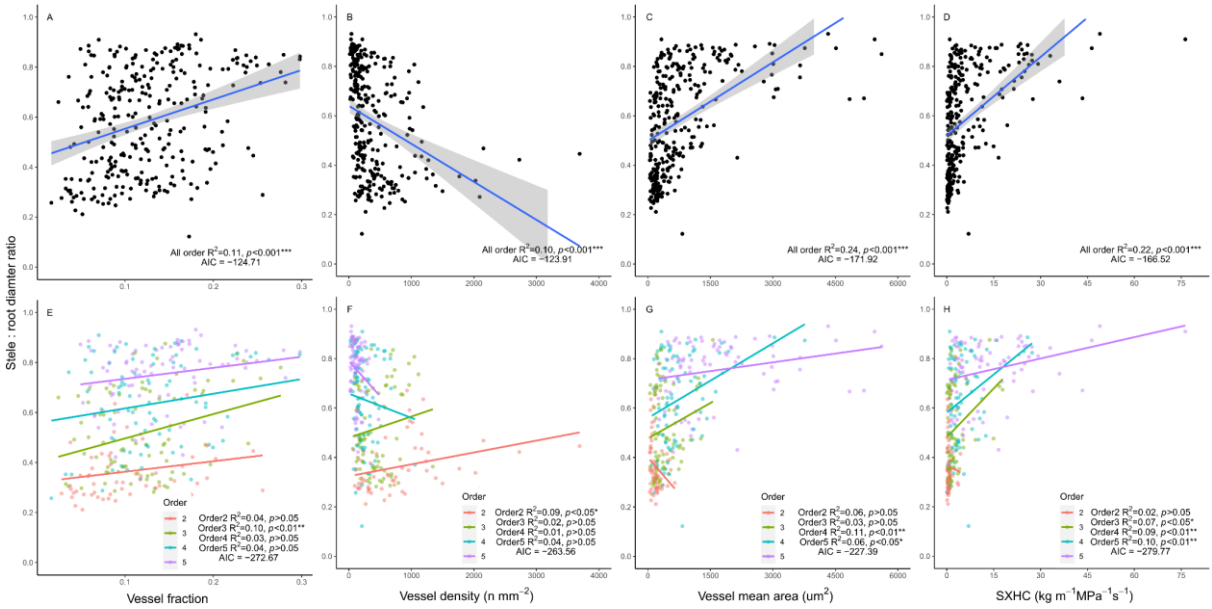

Fig. 4 Interspecific relationships between stele: root diameter ratio and vessel fraction (A and E), vessel density (B and F), vessel mean area (C and G) and specific xylem hydraulic conductivity (SXHC) (D and H), across all root orders (A, B, C and D, as controls) or by root order (E, F, G and H). AIC stands for model evaluation without (A, B, C and D) and with (E, F, G and H) the effect of root order, respectively. Colored dots represent different root orders.

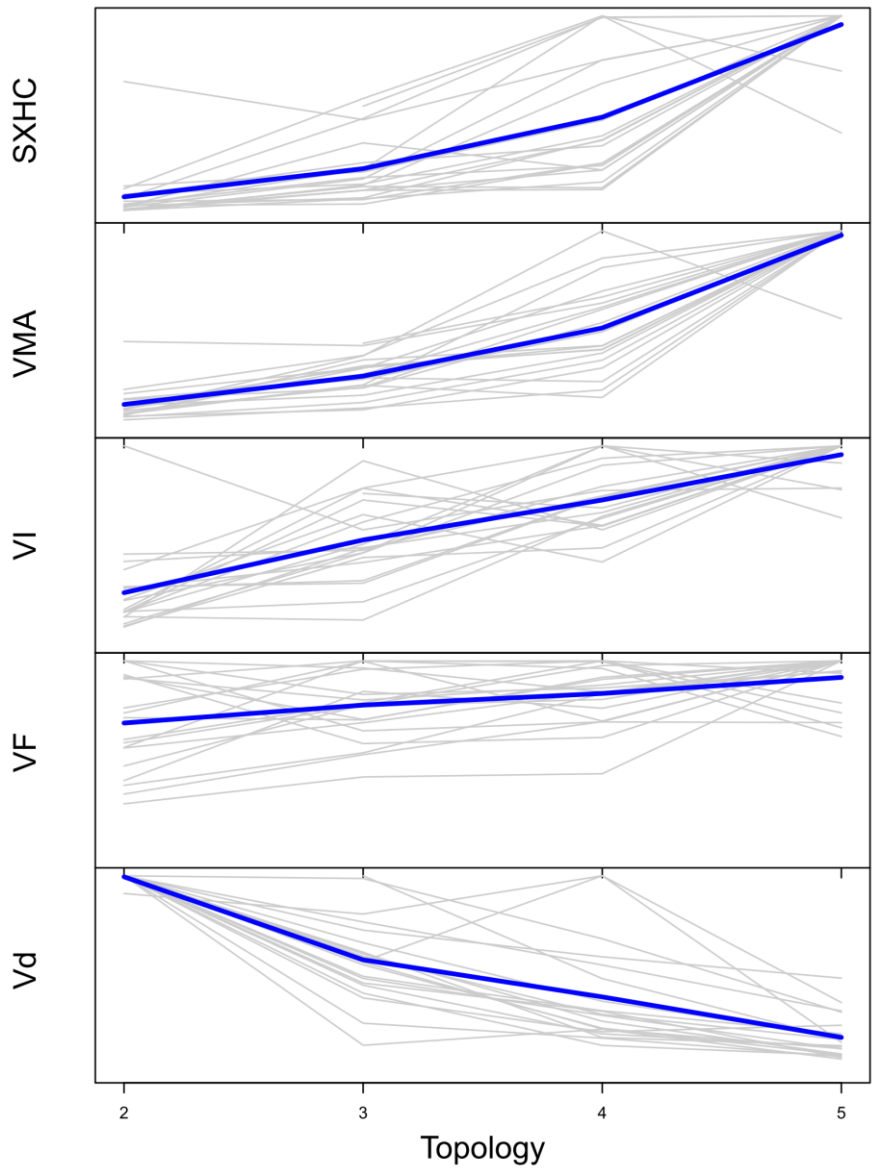

Fig. 5 Conceptual models for the variation of fine root hydraulics along the root order. The grey lines represent the variation of hydraulic-related traits for each tree species, and the blue line represents the variation of hydraulic-related traits for average of all tree species. See Table 2 for trait abbreviations.

SUPPLEMENTARY MATERIALS

Table S1 Pearson correlation coefficient for order and anatomical traits across 400 root branches from 20 tree species. Significant effects are in bold ($P < 0.05$). See Table 2 for trait abbreviations.

	Order	VF	Vd	VMA	MHD	SXHC	VI	RD	CT	SD	S-R	C-R
Order	**1**											
VF	**0.23**	**1**										
Vd	**-0.56**	**0.16**	**1**									
VMA	**0.56**	**0.26**	**-0.43**	**1**								
MHD	**0.67**	**0.34**	**-0.56**	**0.96**	**1**							
SXHC	**0.51**	**0.48**	**-0.34**	**0.89**	**0.88**	**1**						
VI	**0.56**	**0.40**	**-0.37**	**0.53**	**0.65**	**0.65**	**1**					
RD	**0.62**	0.10	**-0.54**	**0.80**	**0.82**	**0.68**	**0.47**	**1**				
CT	**-0.20**	**-0.28**	**-0.16**	**-0.13**	-0.11	**-0.18**	**-0.15**	**0.14**	**1**			
SD	**0.68**	**0.19**	**-0.47**	**0.84**	**0.86**	**0.75**	**0.54**	**0.94**	**-0.16**	**1**		
S-R	**0.76**	**0.31**	**-0.33**	**0.49**	**0.57**	**0.48**	**0.54**	**0.44**	**-0.53**	**0.65**	**1**	
C-R	**-0.75**	**-0.33**	**0.32**	**-0.44**	**-0.51**	**-0.42**	**-0.49**	**-0.42**	**0.63**	**-0.60**	**-0.91**	**1**

Table S2 Pearson correlation coefficient (lower diagonal) and phylogenetically independent contrasts (upper diagonal) among root anatomical traits with all root order pooled from 20 tree species (n=20). Significant effects are in bold ($P < 0.05$). See Table 2 for trait abbreviations.

	VF	Vd	VMA	MHD	SXHC	VI	RD	CT	SD	S-R	C-R
VF	1	0.14	0.21	0.35	**0.53**	0.45	0.29	0.31	0.15	-0.28	0.13
Vd	**0.50**	1	**-0.62**	**-0.62**	**-0.53**	-0.18	**-0.74**	**-0.62**	**-0.64**	0.32	-0.35
VMA	0.01	**-0.66**	1	**0.98**	**0.91**	0.32	**0.68**	0.39	**0.77**	0.08	-0.07
MHD	0.13	**-0.65**	**0.98**	1	**0.96**	0.45	**0.75**	**0.49**	**0.80**	0.01	0.00
SXHC	**0.43**	-0.38	**0.88**	**0.92**	1	**0.57**	**0.74**	**0.53**	**0.74**	-0.12	0.10
VI	0.41	-0.05	0.35	**0.47**	**0.62**	1	**0.58**	**0.57**	**0.47**	-0.18	0.27
RD	-0.23	**-0.84**	**0.71**	**0.73**	**0.54**	0.21	1	**0.82**	**0.90**	-0.29	0.37
CT	-0.20	**-0.83**	**0.58**	**0.63**	0.43	0.20	**0.91**	1	**0.51**	**-0.66**	**0.76**
SD	-0.21	**-0.77**	**0.79**	**0.79**	**0.63**	0.28	**0.95**	**0.75**	1	0.12	-0.01
S-R	0.27	**0.58**	-0.16	-0.18	0.00	0.22	**-0.49**	**-0.70**	-0.23	1	**-0.91**
C-R	-0.32	**-0.70**	0.28	0.32	0.11	-0.08	**0.55**	**0.78**	0.34	**-0.92**	1

Table S3 Pearson correlation coefficient (lower diagonal) and phylogenetically independent contrasts (upper diagonal) among root anatomical traits in root order 2 from 20 tree species (n=19). Significant effects are in bold ($P < 0.05$). See Table 2 for trait abbreviations.

	VF	Vd	VMA	MHD	SXHC	VI	RD	CT	SD	S-R	C-R
VF	1	0.24	0.29	0.33	**0.57**	**0.47**	-0.09	-0.17	-0.08	0.07	-0.35
Vd	**0.52**	1	**-0.74**	**-0.76**	**-0.53**	-0.46	**-0.77**	**-0.70**	**-0.82**	0.33	-0.03
VMA	0.19	**-0.64**	1	**0.99**	**0.86**	**0.66**	**0.78**	**0.68**	**0.86**	-0.36	-0.07
MHD	0.22	**-0.65**	**0.99**	1	**0.87**	**0.69**	**0.79**	**0.69**	**0.86**	-0.38	-0.09
SXHC	**0.62**	0.25	**0.78**	**0.78**	1	**0.89**	0.45	0.37	**0.55**	-0.10	-0.12
VI	0.37	-0.38	**0.69**	**0.72**	**0.85**	1	0.37	0.30	0.45	-0.01	-0.08
RD	**-0.49**	**-0.82**	**0.65**	**0.66**	0.11	0.29	1	**0.97**	**0.97**	**-0.72**	0.25
CT	**-0.52**	**-0.80**	**0.60**	**0.61**	0.07	0.24	**0.99**	1	**0.91**	**-0.77**	0.46
SD	-0.44	**-0.80**	**0.71**	**0.71**	0.17	0.33	**0.97**	**0.95**	1	**-0.55**	0.12
S-R	0.37	**0.68**	-0.42	-0.44	-0.13	-0.17	**-0.70**	**-0.72**	**-0.58**	1	**-0.50**
C-R	**-0.52**	**-0.58**	0.29	0.27	0.00	0.07	**0.60**	**0.69**	**0.52**	**-0.81**	1

Table S4 Pearson correlation coefficient (lower diagonal) and phylogenetically independent contrasts (upper diagonal) among root anatomical traits in root order 3 from 20 tree species (n=20). Significant effects are in bold ($P < 0.05$). See Table 2 for trait abbreviations.

	VF	Vd	VMA	MHD	SXHC	VI	RD	CT	SD	S-R	C-R
VF	1	0.36	0.31	0.38	**0.51**	0.23	0.21	0.24	0.13	-0.01	0.07
Vd	**0.55**	1	**-0.69**	**-0.70**	**-0.50**	-0.43	**-0.63**	**-0.51**	**-0.74**	-0.02	-0.17
VMA	0.12	**-0.69**	1	**0.97**	**0.84**	0.39	**0.78**	**0.65**	**0.83**	0.00	0.18
MHD	0.16	**-0.68**	**0.99**	1	**0.90**	**0.57**	**0.78**	**0.64**	**0.86**	0.08	0.12
SXHC	**0.44**	-0.34	**0.84**	**0.86**	1	**0.67**	**0.60**	**0.58**	**0.61**	-0.01	0.23
VI	0.32	-0.21	**0.58**	**0.66**	0.82	1	0.33	0.21	**0.48**	0.35	-0.15
RD	-0.18	**-0.79**	**0.78**	**0.77**	0.41	0.25	1	**0.92**	**0.88**	-0.27	0.36
CT	-0.24	**-0.81**	**0.68**	**0.67**	0.33	0.10	**0.94**	1	**0.65**	**-0.57**	**0.66**
SD	-0.10	**-0.71**	**0.82**	**0.83**	**0.50**	**0.45**	**0.92**	**0.75**	1	0.18	-0.03
S-R	0.37	**0.50**	-0.13	-0.10	0.06	0.33	-0.35	**-0.62**	0.00	1	**-0.92**
C-R	-0.40	**-0.66**	0.29	0.27	0.08	-0.16	**0.46**	**0.70**	0.17	**-0.94**	1

Table S5 Pearson correlation coefficient (lower diagonal) and phylogenetically independent contrasts (upper diagonal) among root anatomical traits in root order 4 from 20 tree species (n=20). Significant effects are in bold ($P < 0.05$). See Table 2 for trait abbreviations.

	VF	Vd	VMA	MHD	SXHC	VI	RD	CT	SD	S-R	C-R
VF	1	0.07	0.05	0.19	**0.55**	0.29	0.08	0.25	-0.20	-0.34	0.23
Vd	0.41	1	**-0.86**	**-0.88**	**-0.65**	**-0.46**	**-0.76**	0.06	**-0.83**	-0.35	0.25
VMA	0.05	**-0.63**	1	**0.98**	**0.82**	0.25	**0.67**	-0.31	**0.89**	**0.50**	**-0.45**
MHD	0.17	**-0.65**	**0.97**	1	**0.87**	0.40	**0.72**	-0.20	**0.85**	0.40	-0.36
SXHC	**0.61**	-0.28	**0.78**	**0.84**	1	0.38	**0.51**	-0.16	**0.59**	0.23	-0.24
VI	**0.45**	0.10	0.09	0.23	0.40	1	**0.54**	**0.48**	0.18	-0.28	0.28
RD	-0.29	**-0.78**	**0.56**	**0.57**	0.23	-0.13	1	0.43	**0.70**	-0.05	0.21
CT	-0.22	-0.38	-0.09	-0.03	-0.19	-0.08	**0.69**	1	-0.28	**-0.77**	**0.94**
SD	-0.24	**-0.74**	**0.89**	**0.84**	**0.52**	-0.07	**0.70**	0.08	1	**0.66**	-0.43
S-R	0.14	0.18	0.28	0.22	0.31	0.16	**-0.47**	**-0.77**	0.27	1	**-0.79**
C-R	-0.26	-0.32	-0.15	-0.10	-0.23	-0.21	**0.59**	**0.96**	0.01	**-0.77**	1

Table S6 Pearson correlation coefficient (lower diagonal) and phylogenetically independent contrasts (upper diagonal) among root anatomical traits in root order 5 from 20 tree species (n=20). Significant effects are in bold ($P < 0.05$). See Table 2 for trait abbreviations.

	VF	Vd	VMA	MHD	SXHC	VI	RD	CT	SD	S-R	C-R
VF	1	0.03	0.22	0.36	**0.53**	**0.56**	**0.62**	0.03	**0.52**	-0.04	-0.03
Vd	0.12	1	**-0.81**	**-0.79**	**-0.66**	-0.22	-0.43	-0.43	**-0.46**	-0.21	-0.38
VMA	0.17	**-0.80**	1	**0.98**	**0.92**	**0.49**	**0.64**	0.36	**0.68**	0.30	0.16
MHD	0.28	**-0.81**	**0.99**	1	**0.96**	**0.59**	**0.71**	0.38	**0.73**	0.28	0.18
SXHC	**0.51**	**-0.59**	**0.89**	**0.93**	1	**0.69**	**0.77**	0.36	**0.76**	0.18	0.17
VI	0.41	-0.24	**0.45**	**0.53**	**0.70**	1	**0.63**	0.38	**0.58**	0.04	0.24
RD	0.18	**-0.72**	**0.76**	**0.78**	**0.65**	0.33	1	0.10	**0.96**	0.15	-0.02
CT	0.05	-0.41	0.33	0.34	0.22	0.10	0.22	1	-0.06	**-0.48**	**0.94**
SD	0.20	**-0.72**	**0.78**	**0.81**	**0.70**	0.40	**0.98**	0.09	1	0.43	-0.20
S-R	0.18	-0.17	0.28	0.29	0.34	0.39	0.14	**-0.50**	0.33	1	**-0.58**
C-R	-0.11	-0.32	0.14	0.16	0.05	-0.05	0.05	**0.92**	-0.08	**-0.62**	1

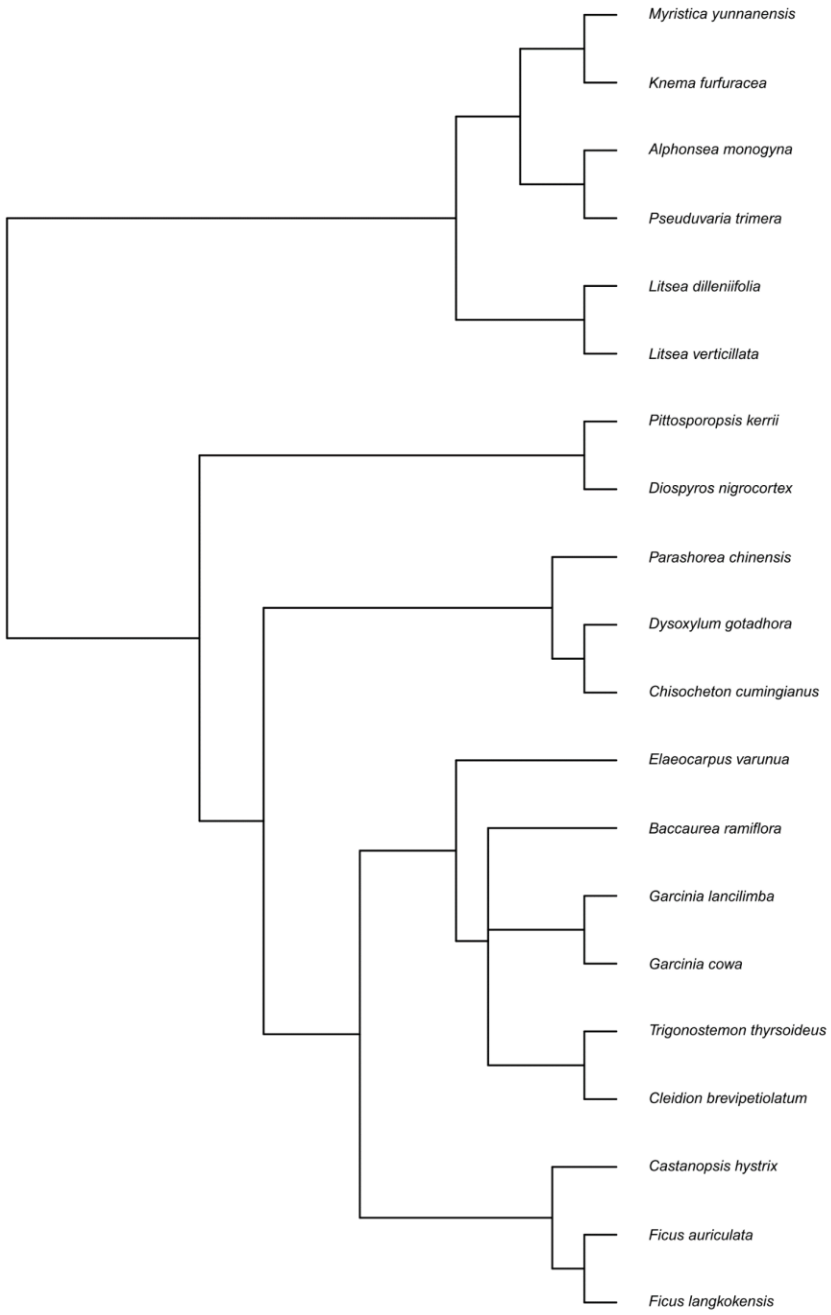

Fig. S1 Phylogenetic tree of 20 Chinese tropical tree species. The cladogram is based on the Angiosperm Phylogeny Group (APG) III classification.

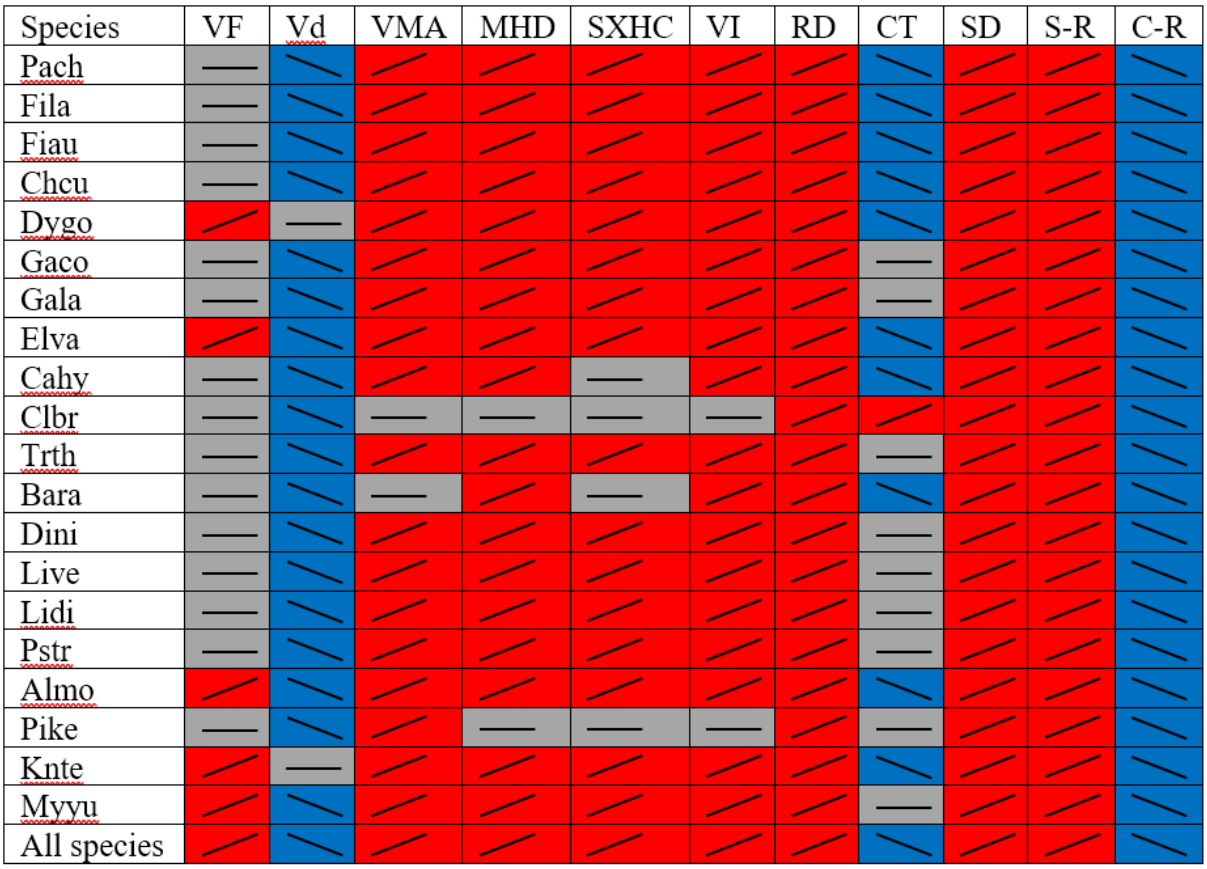

Fig. S2 Changing trend of anatomical traits from low-order root to high-order within species and across all species. The direction of the line and table color indicate the variation of the trait: diagonally upward and red mean increase, horizontal and grey mean unchanged, and diagonally downward and blue mean decrease. See Table 1 and 2 for species and trait abbreviations.

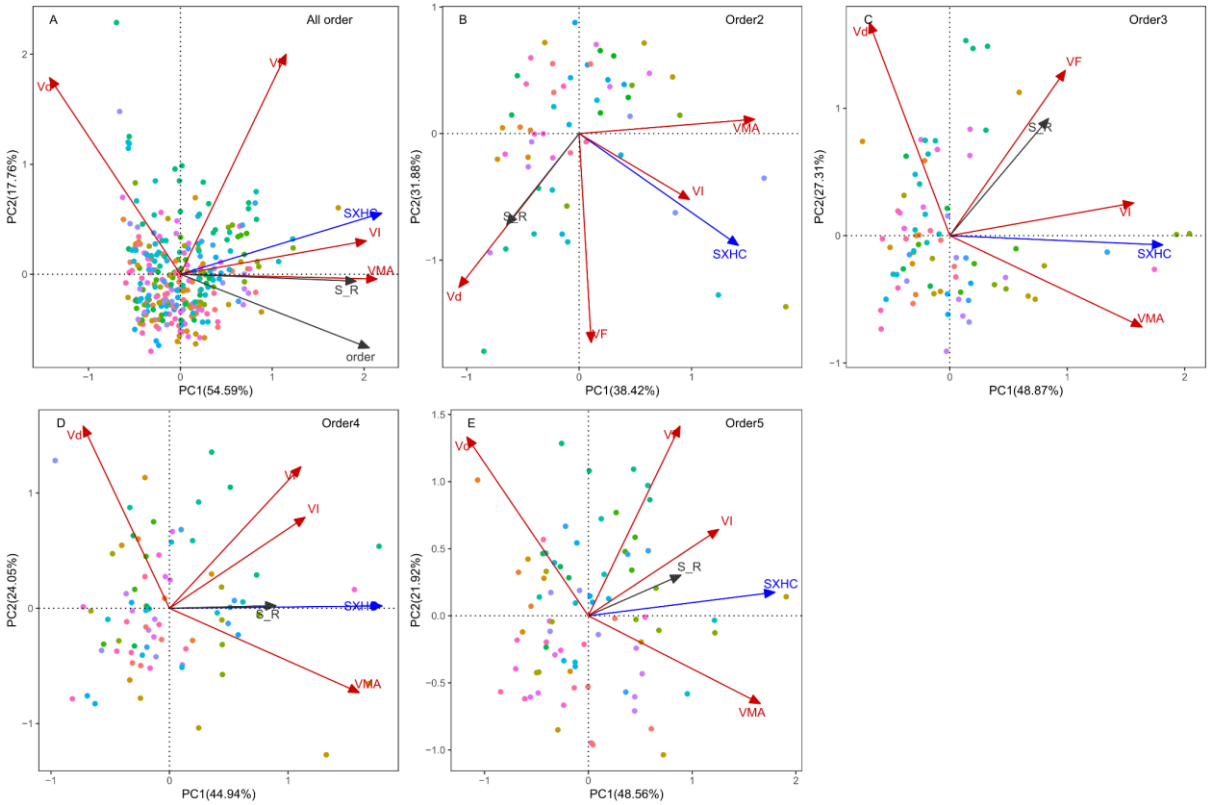

Fig. S3 Principal components analysis (PCA) on root vessel traits among 20 Chinese tropical tree species for all order (A) and each order (B, C, D, E). See Table 2 for trait abbreviations. Colored small circles represent different tree species.

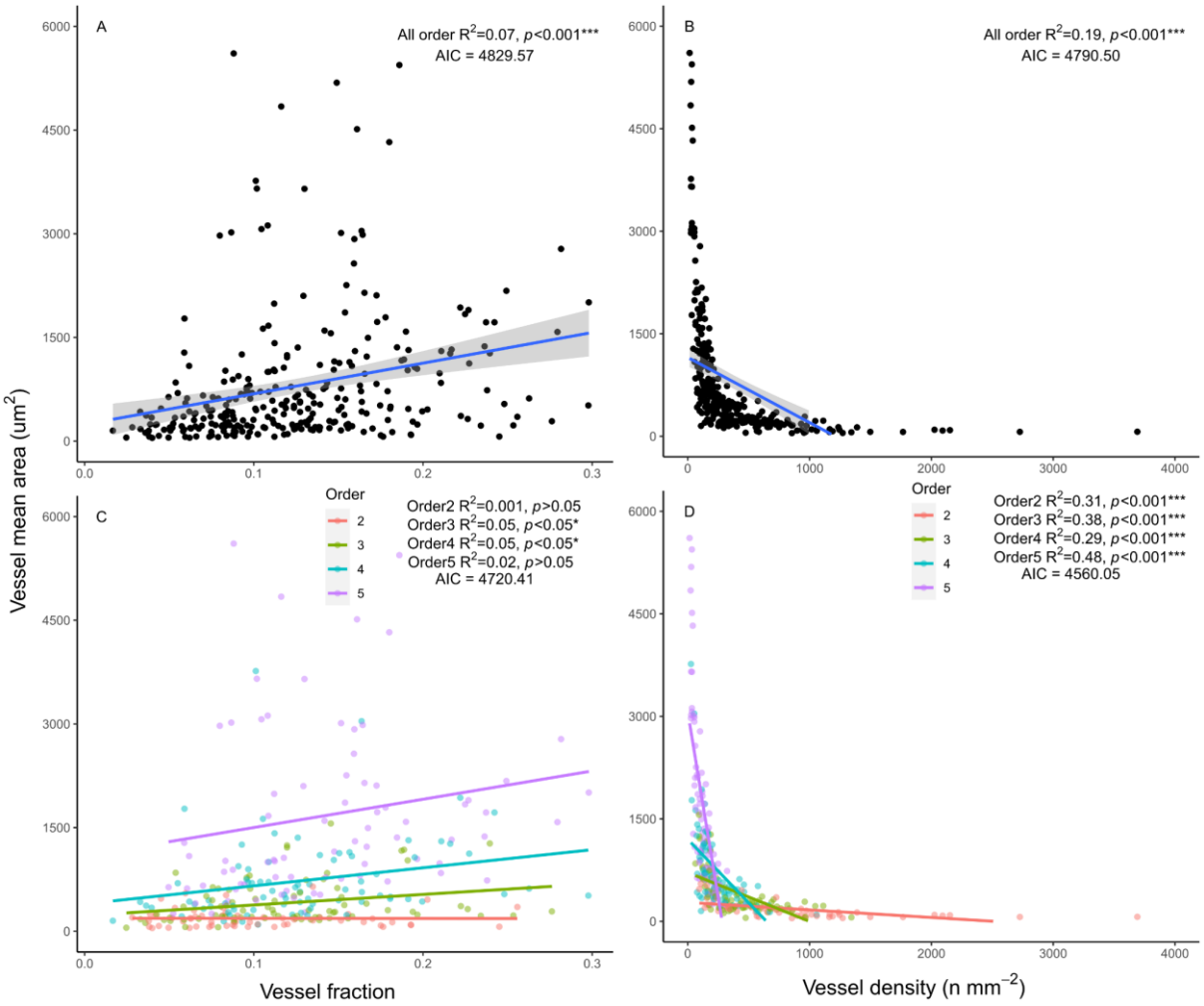

Fig. S4 Relationships between vessel density and vessel fraction (A, C), vessel mean area (B, D) with all root order pooled and in each root order for 20 Chinese tropical tree species. AIC stands for model evaluation without (A, B) and with (C, D) the effect of root order. Colored dots represent different root orders.

Résumé exhaustif: Objectifs, résultats, conclusions générales (In French)

Objectifs généraux et hypothèses:

Au cours de leur croissance, les plantes effectuent une série d'activités physiologiques et de fonctions écologiques, telles que la photosynthèse, la respiration, le transport de l'eau, la défense, etc. Chaque plante a sa propre façon d'agir, c'est-à-dire qu'elle a sa propre stratégie écologique. En d'autres termes, les stratégies écologiques des plantes font référence à la manière dont une espèce assure la subsistance d'une population en remplissant ses fonctions, et en opérant en présence d'espèces concurrentes, dans des paysages variés et sous des régimes de perturbation. Les traits fonctionnels qui ont un impact indirect sur l'aptitude des plantes par le biais de leurs effets sur la croissance, la reproduction et la survie sont considérés comme l'outil largement accepté pour étudier les stratégies des plantes. Les traits anatomiques du xylème et les glucides non structuraux (NSC) sont de plus en plus reconnus comme des traits fonctionnels essentiels des plantes et jouent un rôle important dans la survie et la performance fonctionnelle des arbres.

Les fractions du parenchyme pourraient agir comme un indicateur de la capacité de stockage des NSC et des études récentes ont trouvé des corrélations positives entre le parenchyme radial et axial (RAP) et la teneur en NSC dans les troncs et les branches ligneuses. Cependant, ces études se sont concentrées sur un nombre limité d'espèces ou sur des biomes uniques. En outre, les mesures sur le terrain fournissent des données utiles mais, en raison de la saisonnalité des flux de NSC, les études à grande échelle sont difficiles à réaliser car des échantillonnages répétés doivent être effectués tout au long de l'année. Une revue systématique des données disponibles avec de multiples points d'échantillonnage saisonniers peut donc fournir une perspective alternative et des preuves complémentaires pour valider la relation entre NSC et RAP dans les tiges d'arbres à travers les espèces et les climats.

Les fonctions liées aux différents types de cellules du xylème sont interdépendantes, et comme le xylème du bois accomplit plus d'une tâche, il existe des demandes contradictoires qui conduisent à des compromis entre structure et fonction. En outre, les différences de fonction entre les espèces peuvent être dues à la disposition spatiale des cellules, comme la porosité, dans l'espace du xylème, mais le lien entre la fonction des cellules et leur disposition spatiale est mal compris. La conception de l'espace du xylème qui en résulte influence activement les processus physiologiques qui se produisent à l'intérieur des arbres, ce qui peut entraîner la survie ou le dépérissement lorsque les conditions environnementales locales changent. La compréhension de la conception de l'espace du xylème nous permettra donc d'identifier les stratégies qui contribuent à la survie des arbres sous différents climats.

Les NSC produits par la photosynthèse peuvent être rapidement utilisés pour des fonctions immédiates ou stockés pour les réserves et la défense, ce qui suggère un compromis basé sur l'allocation entre la demande et l'offre de carbone. Plusieurs études ont rapporté le compromis entre l'économie des ressources et les différents tissus, c'est-à-dire les tissus foliaires, les tissus ligneux, les tissus racinaires, ainsi qu'au niveau de la plante entière. Ces études ont démontré que les caractéristiques des feuilles, des tiges et des racines sont coordonnées et fournissent ainsi un cadre utile pour explorer le compromis entre l'acquisition et la conservation des ressources au niveau de la plante entière. Pourtant, bien qu'il existe de nombreuses études sur la stratégie économique des plantes, peu de recherches ont été menées pour explorer la coordination directe entre les NSC dans différents organes et les traits économiques fonctionnels qui conçoivent les stratégies écologiques des plantes.

Suite aux lacunes de recherche mentionnées ci-dessus, les objectifs spécifiques de la thèse étaient de:

1) explorer les relations directes entre les contenus en NSC et les fractions du parenchyme dans un large éventail d'espèces d'arbres afin de fournir une nouvelle perspective et un aperçu supplémentaire sur leurs relations à travers les climats et la subdivision évolutive des arbres, en se basant sur une revue systématique.

2) étudier les compromis entre les multiples structures et fonctions du xylème en examinant les caractéristiques anatomiques, hydrauliques, mécaniques et de stockage dans un large éventail d'espèces d'arbres adultes et de climats.

3) découvrir les coordinations entre les contenus de NSC et les traits de l'économie fonctionnelle de l'arbre (c'est-à-dire l'azote, la masse foliaire par surface et la densité du bois, etc.) au niveau de l'arbre entier pour évaluer le rôle des NSC dans les processus physiologiques de l'arbre et les stratégies écologiques à travers un large éventail d'espèces et de climats.

Dans le chapitre 2, nous avons réalisé une étude systématique en compilant une base de données sur les NSC, les RAP, la densité du bois et la hauteur maximale des arbres pour 68 espèces d'arbres. Conformément aux résultats précédents, nous émettons l'hypothèse suivante: (H1) les troncs des arbres présentant des fractions RAP importantes ont également une teneur élevée en NSC et les fractions de parenchyme radial joueraient un rôle plus important dans le stockage des NSC que les fractions de parenchyme axial. (H2) Les fractions RAP et la teneur en NSC augmentent avec la densité du bois mais diminuent dans les arbres plus hauts, (H3) Les fractions RAP, la teneur en NSC et la densité du bois augmentent toutes avec la température annuelle moyenne, mais diminuent avec les précipitations annuelles moyennes.

Dans le chapitre 3, j'ai étudié la conception de l'espace du xylème dans les troncs et les racines grossières de 60 espèces d'arbres provenant de climats tempérés, méditerranéens et tropicaux, et j'ai examiné comment les modèles de RAP affectaient la teneur en NSC. Je me suis

demandé si la conception de l'espace du xylème coordonne les compromis entre la structure et la fonction dans les tiges et les racines, et si cette coordination est liée au climat, et (H1) je m'attends à ce que toute variance dans les motifs du xylème soit affectée par l'histoire de l'évolution, mais que l'histoire de l'évolution elle-même ne change pas le compromis fondamental entre la structure et la fonction du xylème. Si la conception de l'espace du xylème dépend du climat et de la fonction de l'organe, les modèles du parenchyme axial apotrachéal et paratrachéal sont-ils liés à la porosité qui change entre la tige et la racine? Comme la fonction hydraulique est largement assurée par la formation de nouveaux vaisseaux dans le bois initial des espèces à porosité annulaire des régions tempérées et méditerranéennes, je suppose (H2) que le parenchyme axial apotrachéal existe en plus grande quantité dans les tiges des espèces à porosité annulaire des climats tempérés, et que le parenchyme axial paratrachéal est plus abondant dans le xylème à porosité diffuse, y compris dans les racines qui sont généralement à porosité diffuse avec de gros vaisseaux. Je m'attends également (H3) à ce que le xylème avec de grands vaisseaux et une conductivité hydraulique accrue contienne une densité réduite et plus de NSC qui maintiennent l'osmorégulation et aident au remplissage des vaisseaux embolisés, en particulier dans les régions méditerranéennes qui subissent de longues périodes sèches.

Dans le chapitre 4, j'ai exploré la coordination des traits fonctionnels avec le spectre de l'économie végétale reliant le port des feuilles en mesurant des suites de traits similaires représentant les feuilles, les tiges et les racines de 90 espèces d'angiospermes provenant de forêts tempérées, méditerranéennes et tropicales. J'ai étudié les questions suivantes: Le contenu en NSC dans les feuilles, les tiges et les racines est-il coordonné avec les traits fonctionnels associés aux stratégies de ressources acquisitives et conservatrices? (H1) J'ai émis l'hypothèse que la teneur en NSC des feuilles serait coordonnée avec les traits économiques fonctionnels, tandis que la teneur en NSC des tiges et des racines serait

indépendante du spectre des stratégies d'acquisition ou de conservation ressources. Les caractéristiques des feuilles, des tiges et des racines coïncident-elles et s'intègrent-elles avec le spectre économique des plantes? (H2) J'ai émis l'hypothèse que les caractéristiques des feuilles, des tiges et des racines seraient corrélées à l'ensemble du spectre économique des plantes. Le spectre économique des plantes est-il structuré par les zones climatiques et les habitudes foliaires? (H3) J'ai émis l'hypothèse que le spectre économique des plantes est influencé par les zones climatiques et que les espèces à feuilles caduques adopteraient une stratégie d'acquisition des ressources, tandis que les espèces à feuilles persistantes adopteraient une stratégie de conservation des ressources pour les espèces d'arbres à grande échelle et interrégionales.

Dans le chapitre 5, je résume les résultats clés de la thèse et discute de la cohérence et de la différenciation avec d'autres études. J'ai également fourni quelques perspectives pour des études ultérieures.

Principaux résultats:

Dans le chapitre 2, avec la revue systématique, nous avons étudié les relations entre la NSC, la RAP, la densité du bois et la hauteur maximale potentielle des arbres, ainsi que les facteurs climatiques, pour 68 espèces d'arbres. Nous avons constaté que la teneur en NSC était fortement liée à la RAP lorsque toutes les espèces étaient regroupées, ce qui démontre que les cellules du parenchyme constituent un dépôt important de NSC. Cependant, cette corrélation a été trouvée chez les angiospermes mais pas chez les gymnospermes et seulement chez les espèces tempérées lorsque l'on se concentre sur les régions climatiques. En outre, pour toutes les espèces, la teneur en NSC était positivement corrélée au parenchyme radial mais pas au parenchyme axial. La densité du bois était positivement corrélée à la proportion de parenchyme radial dans les tiges des arbres, mais il n'y avait aucune relation significative

entre la densité du bois et les teneurs en NSC. La hauteur des arbres était fortement et négativement corrélée à la densité du bois et à la RAP dans l'ensemble, mais les NSC étaient plus abondants dans les espèces tropicales plus hautes. Les NSC et la RAP ont tous deux augmenté chez les espèces tropicales, reflétant la forte relation positive avec la température annuelle moyenne. Les précipitations annuelles moyennes étaient faiblement et positivement corrélées avec la teneur en NSC mais pas avec la RAP. Ni la densité du bois ni la hauteur maximale des arbres n'étaient corrélées à la température annuelle moyenne ou aux précipitations. La parenté phylogénétique n'a pas affecté les modèles de corrélation entre les caractéristiques fonctionnelles du bois, ce qui montre que le RAP est un indicateur approprié de la capacité potentielle de stockage des NSC dans les tronc.

Dans le chapitre 3, j'ai étudié les traits du xylème du tronc et des racines de 60 espèces d'arbres de climats tempérés, méditerranéens et tropicaux afin d'examiner comment la conception de l'espace du xylème coordonne les compromis entre la structure et la fonction des tiges et des racines. J'ai constaté que tous les traits du xylème présentaient une variation interspécifique marquée et que certains traits du xylème étaient également significativement différents entre le tronc et les racines: la densité du bois, la fraction des vaisseaux et la densité des vaisseaux étaient plus élevées dans les tiges, tandis que les fractions du parenchyme axial, les fractions RAP et les contenus NSC étaient plus élevés dans les racines. En outre, les traits du xylème variaient également de manière significative selon les climats et les types d'agencement du xylème. Les espèces tempérées avaient une densité de bois plus faible dans le tronc et les racines par rapport aux espèces méditerranéennes et tropicales. La RAP et le parenchyme axial dans le tronc et les racines étaient également plus faibles chez les espèces tempérées, tandis que le parenchyme radial ne variait pas entre les trois climats. La fraction des vaisseaux dans le tronc et les racines était la plus importante chez les espèces tempérées, tandis que le diamètre moyen des vaisseaux dans le tronc et les racines était le plus élevé chez

les espèces tropicales. En revanche, la densité des vaisseaux du tronc et des racines était la plus faible chez les espèces tropicales. La conductivité hydraulique spécifique du xylème (SXHC) du tronc et des racines était plus faible chez les espèces méditerranéennes que chez les espèces tempérées et tropicales. La densité du bois, la fraction des vaisseaux, la densité des vaisseaux, la SXHC et la NSC étaient plus faibles (mais le parenchyme axial et le diamètre moyen des vaisseaux étaient plus grands) dans les tiges des espèces à porosité diffuse par rapport aux espèces à porosité semi-circulaire, alors que la plupart des caractéristiques du xylème n'étaient pas significativement différentes entre les espèces à porosité diffuse et les espèces à porosité semi-circulaire. Lorsque l'on divise les espèces en espèces à parenchyme axial apotrachéal et à parenchyme axial paratrachéal selon la disposition du parenchyme axial, les espèces à parenchyme axial apotrachéal présentent un parenchyme radial plus élevé dans le tronc et les racines et une densité de bois plus élevée dans le tronc par rapport aux espèces à parenchyme axial paratrachéal. En outre, les espèces à parenchyme axial paratrachéal présentaient des vaisseaux plus gros et une plus grande SXHC dans le tronc. La densité du bois était positivement corrélée avec les fractions du parenchyme total dans le tronc et les racines, tandis qu'elle était négativement corrélée avec la fraction des vaisseaux, le diamètre moyen des vaisseaux et le SXHC, ce qui a révélé un compromis entre le support mécanique du xylème et la conductivité hydraulique. De plus, les teneurs en NSC étaient significativement et positivement associées à la SXHC dans le xylème du tronc, alors que des corrélations négatives ont été trouvées entre les teneurs en NSC et la SXHC dans les racines. La densité du bois, les caractéristiques des vaisseaux, la SXHC et les teneurs en NSC ont montré des signaux phylogénétiques significatifs, mais l'histoire de l'évolution ne semble pas modifier les compromis fondamentaux entre les caractéristiques fonctionnelles.

Dans le chapitre 4, j'ai étudié la coordination des traits fonctionnels, y compris le contenu en NSC, associés au spectre économique des plantes parmi 90 espèces d'angiospermes aux

habitudes foliaires contrastées. J'ai constaté que la plupart des traits fonctionnels étaient significativement corrélés entre eux. La masse foliaire par surface était significativement et positivement corrélée au contenu en carbone des feuilles et des racines, et négativement liée au contenu en azote des feuilles et des racines. Les espèces ayant une densité de bois de tige élevée ont tendance à avoir une densité de bois de racine élevée, mais seule la densité de bois de racine était négativement corrélée avec la teneur en azote des feuilles et positivement corrélée avec la masse foliaire par surface. La teneur en NSC des feuilles a montré une corrélation positive avec la teneur en azote et une corrélation négative avec la masse foliaire par surface, tandis que la teneur en NSC de la tige n'a pas montré de corrélations significatives avec les caractéristiques des feuilles. La teneur en NSC de la racine était corrélée positivement avec la teneur en azote de la feuille, et négativement avec la teneur en carbone de la feuille. J'ai également constaté que la teneur en NSC des feuilles n'était pas corrélée à la teneur en NSC des tiges et des racines, mais que la teneur en NSC des tiges était significativement corrélée à la teneur en NSC des racines. La RAP des tiges et des racines était négativement liée à la teneur en azote des feuilles, et seule la RAP des tiges était positivement liée à la masse surfacique des feuilles. La fraction des vaisseaux de la tige et de la racine était négativement liée à la masse de la feuille par surface, et seule la fraction des vaisseaux de la tige était positivement liée à la teneur en azote de la feuille. À l'exception de la teneur en azote des feuilles qui présentait une corrélation négative significative avec la fraction de fibres de la tige, les corrélations entre les autres caractéristiques des feuilles et la fraction de fibres n'étaient pas significatives. En outre, j'ai constaté que la teneur en NSC des feuilles était coordonnée avec les caractéristiques économiques des feuilles, tandis que les organes ligneux, en particulier la teneur en NSC des tiges, semblent être indépendants du spectre économique des ressources, probablement en raison de l'âge différent des NSC stockés dans les feuilles et les organes ligneux. En outre, j'ai également constaté qu'il existait une relation découplée

entre les caractéristiques économiques des feuilles et des tiges, tandis que les caractéristiques chimiques et anatomiques des racines étaient toujours coordonnées avec les caractéristiques fonctionnelles des feuilles. L'histoire de l'évolution des espèces n'a pas influencé les modèles de corrélation des traits des organes végétaux. J'ai pu clairement constater que les espèces d'arbres de différents climats et ayant des habitudes foliaires différentes présentaient des stratégies d'allocation des ressources différentes, les espèces tempérées et méditerranéennes et les espèces à feuilles caduques adoptant une stratégie d'acquisition des ressources, tandis que les espèces tropicales et les espèces à feuilles caduques adoptent une stratégie de conservation des ressources. Notre étude élargit les horizons des compromis dans l'allocation des ressources le long du spectre économique du point de vue de l'arbre entier adulte, et d'autres études liées aux données empiriques et à la méta-analyse sont encore nécessaires à grande échelle et à l'échelle locale.

Conclusions générales:

L'objectif principal de l'étude présentée dans ma thèse était de fournir des connaissances fondamentales sur les compromis dans l'allocation des ressources du point de vue de la plante entière, et de mieux quantifier la structure et la fonction du xylème liées au transport de l'eau, au support mécanique et au stockage. Dans le chapitre 2, j'ai effectué une revue systématique en compilant une base de données comprenant des données sur les NSC, la RAP, la densité du bois et la hauteur maximale des arbres pour 68 espèces d'arbres afin d'explorer les relations entre ces caractéristiques, en particulier la relation entre la NSC et la fraction du parenchyme. Dans les chapitres 3 et 4, j'ai prélevé des feuilles, des tiges et des racines dans le xylème de 90 espèces cultivées sous trois climats et j'ai mesuré les caractéristiques fonctionnelles, notamment la NSC, le carbone, l'azote, la surface foliaire spécifique, la densité du bois des tiges et des racines et les caractéristiques anatomiques du xylème, afin de démêler la façon

dont les caractéristiques des NSC et du xylème sont liées aux processus physiologiques et aux stratégies écologiques des arbres et d'explorer le compromis entre la structure et la fonction du xylème.

Le carbone fixé pendant la photosynthèse est exporté des feuilles vers les organes puits sous forme de NSC, qui constituent une source d'énergie essentielle pour les processus métaboliques des arbres. Dans le xylème, les NSC sont stockés dans les cellules des rayons vivants et du parenchyme axial. Par conséquent, la taille de la fraction du parenchyme détermine la capacité de stockage des NSC chez les arbres. Cette recherche a fourni des preuves préliminaires mais claires que les fractions RAP et la capacité de stockage des NSC sont étroitement liées, soulignant le rôle important des cellules du parenchyme de la tige dans le stockage des NSC. En étudiant les caractéristiques anatomiques et fonctionnelles du xylème, j'ai également révélé des compromis complexes entre la structure et les fonctions du xylème dans les tiges et les racines. J'ai conclu que les caractéristiques du xylème variaient beaucoup selon les organes ligneux, les climats et les dispositions anatomiques. En particulier, les traits liés à la conductivité hydraulique étaient plus faibles chez les espèces d'arbre méditerranéennes, tandis que les traits liés à la mécanique et au stockage étaient plus faibles chez les espèces d'arbre tempérées et tropicales. J'ai également conclu que la densité du bois était négativement corrélée avec la fraction des vaisseaux, le diamètre moyen des vaisseaux et la SXHC, ce qui a révélé un compromis entre le support mécanique du xylème et la conductivité hydraulique. En outre, il y avait des modèles de corrélation contraires entre la teneur en NSC et la SXHC dans les troncs et les racines, ce qui suggère que le tronc et la racine ont tendance à se concentrer sur des stratégies de stockage hydraulique différentes et indique une capacité de stockage élevée de NSC avec une conductivité hydraulique élevée dans le tronc, mais avec une faible conductivité hydraulique dans la racine. En explorant les associations entre la teneur en NSC et les stratégies de ressources du spectre économique des

plantes, je conclue que la teneur en NSC des feuilles est coordonnée avec les caractéristiques économiques des feuilles, tandis que les organes ligneux, en particulier la teneur en NSC des troncs, semblent être indépendants de l'économie des ressources. Je souligne également que les stratégies écologiques des arbres ont été influencées par les climats, et que les espèces à feuilles caduques et à feuilles persistantes ont montré différentes stratégies d'allocation des ressources, les espèces à feuilles caduques ayant une stratégie d'acquisition des ressources et les espèces à feuilles persistantes une stratégie de conservation des ressources. Les résultats présentés dans cette thèse approfondissent notre compréhension de la façon dont les fractions du parenchyme affectent le stockage des NSC et le rôle des NSC dans les processus physiologiques des arbres, en particulier à travers une large gamme d'espèces d'arbres et de climats. Ces résultats ont non seulement élargi le champ de nos connaissances sur le stockage et la physiologie des NSC chez les arbres, mais ont également fourni un aperçu des stratégies fonctionnelles liées à la conception de l'espace du xylème chez les angiospermes. Néanmoins, la recherche scientifique est sans fin, et d'autres études approfondies sont nécessaires à grande échelle afin d'acquérir une compréhension solide de la façon dont les différentes fonctions de l'aubier (y compris le stockage du NSC, le transport de l'eau, la respiration, l'intégrité mécanique et la résistance aux agents pathogènes) sont liées entre les espèces, les formes de croissance et le climat.